AEROELASTIC ROTOR STABILITY ANALYSIS

Robert A. Johnston, et al

United Technologies Corporation

Prepared for:

Army Air Mobility Research and Development Laboratory

January 1976

USAAMRDL-TR-75-40

057172

AEROELASTIC ROTOR STABILITY ANALYSIS

Sikorsky Aircraft
Division of United Technologies Corporation
Stratford, Conn. 06497

January 1976

Final Report

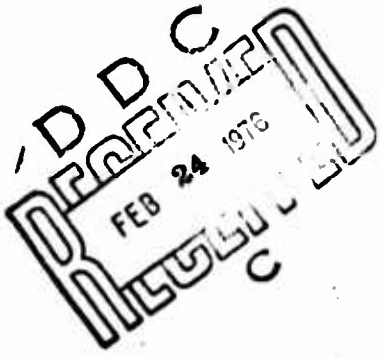

Prepared for

EUSTIS DIRECTORATE
U. S. ARMY AIR MOBILITY RESEARCH AND DEVELOPMENT LABORATORY
Fort Eustis, Va. 23604

EUSTIS DIRECTORATE POSITION STATEMENT

This report has been reviewed by the Eustis Directorate, U. S. Army Air Mobility Research and Development Laboratory and is considered to be technically sound. The purpose of this program was to develop a computer analysis to study the stability of a coupled helicopter main or tail rotor/airframe/control system in hover, forward flight, or pure axial flow.

The program was conducted under the technical management of Paul Mirick of the Technical Applications Division of this directorate.

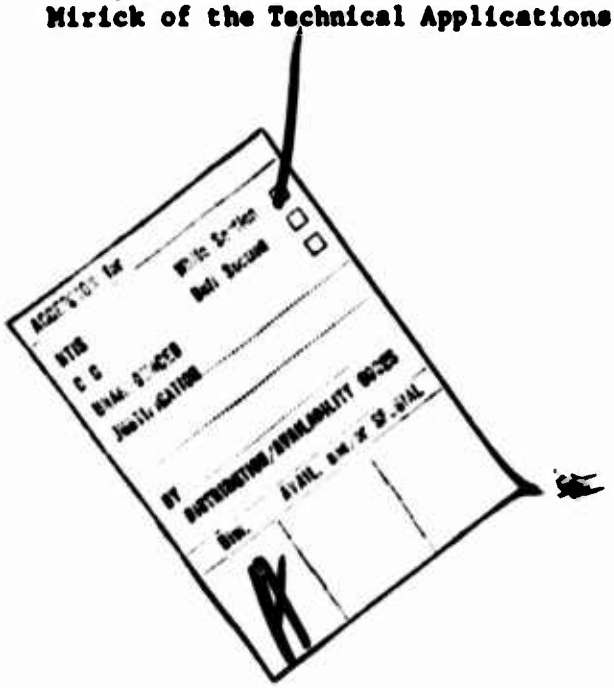

DISCLAIMERS

The findings in this report are not to be construed as an official Department of the Army position unless so designated by other authorized documents.

When Government drawings, specifications, or other data are used for any purpose other than in connection with a definitely related Government procurement operation, the United States Government thereby incurs no responsibility nor any obligation whatsoever; and the fact that the Government may have formulated, furnished, or in any way supplied the said drawings, specifications, or other data is not to be regarded by implication or otherwise as in any manner licensing the holder or any other person or corporation, or conveying any rights or permission, to manufacture, use, or sell any patented invention that may in any way be related thereto.

Trade names cited in this report do not constitute an official endorsement or approval of the use of such commercial hardware or software.

DISPOSITION INSTRUCTIONS

Destroy this report when no longer needed. Do not return it to the originator.

UNCLASSIFIED

SECURITY CLASSIFICATION OF THIS PAGE (When Data Entered)

REPORT DOCUMENTATION PAGE	READ INSTRUCTIONS BEFORE COMPLETING FORM
1. REPORT NUMBER: USAAMRDL-TR-75-40	2. GOVT ACCESSION NO. / 3. RECIPIENT'S CATALOG NUMBER
4. TITLE (and Subtitle): AEROELASTIC ROTOR STABILITY ANALYSIS	5. TYPE OF REPORT & PERIOD COVERED: Final Report
	6. PERFORMING ORG. REPORT NUMBER
7. AUTHOR(s): Robert A. Johnston, S. J. Cassarino	8. CONTRACT OR GRANT NUMBER(s): DAAJ02-74-C-0010
9. PERFORMING ORGANIZATION NAME AND ADDRESS: Sikorsky Aircraft, Division of United Technologies Corporation, Stratford, Connecticut 06497	10. PROGRAM ELEMENT, PROJECT, TASK AREA & WORK UNIT NUMBERS: 62208A 1F262208AH90 01, 003 EK
11. CONTROLLING OFFICE NAME AND ADDRESS: Eustis Directorate, U. S. Army Air Mobility Research and Development Laboratory, Fort Eustis, Virginia 23604	12. REPORT DATE: January 1976
	13. NUMBER OF PAGES: ~~200~~ 200
14. MONITORING AGENCY NAME & ADDRESS (if different from Controlling Office)	15. SECURITY CLASS. (of this report): Unclassified
	15a. DECLASSIFICATION/DOWNGRADING SCHEDULE

16. DISTRIBUTION STATEMENT (of this Report)

Approved for public release; distribution unlimited.

17. DISTRIBUTION STATEMENT (of the abstract entered in Block 20, if different from Report)

18. SUPPLEMENTARY NOTES

19. KEY WORDS (Continue on reverse side if necessary and identify by block number)

Helicopter, Main Rotor, Tail Rotor, Stability, Hover, Forward Flight, Coupled Rotor/Airframe/Control System

20. ABSTRACT (Continue on reverse side if necessary and identify by block number)

This report describes an aeroelastic analysis that provides a complete description of the dynamics and aerodynamics of fully coupled helicopter main or tail rotor/airframe/control systems. The analysis is designed to study stability characteristics in conditions of pure axial flow or in forward flight, for which it computes the system eigenvalues and eigenvectors. For hover studies, the aerodynamic derivatives include stall and compressibility effects, and circulatory and noncirculatory unsteady effects are accounted for through use

DD FORM 1 JAN 73 1473 EDITION OF 1 NOV 65 IS OBSOLETE

UNCLASSIFIED

SECURITY CLASSIFICATION OF THIS PAGE (When Data Entered)

20. ABSTRACT - continued

of Theodorsen and Loewy type lift deficiency functions. The forward-flight aerodynamic derivatives are obtained from any appropriate linear or nonlinear time history analysis. The approximations made in the forward-flight analysis limit such applications to an advance ratio of about 0.5.

The results of parametric and sensitivity studies conducted using the analysis are shown. Here, semiarticulated and hingeless, composite bearingless tail rotors were used as baselines. Studies were conducted at advance ratios of 0.0, 0.25, and 0.5. As might be expected, the studies showed that the cyclic system modes are most affected by advance ratio. The cyclic flapping modes, for example, are significantly destabilized as advance ratio is increased.

TABLE OF CONTENTS

LIST OF FIGURES

LIST OF FIGURES (continued)

LIST OF FIGURES (continued)

LIST OF FIGURES (continued)

LIST OF FIGURES (continued)

LIST OF TABLES

INTRODUCTION

There are few aeromechanical systems that operate in a more hostile aerodynamic environment than the helicopter rotor. In hover, the wakes shed by the rotor blades can tend to pile up beneath the rotor and lead to unfavorable blade aeroelastic response. In forward flight the rotors are required to provide lift and propulsive force while the blades are being subjected to rapidly varying aerodynamic forces. The advancing blades can operate at high tip Mach numbers and might experience adverse compressibility effects, while the retreating blades experience both reversed flow and stall effects. Since the rotor blades are relatively flexible, these aerodynamic phenomena can, under certain conditions, lead to aeroelastic instability. Typical of these are advancing blade static pitch divergence and classical flutter, while the retreating blades can encounter stall flutter and drag divergence. Other phenomena that lead to oscillations of the tip path plane are also possible. In hover, the shed wakes can induce blade flutter and the tip vortices shed by the blades can cause subharmonic blade oscillation and can also result in the blades going out of track.

In addition to the above, other instabilities can be encountered that are a direct result of blade kinematic coupling. Among these are classical pitch-flap and pitch-lag instabilities, caused by adverse coupling between the pitching and out-of-plane and inplane motions of the blades. Also, the fact that the blades are relatively flexible can give rise to frequency relationships that result in a class of instability generally referred to as flap-lag instability.

Many of the phenomena encountered by helicopter rotors are little affected by motions of the rotor hub. These can generally be classed as rotor instabilities. However, a number of unstable phenomena that have been experienced are a direct result of coupling between rotor motions and hub motions. The most classical of these is ground resonance, or more aptly, mechanical instability. This can occur when the frequencies and damping of the modes of the helicopter on the ground bear a certain relationship to the rotor blade inplane frequency and damping, when this inplane frequency is less than the rotor speed. This instability is purely mechanical, that is, it requires no aerodynamic influence. A similar phenomenon that does require aerodynamics occurs when the helicopter is airborne. This is generally referred to as air resonance and normally involves the airframe rigid-body modes, bending modes, or local transmission modes. When a rotor is in high-speed axial flight, for example, a propeller rotor, an instability that causes whirling of the rotor hub can occur. The precise form of this instability and the nature of the whirling, advancing or regressing, depend on the degree of flexibility of the blades, or more exactly, the blade out-of-plane and inplane frequencies. Another type of whirling instability that involves rotor coning and blade flapping has recently been encountered during an NASA-sponsored test program at Sikorsky Aircraft.

Rotor blade pitch control systems have a wide variety of designs and dynamic characterics. They invariably include servo actuators and can significantly affect the rotor system aeroelastic response. The blade pitch frequency can be substantially reduced by coupling with the control system which can lead to an otherwise stable system's becoming unstable if the reduction in frequency results in adverse blade modal interactions. Airframe motion feedback through the servo supports or input valve can also affect the rotor response.

Based on the foregoing, it seems clear that if predictions relating to rotor stability are to be believed, then the mathematical models of the system being analyzed should include adequate descriptions of not only the rotor blades and aerodynamics, but also of control systems and hub impedances when there is any possibility that these may influence the results. The analysis described in this report provides this capability by incorporating realistic descriptions of the dynamics of fully coupled rotor/airframe/control systems. It also provides a refined description of the aerodynamics that includes stall, compressibility, and unsteady effects.

The analysis can be used to study the stability of main or tail rotors or propellers in hover, forward flight, or pure axial flow. Since a major objective of the contract under which this work was completed was to provide the Army with the analysis and an operational computer program, the method of developing the analysis, its important features, and the equations of motion are given in detail in Appendixes A and B. A program user's manual has been provided as a separate document.

Also included in the report are the results of parametric and sensitivity studies of semiarticulated and hingeless, composite bearingless type tail rotors using the present analysis. It should be noted that not all of the options available in the analysis were exercised during these studies. Specifically, blade motions were described by only three modes, no control system dynamics were included, hub motions were described by only two modes, certain forward flight dynamic effects were not incorporated, and unsteady aerodynamics were not used. These facts should be taken into consideration when conclusions are drawn from the results of the studies.

DESCRIPTION OF BASELINE TAIL ROTORS

Two baseline tail rotors that are representative of current Sikorsky Aircraft designs were selected. The physical and structural characteristics of the rotor blades and rotor hubs are presented respectively in Tables 1 and 2. Both rotors were nonarticulated in the inplane direction. The tail rotor that is articulated in the out-of-plane direction will be referred to as tail rotor no. 1, while the tail rotor having a rigid root boundary condition for out-of-plane motion will be referred to as tail rotor no. 2. It should be noted that the hinge offset for out-of-plane motion listed for tail rotor no. 2 in Table 1 represents an equivalent hinge offset, or the radial location at which the rotor blade flexibility can be assumed to become finite in the flatwise direction.

Additional rotor blade characteristics are presented for both rotors in Figures 1 through 6. These show respectively the radial distributions of chord, twist, weight, flatwise and edgewise area moments of inertia, and torsional inertia. The blade flatwise mass moment of inertia was assumed to be zero, while the edgewise mass moment of inertia was assumed to equal the torsional mass moment of inertia. The blades were assumed to be torsionally inelastic, the torsional frequency depending only on the control system stiffnesses and the blade torsional inertia.

All conditions investigated assumed sea level, standard day operating conditions (air mass density was .002378 slug/ft^3 and speed of sound was 1116 ft/sec).

Two coupled flatwise/edgewise blade modes were used for each rotor. The first mode, which was primarily flatwise for both rotors, represents rigid-body flapping for tail rotor no. 1 and flatwise bending for tail rotor no. 2. The second mode was mostly edgewise and described a bending mode for both rotors.

TABLE 1. TAIL ROTOR BLADE CHARACTERISTICS

Parameter Description	Tail Rotor No. 1	Tail Rotor No. 2	Units
Radius	10.0	5.5	ft
Hinge offset for out-of-plane motion	.4160	.2917*	ft
Number of blades	4	4	
Rotor speed	700.0	1214	rpm
Tip loss factor	.97	.97	
Prelag angle	3.33	0.00	deg
Precone angle	0.00	0.00	deg
Airfoil section	NACA 0012	NACA 0012	
Young's modulus	10^7	10^6	psi
Pitch horn radial location	9.5	7.375	in
Chordwise distance from elastic axis to pushrod - positive toward leading edge	4.5	5.0	in
Pitch beam arm length	10.64	8.91	in
Critical pitch damping	6.	2.	%
Critical blade bending mode damping	.5	1.5	%
Blade root flapping boundary condition	artic.	rigid	
Blade root inplane boundary condition	riged	rigid	
Radial location of inner snubber		13.5	in
Radial location of outer snubber		30.0	in
Weight at blade pushrod	2.1	.75	lb
Stiffness of pitch beam arm	15,200	32,600	lb/in
Damping associated with pitch beam arm	0.00	0.00	lb sec/in
Stiffness of actuator shaft for pure moment applied at pitch beam end	754,000	935,000	in-lb/rad
Number of blade modes (flatwise/edgewise)	2	2	

*equivalent hinge offset

TABLE 2. TAIL ROTOR HUB CHARACTERISTICS

Parameter Description	Tail Rotor No. 1	Tail Rotor No. 2	Units
Number of modes	2	2	
Generalized mass of mode 1	6439	44.6	in-lb-sec^2
Generalized mass of mode 2	11739	75.1	in-lb-sec^2
Frequency of mode 1	1750	2530	cpm
Frequency of mode 2	502	2160	cpm
Damping of mode 1	3.4	4.0	%
Damping of mode 2	4.1	4.0	%
Lateral displacement of mode 1	0.00	0.00	in
Lateral displacement of mode 2	0.00	0.00	in
Longitudinal displacement of mode 1	-37.6	-12.77	in
Longitudinal displacement of mode 2	0.00	0.00	in
Vertical displacement of mode 1	0.00	0.00	in
Vertical displacement of mode 2	37.4	12.77	in
Yaw displacement of mode 1	1.00	1.00	rad
Yaw displacement of mode 2	0.00	0.00	rad
Pitch displacement of mode 1	0.00	0.00	rad
Pitch displacement of mode 2	1.00	1.00	rad

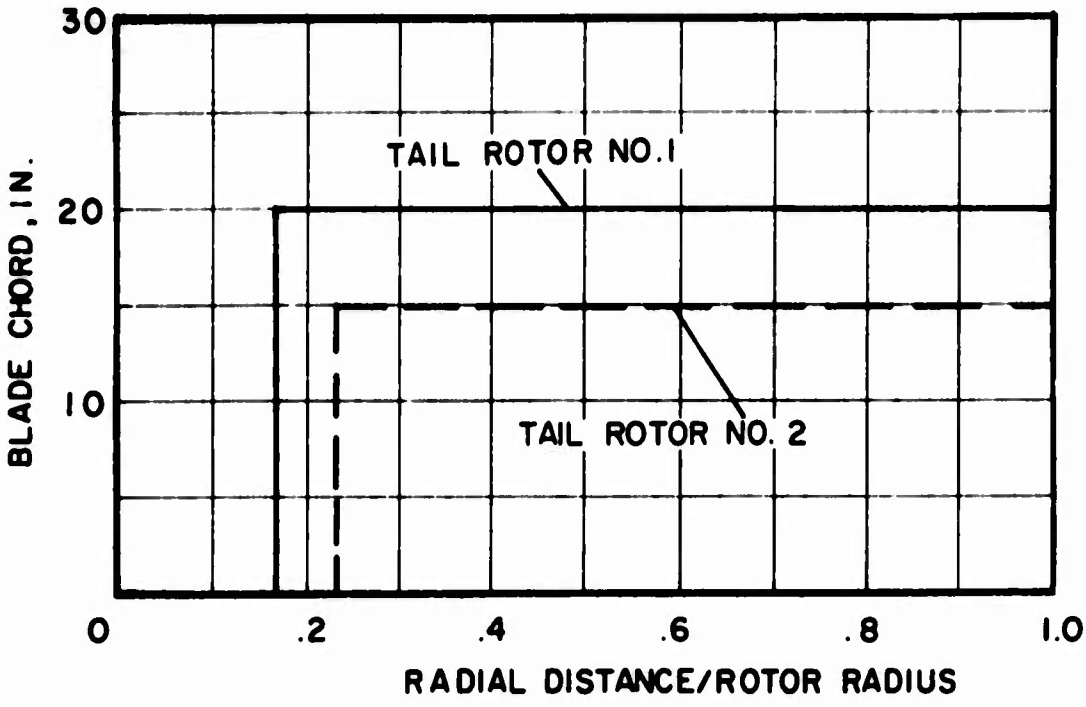

Figure 1. Tail Rotor Blade Chord Distribution.

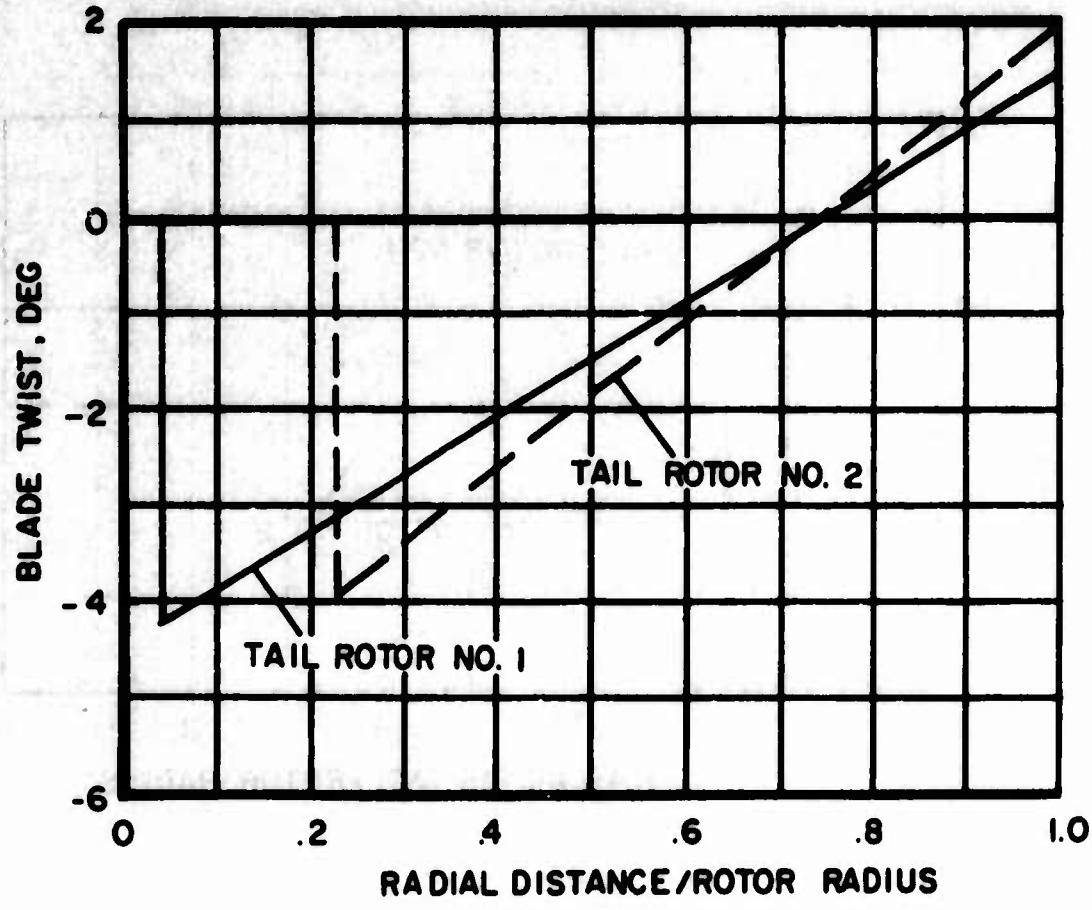

Figure 2. Tail Rotor Blade Twist Distribution.

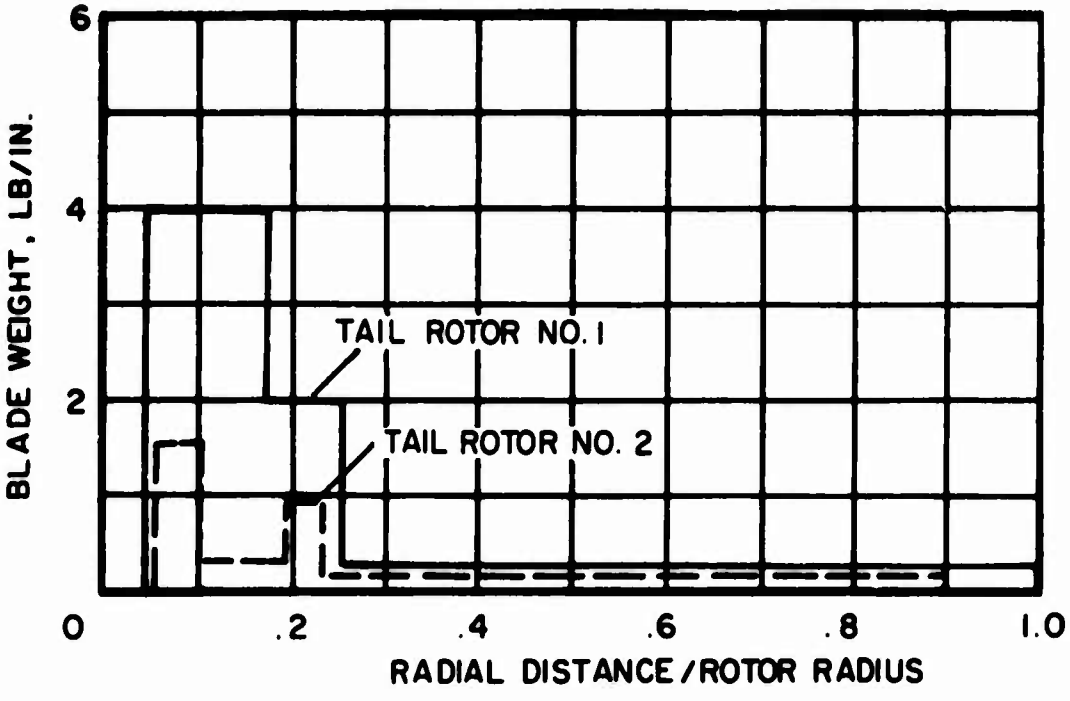

Figure 3. Tail Rotor Blade Weight Distribution.

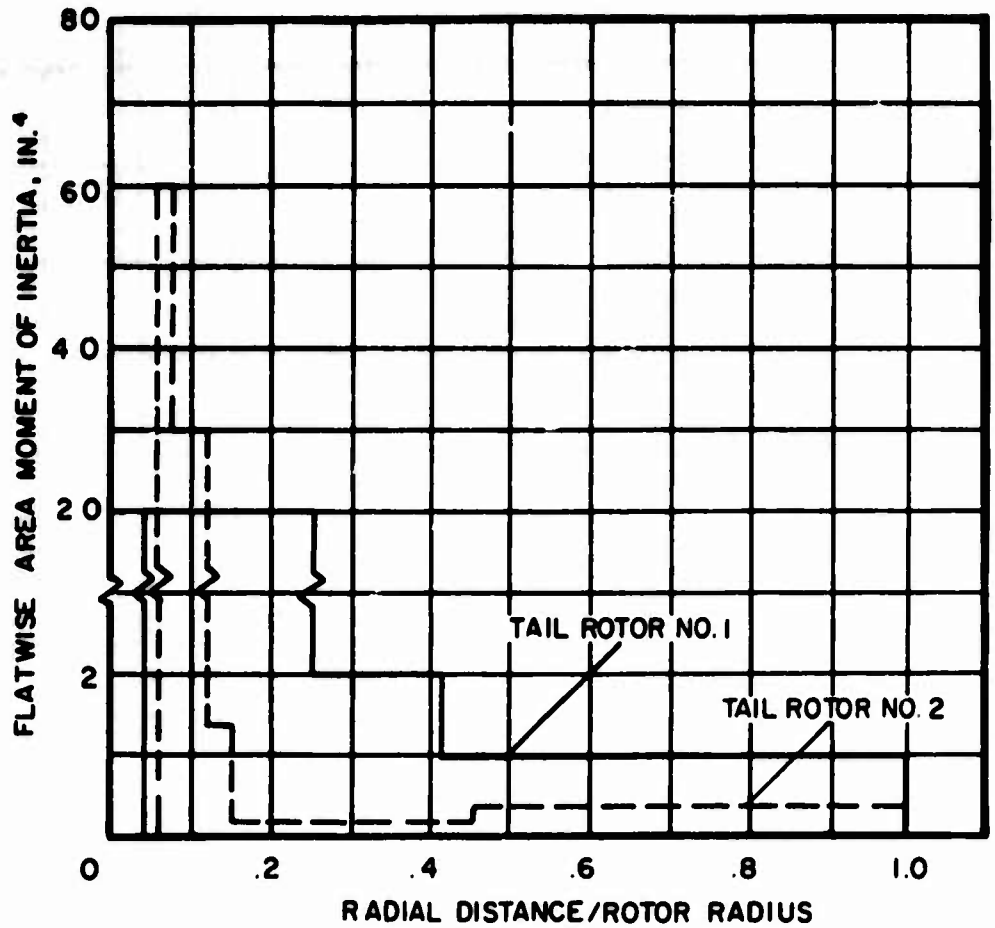

Figure 4. Tail Rotor Blade Flatwise Area Moment of Inertia Distribution.

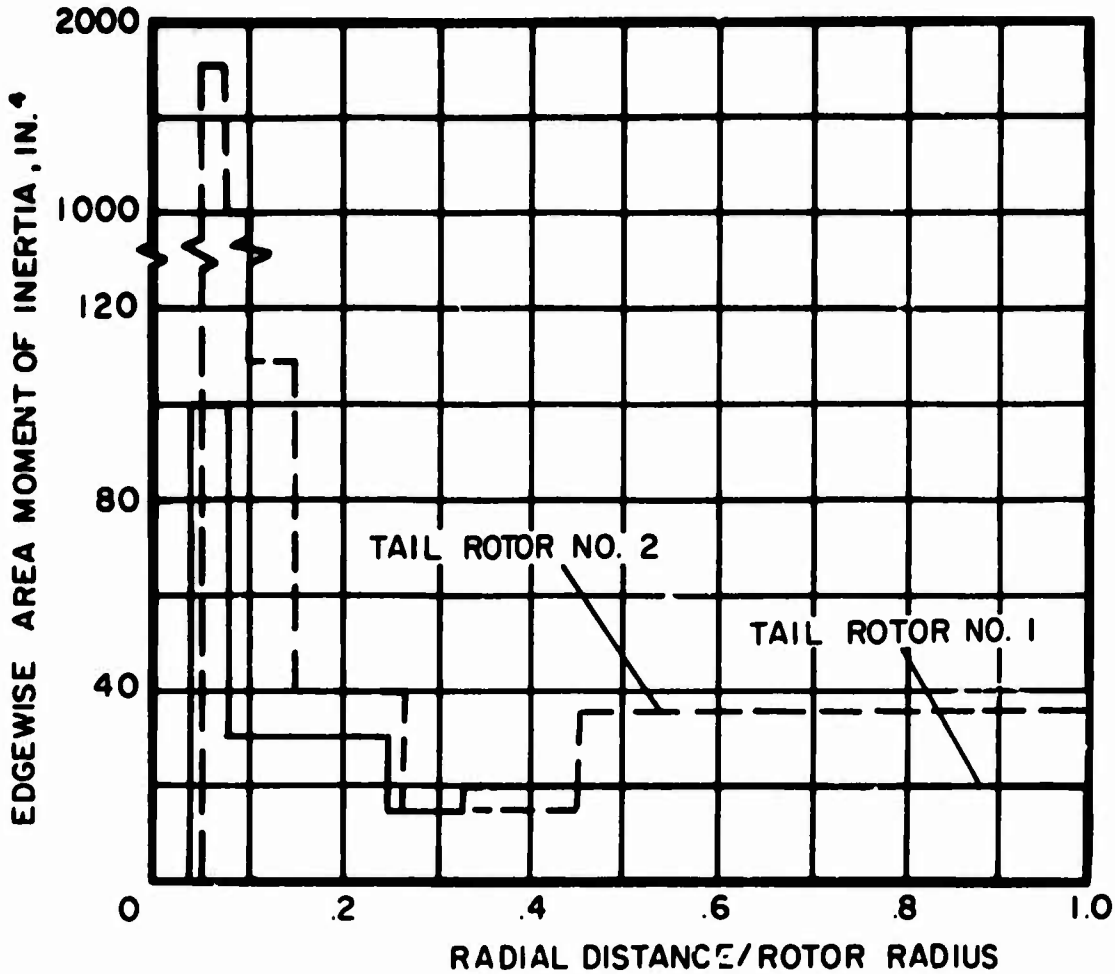

Figure 5. Tail Rotor Blade Edgewise Area Moment of Inertia Distribution.

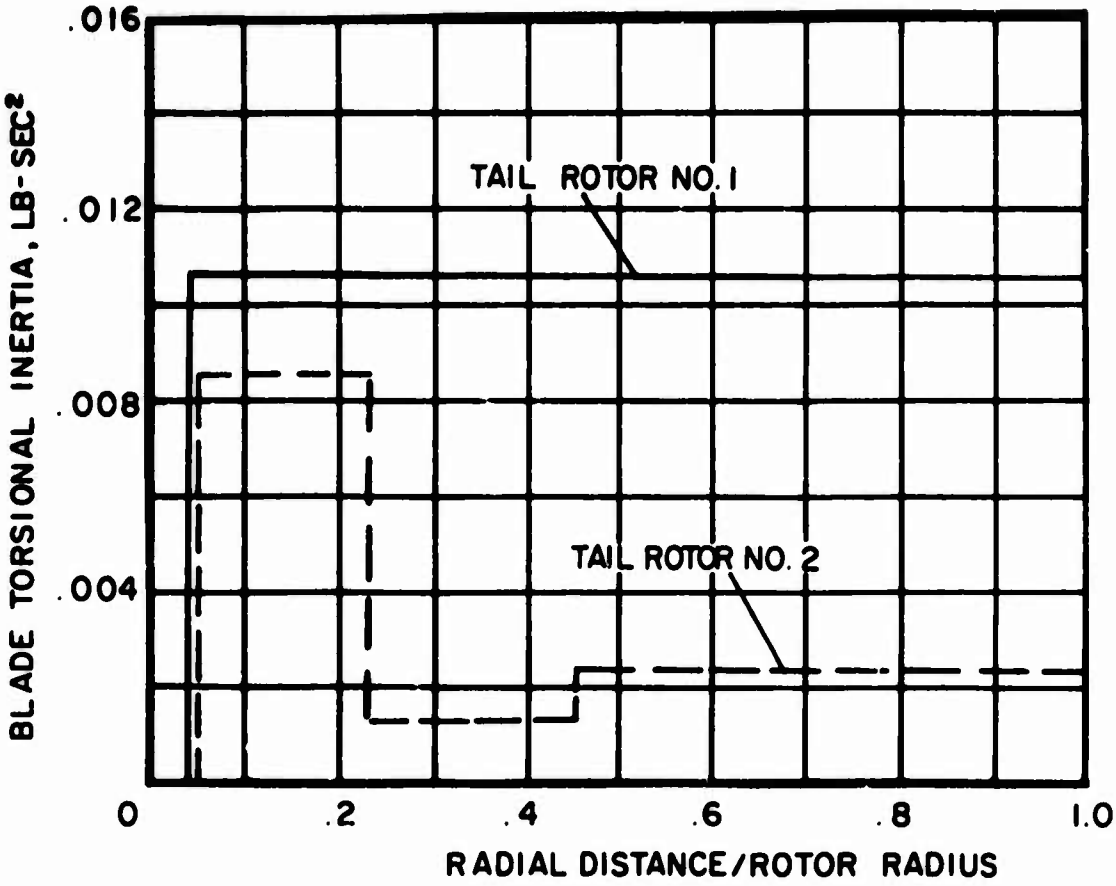

Figure 6. Tail Rotor Blade Torsional Inertia Distribution.

AEROELASTIC STABILITY CHARACTERISTICS IN HOVER AND FORWARD FLIGHT

The aeroelastic stability characteristics of the two baseline tail rotors were developed for advance ratios of 0, 0.25, and 0.50. The blade collective pitch at the 75 percent radial location was varied from -30 to 30 degrees for the hover condition, while the forward flight range was from -20 to 20 degrees. The modal damping and frequency are presented in Figures 7 through 13 for tail rotor No. 1 and in Figures 14 through 20 for tail rotor No. 2. For each rotor, the stability characteristics of the following modes are shown as a function of blade collective pitch:

1. blade flatwise symmetric mode
2. blade flatwise forward whirl mode
3. blade flatwise backward whirl mode
4. blade edgewise symmetric mode
5. blade edgewise forward whirl mode
6. blade edgewise backward whirl mode
7. blade torsional symmetric mode
8. blade torsional forward whirl mode
9. blade torsional backward whirl mode
10. rotor hub pitch mode
11. rotor hub yaw mode

It should be noted that the modal damping given for the blade whirl modes in this report use a blade frequency referred to a rotating-axis system. Thus, the fixed-axis forward whirl blade frequency is decreased by the rotor speed, while the backward whirl frequency is increased by the rotor speed. In most cases, when the blade flatwise and edgewise whirl frequencies are transferred to a rotating-axis system, they agree quite well with the values for the symmetric modes.

The hover stability response of the blade flatwise symmetric and whirl modes is similar for both rotors, as seen in Figures 7 (a) and 14 (a). These show that the rotor system stability characteristics are essentially symmetrical about the zero blade collective pitch line. This result is substantiated further by an inspection of Figures 7 (b) and 14 (b) for the blade edgewise modal damping. It is also noted that the edgewise response of baseline tail rotor No. 2 is much more sensitive to changes in collective pitch than tail rotor No. 1. Both rotors show reductions in stability at zero collective pitch and at high values of blade pitch. Figures 7 (c) and 14 (c) illustrate that the stability of the blade torsional modes is not significantly affected by a large change in blade collective pitch.

The stability characteristics of the rotor hub pitch and yaw modes in hover appear in Figures 7 (d) and 14 (d) for tail rotors No. 1 and No. 2 respectively. As seen from Table 2, the first hub mode represents a rigid-body rotation about the airframe yaw axis which results in a longitudinal

displacement at the rotor head. Similarly, the second hub mode is rigid-body rotation about the pitch axis which yields a vertical displacement at the rotor head. The damping of the hub modes increases with collective pitch up to 10 degrees. As blade pitch is increased further, a reduction in stability is evident.

The modal frequency response with rotor blade collective pitch in hover is presented in Figure 8 for tail rotor No. 1 and in Figure 15 for tail rotor No. 2. The two rotors exhibit similar behavior, although rotor No. 1 shows larger variations in modal frequency with blade pitch. It is seen that increasing or decreasing blade pitch from zero results in reduction in the flatwise and edgewise modal frequencies. The torsional whirl mode of tail rotor No. 1 at first increases with blade pitch up to -20 degrees and then decreases. The blade torsional symmetric frequency for both rotors is not plotted in Figures 8 and 15, being much higher than all others: 5.48 cycles/rev for rotor No. 1 and 13.85 cycles/rev for rotor No. 2. It is unaffected by pitch changes since it is mostly a function of physical parameters not associated with blade pitch or thrust. The frequencies of the rotor hub pitch and yaw modes do not vary with blade pitch. It is noted that the edgewise frequency for both rotors is above one cycle/rev; such rotors are classified as stiff-inplane rotors.

The aeroelastic stability characteristics of the two baseline tail rotors in forward flight are illustrated in Figures 9 through 12 for rotor No. 1 and in Figures 16 through 19 for rotor No. 2. Advance ratios of .25 and .50 were investigated. These advance ratios correspond to forward velocities of 109 and 217 knots for rotor No. 1 and 104 and 207 knots for rotor No. 2. Only the modal damping of the blade flatwise and edgewise modes is presented since the blade torsional and rotor hub modal response is not affected significantly by advance ratio. To facilitate comparisons of stability trends with advance ratio, the modal damping of the blade flatwise symmetric mode and of the edgewise forward whirl mode is plotted in Figures 13 and 20 for rotor No. 1 and 2 respectively. These plots indicate generally a reduction in system stability of both modes with advance ratio. This effect is greatest near blade pitches of -10 degrees. The region of highest stability of the blade flatwise symmetric mode is near a pitch angle of zero degrees. The damping decreases as advance ratio increases for both tail rotors. A similar behavior is exhibited by the flatwise backward and forward whirl modes.

A comparison of the modal frequency response illustrated in Figures 8, 10, and 12 for rotor No. 1 and in Figures 15, 17 and 19 for rotor No. 2 reveals that the effect of advance ratio on frequency is small for all modes except the blade torsional whirl mode, which shows a slight decrease in frequency with advance ratio.

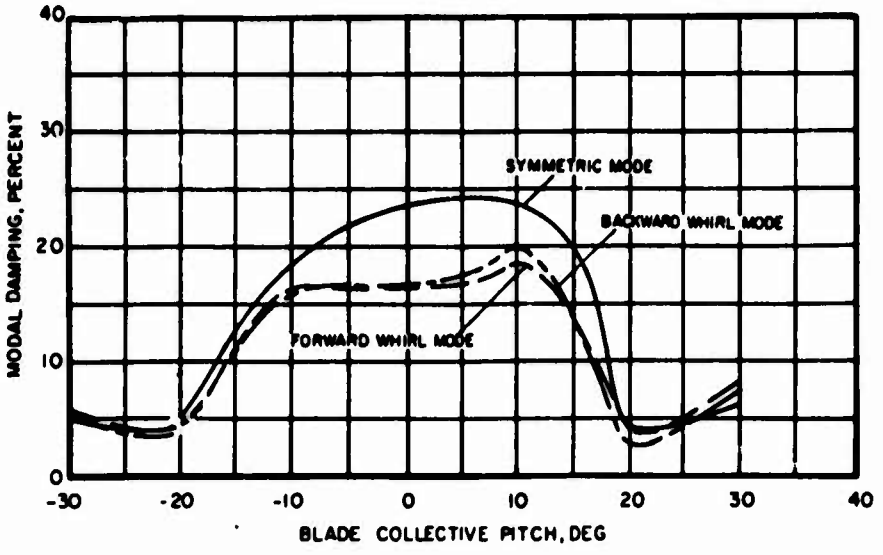

(a) Blade Flatwise Mode

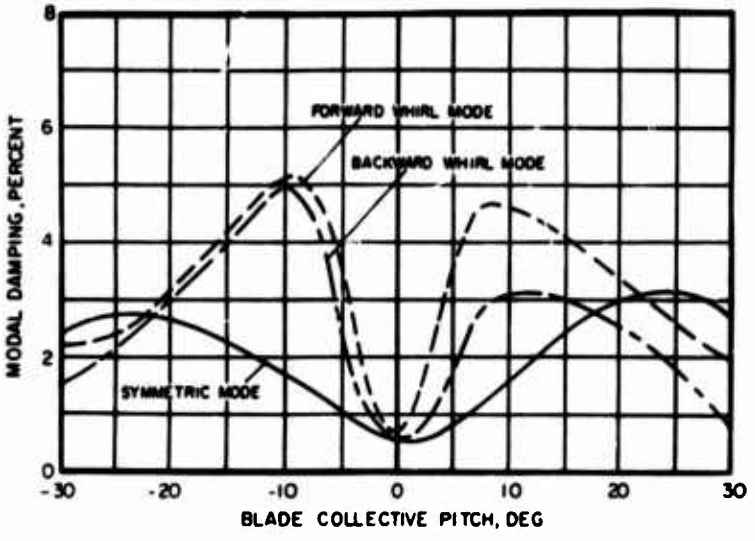

(b) Blade Edgewise Mode

Figure 7. Modal Damping Response With Blade Collective Pitch for Tail Rotor No. 1 in Hover.

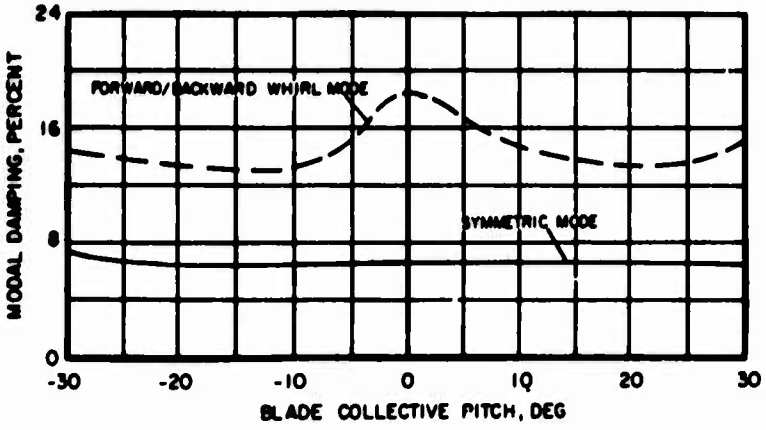

(c) Blade Torsional Mode

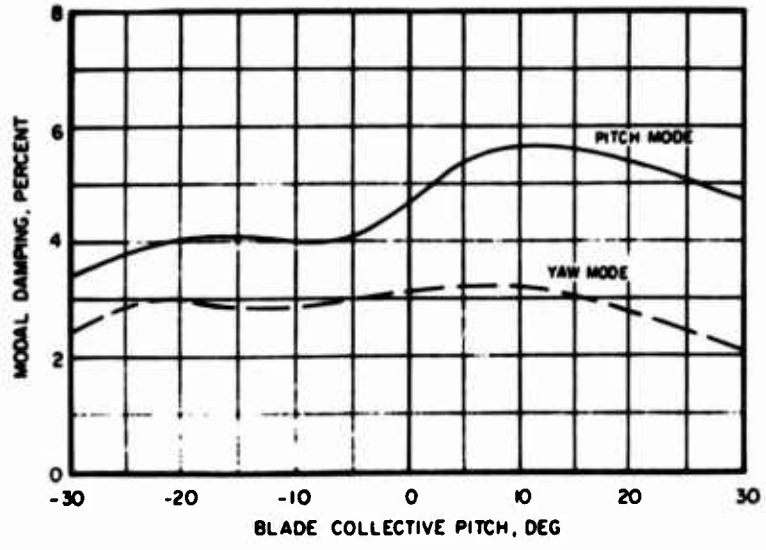

(d) Rotor Hub Modes

Figure 7. Concluded.

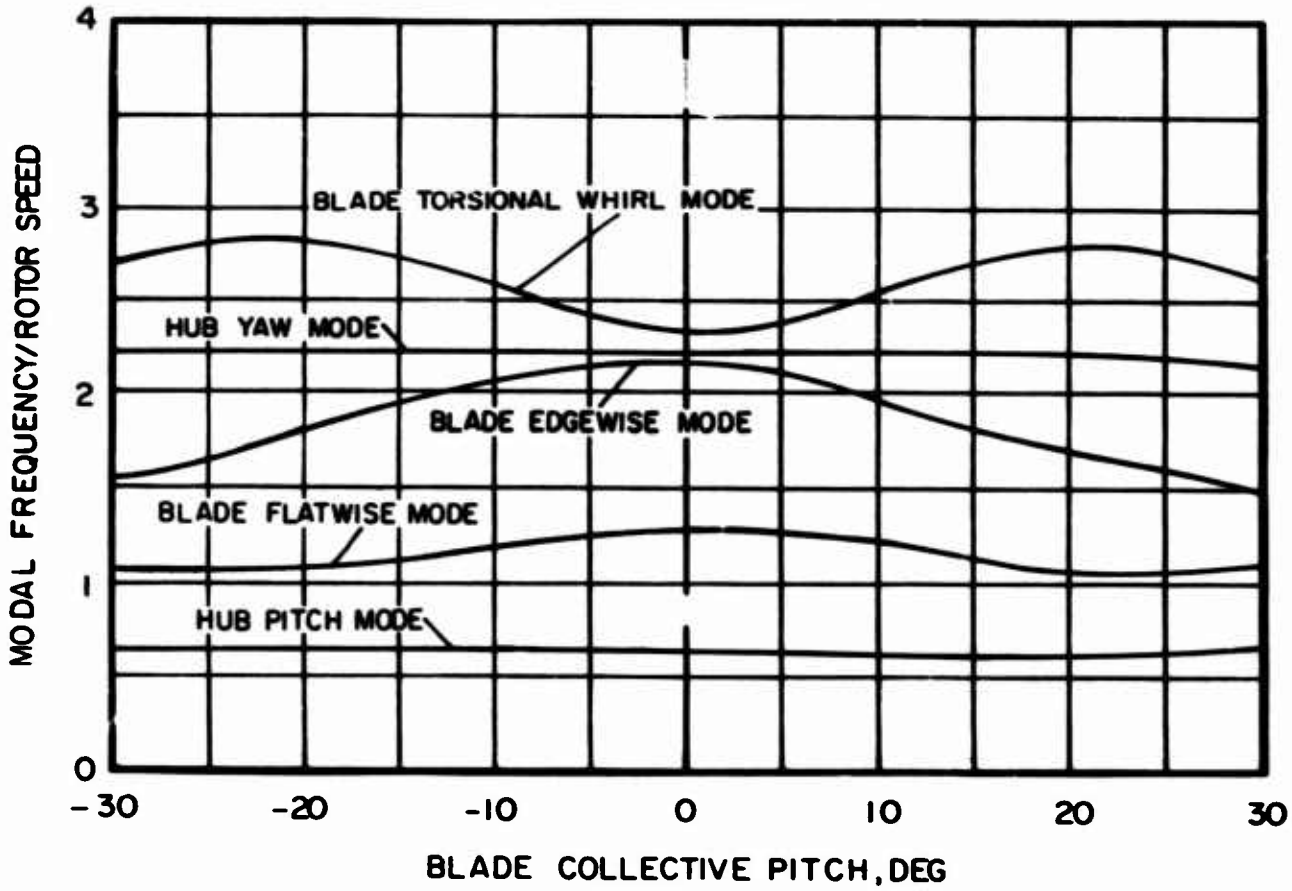

Figure 8. Modal Frequency Response With Blade Collective Pitch for Tail Rotor No. 1 in Hover.

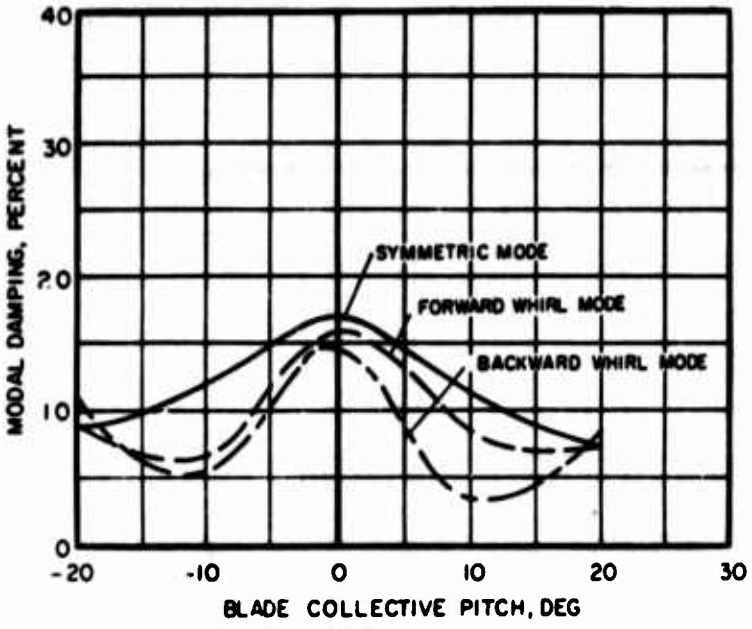

(a) Blade Flatwise Mode

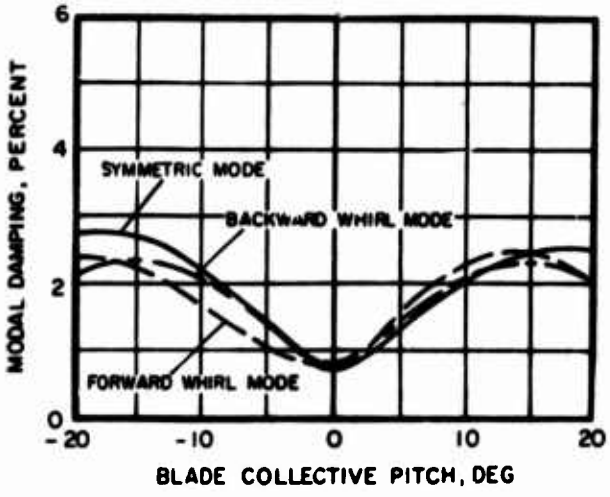

(b) Blade Edgewise Mode

Figure 9. Modal Damping Response With Blade Collective Pitch for Tail Rotor No. 1 at $\mu = .25$.

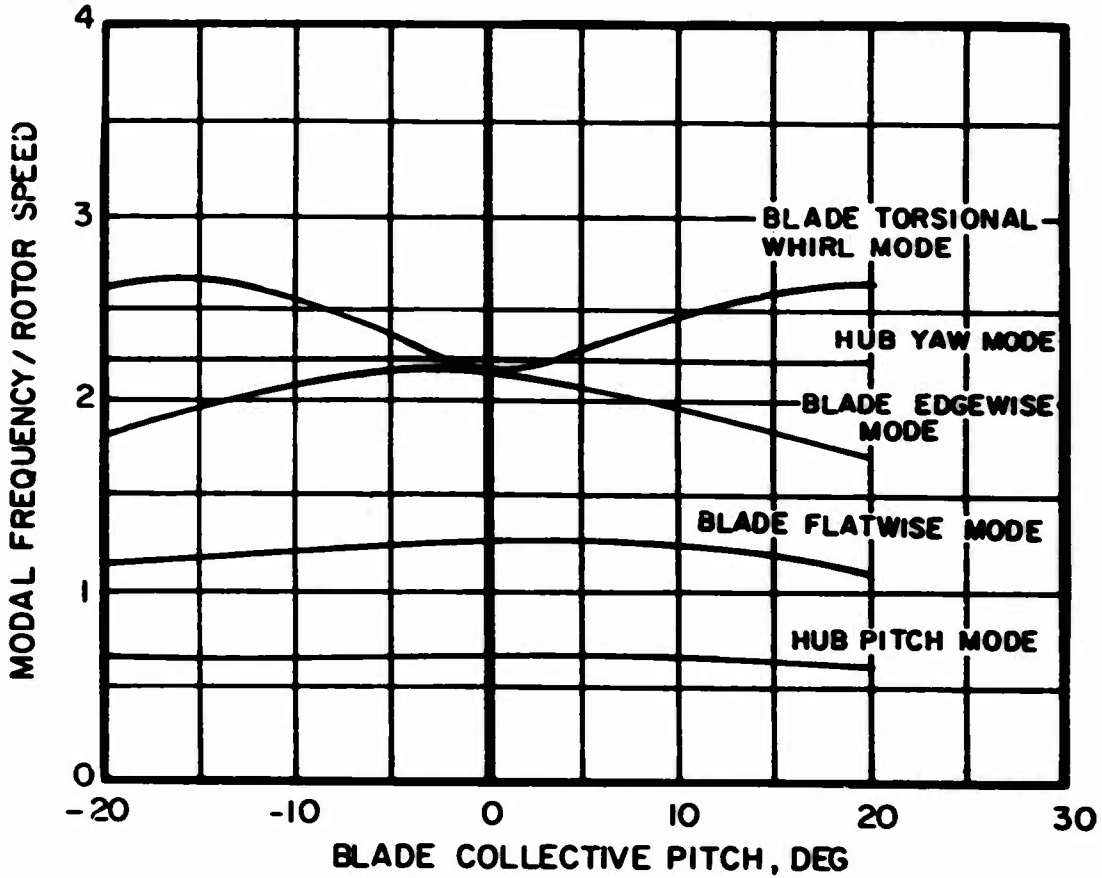

Figure 10. Modal Frequency Response With Blade Collective Pitch for Tail Rotor No. 1 at $\mu = .25$.

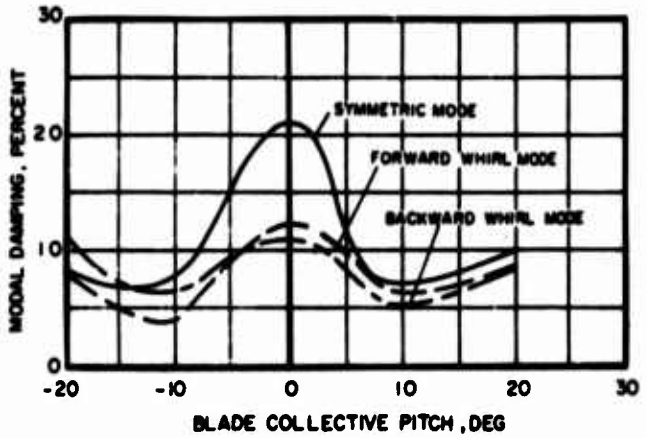

(a) Blade Flatwise Mode

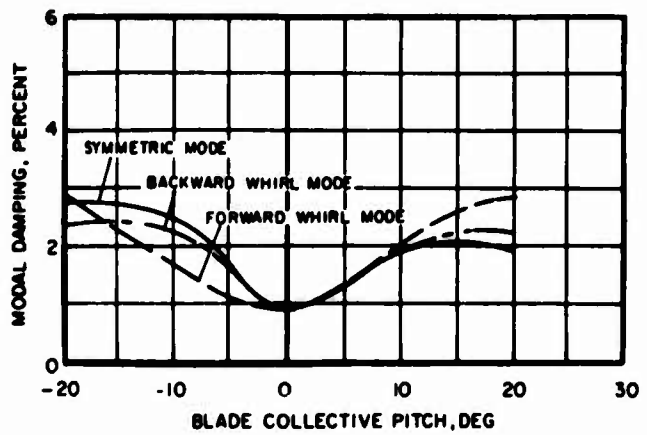

(b) Blade Edgewise Mode

Figure 11. Modal Damping Response With Blade Collective Pitch for Tail Rotor No. 1 at μ = .50.

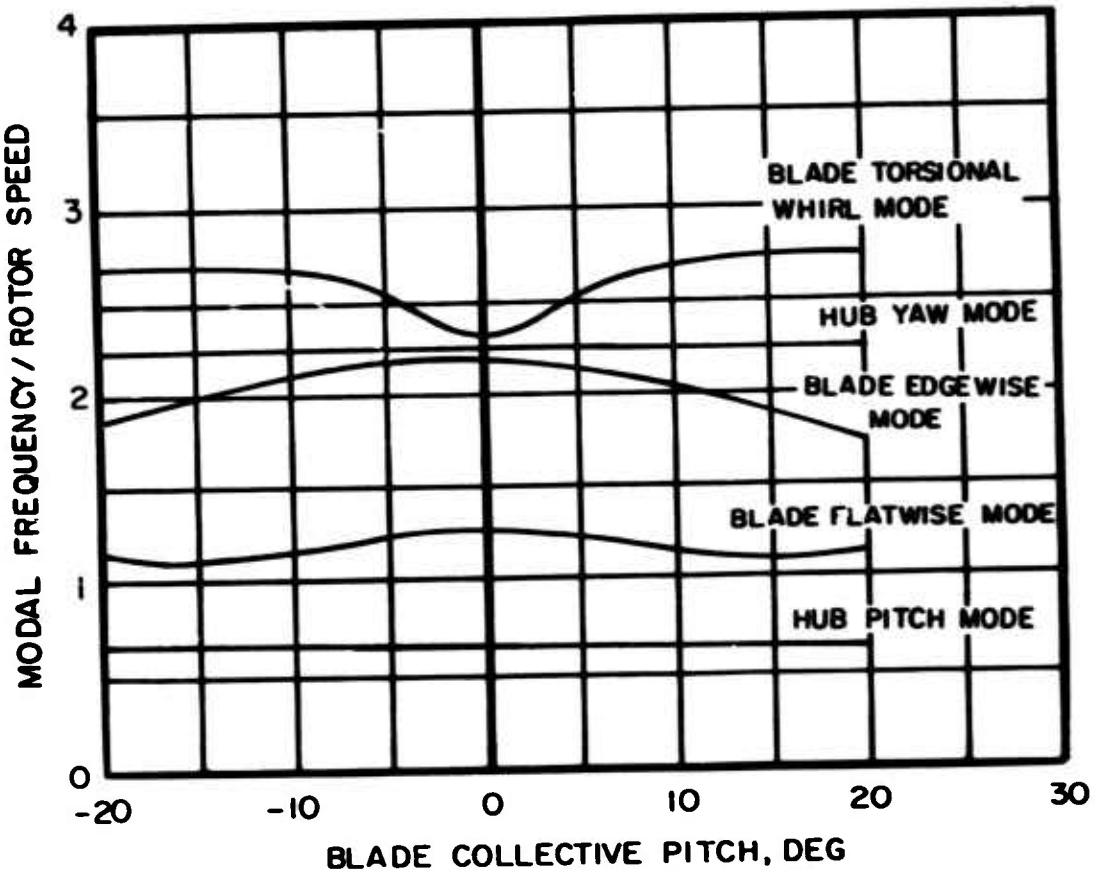

Figure 12. Modal Frequency Response With Blade Collective Pitch for Tail Rotor No. 1 at $\mu = .50$.

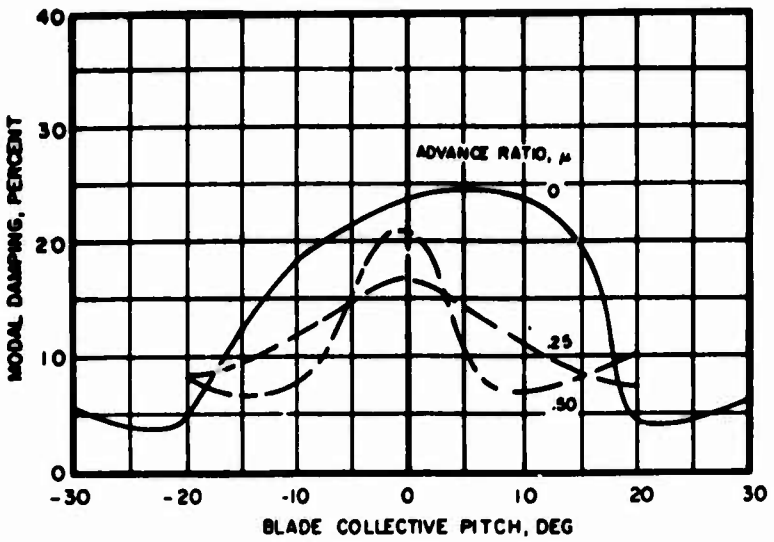

(a) Blade Flatwise Symmetric Mode

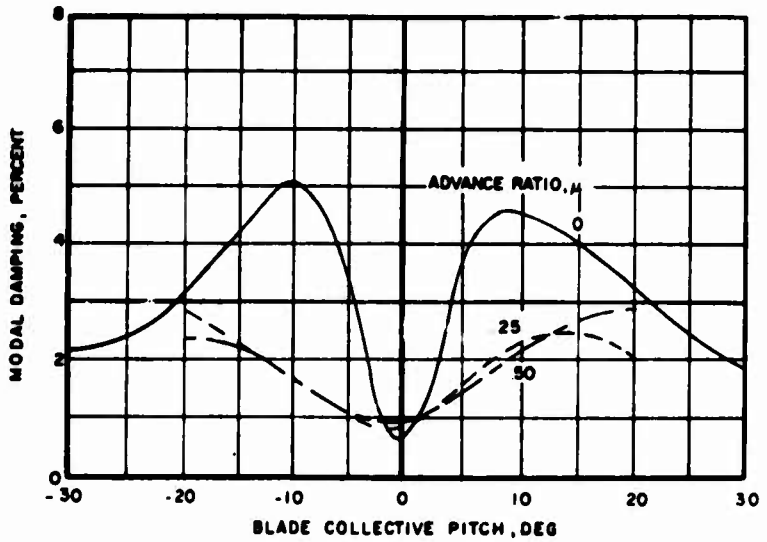

(b) Blade Edgewise Forward Whirl Mode

Figure 13. Effect of Advance Ratio on Modal Damping for Tail Rotor No. 1.

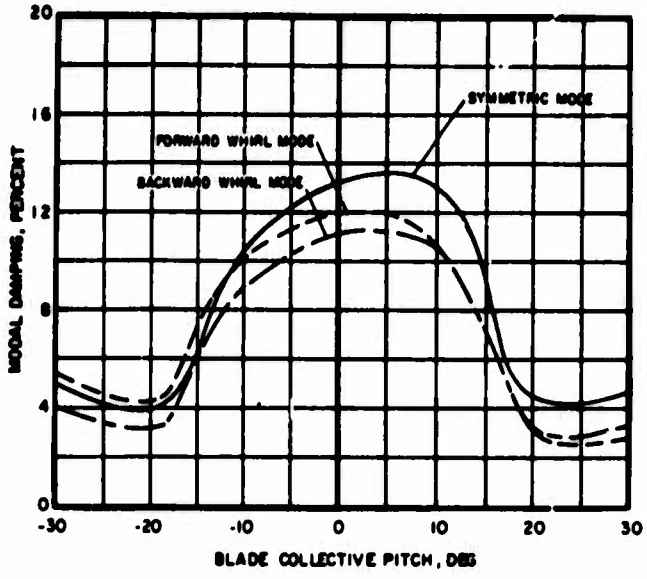

(a) Blade Flatwise Mode

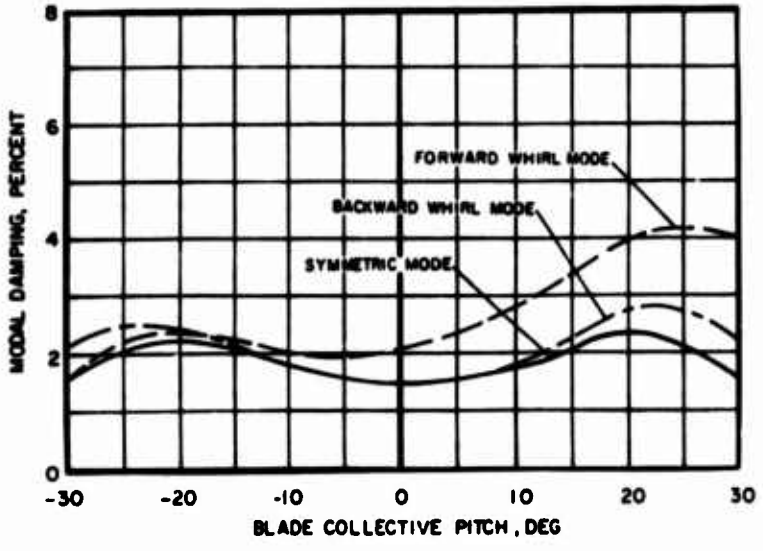

(b) Blade Edgewise Mode

Figure 14. Modal Damping Response With Blade Collective Pitch for Tail Rotor No. 2 in Hover.

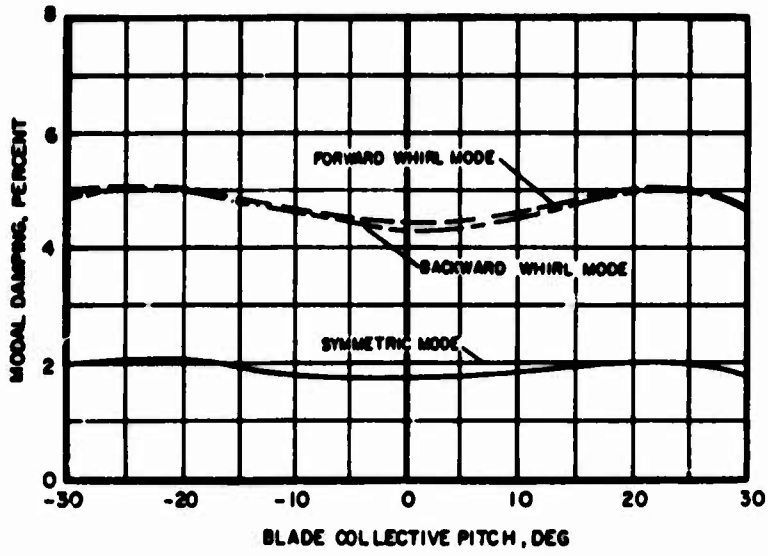

(c) Blade Torsional Mode

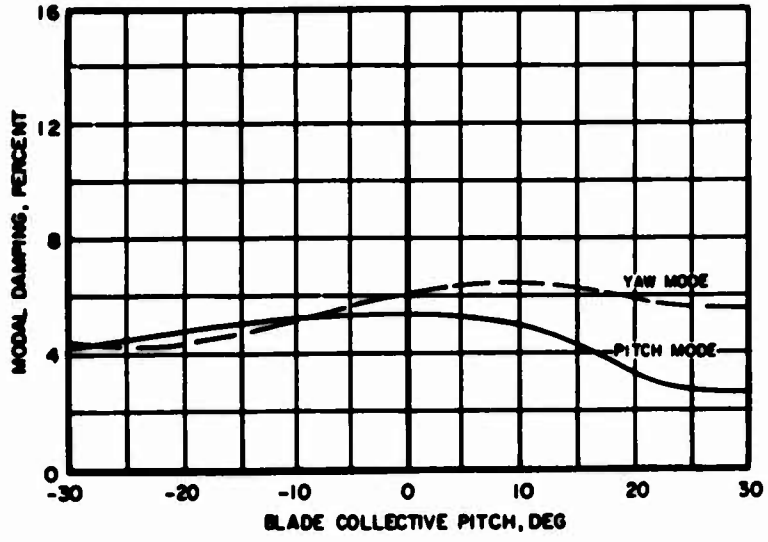

(d) Rotor Hub Modes

Figure 14. Concluded.

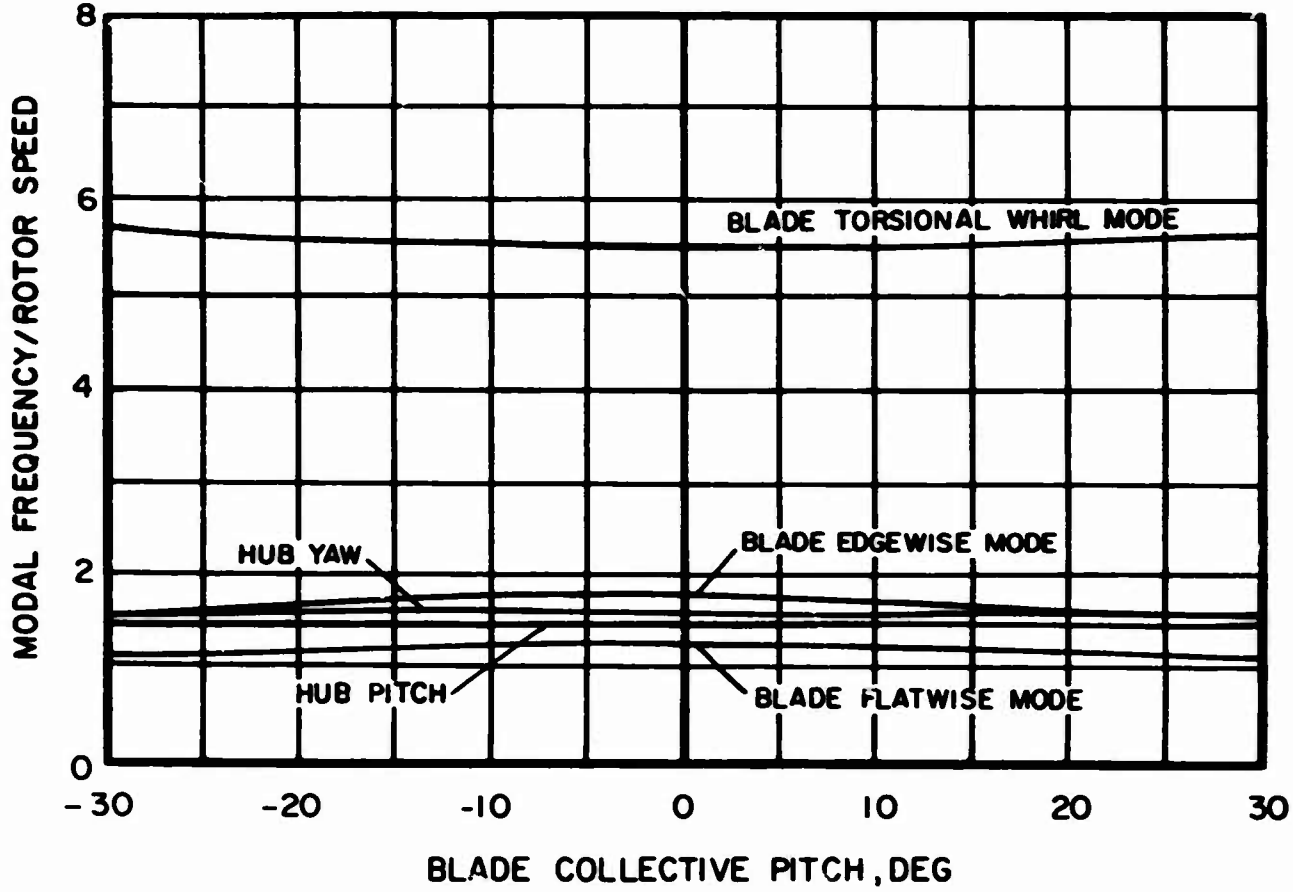

Figure 15. Modal Frequency Response With Blade Collective Pitch for Tail Rotor No. 2 in Hover.

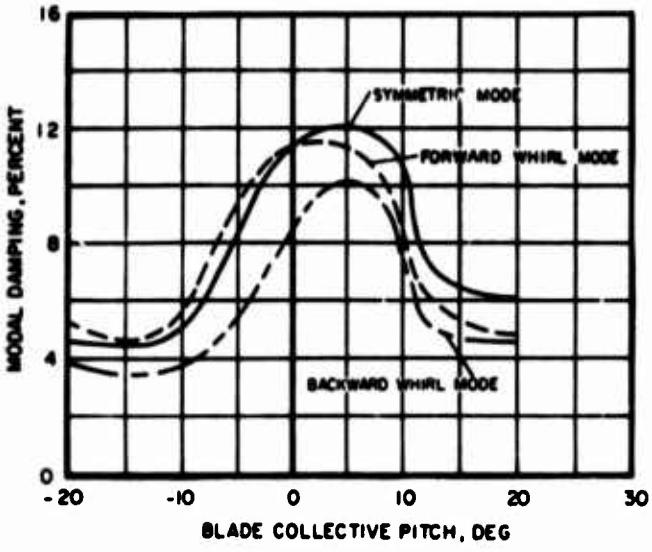

(a) Blade Flatwise Mode

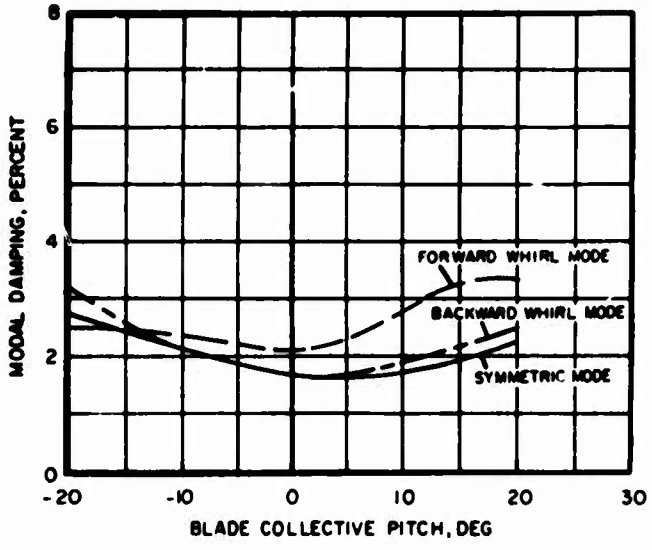

(b) Blade Edgewise Mode

Figure 16. Modal Damping Response With Blade Collective Pitch for Tail Rotor No. 2 at $\mu = .25$.

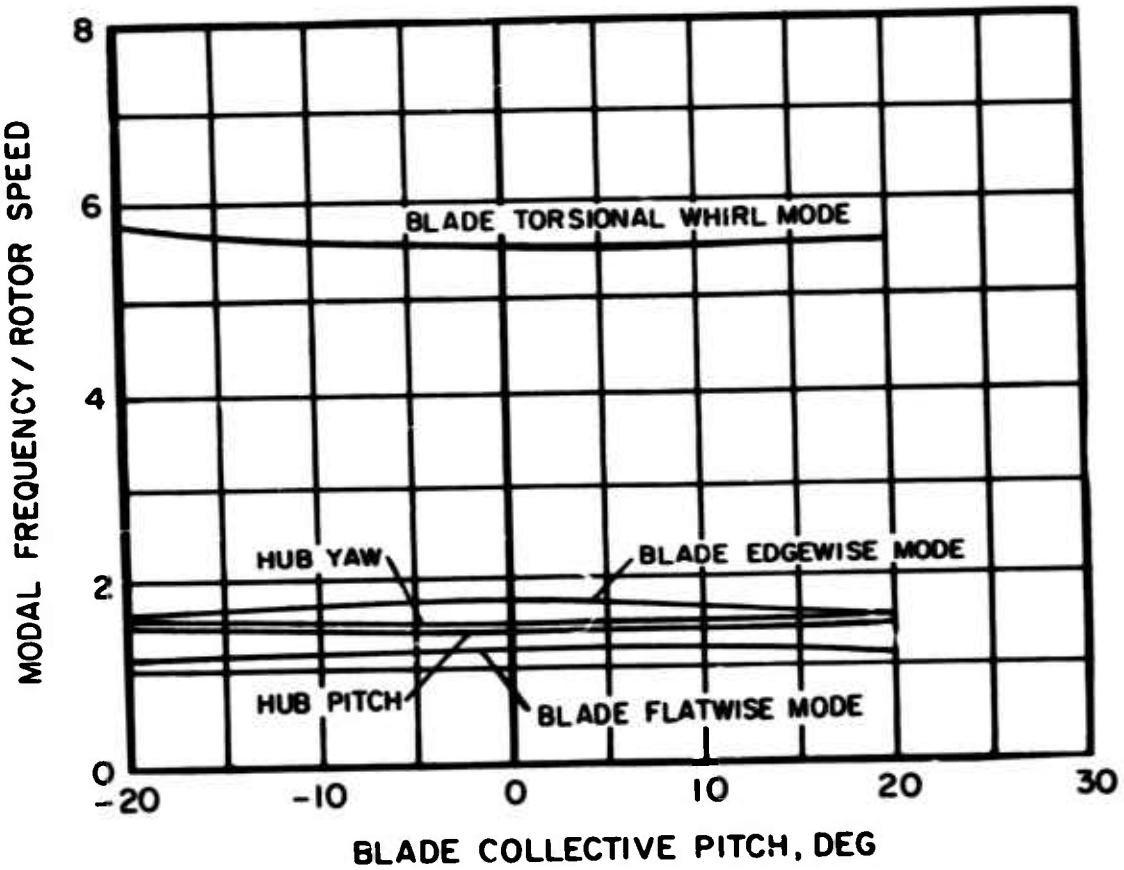

Figure 17. Modal Frequency Response With Blade Collective Pitch for Tail Rotor No. 2 at $\mu = .25$.

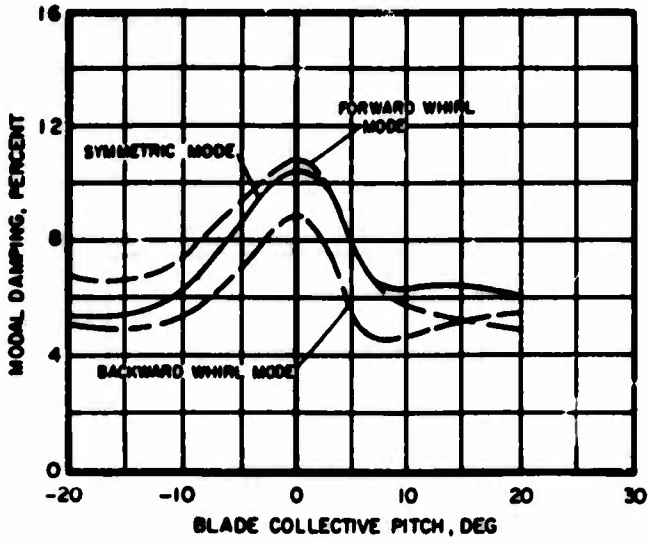

(a) Blade Flatwise Mode

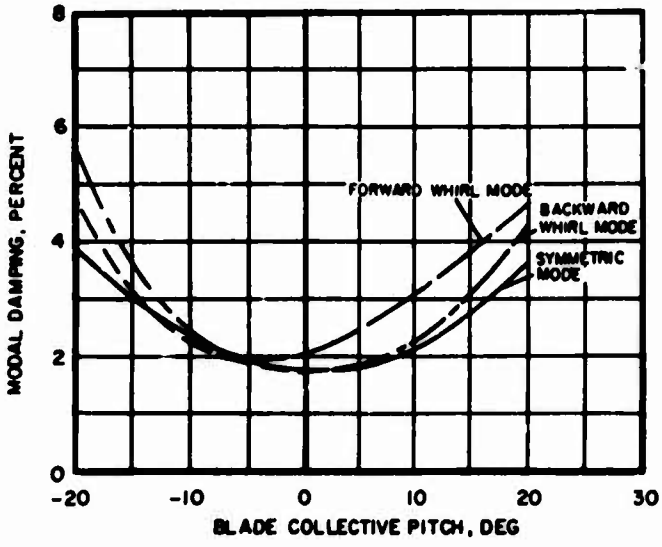

(b) Blade Edgewise Mode

Figure 18. Modal Damping Response With Blade Collective Pitch for Tail Rotor No. 2 at $\mu = .50$.

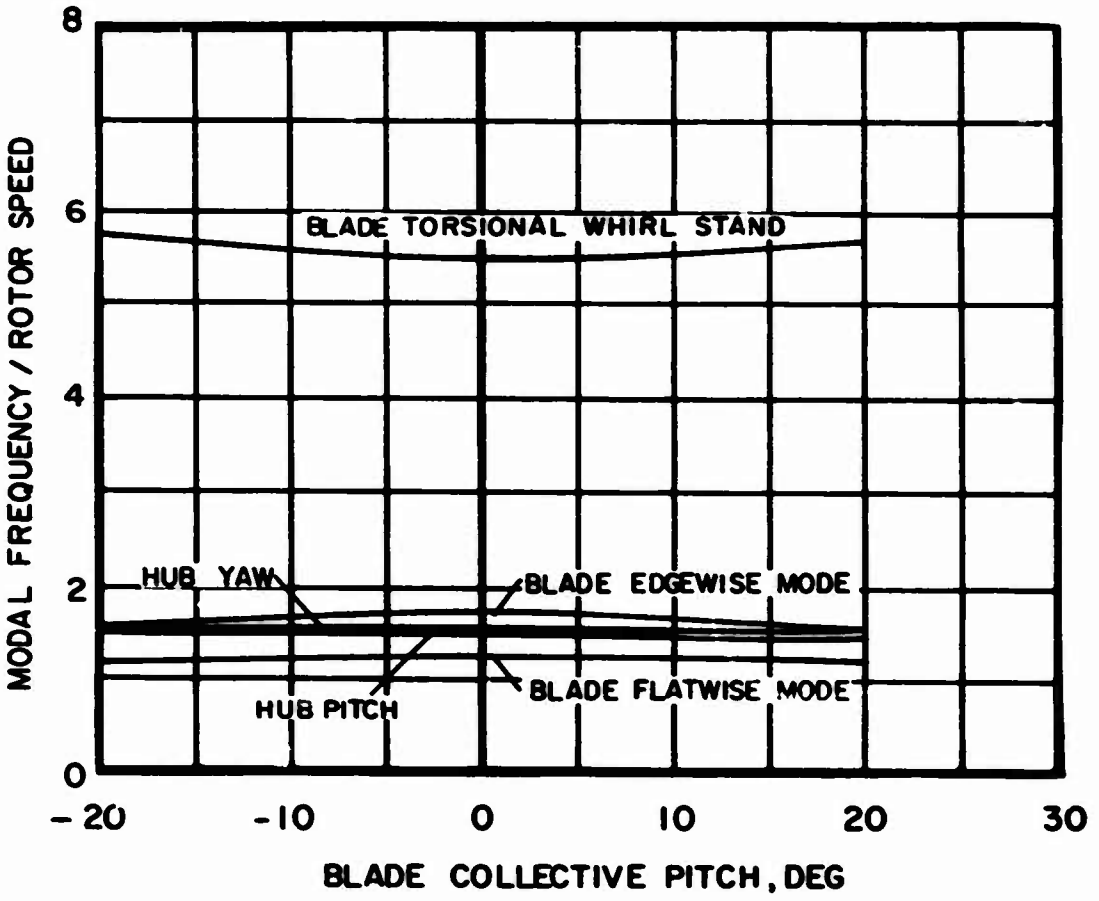

Figure 19. Modal Frequency Response With Blade Collective Pitch for Tail Rotor No. 2 at $\mu = .50$.

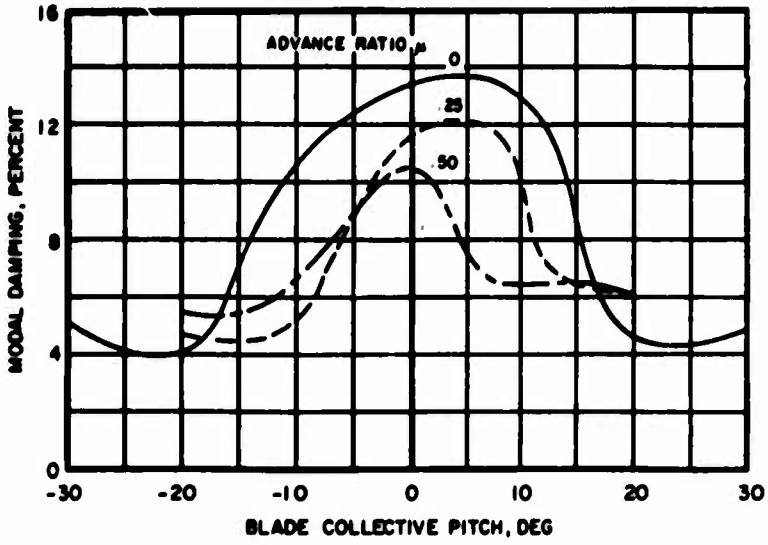

(a) Blade Flatwise Symmetric Mode

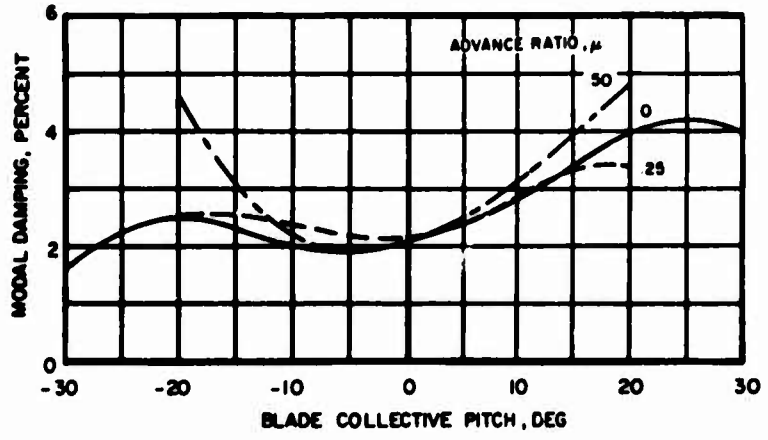

(b) Blade Edgewise Forward Whirl Mode

Figure 20. Effect of Advance Ratio on Modal Damping for Tail Rotor No. 2.

PARAMETRIC INVESTIGATION OF STABILITY CHARACTERISTICS

The effects of independent variations of several design parameters on the stability characteristics of the two baseline tail rotors were investigated in hover and at an advance ratio of .50. The blade collective pitch was 8 degrees throughout the study. The following parameters were examined:

1. control system asymmetric stiffness, K_3
2. control system symmetric stiffness, K_1
3. blade torsional natural frequency, ω_{T_1}, ω_{T_2}
4. pitch-flap coupling, δ_3
5. blade edgewise natural frequency, ω_{EN}
6. rotor hub frequencies (pitch and yaw), ω_P, ω_Y
7. blade precone angle, β_o
8. pitch-lag coupling, α_1

The results of the parametric study are presented in a nondimensional form to enhance their general applicability. All system frequencies are nondimensionalized by the rotor speed.

The variations in control system asymmetric stiffness are illustrated in terms of an equivalent blade torsional frequency defined by

$$\omega_{T_1}^2 = L_2^2 K_3 / I_\theta \qquad (1)$$

where

L_2 = chordwise distance from elastic axis to the pushrod, positive toward leading edge, in.

I_θ = blade torsional mass moment of inertia, in-lb-sec^2

K_3 = control system asymmetric stiffness, lb/in.

The control system asymmetric stiffness is defined by

$$K_3 = 2K_2K_1/(2K_2 + NK_1L_1) \qquad (2)$$

where

K_2 = stiffness of actuator shaft for pure moment applied at pitch beam end, in-lb/rad

K_1 = control system symmetric stiffness (or pitch beam arm stiffness), lb/in.

N = number of rotor blades

L_1 = pitch beam arm length, in.

The variable in Equation 2 is the actuator shaft moment stiffness K_2. The baseline values for ω_{T_1}/Ω are 2.32 cycles/rev for tail rotor No. 1 and 5.42 cycles/rev for tail rotor No. 2.

The parametric trends obtained for the control system symmetric stiffness are also expressed in terms of an equivalent blade torsional frequency, which is defined by

$$\omega_{T_2}^2 = L_2^2 K_1 / I_\theta \tag{3}$$

Here the variable is the pitch beam arm stiffness K_1. The baseline values of ω_{T_2}/Ω are 5.48 cycles/rev for tail rotor No. 1 and 13.85 cycles/rev for tail rotor No. 2.

The blade torsional natural frequency is derived from Equation 3 when symmetric mode stability characteristics are presented and from Equation 1 when unsymmetric mode stability characteristics are presented. Thus, a comparison can be made of the parametric trends developed as a function of the blade torsional frequency due to independent variations in stiffness or inertia.

The rotor blade pitch-flap coupling is defined below for tail rotor No. 1, which is articulated in the flatwise direction.

$$\text{TAN } \delta_3 = (L_3 - e)/L_2 \tag{4}$$

where

L_3 = pitch horn radial location, in.

e = blade flapping hinge offset, in.

For the hingeless tail rotor No. 2 an effective pitch-flap coupling can be evaluated from

$$\text{TAN } \delta_3 = {}^{R}/_{L_2}[\phi_{F1} + (\phi_{F1} - \phi_{F2})(r_1 - L_3)/(r_2 - r_1)] \tag{5}$$

where

R = blade radius, in.

r_1 = radial location of inner snubber, in.

r_2 = radial location of outer snubber, in.

ϕ_{F1} = flatwise mode shape at r_1

ϕ_{F2} = flatwise mode shape at r_2

Variations in the blade edgewise natural frequency were made by changing the radial distribution of the blade edgewise area moment of inertia which appears in Figure 5.

The values of the rotor hub pitch and yaw frequencies that are referred to as reference hub frequencies are defined in terms of the generalized stiffness $K_{G,i}$ and mass $M_{G,i}$ of the i^{th} fixed system mode as follows:

$$\omega_i = \sqrt{K_{G,i}/M_{G,i}} \tag{6}$$

Variations in the fixed system reference frequencies were made by changing the generalized stiffness. The reference values were varied simultaneously by similar amounts.

In summary, the variables associated with each of the eight parameters investigated are:

1. actuator shaft moment stiffness, K_2
2. pitch beam stiffness, K_1
3. blade torsional mass moment of inertia, I_θ
4. chordwise distance from elastic axis to pushrod, L_2
5. blade edgewise area moment of inertia, I_{YY}
6. rotor hub frequencies, ω_P and ω_Y
7. blade precone angle, β_o
8. pitch-lag coupling, α_1

The baseline values of all parameters investigated are listed in Table 3 for both tail rotors. All baseline values apply at advance ratios of zero and 0.50.

TABLE 3. TAIL ROTOR BASELINE PARAMETERS FOR PARAMETRIC STUDY

Number	Parameter Symbol	Parameter Value: Tail Rotor No. 1	Parameter Value: Tail Rotor No. 2	Units
1	K_3	2725	4990	lb/in.
2	K_1	15200	32600	lb/in.
3a	ω_{T_1}/Ω	2.32	5.42	cycles/rev
3b	ω_{T_2}/Ω	5.48	13.85	cycles/rev
4	δ_3	45.	40.5	deg
5	ω_{EN}/Ω	2.06	1.74	cycles/rev
6a	ω_P/Ω	0.72	1.78	cycles/rev
6b	ω_Y/Ω	2.50	2.08	cycles/rev
7	β_o	0.0	0.0	deg
8	α_1	0.0	0.0	deg

Effect of Control System Asymmetric Stiffness

The effect of control system asymmetric stiffness on the aeroelastic stability characteristics of the baseline tail rotors is shown in Figures 21 through 26 at advance ratios of zero and 0.50.

Only the blade whirl or unsymmetric modes are presented in these figures, since the symmetric blade mode equations are not affected by changes in the actuator shaft moment stiffness. Control system asymmetric stiffness increases with actuator shaft moment stiffness. This is evident from Equation 2, when expressed in the following form:

$$K_3 = K_1/(1+NK_1L_1^2/2K_2) \qquad (2a)$$

The blade torsional frequency ω_{T_1} is proportional to the control system asymmetric stiffness, as can be seen from Equation 1.

Variations in actuator shaft moment stiffness resulted in a range of blade torsional frequencies of 1.25 to 4.37 cycles/rev for tail rotor No. 1 and from 2.88 to 10.65 cycles/rev for tail rotor No. 2. Four values of stiffness were used to generate the curves. The baseline value of the parameter being investigated is indicated by an arrow along the abscissa of all plots.

From an inspection of Figures 21 and 22, it is observed that as the moment stiffness of the actuator shaft increases, the hover stability of the blade flatwise whirl mode increases, while the modal damping associated with the blade torsional and edgewise whirl modes and the rotor hub pitch and yaw modes decreases for both baseline tail rotors. However, it appears that the effect of variations in actuator shaft moment stiffness on rotor stability is more pronounced for tail rotor No. 1, especially for the blade flatwise whirl mode. This mode becomes unstable as the blade torsional frequency approaches 1.25 cycles/rev.

The trends at an advance ratio of 0.50, shown in Figures 23 and 24, are basically the same as in hover except that for tail rotor No. 1 at the lower blade torsional frequencies a strong interaction seems to exist between the blade edgewise and torsional backward whirl modes. The edgewise mode exhibits a large increase in modal damping, while the torsional response becomes less stable. Also, the hub yaw mode for rotor No. 1 shows a slight increase in stability with stiffness at an advance ratio of 0.50, while it remained largely unaffected in the hover condition.

The effect of control system asymmetric stiffness on hover modal frequency is illustrated in Figures 25 and 26 for tail rotors No. 1 and 2 respectively. It is observed that the modal frequencies of the blade flatwise and edgewise whirl modes, as well as the hub modes, are not affected by large variations in control system asymmetric stiffness. As might be expected, the blade torsional whirl frequency for both rotors has nearly the same value as the equivalent torsional frequency ω_{T_1}, defined by Equation 1.

The parametric trends of modal frequency predicted for all parameters investigated in this study for both baseline rotors were not affected by a change in advance ratio from zero to 0.50. Thus, only the frequency results in hover are shown.

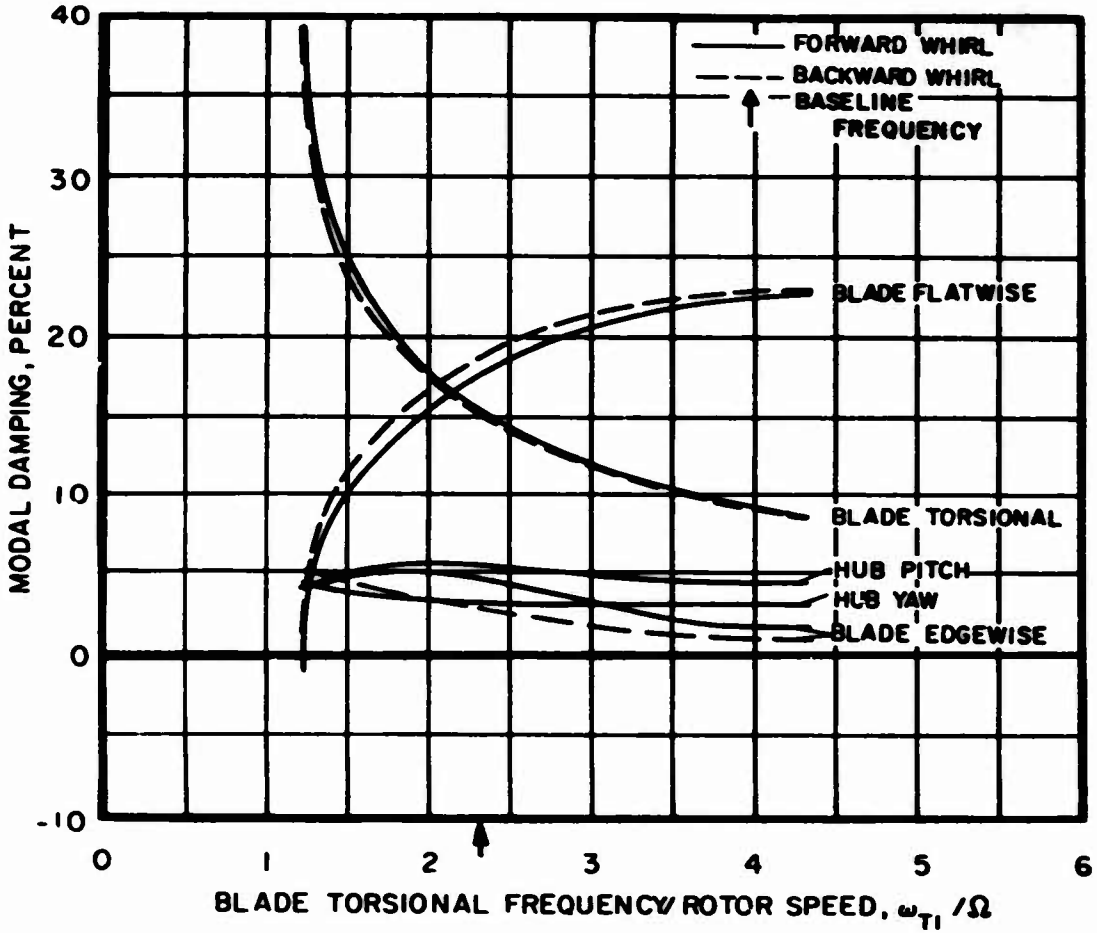

Figure 21. Effect of Blade Torsional Frequency (as a Function of Actuator Shaft Moment Stiffness) on Modal Damping for Tail Rotor No. 1 in Hover.

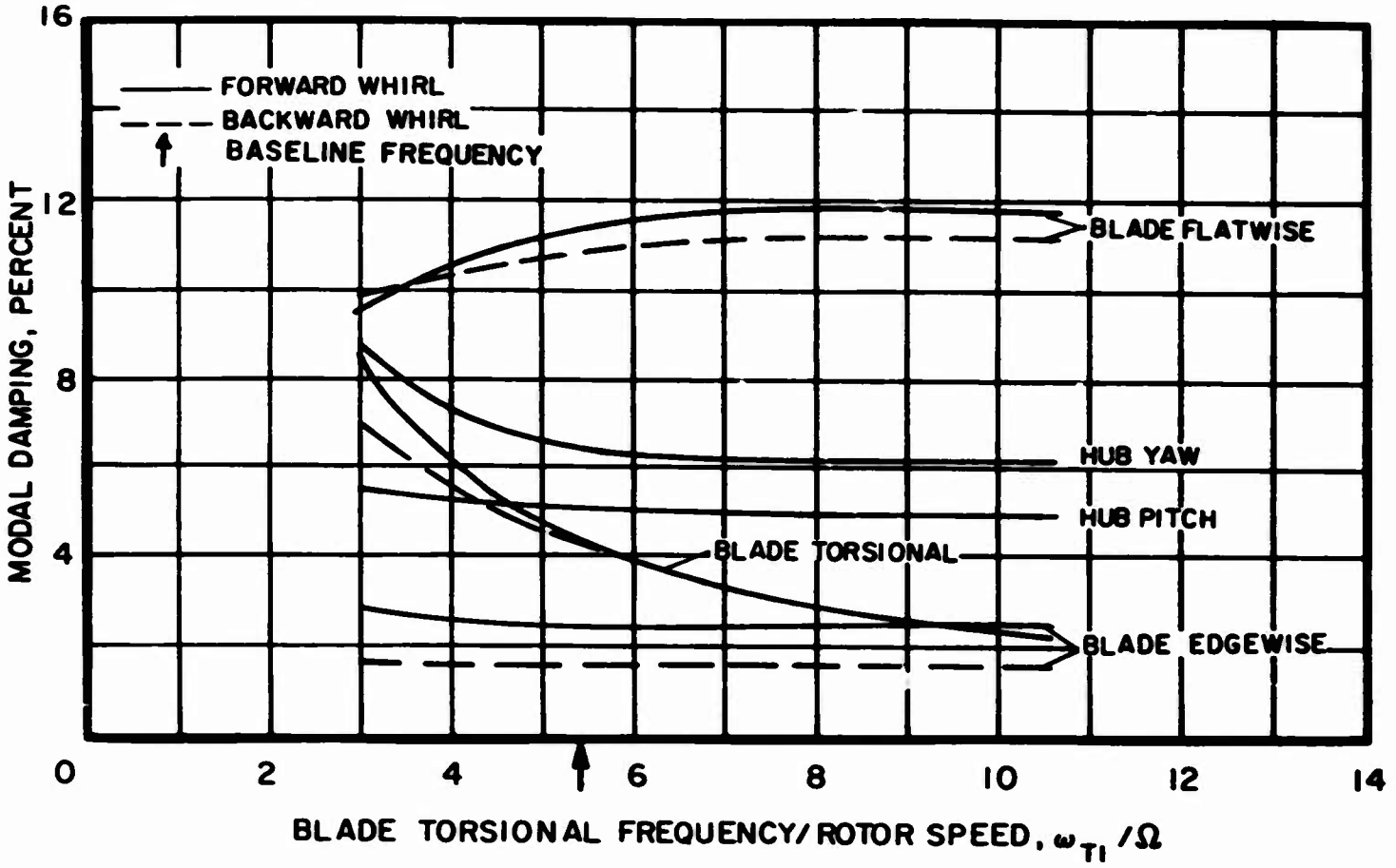

Figure 22. Effect of Blade Torsional Frequency (as a Function of Actuator Shaft Moment Stiffness) on Modal Damping for Tail Rotor No. 2 in Hover.

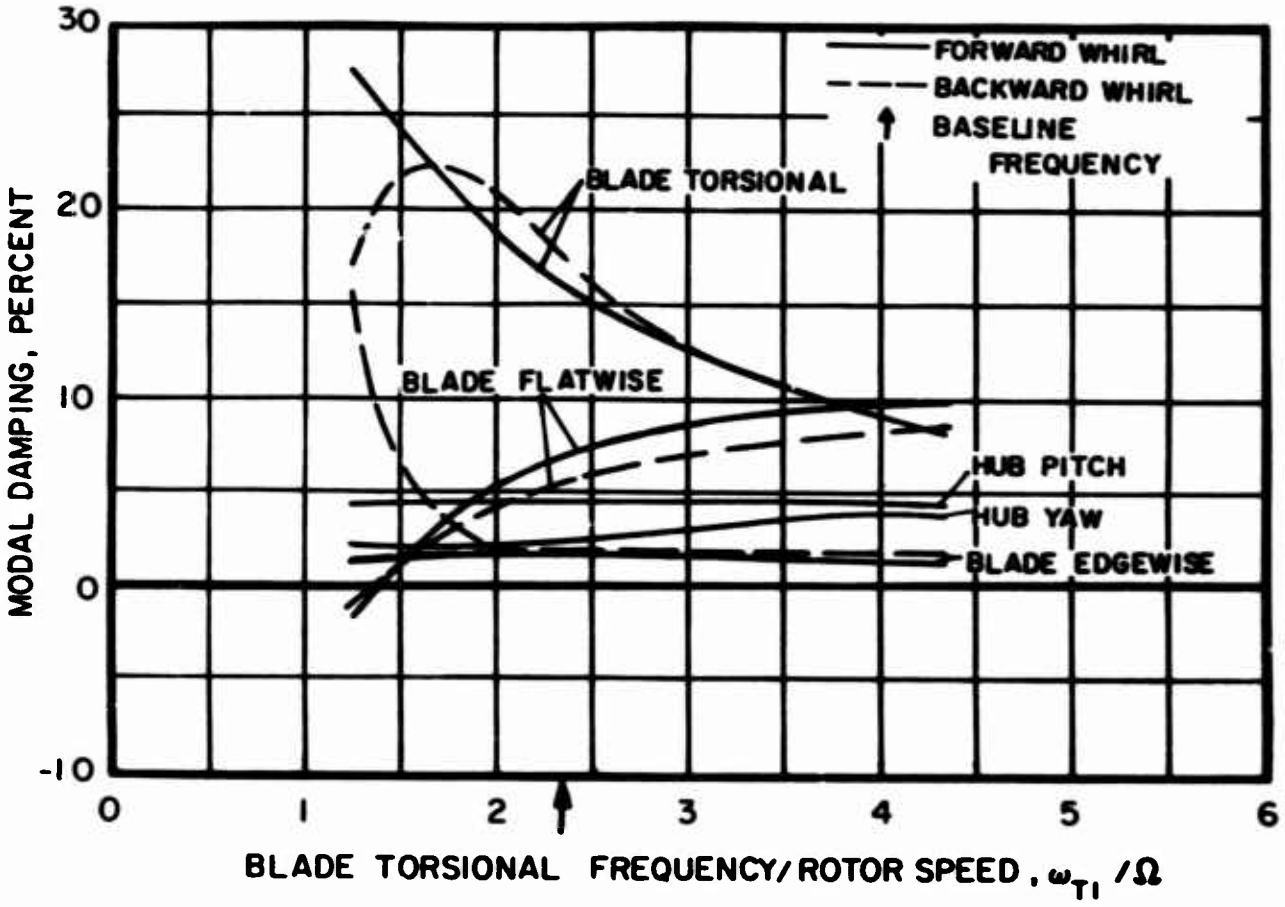

Figure 23. Effect of Blade Torsional Frequency (as a Function of Actuator Shaft Moment Stiffness) on Modal Damping for Tail Rotor No. 1 at $\mu = .50$.

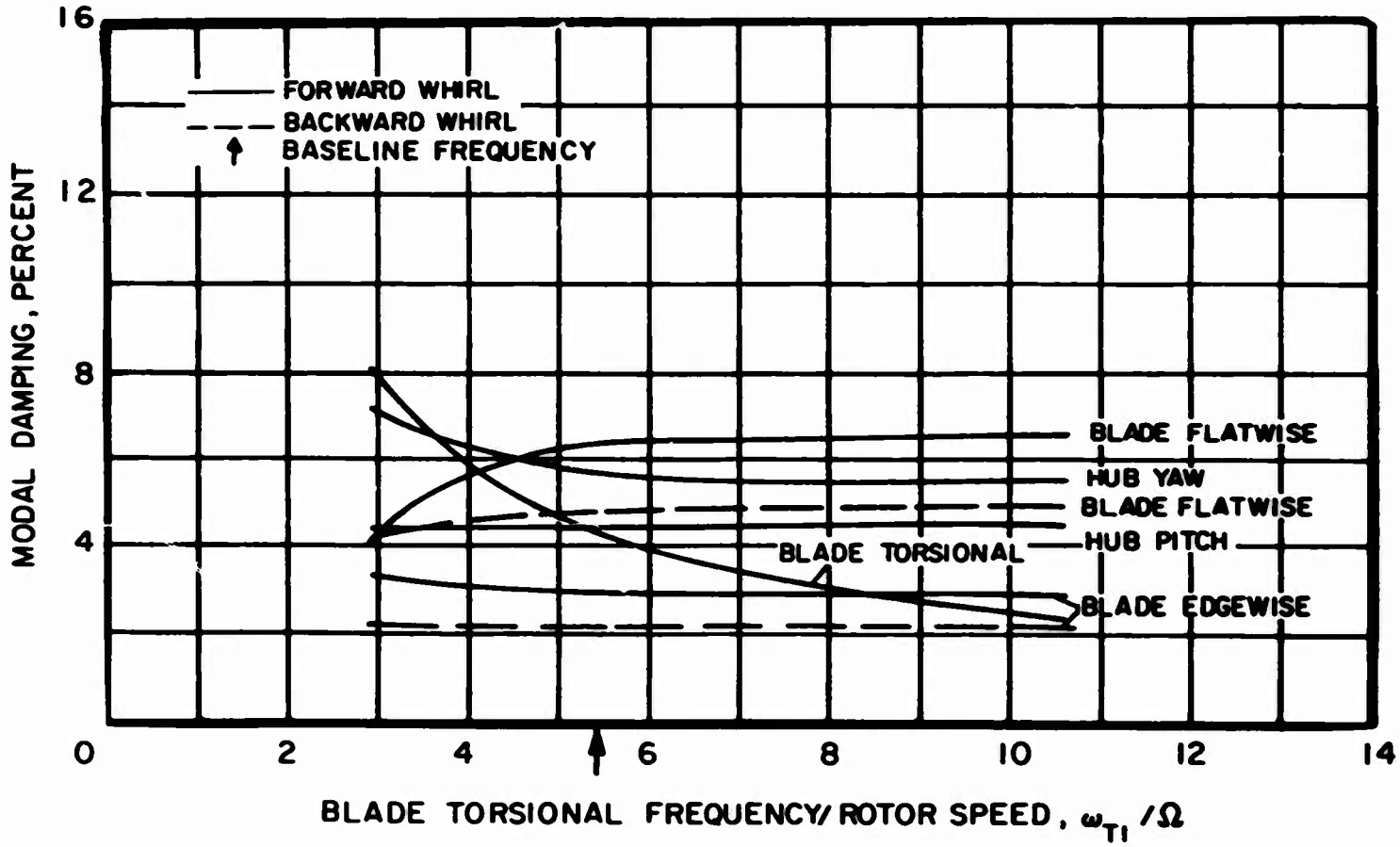

Figure 24. Effect of Blade Torsional Frequency (as a Function of Actuator Shaft Moment Stiffness) on Modal Damping for Tail Rotor No. 2 at $\mu = .50$.

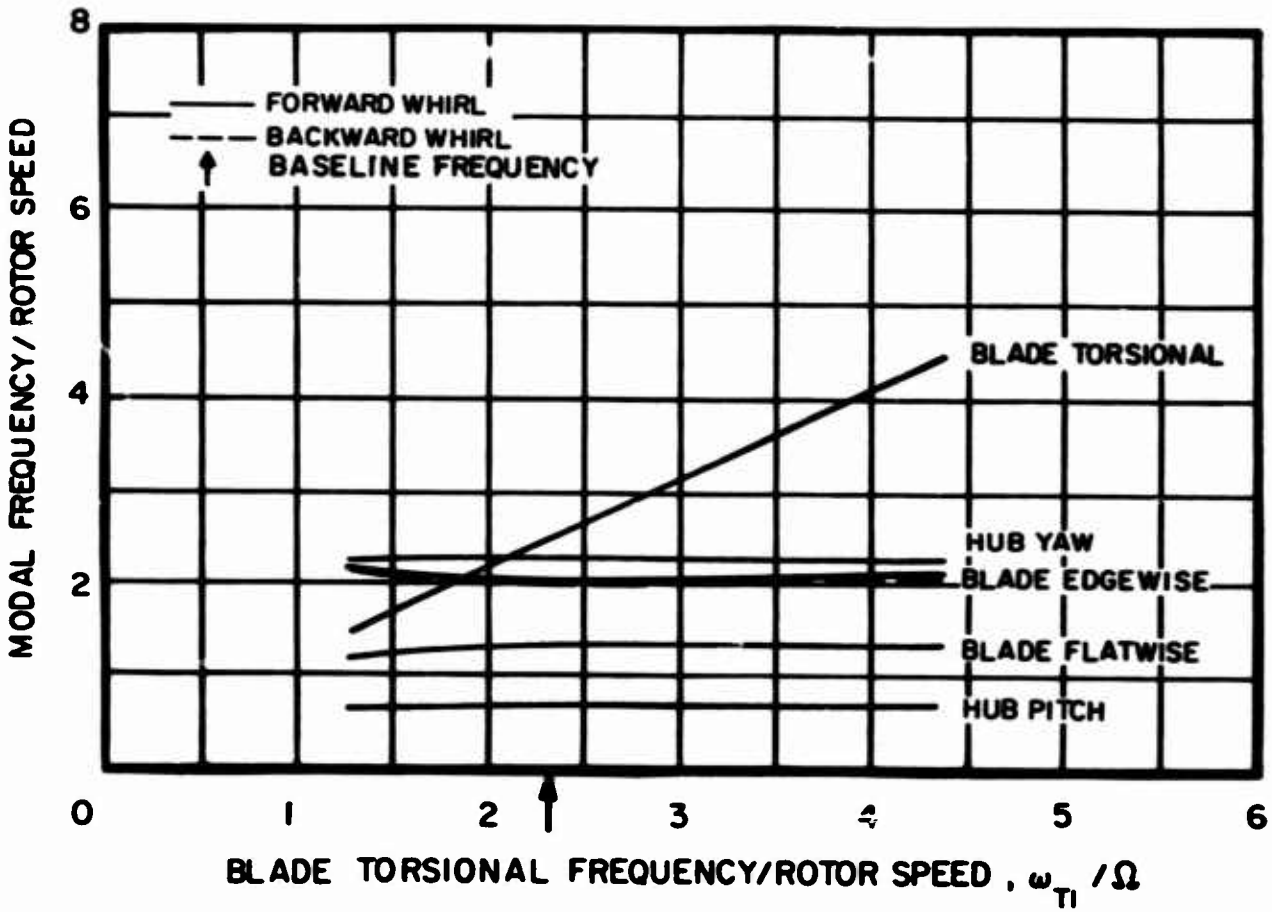

Figure 25. Effect of Blade Torsional Frequency (as a Function of Actuator Shaft Moment Stiffness) on Modal Frequency for Tail Rotor No. 1 in Hover.

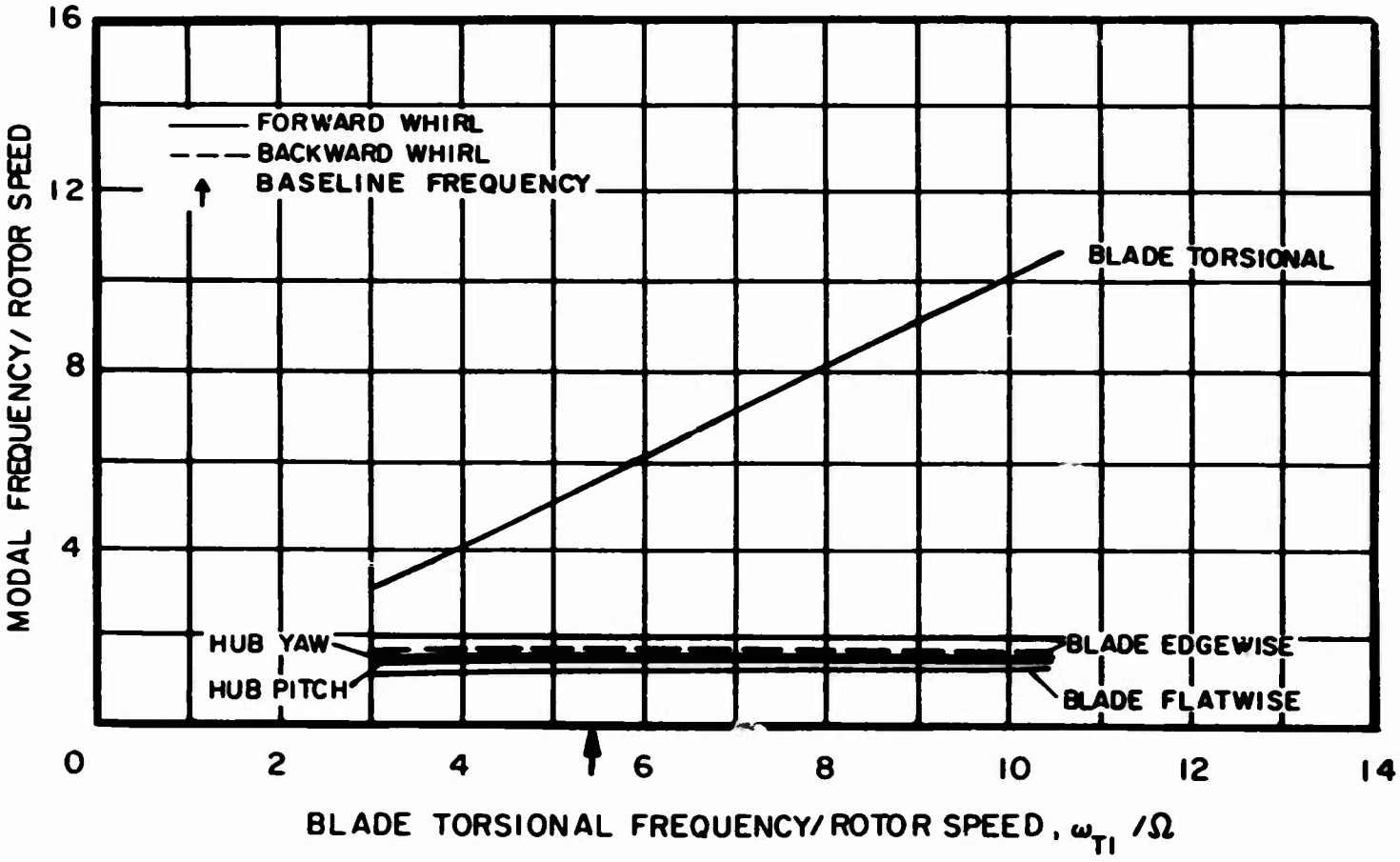

Figure 26. Effect of Blade Torsional Frequency (as a Function of Actuator Shaft Moment Stiffness) on Modal Frequency for Tail Rotor No. 2 in Hover.

Effect of Control System Symmetric Stiffness

Variations in the control system symmetric stiffness, otherwise referred to as the pitch beam arm stiffness, yielded the stability characteristics presented in Figures 27 through 32. The blade torsional frequency ω_{T2}, defined by Equation 3, ranged from 2.74 to 15.50 cycles/rev for tail rotor No. 1 and from 6.90 to 39.20 cycles/rev for tail rotor No. 2. Four values of stiffness were used to generate the curves. From Equation 2, it can be seen that a change in control system symmetric stiffness K_1 results in a new value of control system asymmetric stiffness K_3 unless the actuator shaft moment stiffness K_2 is varied accordingly. This was done in order to separate the effect of the control system asymmetric stiffness discussed in the previous section from that of the control system symmetric stiffness. Thus, the modal damping and frequency for the blade whirl modes and the rotor hub modes remain unchanged.

The modal damping and frequency of the blade symmetric modes are shown as a function of pitch beam stiffness or equivalent blade torsional frequency, ω_{T2}, in Figures 27 through 32. An inspection of Figures 27 through 30 reveals that the damping of the blade torsional mode decreases while the damping of the flatwise mode increases with torsional frequency. The effect on the edgewise mode is very slight. These results apply to both baseline rotors at advance ratios of zero and 0.50. Figures 31 and 32 show that the flatwise and edgewise blade symmetric frequencies remain constant. The blade symmetric torsional frequency is almost the same as that defined by Equation 3. The effect of variations of pitch beam stiffness on the blade symmetric modes is generally similar to the effect of actuator shaft moment stiffness variations on the blade whirl or unsymmetric modes.

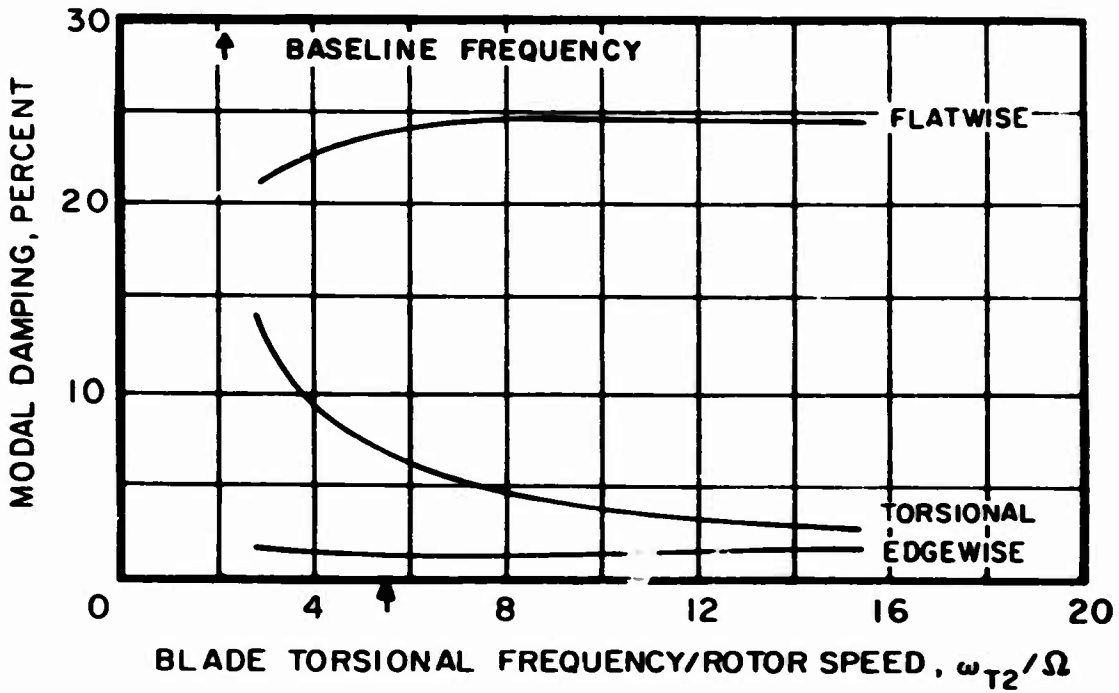

Figure 27. Effect of Blade Torsional Frequency (as a Function of Pitch Beam Arm Stiffness) on Modal Damping for Tail Rotor No. 1 in Hover.

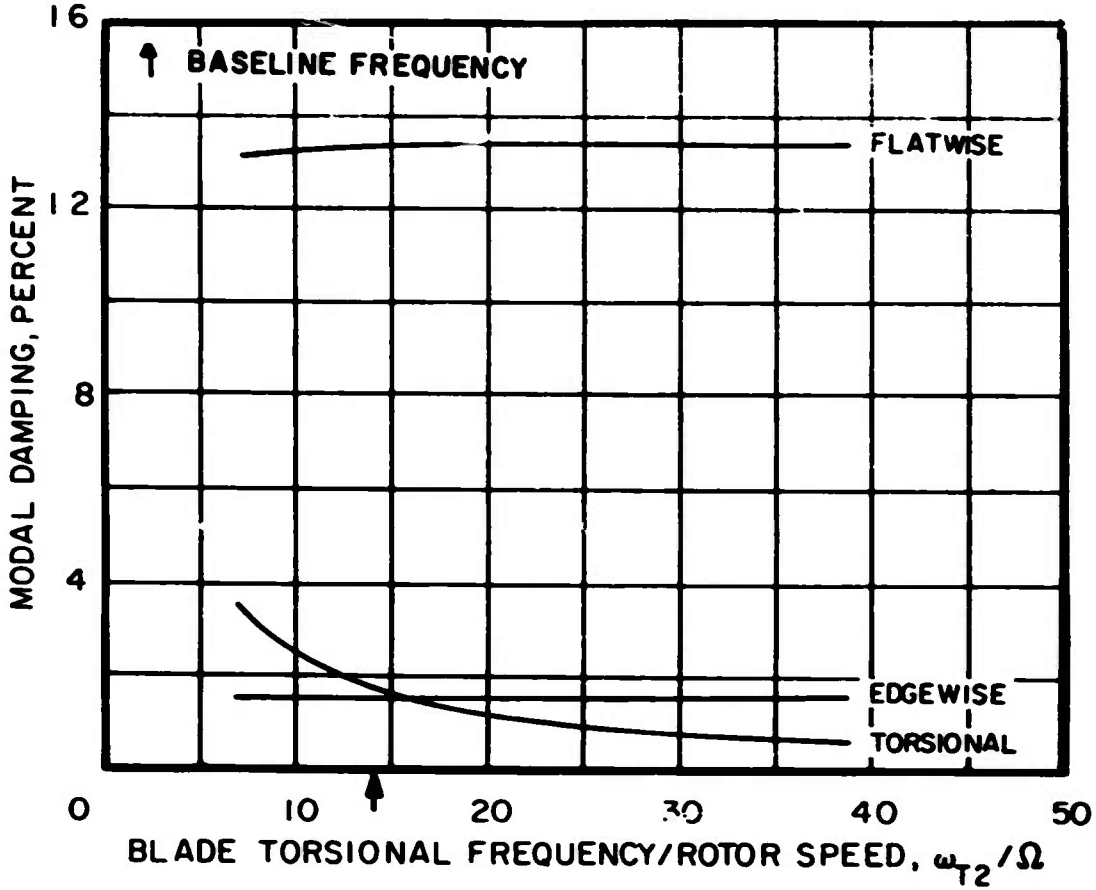

Figure 28. Effect of Blade Torsional Frequency (as a Function of Pitch Beam Arm Stiffness) on Modal Damping for Tail Rotor No. 2 in Hover.

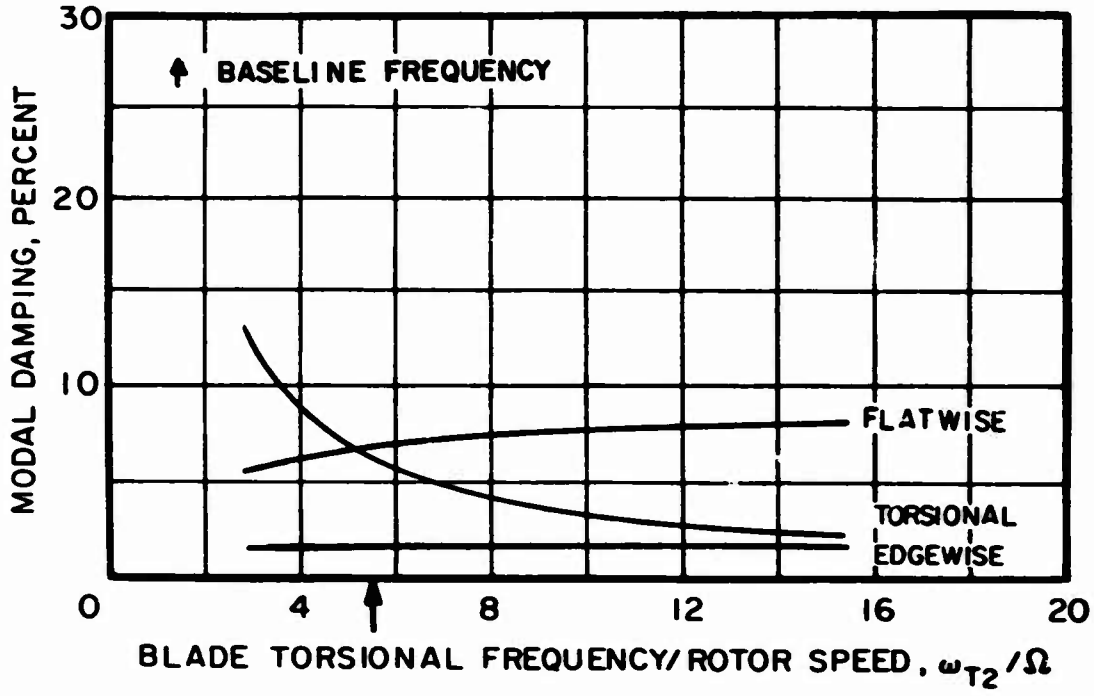

Figure 29. Effect of Blade Torsional Frequency (as a Function of Pitch Beam Arm Stiffness) on Modal Damping for Tail Rotor No. 1 at $\mu = .50$.

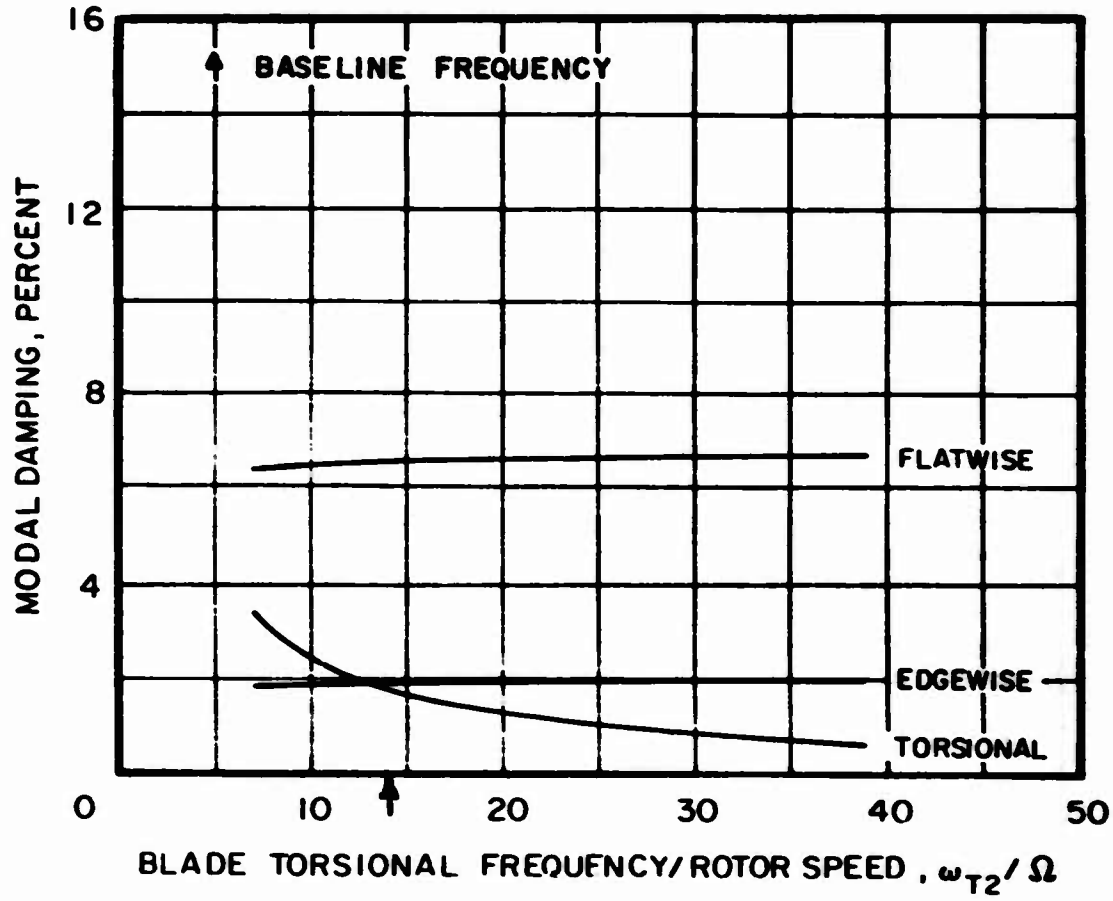

Figure 30. Effect of Blade Torsional Frequency (as a Function of Pitch Beam Arm Stiffness) on Modal Damping for Tail Rotor No. 2 at $\mu = .50$.

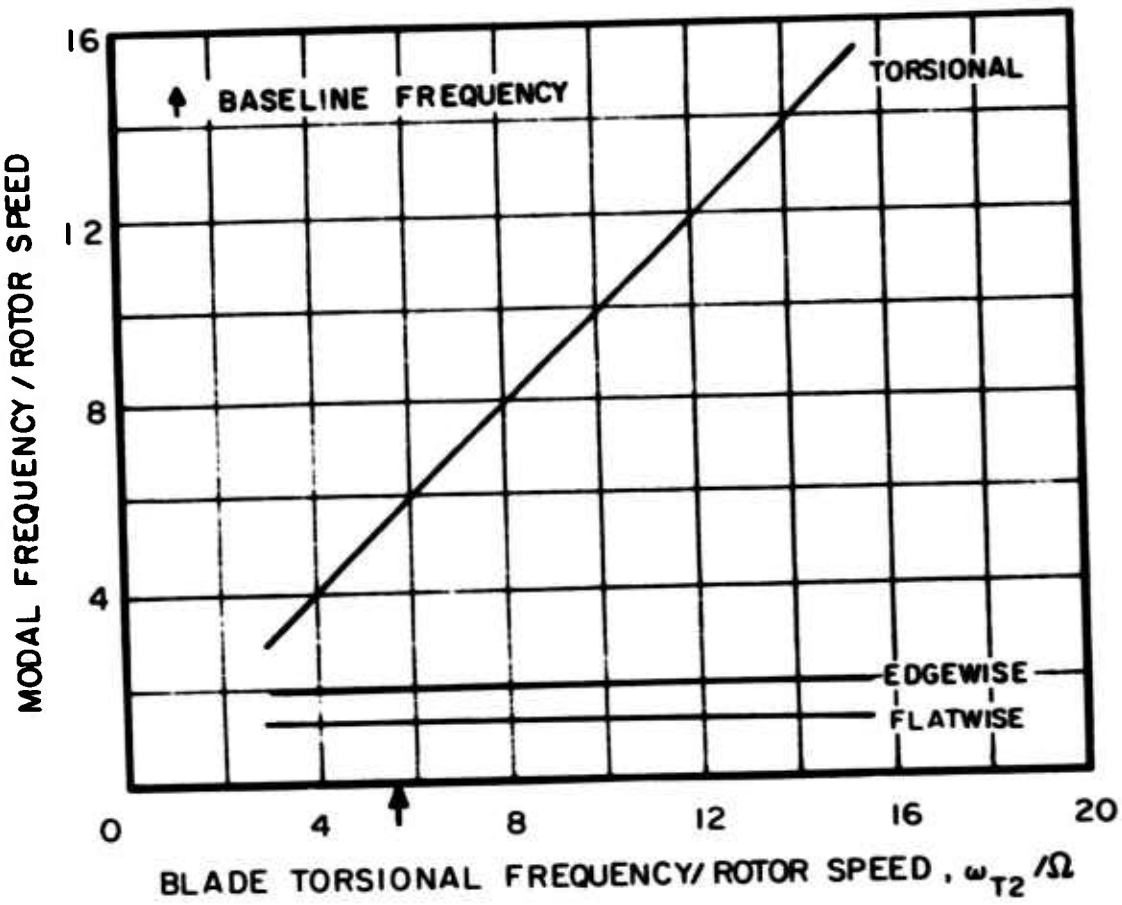

Figure 31. Effect of Blade Torsional Frequency (as a Function of Pitch Beam Arm Stiffness) on Modal Frequency for Tail Rotor No. 1 in Hover.

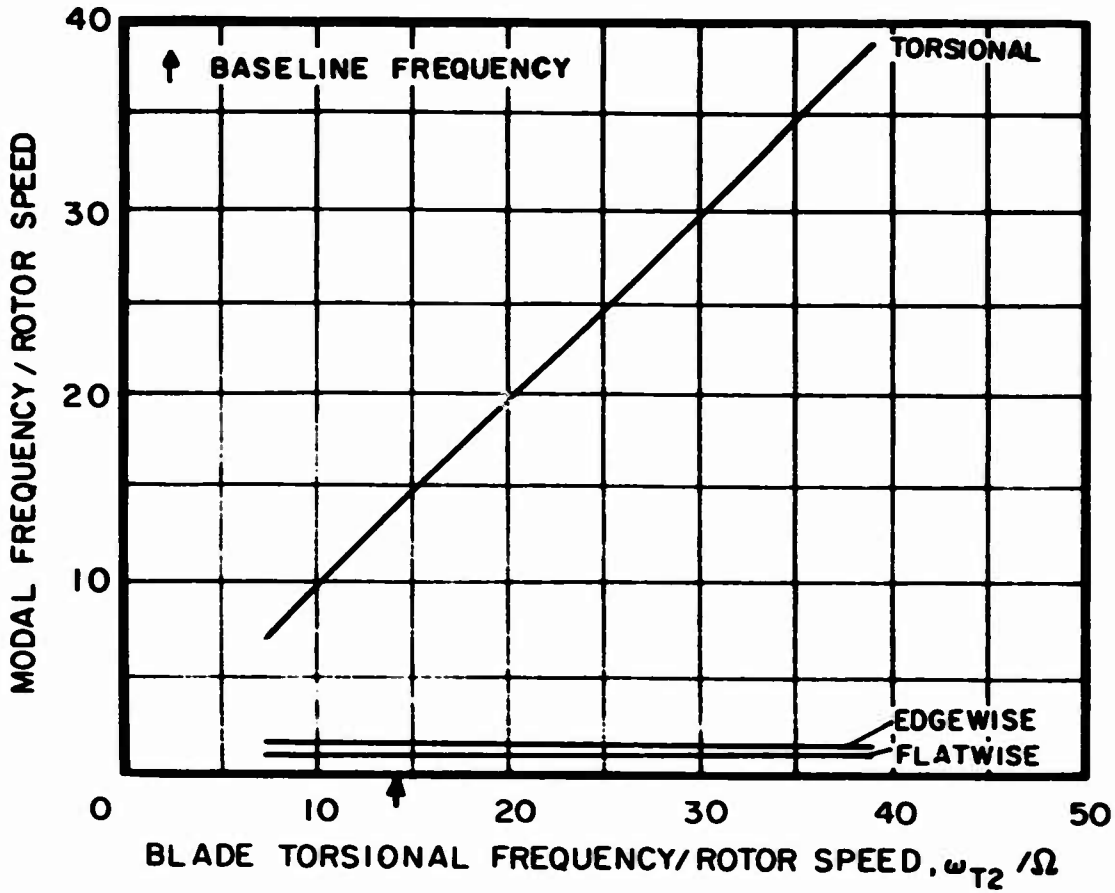

Figure 32. Effect of Blade Torsional Frequency (as a Function of Pitch Beam Arm Stiffness) on Modal Frequency for Tail Rotor No. 2 in Hover.

Effect of Blade Torsional Natural Frequency

The effect of changes in blade torsional moment of inertia on the modal damping and frequency of the two baseline tail rotors is illustrated in Figures 33 through 38. All blade modes are shown in these figures since the blade torsional moment of inertia, I_θ, appears in both Equations 1 and 3, which affect respectively the blade unsymmetric and symmetric degrees of freedom.

The blade torsional frequency, ω_{T2}, defined by Equation 3, is used to illustrate the results for the blade symmetric modes. This frequency ranged from 2.11 to 7.60 cycles/rev for tail rotor No. 1 and from 4.94 to 17.60 cycles/rev for tail rotor No. 2. Six values of frequency were used to generate the curves.

The modal damping and frequencies for the blade whirl modes and the rotor hub modes are presented as a function of the blade torsional frequency, ω_{T1}, as calculated from Equation 1. This frequency ranged from 0.89 to 3.22 cycles/rev for tail rotor No. 1 and from 2.98 to 6.90 cycles/rev for tail rotor No. 2. Six values of frequency were used to generate the curves.

A comparison of the stability characteristics presented in this section for the blade symmetric modes can be made with the results given in Figures 27 through 32, which show the effect of the pitch beam arm stiffness. Similarly, the behavior of the blade whirl and hub modes can be compared with those in Figures 21 through 26, which show the effect of actuator shaft moment stiffness.

The modal damping of the blade symmetric modes in hover appears in Figures 33(a) and 34(a) for tail rotors Nos. 1 and 2 respectively. It is noted that in the common frequency range, 2.74 to 7.60 cycles/rev for tail rotor No. 1 and 6.90 to 17.60 cycles/rev for tail rotor No. 2, the parametric trends for both rotors are similar for the blade torsional and edgewise modes. The flatwise mode of tail rotor No. 1 shows a slight decrease in stability with decreasing torsional inertia, Figure 33(a), while the same mode becomes more stable (Figure 27) as pitch beam stiffness increases. Rapid changes in stability are predicted at low torsional frequencies, between 2 and 3 cycles/rev, for tail rotor No. 1 in Figure 33(a). The blade torsional mode shows an abrupt reduction in stability, while the edgewise and flatwise modes exhibit large increases in damping. This result may be explained by the modal interaction indicated in Figure 37(a) for the edgewise and torsional modes as they both approach a value of 2 cycles/rev. For tail rotor No. 2, the torsional frequency is well removed from the edgewise and flatwise frequencies, as shown in Figure 38(a).

The stability characteristics of the blade symmetric modes at an advance ratio of 0.50 are illustrated in Figures 35(a) and 36(a) for tail rotors Nos. 1 and 2 respectively. The parametric trends shown in these figures are similar to those already discussed for the hover condition.

The modal frequencies of the blade symmetric flatwise and edgewise modes are not affected by changes in blade torsional inertia, as shown in Figures 37(a) and 38(a) for both rotors. The blade symmetric torsional frequency is practically the same as the equivalent torsional frequency, ω_{T2}. These results are similar to those presented in Figures 31 and 32 for pitch beam arm stiffness variations.

The variations in modal damping with blade torsional inertia for the blade unsymmetric modes and the rotor hub modes are presented in Figure 33(b) for tail rotor No. 1 and in Figure 34(b) for tail rotor No. 2 for the hover condition. These results can be compared with those from Figures 21 and 22 in the common frequency range of 1.25 to 3.22 cycles/rev for tail rotor No. 1 and 2.98 to 6.90 cycles/rev for tail rotor No. 2. Good agreement exists in the trends shown by all blade and hub modes for tail rotor No. 1 and by the blade edgewise and torsional modes for tail rotor No. 2. However, tail rotor No. 2 indicates a slight decrease in the stability of the blade flatwise whirl mode as the blade torsional moment of inertia decreases (Figure 34(b)), while in Figure 22, the damping of this mode increases with actuator shaft moment stiffness. For this rotor, it is also noted that the behavior of the rotor hub modes, especially the yaw mode, is quite different for the two parameter variations as the blade torsional frequency is reduced below 5 cycles/rev.

As advance ratio is increased to 0.50, the stability trends predicted for the blade whirl and rotor hub modes as a function of blade torsional inertia are generally the same as in the hover condition for both tail rotors. These results are illustrated in Figures 35(b) and 36(b) for tail rotor No. 1 and 2 respectively. However, some differences in behavior exist in the blade edgewise mode for tail rotor No. 1 and the blade flatwise forward whirl mode for tail rotor No. 2. These differences probably result from the coupling of the symmetric and unsymmetric blade modes which exists in forward flight.

The variations in modal frequency with blade torsional frequency for the blade whirl and rotor hub modes are shown in Figure 37(b) for tail rotor No. 1 and in Figure 38(b) for tail rotor No. 2 in hover. The results for tail rotor No. 1 indicate a strong interaction between the torsional and edgewise whirl modes as the blade torsional frequency, ω_{T1}/Ω, approaches 2 cycles/rev. A further increase in blade torsional moment of inertia, which lowers ω_{T1}/Ω, results in another interaction between the torsional and flatwise whirl modes near a value of ω_{T1}/Ω of 1.70 cycles/rev. It is noted that for tail rotor No. 2, no such interactions in blade whirl frequencies occur since the blade torsional whirl frequency is well

removed from all other system frequencies in the range of ω_{T_1}/Ω investigated.

Both rotors exhibit negligible changes in the hub pitch and yaw modal frequencies. A comparison of the frequency response as a function of blade torsional moment of inertia, Figures 37(b) and 38(b), or actuator shaft moment stiffness, Figures 25 and 26, shows similar trends for both tail rotors. However, the interactions between the blade whirl modes for tail rotor No. 1 are more pronounced in Figure 37(b) than in Figure 25.

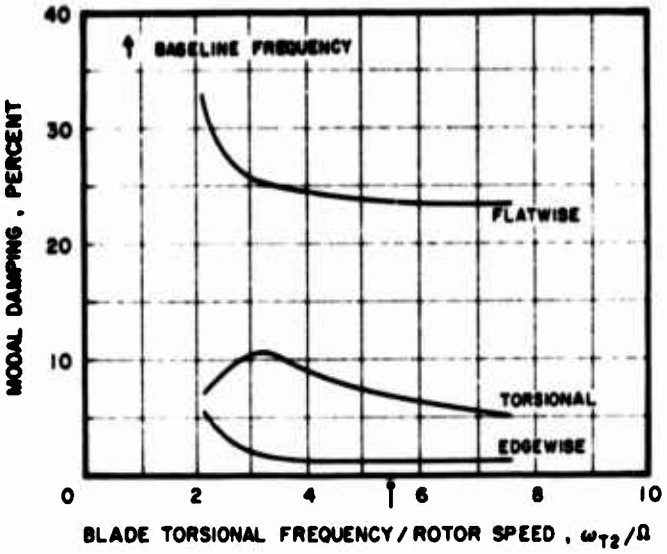

(a) Blade Symmetric Modes

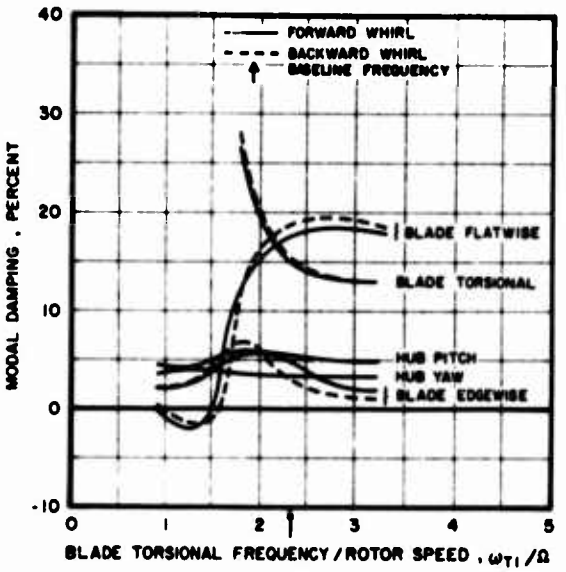

(b) Blade Whirl and Hub Modes

Figure 33. Effect of Blade Torsional Frequency (as a Function of Blade Torsional Inertia) on Modal Damping for Tail Rotor No. 1 in Hover.

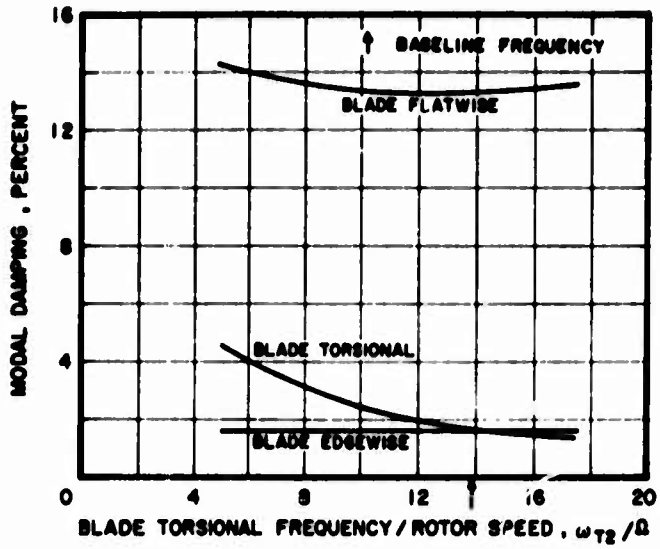

(a) Blade Symmetric Modes

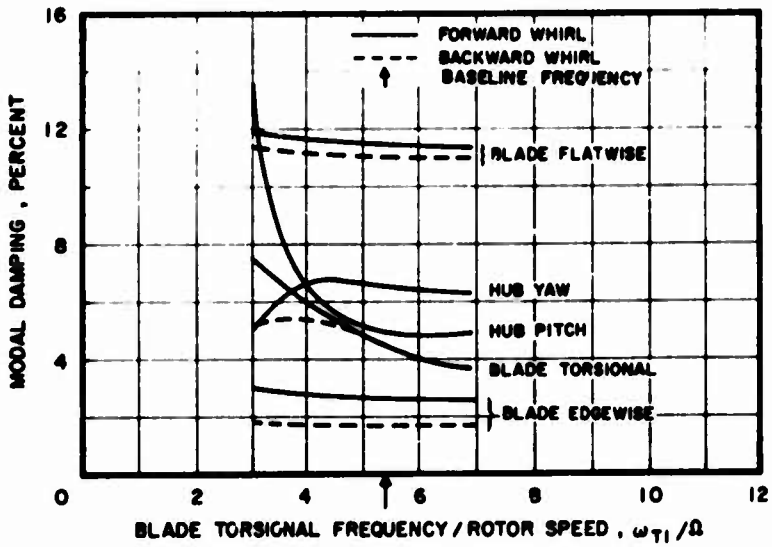

(b) Blade Whirl and Hub Modes

Figure 34. Effect of Blade Torsional Frequency (as a Function of Blade Torsional Inertia) on Modal Damping for Tail Rotor No. 2 in Hover.

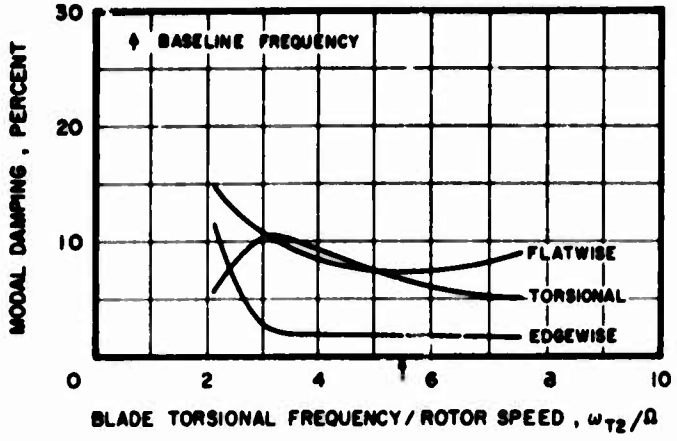

(a) Blade Symmetric Modes

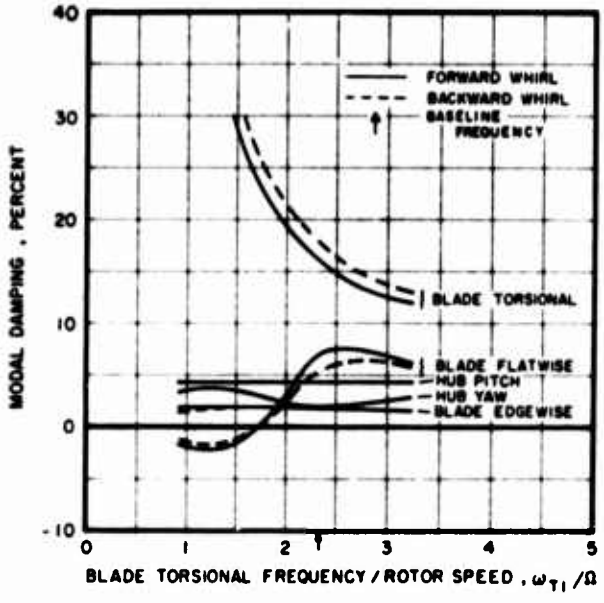

(b) Blade Whirl and Hub Modes

Figure 35. Effect of Blade Torsional Frequency (as a Function of Blade Torsional Inertia) on Modal Damping for Tail Rotor No. 1 at $\mu = .50$.

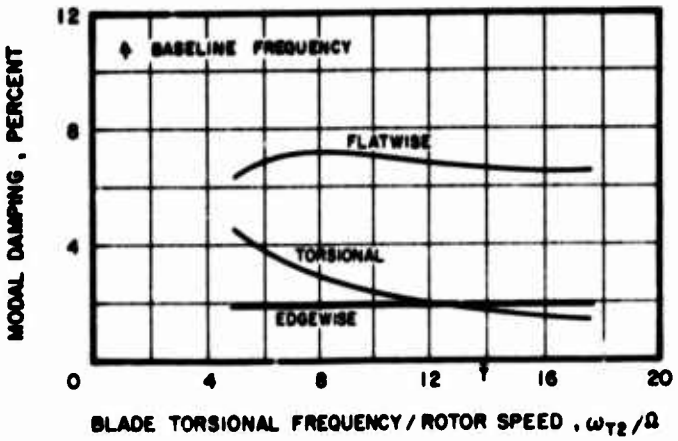

(a) Blade Symmetric Modes

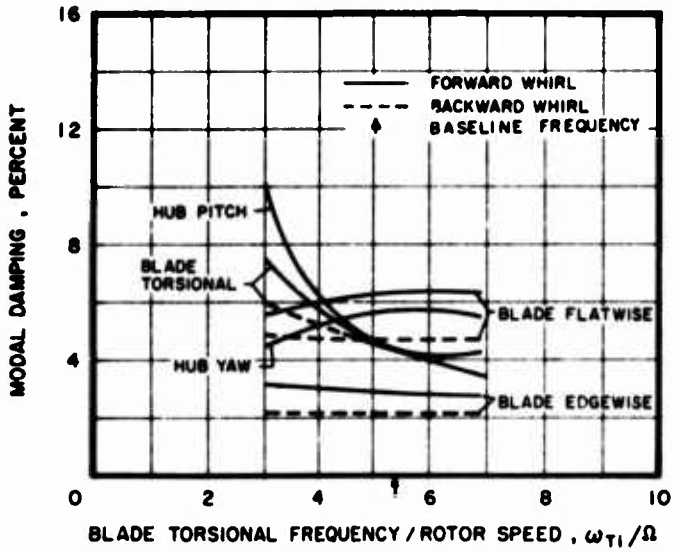

(b) Blade Whirl and Hub Modes

Figure 36. Effect of Blade Torsional Frequency (as a Function of Blade Torsional Inertia) on Modal Damping for Tail Rotor No. 2 at μ = .50.

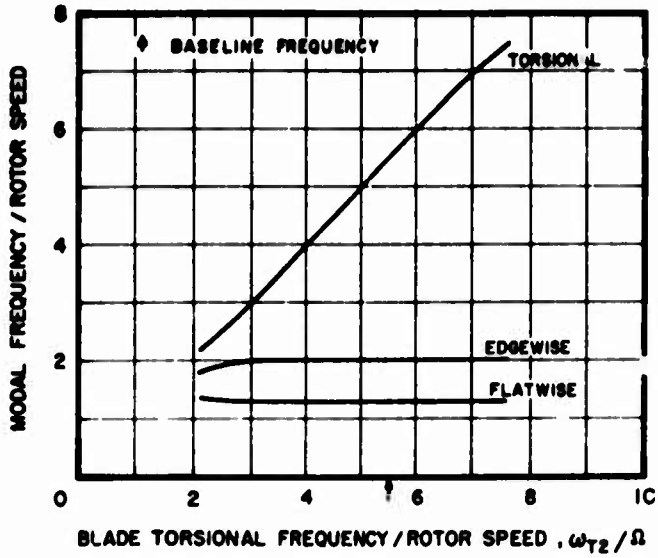

(a) Blade Symmetric Mode

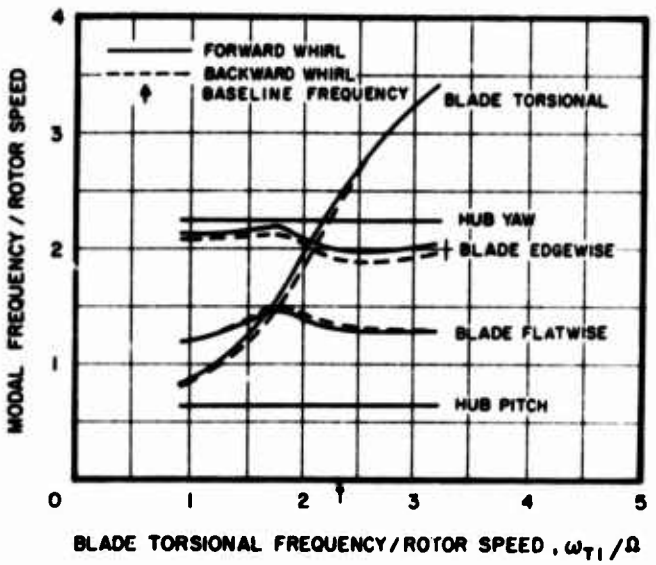

(b) Blade Whirl and Hub Modes

Figure 37. Effect of Blade Torsional Frequency (as a Function of Blade Torsional Inertia) on Modal Frequency for Tail Rotor No. 1 in Hover.

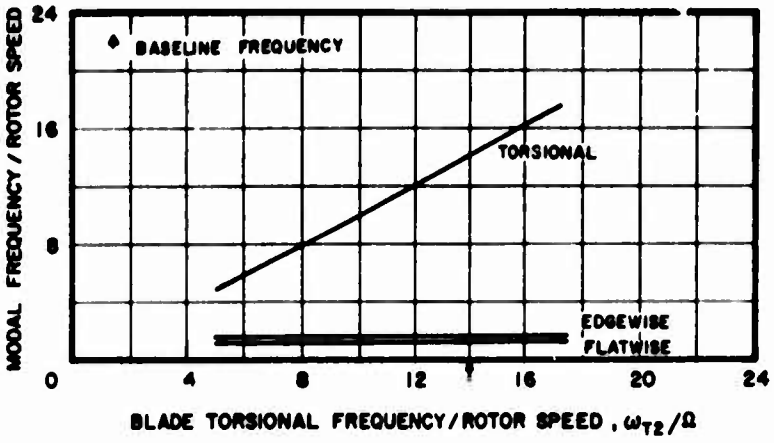

(a) Blade Symmetric Modes

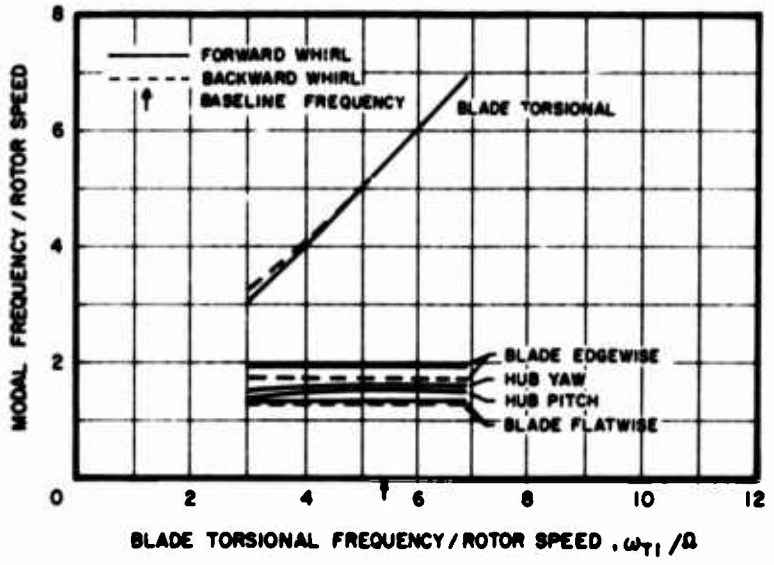

(b) Blade Whirl and Hub Modes

Figure 38. Effect of Blade Torsional Frequency (as a Function of Blade Torsional Inertia) on Modal Frequency for Tail Rotor No. 2 in Hover.

Effect of Pitch-Flap Coupling

The effect of blade pitch-flap coupling on the stability characteristics of the two baseline tail rotors is illustrated in Figures 39 through 44 for advance ratios of zero and 0.50. The range in pitch-flap coupling investigated was from -30 to 60 degrees for both tail rotors. Five values were used. Equation 4 was used to calculate the coupling for tail rotor No. 1, which is articulated in the flatwise direction, while an effective value of pitch-flap coupling was computed from Equation 5 for tail rotor No. 2, which is nonarticulated. The stability characteristics in hover are discussed first.

From Figures 39 and 40, it is noted that pitch-flap coupling stabilizes the blade torsional symmetric and unsymmetric modes and the blade edgewise whirl modes; this effect becomes more pronounced as coupling is increased above 30 degrees for both rotors. A strong destabilization of the blade flatwise modes is evident throughout the entire range of pitch-flap coupling investigated. An instability of the blade flatwise whirl mode of tail rotor No. 1 is predicted at a pitch-flap coupling of 60 degrees (Figure 39). The blade edgewise symmetric mode for tail rotor No. 1 becomes marginally stable as pitch-flap coupling approaches 60 degrees, while no change in stability is shown by the same mode for tail rotor No. 2. From the results presented in Figure 39 and 40, it can be concluded that the stability of the blade torsional and flatwise modes is considerably more sensitive to variations in blade pitch-flap coupling for tail rotor No. 1 than for tail rotor No. 2.

The modal damping of the rotor hub modes for tail rotor No. 1 is generally unaffected by pitch-flap coupling variations. On the other hand, tail rotor No. 2 exhibits a slight reduction in the damping of the rotor pitch mode, while the yaw mode shows a large increase in stability at the higher values of pitch-flap coupling.

The parametric trend of modal damping with pitch-flap coupling at an advance ratio of 0.50 is illustrated in Figures 41 and 42 for tail rotors No. 1 and 2 respectively. A comparison of these results with the results presented in Figures 39 and 40 for the hover condition shows similar effects of pitch-flap coupling on the stability of the rotor blade and hub modes. The only difference in modal damping at an advance ratio of 0.50 is shown by the blade edgewise mode for tail No. 1. The stability of this mode remains unchanged throughout the range of coupling examined.

The modal frequency response with blade pitch-flap coupling is illustrated in Figures 43 and 44. From these figures, it can be seen that the blade flatwise frequency for the symmetric and unsymmetric modes increases with pitch-flap coupling for both tail rotors. On the other hand, the presence of pitch-flap coupling, positive or negative, results in lower blade torsional frequencies, as indicated in Figures 43 and 44. The frequencies of the blade edgewise and rotor hub modes are little affected by pitch-flap coupling variations.

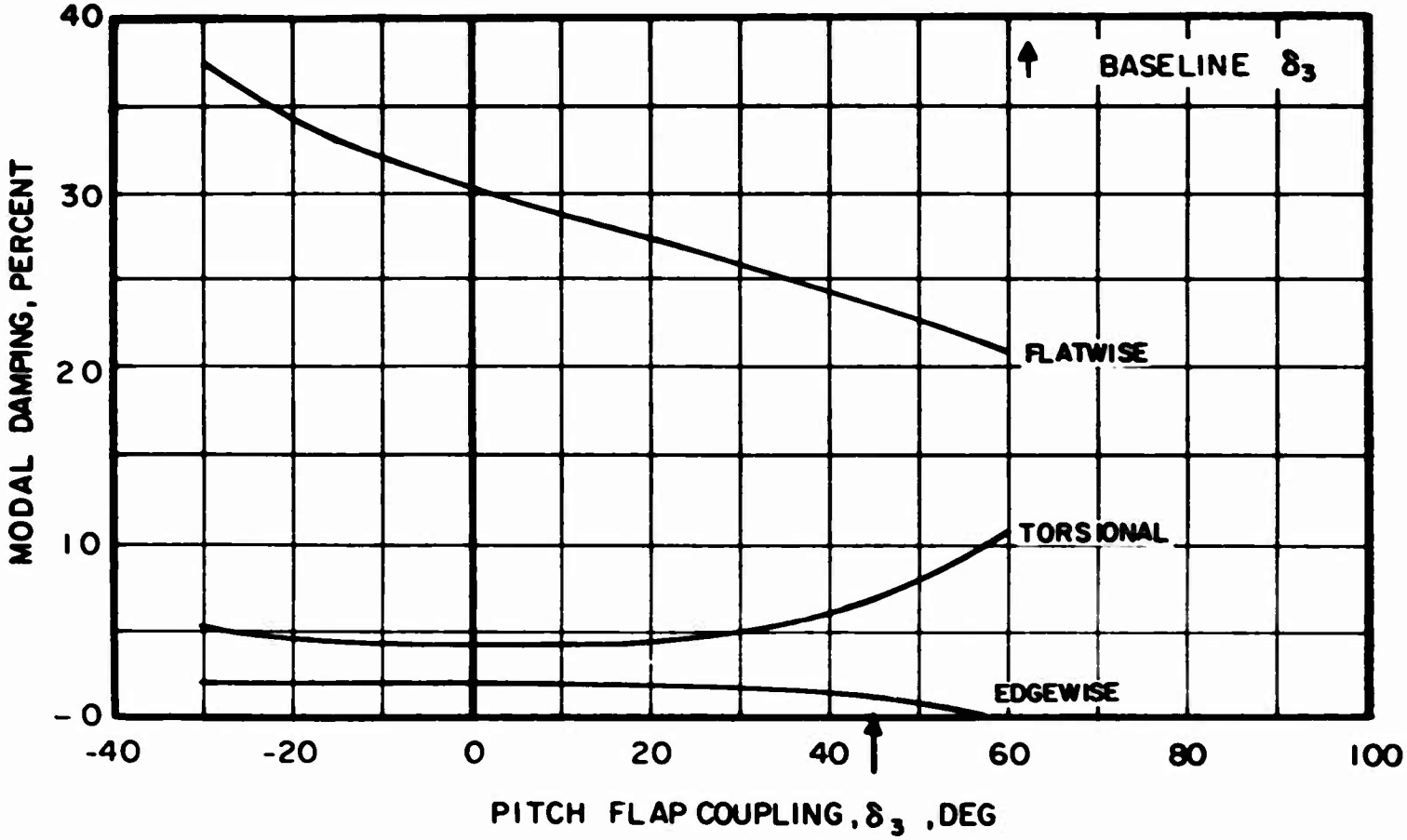

(a) Blade Symmetric Modes

Figure 39. Effect of Pitch-Flap Coupling on Modal Damping for Tail Rotor No. 1 in Hover.

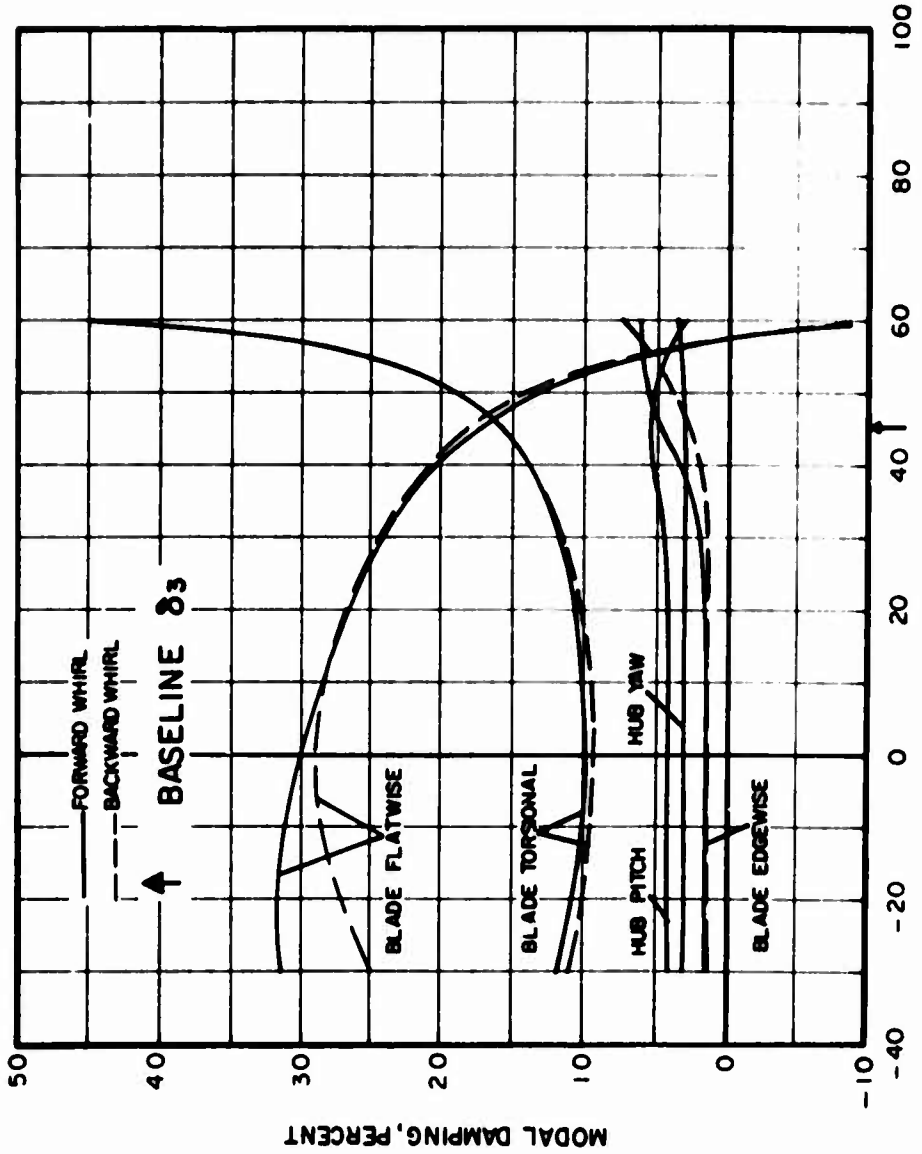

(b) Blade Whirl and Hub Modes

Figure 39. Concluded.

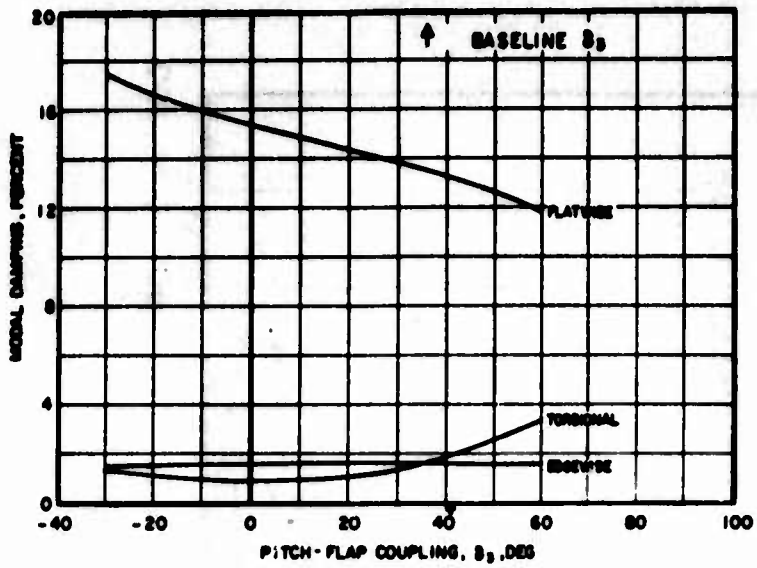

(a) Blade Symmetric Modes

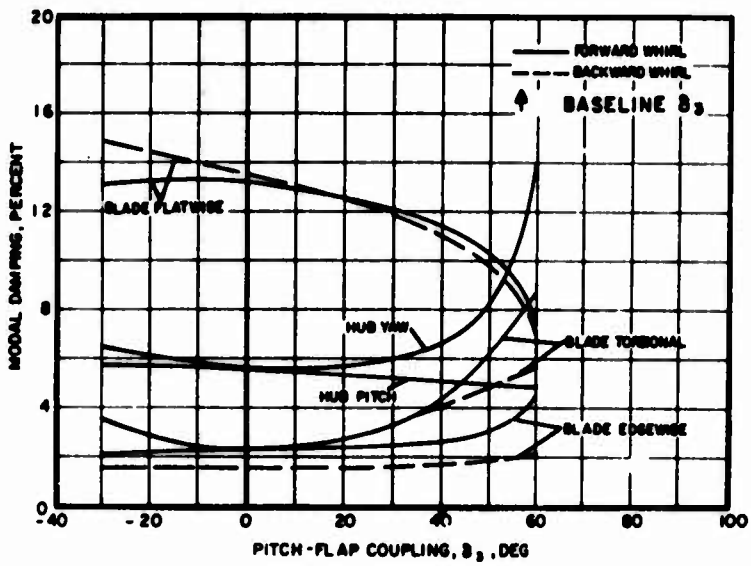

(b) Blade Whirl and Hub Modes

Figure 40. Effect of Pitch-Flap Coupling on Modal Damping for Tail Rotor No. 2 in Hover.

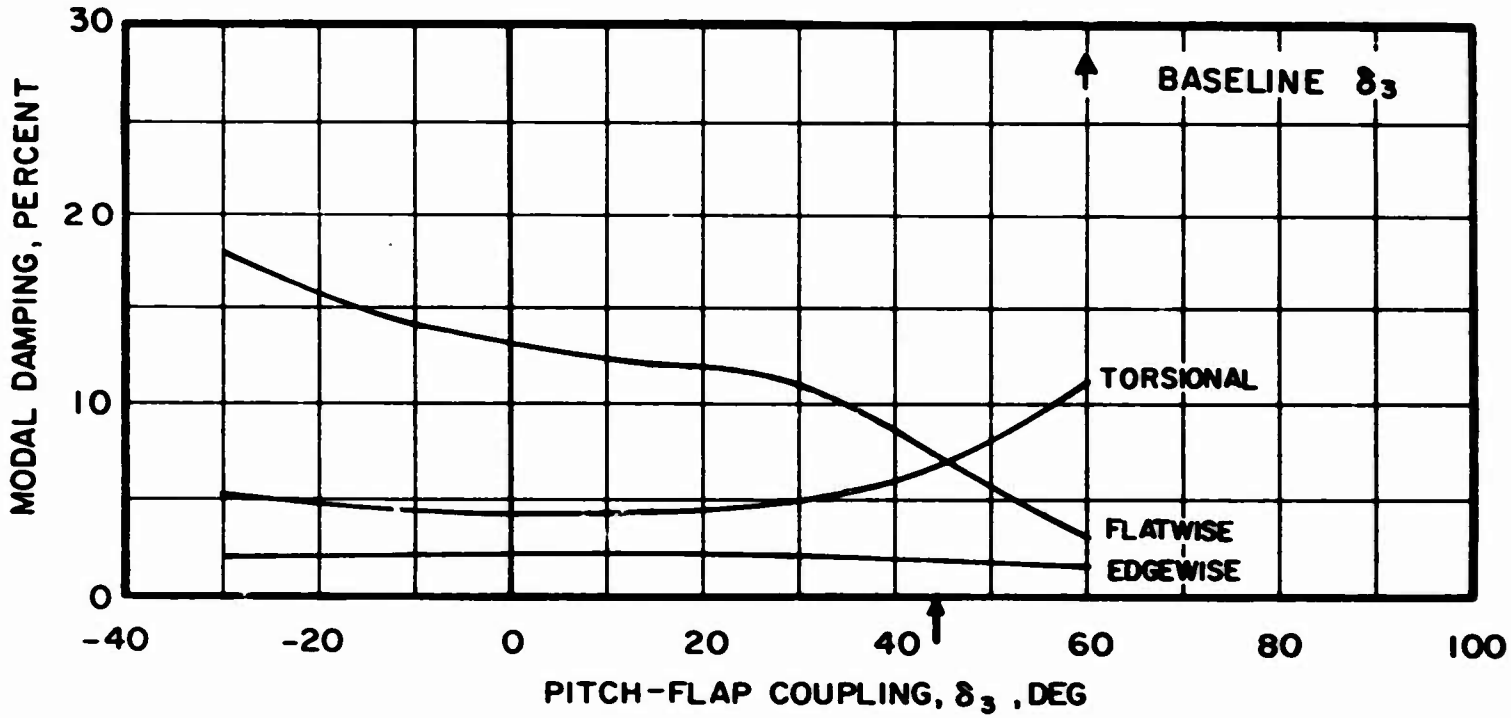

(a) Blade Symmetric Modes

Figure 41. Effect of Pitch-Flap Coupling on Modal Damping for Tail Rotor No. 1 at μ = .50.

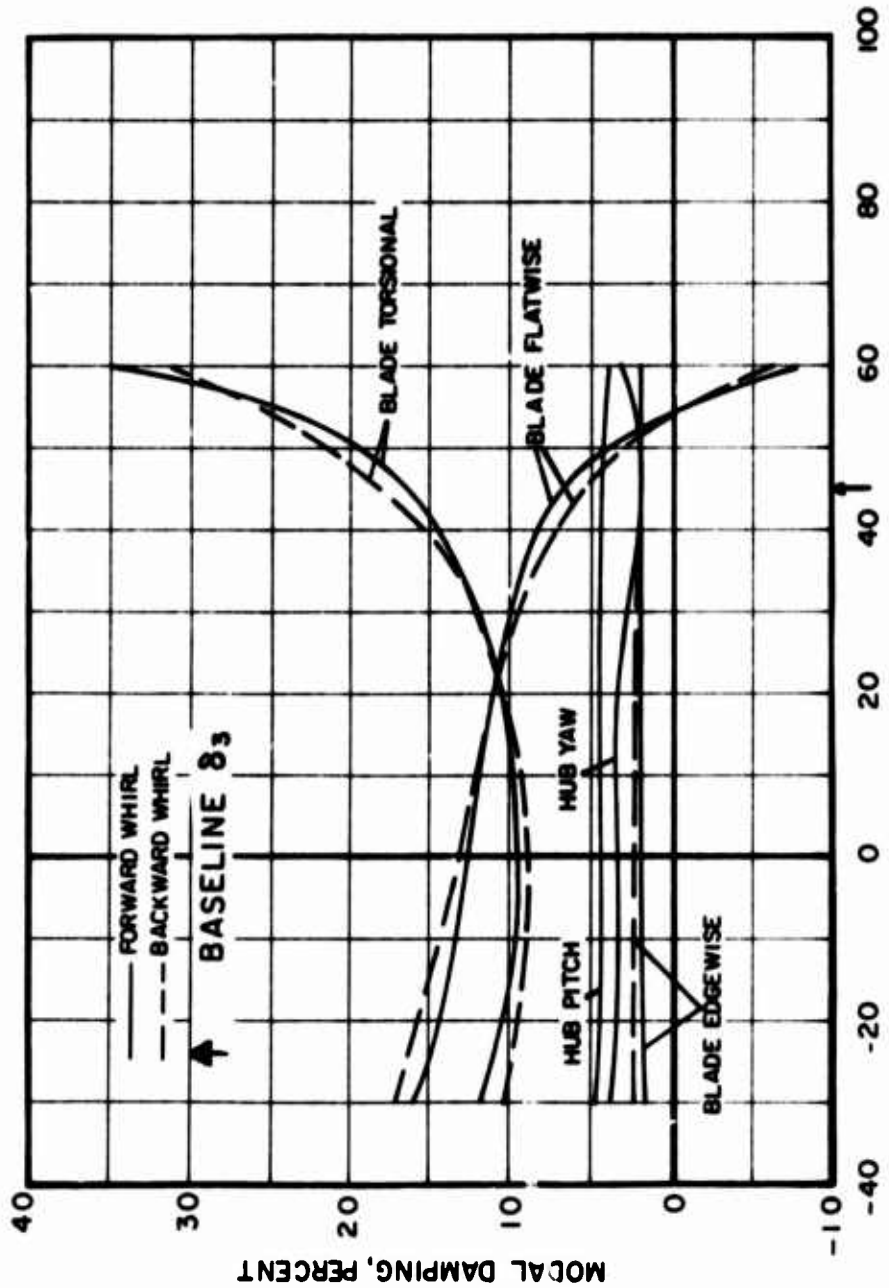

(b) Blade Whirl and Hub Modes

Figure 41. Concluded.

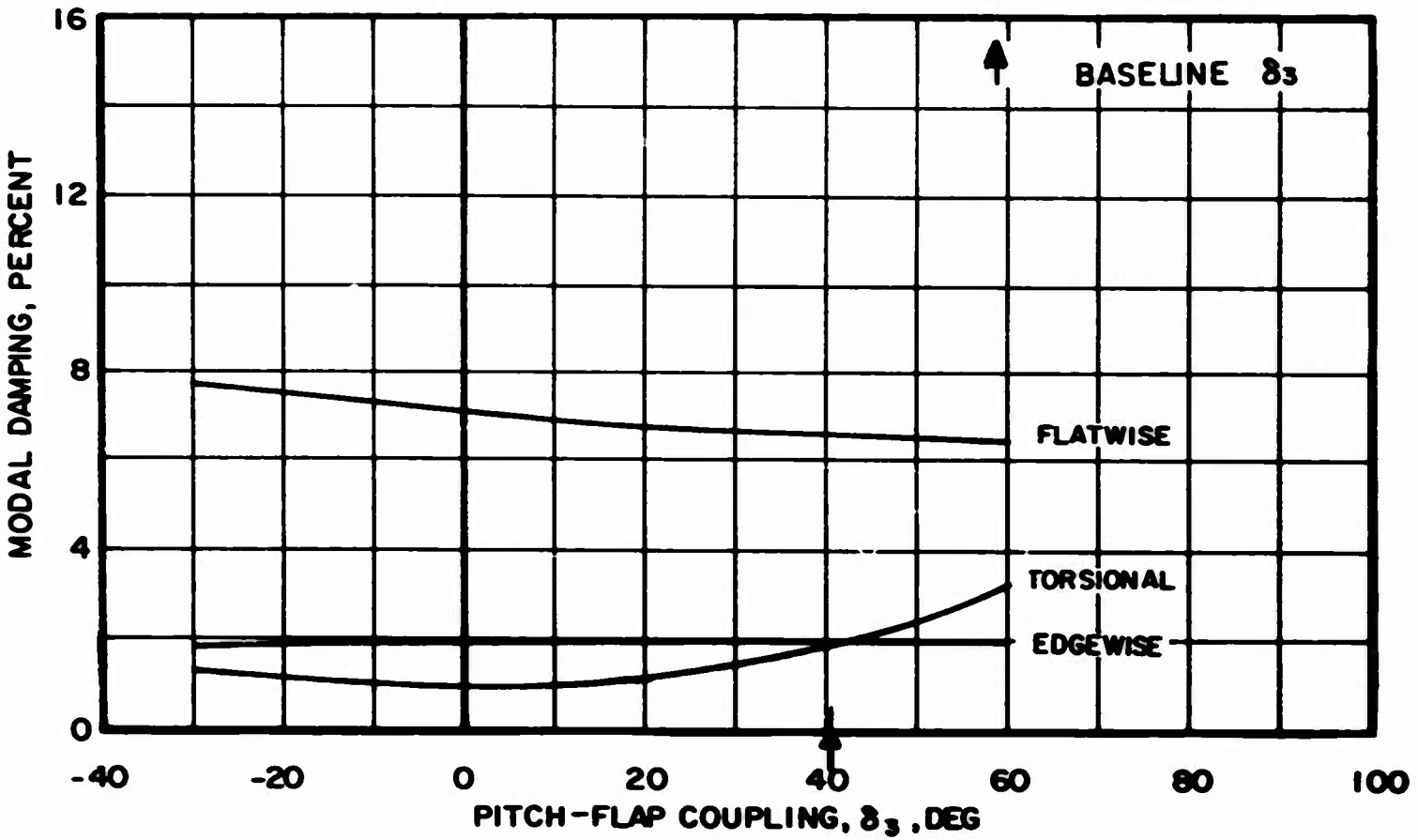

(a) Blade Symmetric Modes

Figure 42. Effect of Pitch-Flap Coupling on Modal Damping for Tail Rotor No. 2 at μ = .50.

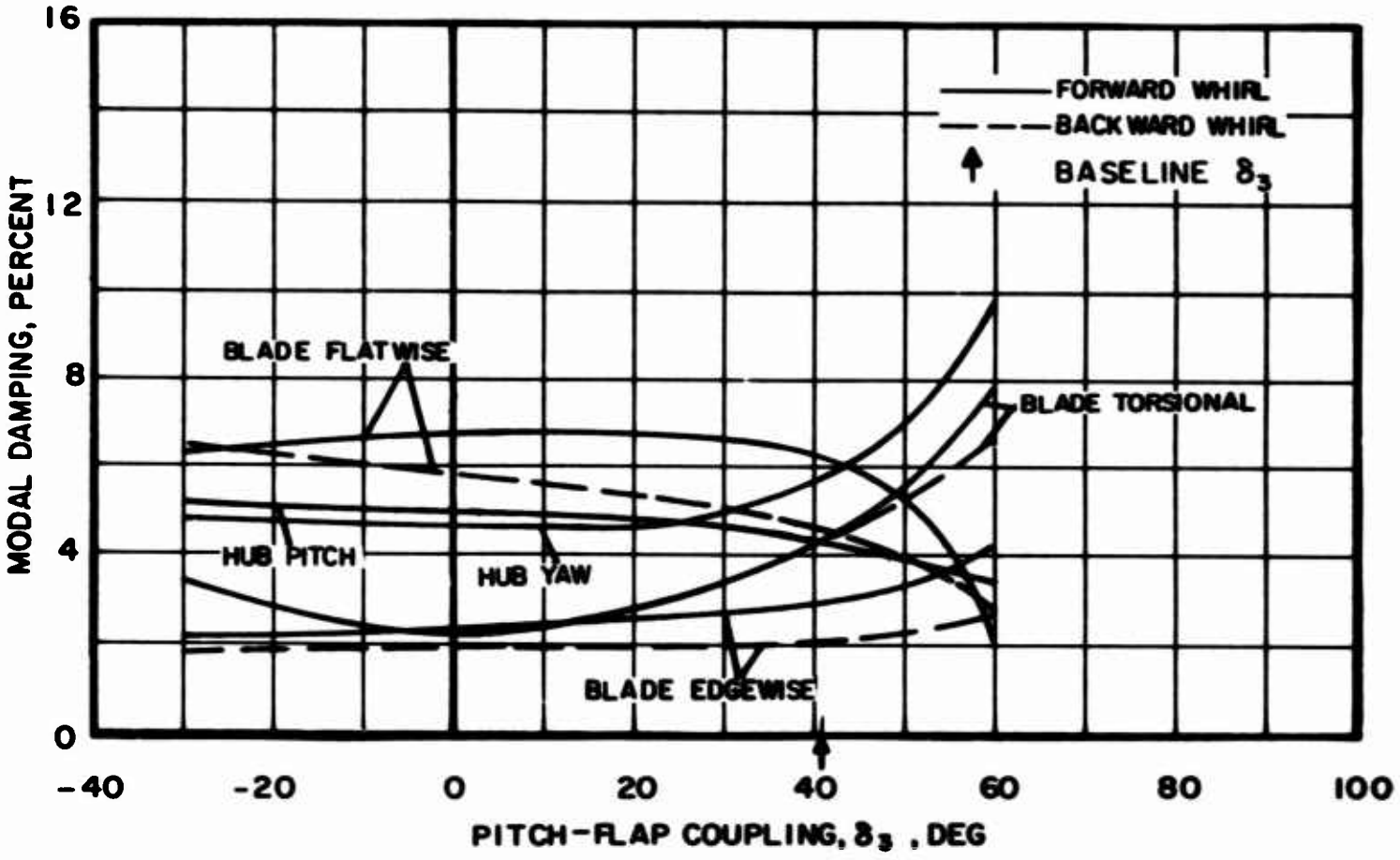

(b) Blade Whirl and Hub Modes

Figure 42. Concluded.

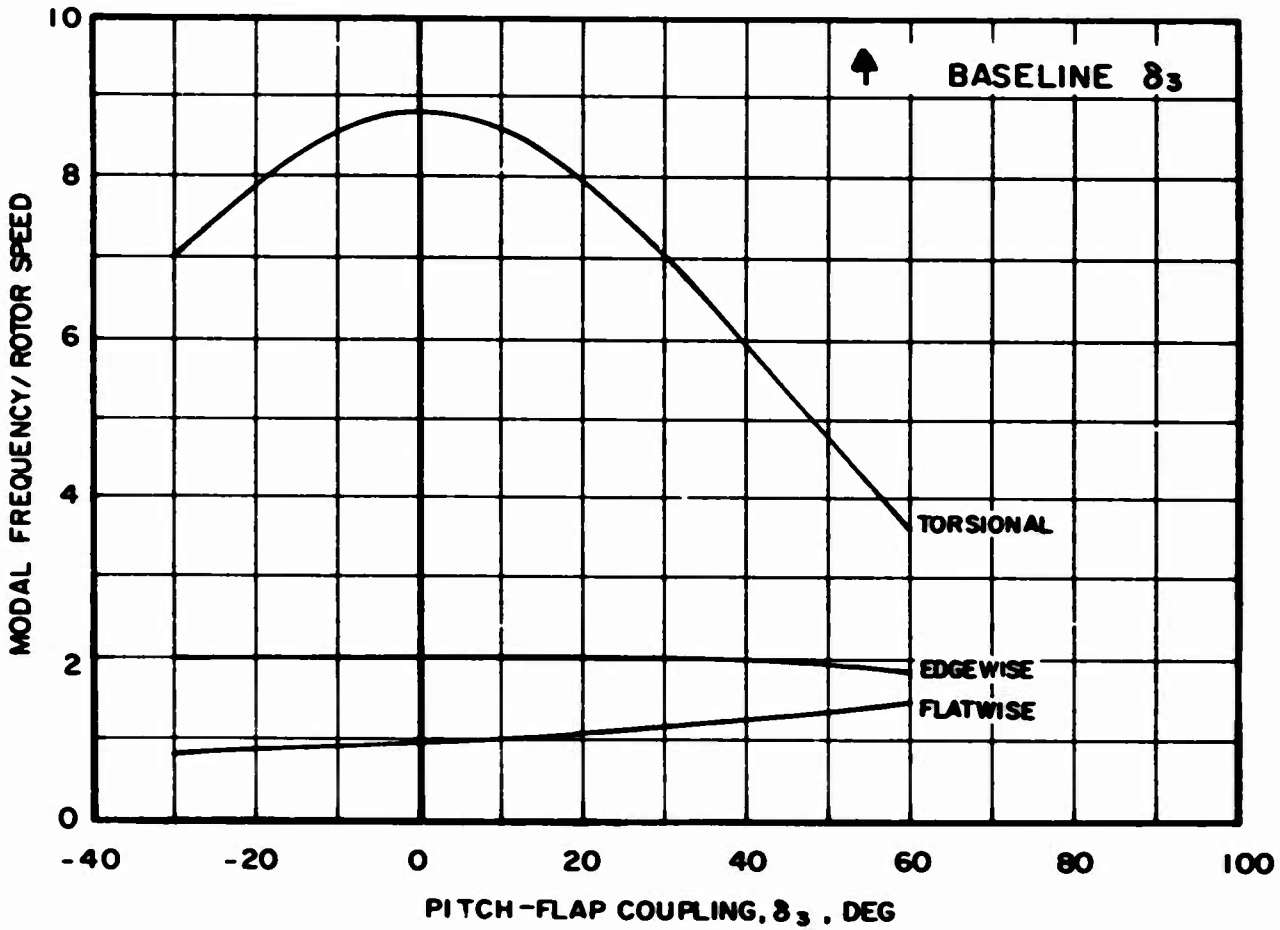

(a) Blade Symmetric Modes

Figure 43. Effect of Pitch-Flap Coupling on Modal Frequency for Tail Rotor No. 1 in Hover.

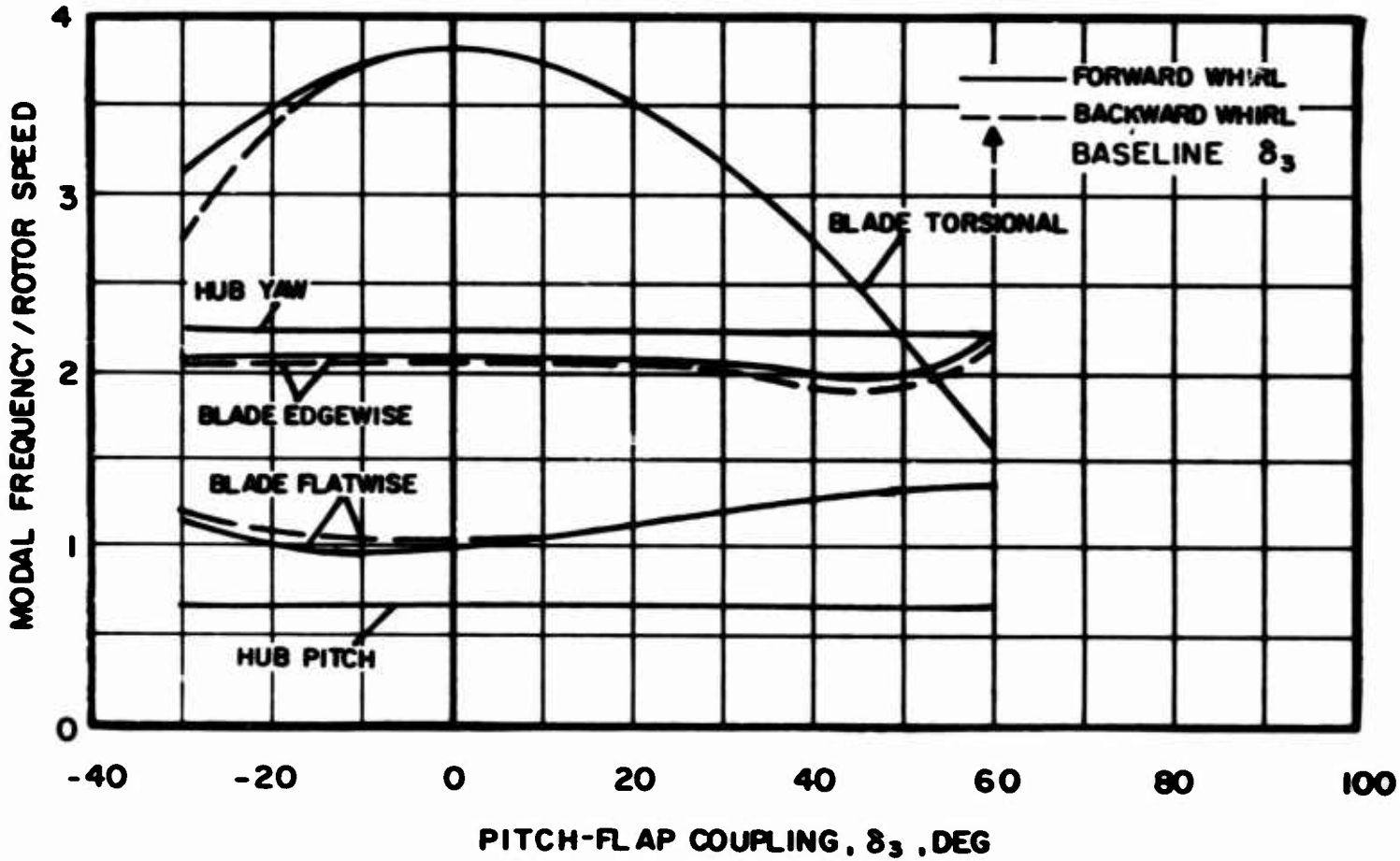

(b) Blade Whirl and Hub Modes

Figure 43. Concluded.

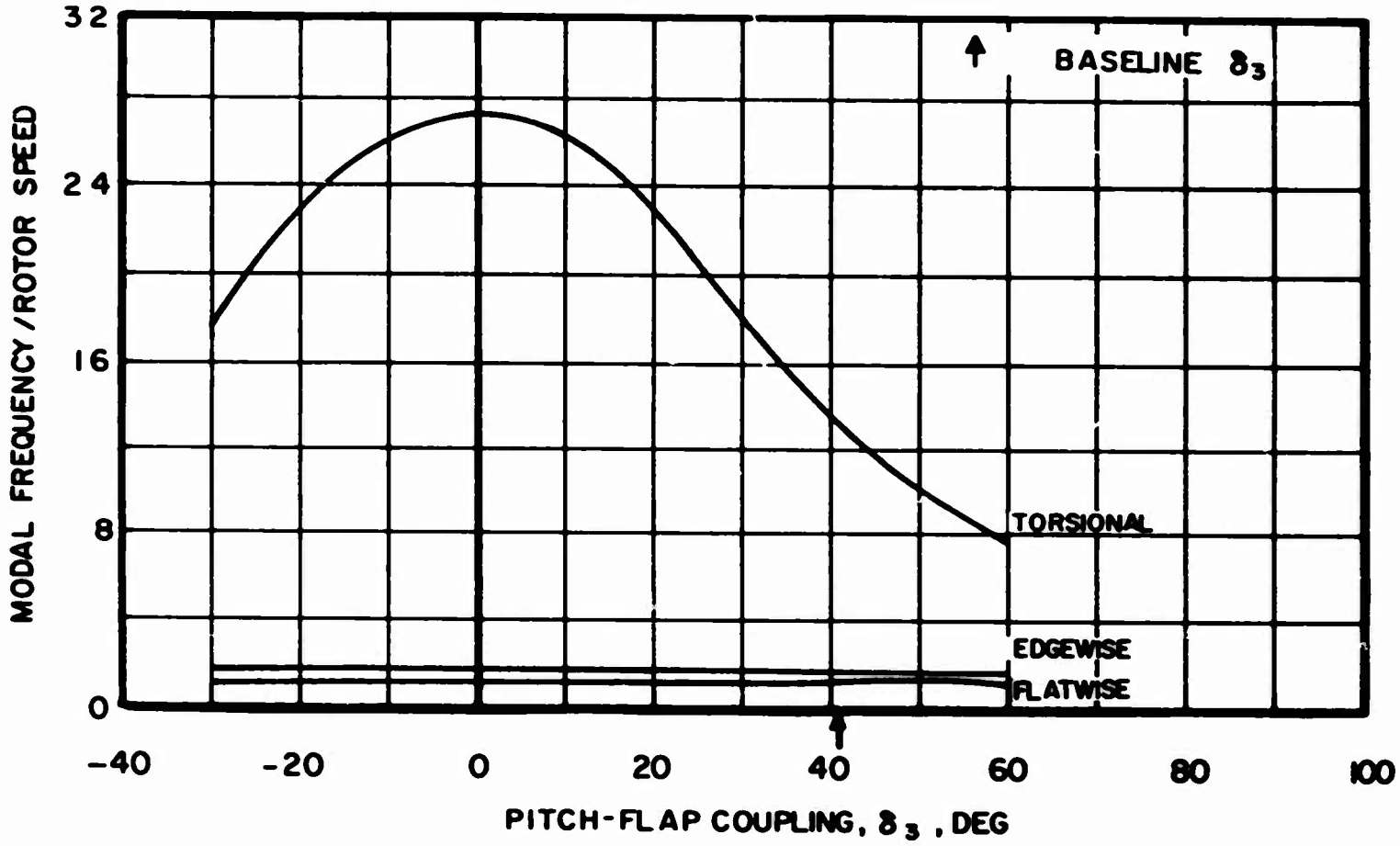

(a) Blade Symmetric Modes

Figure 44. Effect of Pitch-Flap Coupling on Modal Frequency for Tail Rotor No. 2 in Hover.

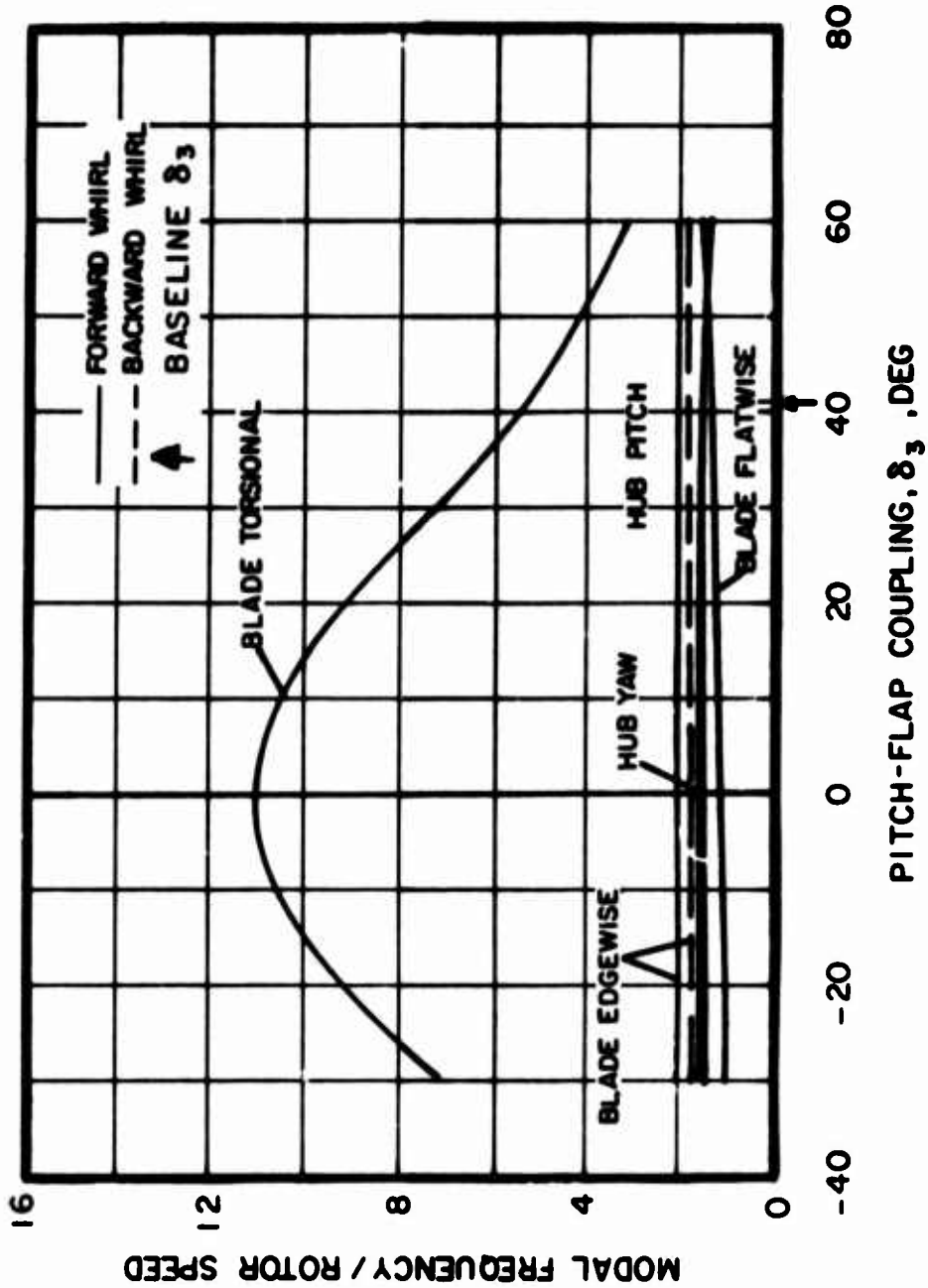

(b) Blade Whirl and Hub Modes

Figure 44. Concluded.

Effect of Blade Edgewise Natural Frequency

The blade edgewise natural frequency was varied by changing the radial distribution of the edgewise area moment of inertia. These variations gave a frequency range of 0.66 to 2.63 cycles/rev for tail rotor No. 1 and 0.68 to 2.66 cycles/rev for tail rotor No. 2. Four values were used.

The modal damping and frequencies obtained for the two rotors in hover and at advance ratio of 0.50 are presented in Figures 45 through 50.

From Figures 45(a) and 46(a), it is observed that the hover stability of the blade symmetric flatwise and torsional modes is little affected by changes in the edgewise natural frequency. The blade symmetric edgewise mode exhibits a slight reduction in modal damping for edgewise frequencies below 1.8 cycles/rev for both rotors. However, as the edgewise frequency is increased further, this mode becomes considerably more stable.

The frequency response of the blade symmetric modes for variations in edgewise natural frequency appears in Figures 49 and 50. The frequencies of the torsional and flatwise modes of both rotors remain constant throughout the range of edgewise frequency investigated. The frequency of the symmetric edgewise mode is almost equal to the edgewise blade natural frequency for both rotor systems. A coalescence of the blade symmetric flatwise and edgewise modal frequencies occurs at an edgewise natural frequency of 1.3 cycles/rev.

The hover stability characteristics of the blade whirl and rotor hub modes are illustrated in Figures 45(b) and 46(b) for tail rotors No. 1 and 2 respectively. From these figures, it is observed that the trend of modal damping with blade edgewise natural frequency is quite different for the two baseline rotors. Tail rotor No. 1 exhibits large changes in system stability as the edgewise natural frequency is increased above 1.6 cycles/rev, while the stability behavior of tail rotor No. 2 shows significant variations for edgewise natural frequencies below 1.6 cycles/rev. The backward whirl mode of the tail rotor No. 1 is marginally stable in the range of ω_{EN}/Ω from 0.66 to 1.80 cycles/rev. Both the forward and backward whirl edgewise modes become quite stable at higher edgewise natural frequencies, while the torsional response shows a large decrease in stability. This behavior may be caused by the interaction between the torsional and edgewise modes shown in Figure 49(b). The blade flatwise whirl mode and the rotor hub pitch and yaw modes for tail rotor No. 1 are not significantly affected by variations in blade edgewise natural frequency. The stability characteristics presented in Figure 46(b) for tail rotor No. 2 indicate that a strong coupling is present between the blade flatwise and edgewise forward whirl modes and the rotor hub pitch mode for edgewise natural frequencies below 1.6 cycles/rev. The stability of the blade flatwise forward whirl and the hub pitch modes decreases, while that of the blade edgewise forward whirl mode increases in this frequency range. From Figure 50(b), it is noted that the frequencies of these modes are all near each other. The response of the blade torsional

mode is not affected by changes in the blade edgewise natural frequency. This result is not surprising, since the blade torsional whirl frequency is well removed from all other system frequencies, as shown in Figure 50(b).

The stability trends with blade edgewise natural frequency presented in Figures 47 and 48 at an advance ratio of 0.50 show behavior similar to that discussed for the hover condition. The only exception is the blade edgewise forward whirl mode for tail rotor No. 1, which is unstable for ω_{FW}/Ω less than one cycle/rev. It may be added that the variations in stability with blade edgewise natural frequency are not as pronounced for the forward flight condition as for hover.

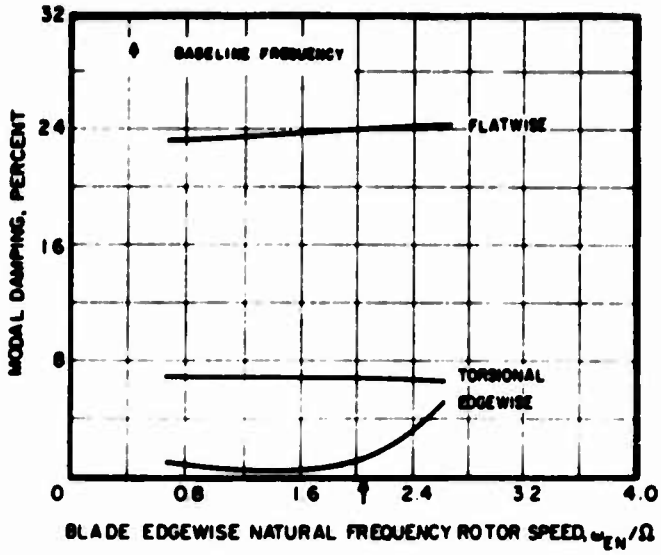

(a) Blade Symmetric Modes

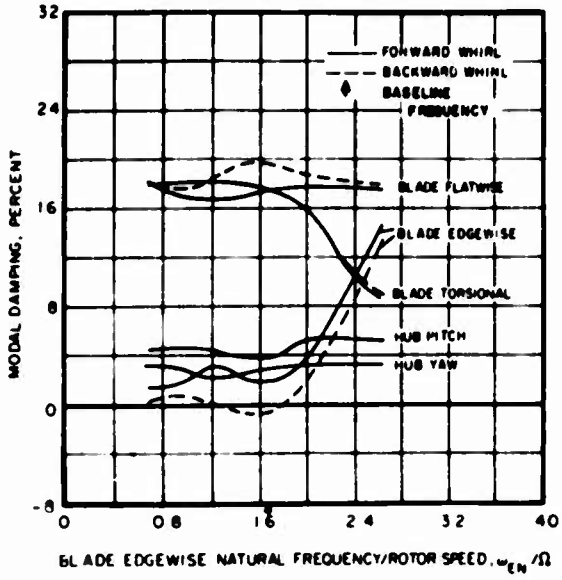

(b) Blade Whirl and Hub Modes

Figure 45. Effect of Blade Edgewise Natural Frequency on Modal Damping for Tail Rotor No. 1 in Hover.

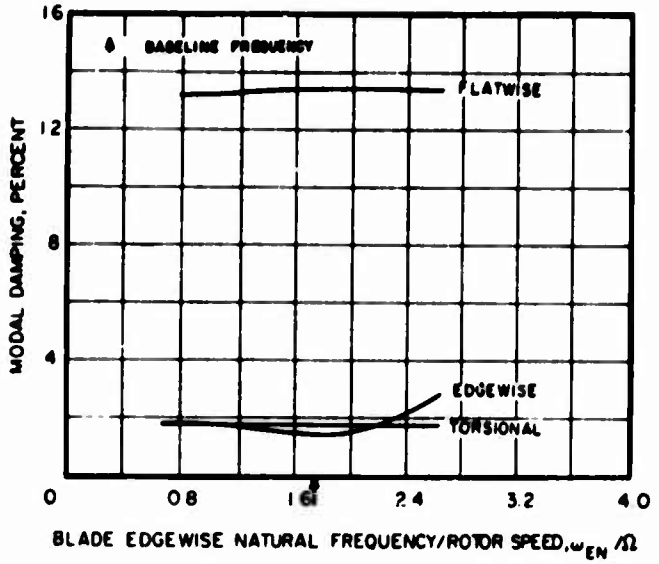

(a) Blade Symmetric Modes

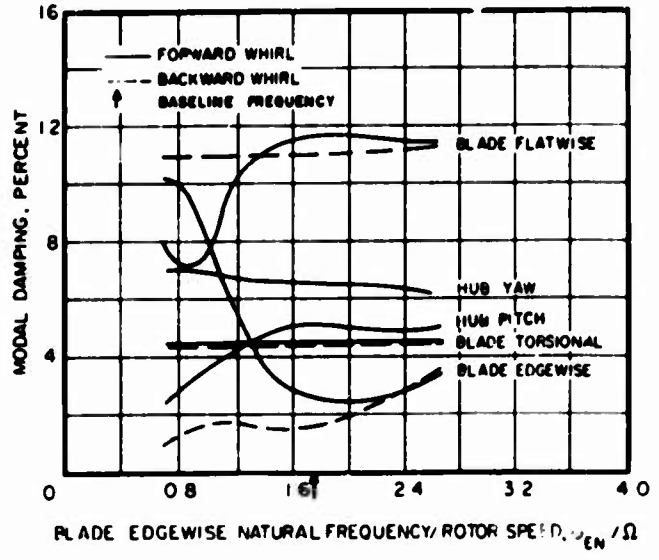

(b) Blade Whirl and Hub Modes

Figure 46. Effect of Blade Edgewise Natural Frequency on Modal Damping for Tail Rotor No. 2 in Hover.

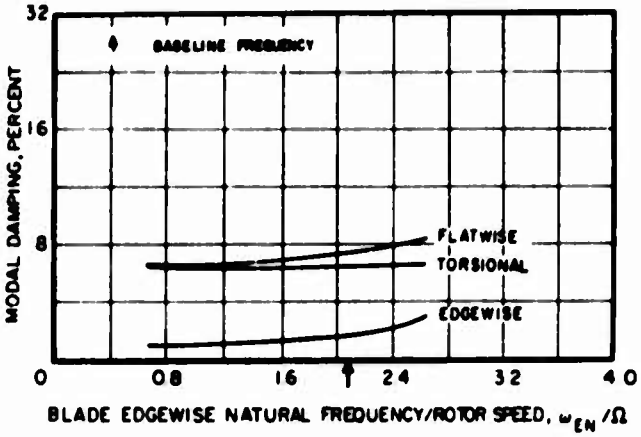

(a) Blade Symmetric Modes

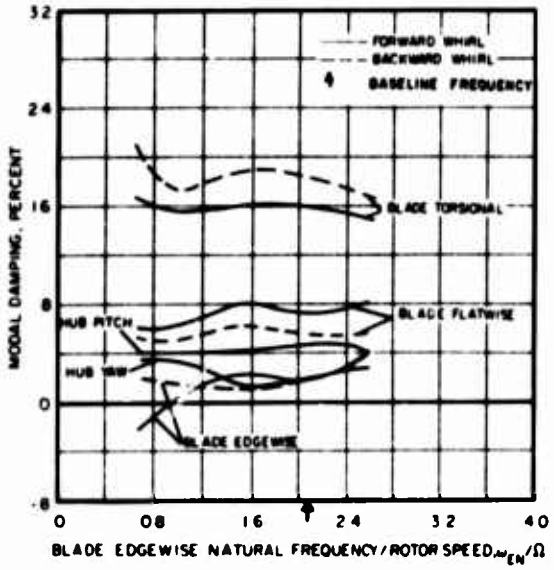

(b) Blade Whirl and Hub Modes

Figure 47. Effect of Blade Edgewise Natural Frequency on Modal Damping for Tail Rotor No. 1 at μ = .50.

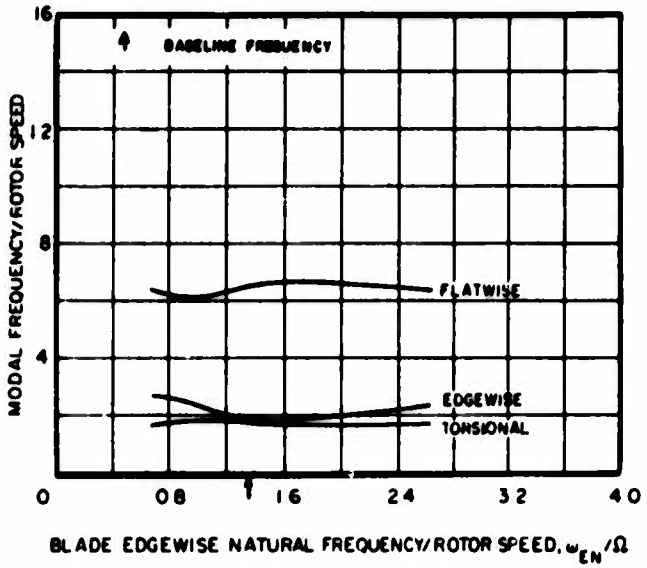

(a) Blade Symmetric Modes

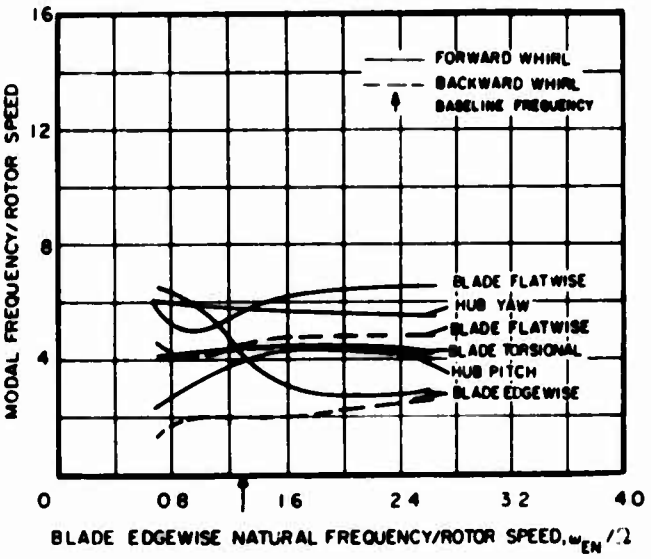

(b) Blade Whirl and Hub Modes

Figure 48. Effect of Blade Edgewise Natural Frequency on Modal Frequency for Tail Rotor No. 2 at $\mu = .50$.

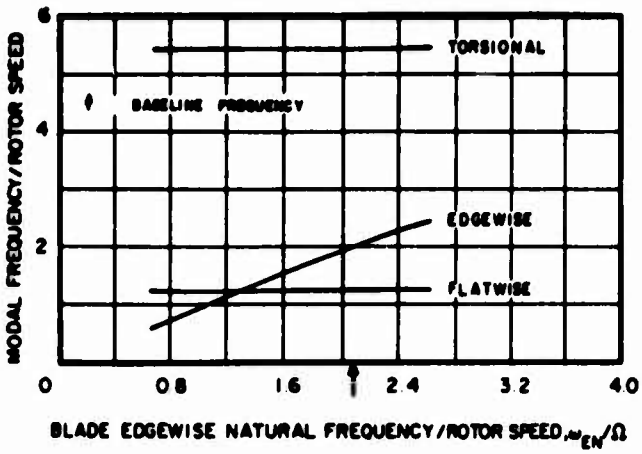

(a) Blade Symmetric Modes

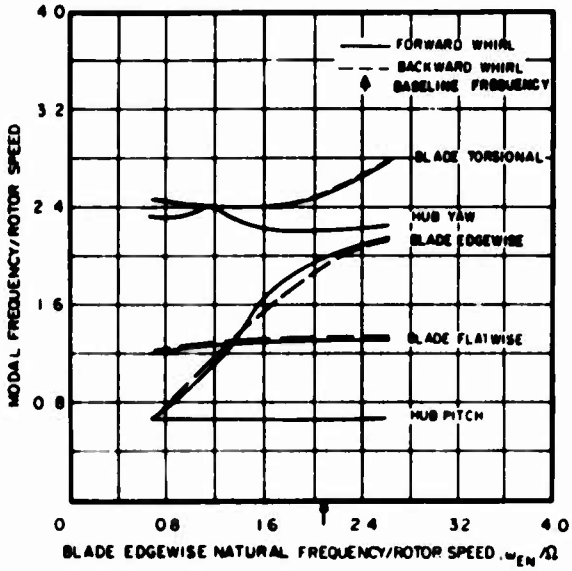

(b) Blade Whirl and Hub Modes

Figure 49. Effect of Blade Edgewise Natural Frequency on Modal Frequency for Tail Rotor No. 1 in Hover.

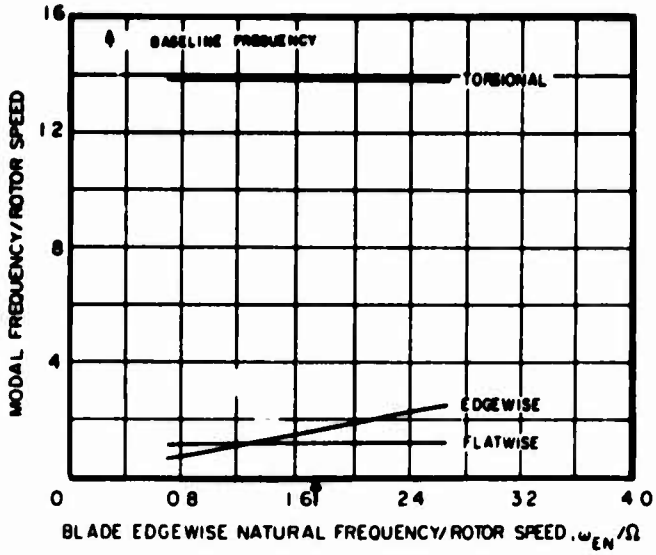

(a) Blade Symmetric Modes

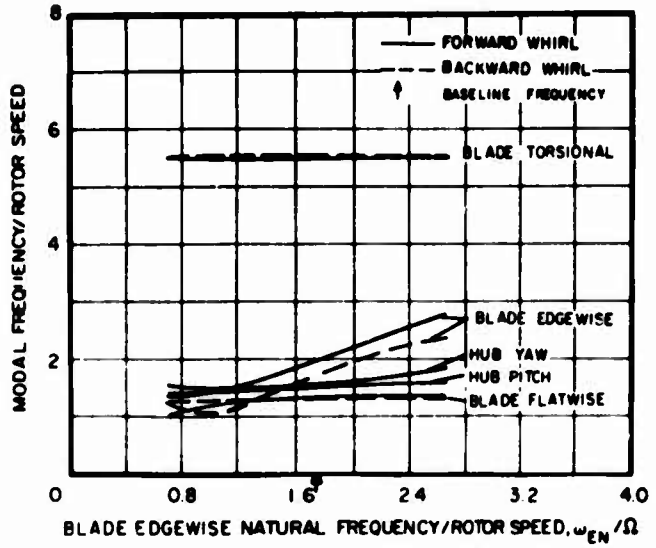

(b) Blade Whirl and Hub Modes

Figure 50. Effect of Blade Edgewise Natural Frequency on Modal Frequency for Tail Rotor No. 2 in Hover.

Effect of Rotor Hub Frequencies

The effect of variations in reference rotor hub frequency on the stability characteristics of the two baseline tail rotors is illustrated in Figure 51 through 56 in hover and at an advance ratio of 0.50. The generalized stiffness of the fixed system yaw and pitch modes was varied to give a range in reference yaw frequency of 0.625 to 20.0 cycles/rev for rotor No. 1 and 0.52 to 16.64 cycles/rev for rotor No. 2. Four values of stiffness were used. In Figures 51 through 56, the reference rotor hub pitch frequency is also shown; it ranges from 0.18 to 5.76 cycles/rev for rotor No. 1 and from 0.445 to 14.24 cycles/rev for rotor No. 2. The modal damping and frequency for the blade whirl and rotor hub modes only are shown in these figures since, for the modes used here, the fixed system motions do not affect the blade symmetric modes.

The stability characteristics in hover are presented in Figures 51 and 52 for tail rotors No. 1 and No. 2 respectively. From these figures, it can be seen that there is no appreciable change in the modal damping of the blade whirl modes at reference rotor hub frequencies above 4 cycles/rev. Below this frequency, however, the interaction between the fixed system motions and the blade flatwise and edgewise modes becomes more pronounced, especially for tail rotor No. 2. This effect may be expected from an inspection of the modal frequency characteristics presented in Figures 55 and 56. At low reference hub frequencies, the blade flatwise backward whirl mode for tail rotor No. 2 has a sharp reduction in modal damping, while the blade edgewise backward whirl becomes more stable. For both rotors, the stability of the rotor hub pitch and yaw modes increases significantly at low reference hub frequencies.

The stability characteristics at an advance ratio of 0.50 are shown in Figure 53 for tail rotor No. 1 and in Figure 54 for tail rotor No. 2. A comparison of these forward flight results with the hover results shows no major differences in the parametric effect of reference hub frequency on modal damping.

The frequency characteristics of both baseline rotors as a function of reference hub pitch and yaw frequencies appear in Figures 55 and 56. It can be seen that reference hub frequency has generally a negligible effect on the blade whirl frequencies. However, as previously discussed, an interaction between the hub and blade modes is present for tail rotor No. 2 at reference hub frequencies below 4 cycles/rev. Linear variations in modal frequency for the rotor hub pitch and yaw modes with reference hub frequency are shown in these figures for both baseline tail rotors. The calculated frequencies are slightly lower than the reference values due to the mass and inertia effects of the rotors.

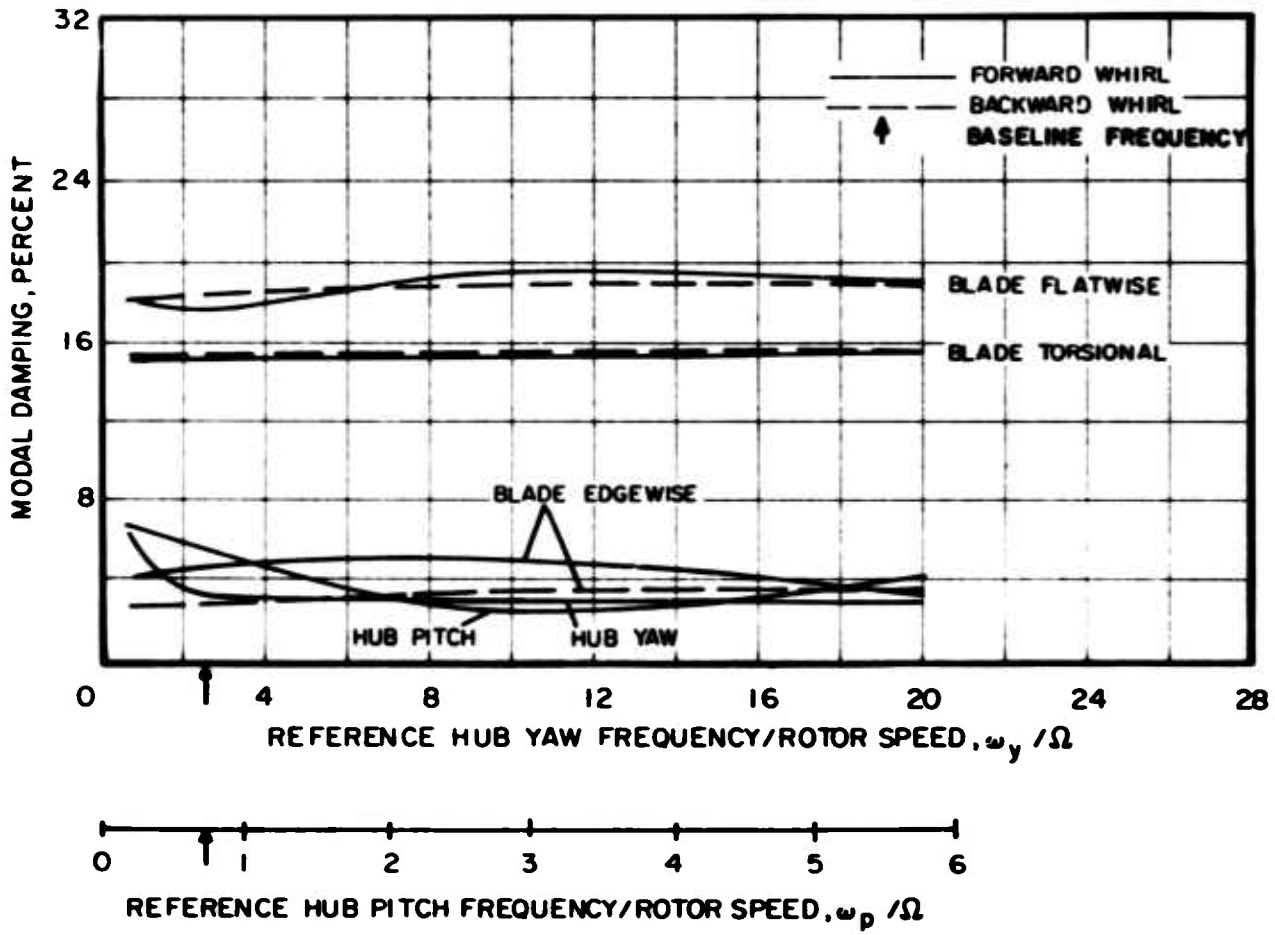

Figure 51. Effect of Rotor Hub Frequency on Modal Damping for Tail Rotor No. 1 in Hover.

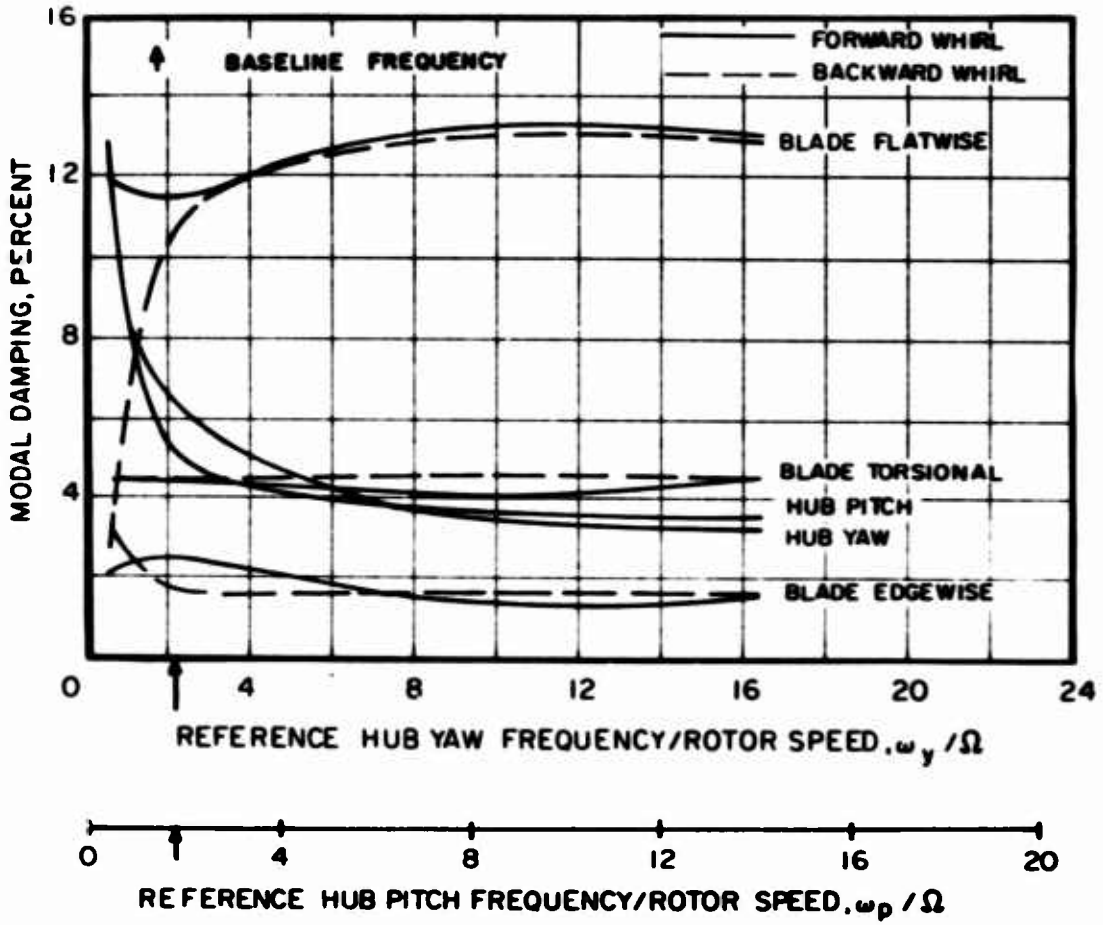

Figure 52. Effect of Rotor Hub Frequency on Modal Damping for Tail Rotor No. 2 in Hover.

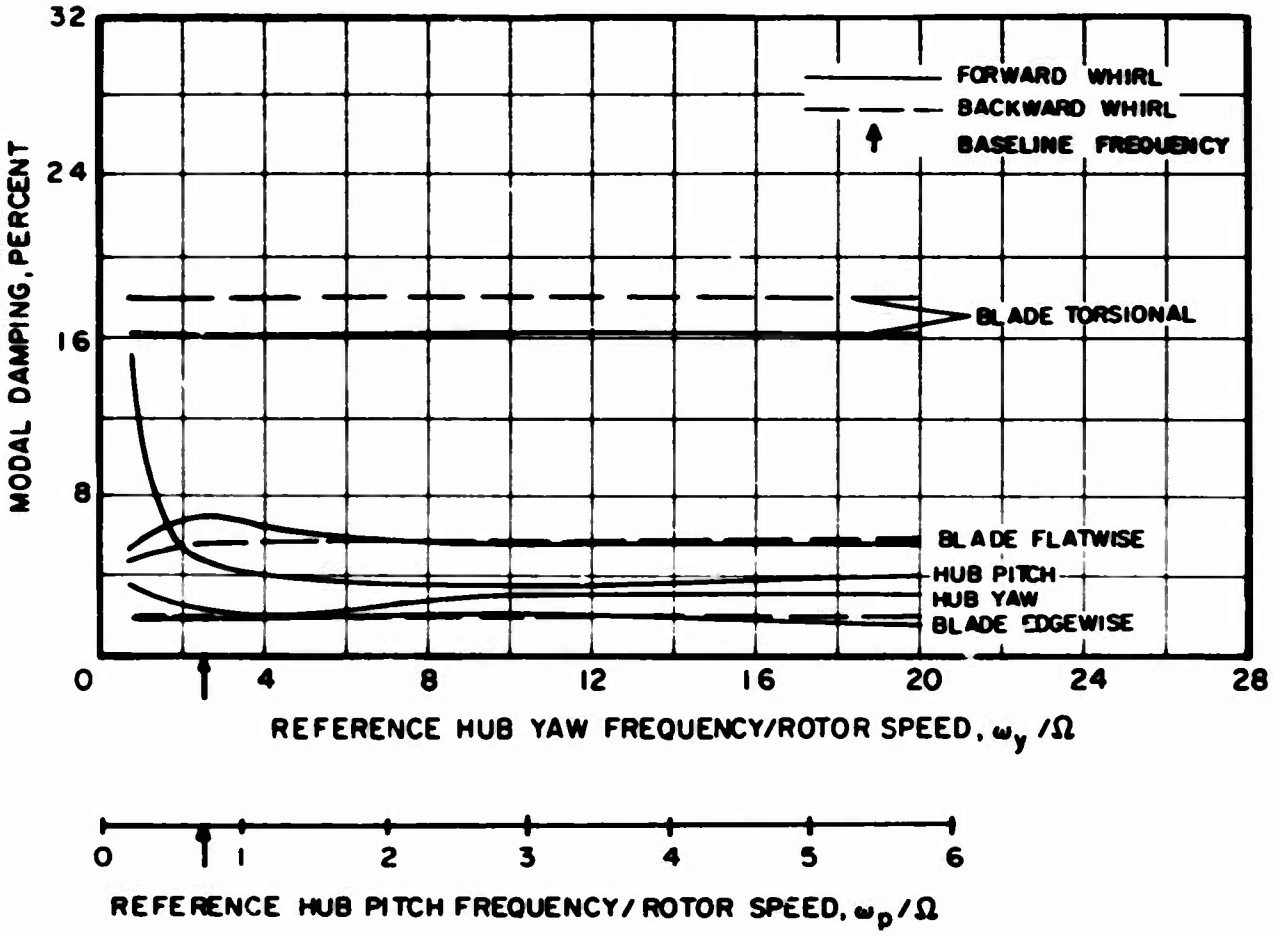

Figure 53. Effect of Rotor Hub Frequency on Modal Damping for Tail Rotor No. 1 at μ = .50.

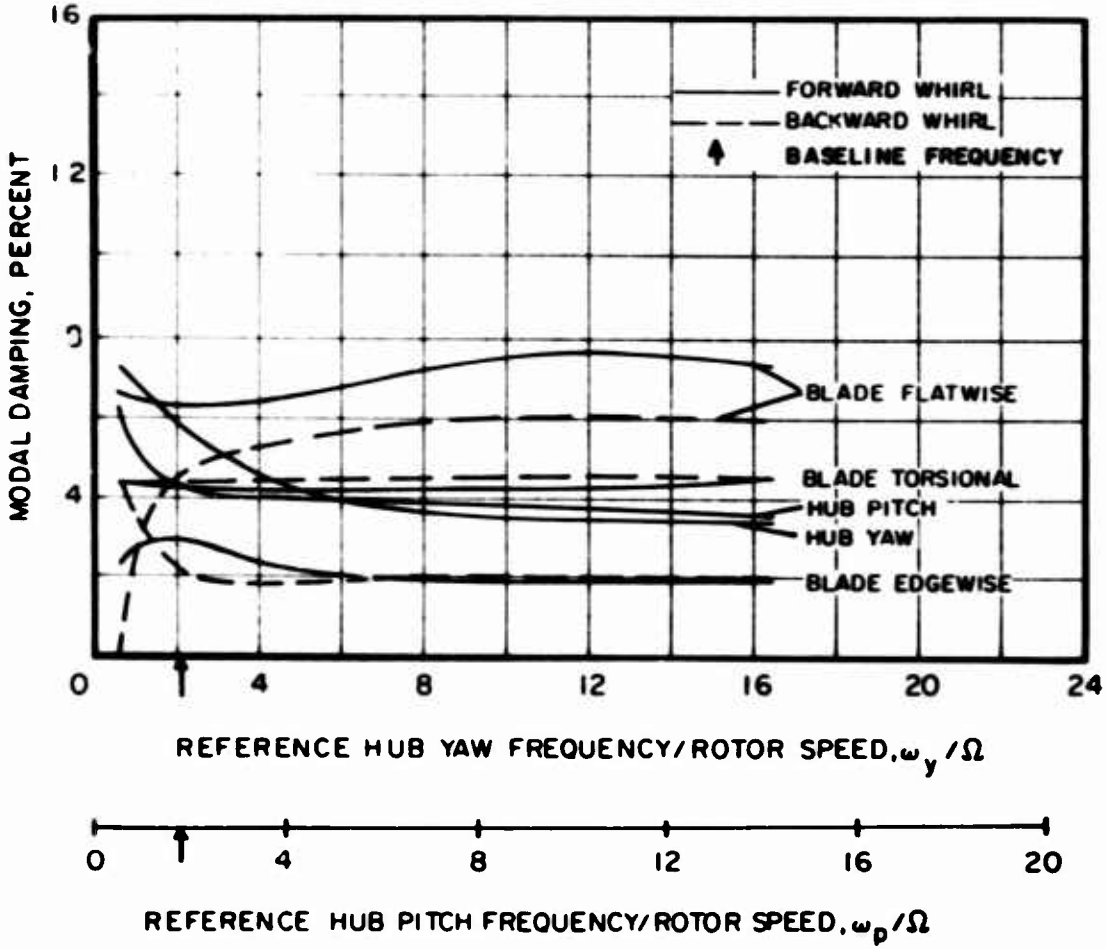

Figure 54. Effect of Rotor Hub Frequency on Modal Damping for Tail Rotor No. 2 at μ = .50.

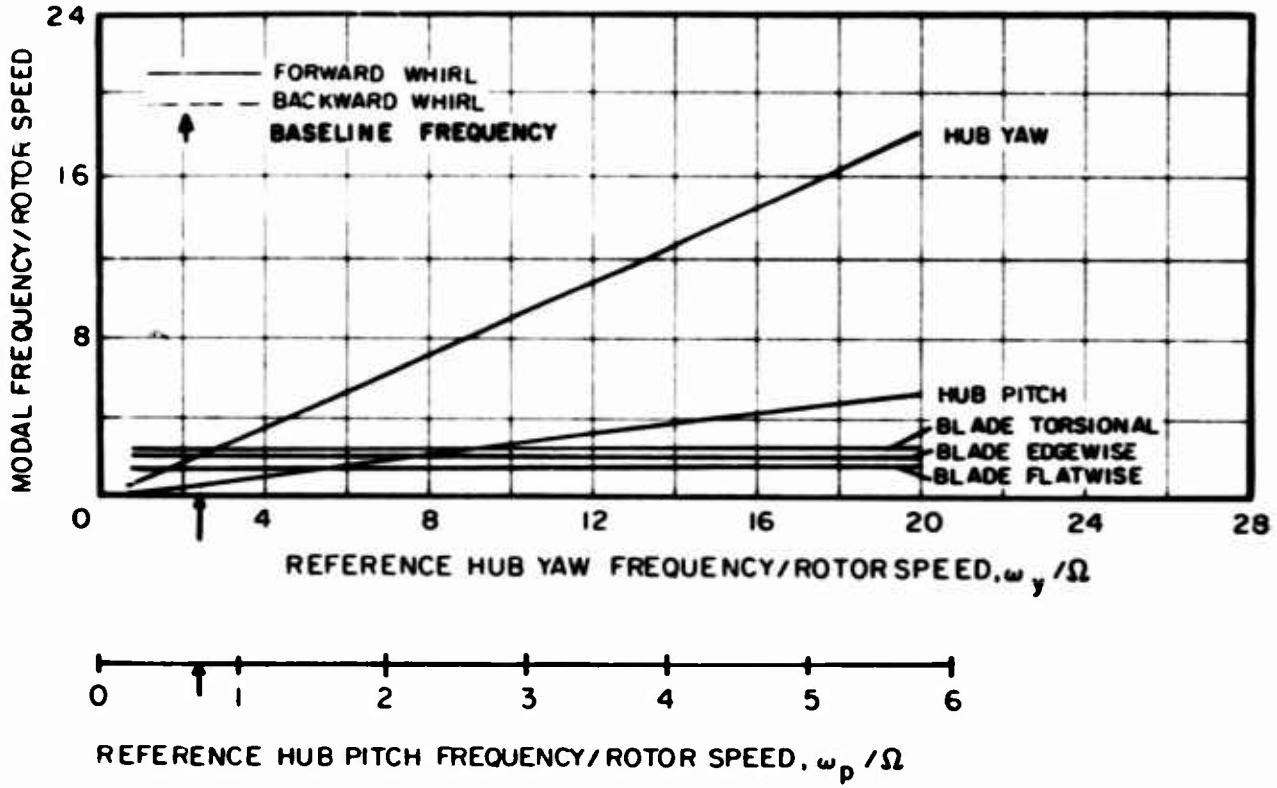

Figure 55. Effect of Rotor Hub Frequency on Modal Frequency for Tail Rotor No. 1 in Hover.

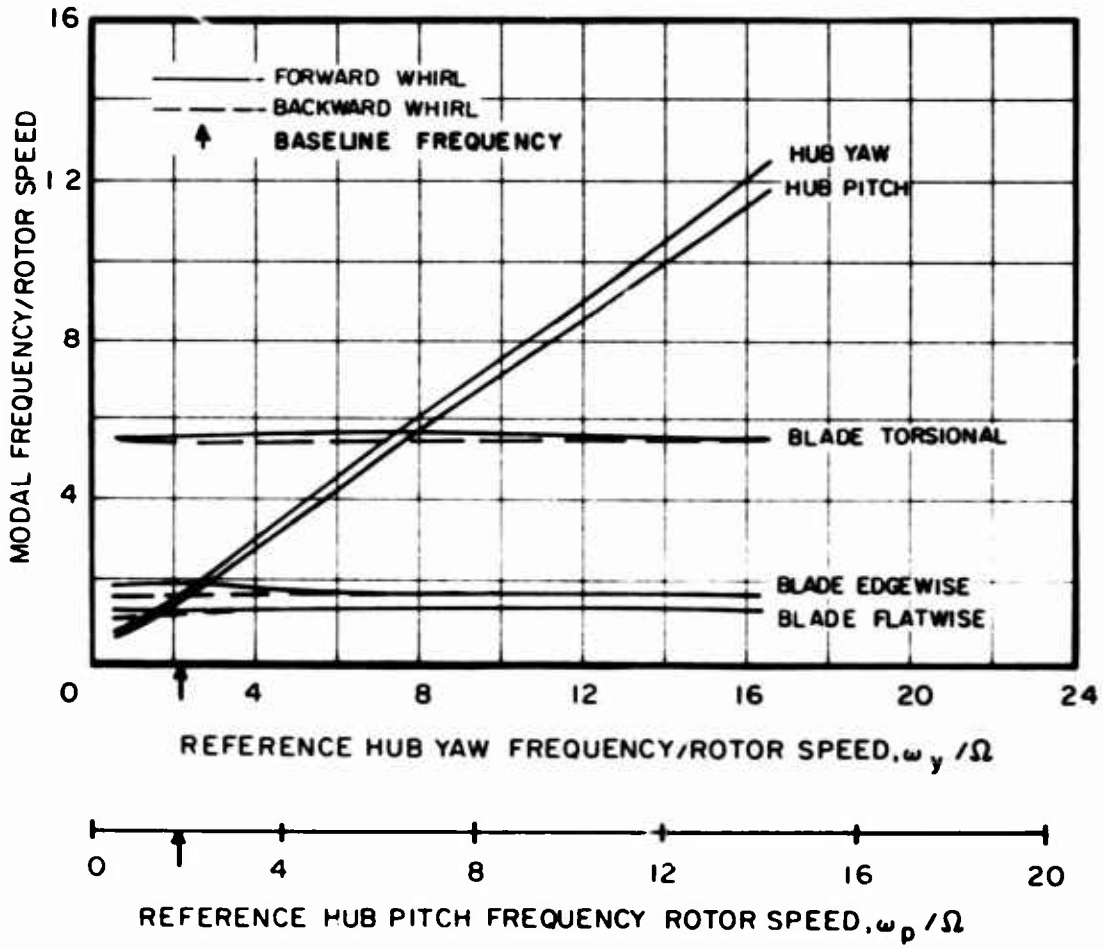

Figure 56. Effect of Rotor Hub Frequency on Modal Frequency for Tail Rotor No. 2 in Hover.

Effect of Blade Precone Angle

The effect of blade precone angle on the stability characteristics of tail rotor No. 2 is presented in Figures 57 through 59. Only tail rotor No. 2 was considered for this portion of the study since it is nonarticulated in the flatwise direction and can thus be preconed. A range in blade precone from -6 to 6 degrees was examined. Five values were used. The results from Figure 57(a) in hover show that blade precone has little effect on the modal damping of the blade symmetric flatwise and edgewise modes, while the torsional mode exhibits an increase in stability as the blade is preconed. However, from Figure 58(a) at an advance ratio of 0.50, the blade symmetric flatwise mode indicates an increase in modal damping with blade precone, while the torsional mode becomes more stable than the hover case.

The variations in modal damping with precone for the blade whirl and rotor hub modes appear in Figures 57(b) and 58(b) for advance ratios of zero and 0.50 respectively. From these figures, it is observed that the blade torsional whirl mode is least stable for zero precone, a behavior similar to that of the symmetric torsional mode. An increase in precone reduces the stability of the blade edgewise whirl mode, while the flatwise whirl mode becomes more stable; these effects are generally greater for the forward flight condition. The rotor hub modes show generally small variations in mode damping response with blade precone except for the pitch mode in hover. The damping of the pitch mode decreases from 6 to 4 percent as precone is increased from -6 to 6 degrees.

A negligible effect of blade precone on modal frequency is exhibited by the results shown in Figure 59(a) for the blade symmetric modes and in Figure 59(b) for the blade unsymmetric and rotor hub modes.

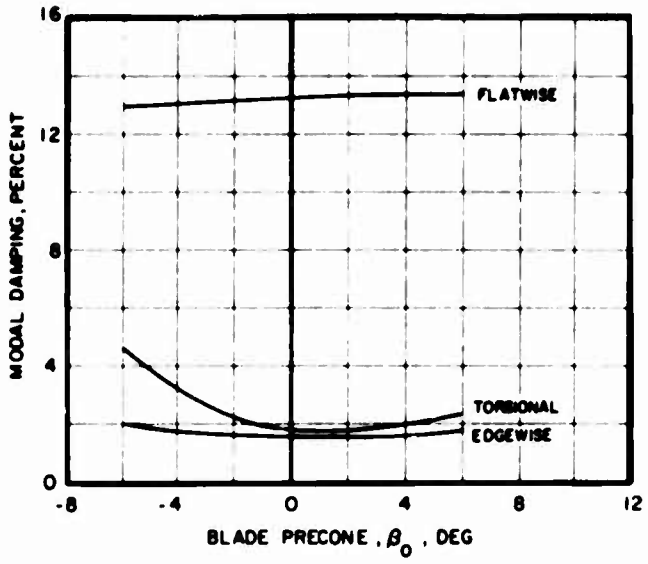

(a) Blade Symmetric Modes

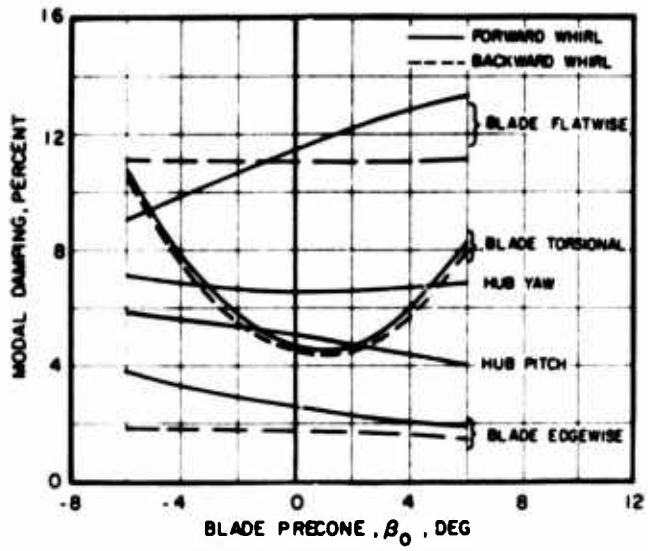

(b) Blade Whirl and Hub Modes

Figure 57. Effect of Blade Precone on Modal Damping for Tail Rotor No. 2 in Hover.

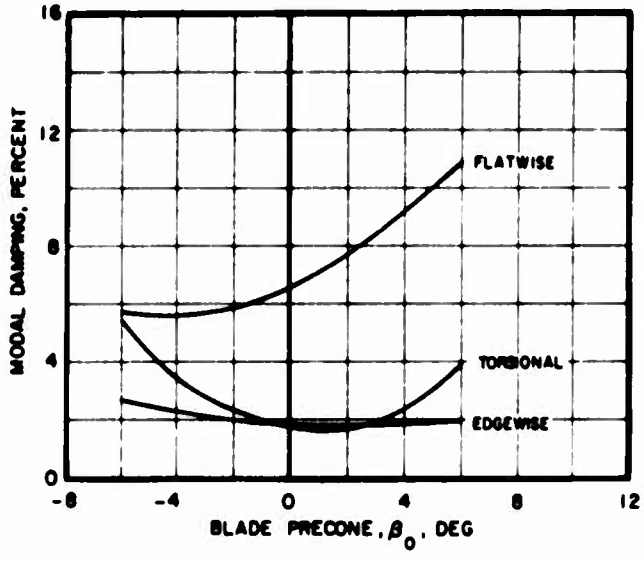

(a) Blade Symmetric Modes

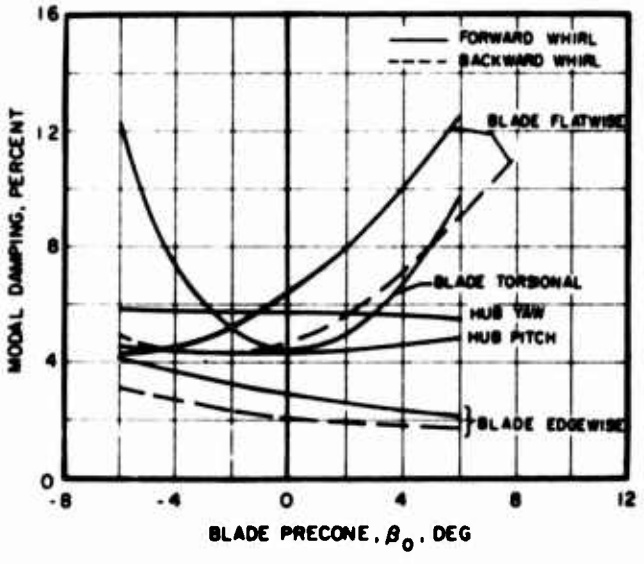

(b) Blade Whirl and Hub Modes

Figure 58. Effect of Blade Precone on Modal Damping for Tail Rotor No. 2 at μ = .50.

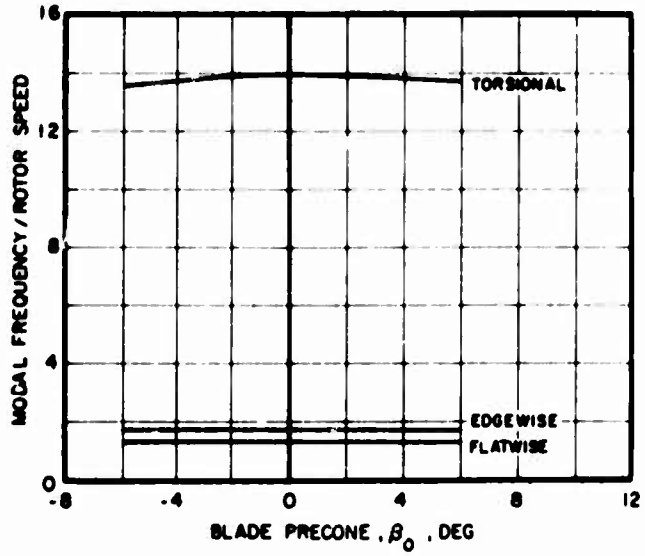

(a) Blade Symmetric Modes

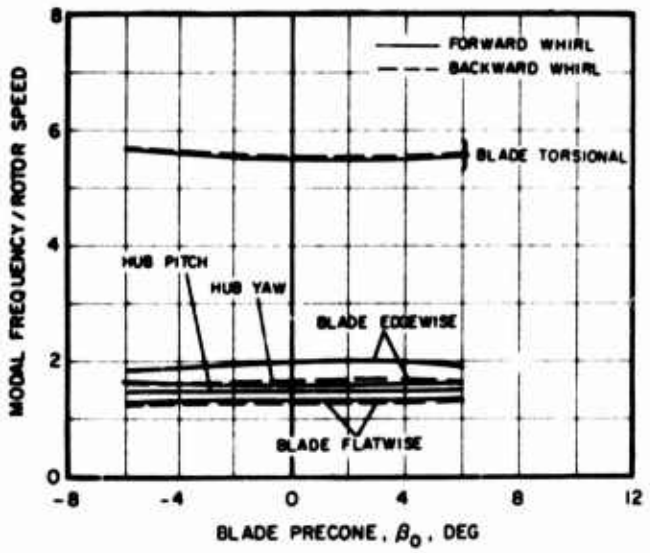

(b) Blade Whirl and Hub Modes

Figure 59. Effect of Blade Precone on Modal Frequency for Tail Rotor No. 2 in Hover.

Effect of Pitch-Lag Coupling

Variations in pitch-lag coupling over the range -0.2 to 0.2 for both baseline rotors in hover and at an advance ratio of 0.5 produced no discernible change in stability. The fact that both rotors are relatively stiff inplane is the cause of this effect. However, it is known that pitch-lag coupling can appreciably affect the stability of soft inplane rotors. Therefore, in such cases the parameter should be accurately defined and incorporated in any analysis.

CONCLUDING REMARKS

The major objectives of this study were, first, to develop a computerized eigenvalue analysis that had a sufficiently complete dynamic and aerodynamic description of coupled rotor/airframe/control systems to allow accurate stability estimations and, second, to demonstrate some of its capabilities through parametric and sensitivity studies of representative semiarticulated and hingeless tail rotor systems. Both of these objectives were achieved.

The studies described in the foregoing were necessarily restricted to simplified systems, but they do serve to illustrate the potential of the analysis. The inclusion of forward flight effects in the analysis is a big step forward and considerably extends the envelope within which the analysis can be applied. Although not exercised in these studies, the unsteady aerodynamics serve to further refine the modelling of aerodynamic effects, thus permitting flutter and wake interaction studies. The models used for the control systems can accurately represent the dynamics of most existing systems, thereby reducing the number of effects not properly accounted for in the overall system. The overall usefulness of the analysis was further extended by inclusion of the gimbaled rotor capability.

Since a number of unstable phenomena involve coupling between rotor system and fixed system motions, it is important that the analysis have the facility to predict these. This is adequately accounted for by inclusion of an airframe (or fixed system) model that can represent rigid body and elastic modes, including local transmission, etc., modes.

The methods employed in the development of the analysis are given in the appendixes, together with the final equations of motion.

A final comment on the computer program of the analysis: although this in its entirety gives a refined description of coupled rotor/airframe/control systems, it was realized that there are many instances when studies employing simple systems are desired. To this end, the program is so designed that the user, by use of simple control cards, can specify the precise degree of freedom, type of control system, mode of flight, and type of aerodynamics that he wishes to use. From this point, the program assumes executive control and automatically performs the desired functions. This feature allows systems with as little as one degree of freedom to be analyzed and makes it possible for inexperienced users to run the program with little difficulty.

RECOMMENDATIONS

The analysis described in this report represents a fairly complete description of a coupled rotor/airframe/control system. Its capacity to treat rotor systems in hover and forward flight has been demonstrated. However, the effects of unsteady aerodynamics and cyclic inputs to the dynamic system equations have not been explored. In addition, the representation of the blade pitch control system in the parametric and sensitivity studies did not account for multi-degree-of-freedom effects or the effects of the control servos and servo feedback parameters. The representation of hub motions was also idealized.

Clearly, in practice such exclusions and simplifications may be neither warranted nor desired. If we wish to define the overall system stability characteristics to the best of our ability, and within the constraints of the accuracy of the analysis we are employing, it behooves us to model that system as accurately as possible. Therefore, we must include in our studies all of the elements that we feel could play an important part in our predictions.

It is, therefore, recommended that the effects of inclusion of unsteady aerodynamics and cyclic inputs to the dynamic system equations be established. Recent studies using a simplified Floquet analysis have, for example, shown that the inclusion of cyclic pitch had a pronounced effect on the pitch lag stability of a rotor. In this case, the classical hover expressions were nonconservative.

It is also recommended that the analysis be subjected to extensive use. It is only by using the analysis and possibly even questioning certain aspects of the modelling that the user can become familiar enough with its general characteristics to effectively incorporate improvements. Also, it is only through use that a complete understanding of the real meaning of the output can be gained.

In its present form, the computer program of the analysis relies on some unlinked transient aeroelastic analysis for production of the derivative terms required for forward flight studies. The analysis currently used for this purpose is the Y-200 Normal Modes Analysis provided to the Army under Contract DAAJ02-71-C-0024. Unfortunately, this analysis has some inconsistencies with the E-927 Aeroelastic Rotor Stability Analysis. Not the least of these are the facts that Y-200 can accept only one blade angle distribution and that it does not permit representation of control system dynamics. It is, therefore, recommended that these and any other inconsistencies be eliminated and that Y-200 be linked to E-927 to facilitate use of the program.

Finally, any analysis is only as good as the confidence we place in its predictions. Obviously, such confidence can only be obtained, or increased, by correlating the analysis with test data. Unfortunately, only limited correlation of the present analysis has been completed. Much remains to be done. To close this gap, it is suggested that consideration be given to the initiation of a model test program to provide the needed data. Such a program could be designed to accurately model not only the rotor blades but also the control system and the test rig characteristics. By making parametric variations of the system dynamic characteristics and conducting hovering and forward flight tests, very valuable data could be acquired. Since the analysis is capable of accurately modelling the systems, very meaningful correlation could be obtained.

APPENDIX A

HOVER ANALYSIS

This appendix gives details of the development of an analysis designed to study the stability of helicopter main or tail rotors in hover, or under conditions of pure axial flow. It can also be used to study the stability of propellers.

Important assumptions are noted below and the coordinate system employed is shown in Figure A1. The coordinates used for the control systems are defined later in the text.

ASSUMPTIONS

1. Dynamic and aerodynamic effects assume small perturbations about steady initial values of the system generalized coordinates.

2. Aerodynamic forces are developed using strip theory.

3. Radial flow effects are neglected.

4. Products involving up to the squares of steady displacements and a perturbation displacement, velocity, or acceleration are retained.

5. Rotor speed is constant.

6. No small-angle assumptions are applied to the blade collective pitch or twist.

7. Because of the rotating system generalized coordinate transformations employed, only rotors with three or more blades can be treated.

8. Stall, compressibility, and unsteady effects are included.

9. Inflow is constant over the rotor disc.

10. Blades have an elastic axis.

11. Blade flap and lag hinges are coincident.

12. The blade feathering bearing can either remain in the plane of the hub or follow the blade root out-of-plane slope. A similar statement can be made regarding inplane motion.

13. The rotor shaft experiences no torsional deformations.

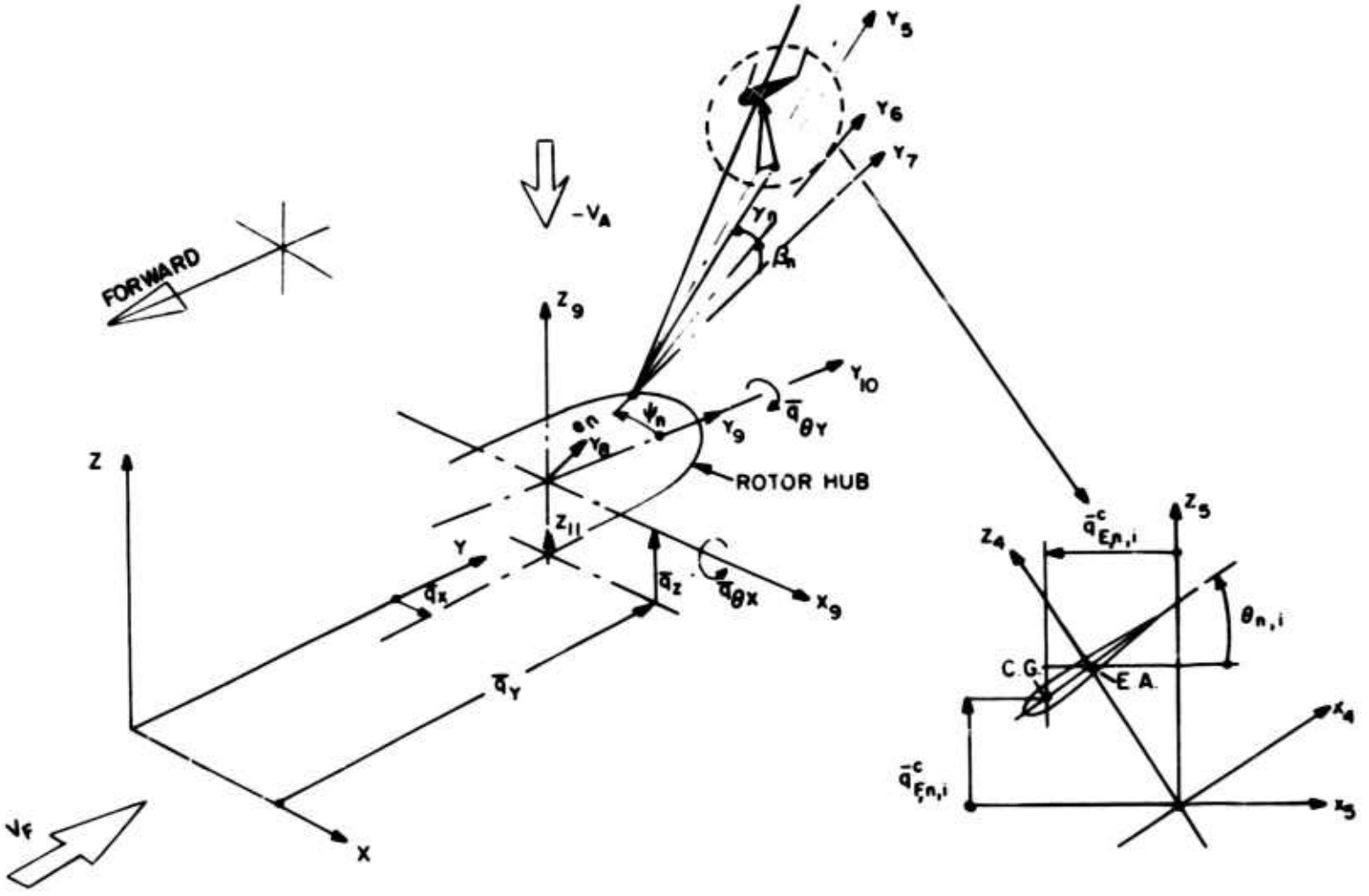

Figure A1. Aeroelastic Rotor Stability Analysis Coordinate System.

14. Only those aerodynamic forces associated with the rotor system are considered. Rotor/airframe interference effects and airframe lift/drag are not included.

DEVELOPMENT OF HOVER ANALYSIS

Dynamic System Equations

The development of the equations of motion of the total dynamic system follows the classical path of first defining the kinetic and potential energies and dissipation potentials of the system, then establishing Lagrange's equations in the form

$$\frac{d}{dt}\left(\frac{\partial T}{\partial \dot{q}_j}\right) - \frac{\partial T}{\partial q_j} + \frac{\partial V}{\partial q_j} + \frac{\partial D}{\partial \dot{q}_j} = 0 \qquad \text{(A1)}$$

In what follows, to preserve clarity, the total dynamic system is broken down into four major subsystems. These are:

1. The rotor blades.
2. The fixed, or airframe, system.
3. The control systems.
4. The servo systems.

Each of these is treated separately, but it will be apparant that their dynamic responses are all close coupled through the motions of the respective coupling generalized coordinates.

Equation A1 is indeed a simple statement of fact, but the development of the terms on the left-hand side does, for a multi-degree-of-freedom system, present a very formidable task that requires extensive expansion and manipulation of large arrays of matrices. In the interests of documenting the analysis in a not too cumbersome fashion, obvious intermediate steps are omitted, but sufficient detail is retained to show how the final forms of the equations of motion were established.

In the development of the equations, a number of transformation matrices and vectors are employed. These are defined below for easy reference.

$$A_{\bar{q}_{\theta Y}} = \begin{bmatrix} \cos\bar{q}_{\theta Y} & 0 & \sin\bar{q}_{\theta Y} \\ 0 & 1 & 0 \\ -\sin\bar{q}_{\theta Y} & 0 & \cos\bar{q}_{\theta Y} \end{bmatrix} \tag{A2}$$

$$A_{\bar{q}_{\theta X}} = \begin{bmatrix} 1 & 0 & 0 \\ 0 & \cos\bar{q}_{\theta X} & -\sin\bar{q}_{\theta X} \\ 0 & \sin\bar{q}_{\theta X} & \cos\bar{q}_{\theta X} \end{bmatrix} \tag{A3}$$

$$A_{\psi,n} = \begin{bmatrix} \cos\psi_n & -\sin\psi_n & 0 \\ \sin\psi_n & \cos\psi_n & 0 \\ 0 & 0 & 1 \end{bmatrix} \tag{A4}$$

$$A_{\beta,n} = \begin{bmatrix} 1 & 0 & 0 \\ 0 & \cos\beta_n & -\sin\beta_n \\ 0 & \sin\beta_n & \cos\beta_n \end{bmatrix} \tag{A5}$$

$$A_{\gamma,n} = \begin{bmatrix} \cos\gamma_n & -\sin\gamma_n & 0 \\ \sin\gamma_n & \cos\gamma_n & 0 \\ 0 & 0 & 1 \end{bmatrix} \tag{A6}$$

$$A_{\theta,n,i} = \begin{bmatrix} \cos\theta_{n,i} & 0 & -\sin\theta_{n,i} \\ 0 & 1 & 0 \\ \sin\theta_{n,i} & 0 & \cos\theta_{n,i} \end{bmatrix} \tag{A7}$$

$$A_{q^{c'}_{E,n,i}} = \begin{bmatrix} \cos q^{c'}_{E,n,i} & -\sin q^{c'}_{E,n,i} & 0 \\ \sin q^{c'}_{E,n,i} & \cos q^{c'}_{E,n,i} & 0 \\ 0 & 0 & 1 \end{bmatrix} \tag{A8}$$

$$A_{q^{c'}_{F,n,i}} = \begin{bmatrix} 1 & 0 & 0 \\ 0 & \cos q^{c'}_{F,n,i} & -\sin q^{c'}_{F,n,i} \\ 0 & \sin q^{c'}_{F,n,i} & \cos q^{c'}_{F,n,i} \end{bmatrix} \tag{A9}$$

$$I_{n,i} = \begin{bmatrix} I_{X,n,i}, & 0 & , & 0 \\ 0 & , I_{Y,n,i}, & & 0 \\ 0 & , & 0 & , I_{Z,n,i} \end{bmatrix} \tag{A10}$$

$$q_{r,i} = \begin{Bmatrix} (\int_0^{r_{n,i}} -\cos q'_{F,n} \sin q'_{E,n} dr) - CG \\ (\int_0^{r_{n,i}} \cos q'_{F,n} \cos q'_{E,n} dr) \\ (\int_0^{r_{n,i}} \sin q'_{F,n} dr) \end{Bmatrix} = \begin{Bmatrix} -q_{E,n,i} - CG \\ r_{n,i} - \int_0^{r_{n,i}} (\frac{(q'_{E,N})^2}{2} + \frac{(q'_{F,n})^2}{2}) dr \\ q_{F,n,i} \end{Bmatrix} \tag{A11}$$

$$\begin{Bmatrix} A_{\theta,n,i} \dot{q}_{n,i} \end{Bmatrix} = \begin{Bmatrix} -(\sum_{t=1}^{NE} \phi_{E,i,t} \dot{q}_{T,n,t}) - (q_{FO,n,i} - CG_{n,i} \sin\theta_{o,n,i}) \dot{\theta}_{n,i} \\ \dot{\bar{r}}_{n,i} \\ (\sum_{t=1}^{NE} \phi_{F,i,t} \dot{q}_{T,n,t}) + (q_{EO,n,i} - CG_{n,i} \cos\theta_{o,n,i}) \dot{\theta}_{n,i} \end{Bmatrix} \tag{A12}$$

$$\dot{\bar{r}}_{n,i} = -\sum_{t=1}^{NE} \sum_{s=1}^{NE} (\int_0^{r_{n,i}} ((-q'_{EO,n} \phi'_{E,t} + q'_{FO,n} \phi'_{F,t}) \dot{q}_{T,n,t} + (\phi'_{E,t} \phi'_{E,s} + \phi'_{F,t} \phi'_{F,s}) q_{T,n,t} \dot{q}_{T,n,s}) dr) \tag{A13}$$

$$\bar{q}^c_{E,n,i} = (\sum_{t=1}^{NE} \phi_{E,i,t} q_{T,n,t}) - q_{EO,n,i} + CG_{n,i} \cos\theta_{n,i} \tag{A14}$$

$$\bar{q}^c_{F,n,i} = (\sum_{t=1}^{NE} \phi_{F,i,t} q_{T,n,t}) + q_{FO,n,i} - CG_{n,i} \sin\theta_{n,i} \tag{A15}$$

$$q^{c'}_{E,n,i} = (\sum_{t=1}^{NE} \phi'_{E,i,t} q_{T,n,t}) - q'_{EO,n,i} \tag{A16}$$

$$q^{c'}_{F,n,i} = (\sum_{t=1}^{NE} \phi'_{F,i,t} q_{T,n,t}) + q'_{FO,n,i} \tag{A17}$$

$$\theta_{n,i} = \theta_{o,n,i} + \phi_{\theta,i} \theta_{T,n} \tag{A18}$$

$$\bar{E}_n = \{ 0 \quad , e_n \quad , 0 \quad \} \tag{A19}$$

$$\bar{q} = \{ \bar{q}_X \quad , \bar{q}_Y \quad , \bar{q}_Z \quad \} \tag{A20}$$

$$\bar{X}_{n,i} = \{ X_{n,i} \quad , Y_{n,i} \quad , Z_{n,i} \quad \} \tag{A21}$$

$$\bar{\theta}_{n,i} = \{ \theta_{X,n,i}, \theta_{Y,n,i}, \theta_{Z,n,i} \} \tag{A22}$$

$$\bar{q}_{\theta Y} = \left(\sum_{s=1}^{NA} \phi_{\theta Y,s} \bar{q}_s \right) \tag{A23}$$

$$\bar{q}_{\theta X} = \left(\sum_{s=1}^{NA} \phi_{\theta X,s} \bar{q}_s \right) \tag{A24}$$

$$\bar{q}_X = \left(\sum_{s=1}^{NA} \phi_{X,s} \bar{q}_s \right) \tag{A25}$$

$$\bar{q}_Y = \left(\sum_{s=1}^{NA} \phi_{Y,s} \bar{q}_s \right) \tag{A26}$$

$$\bar{q}_Z = \left(\sum_{s=1}^{NA} \phi_{Z,s} \bar{q}_s \right) \tag{A27}$$

Relations A2 through A9 are the coordinate transformation matrixes. A10 is the matrix of the blade flatwise, torsional, and edgewise mass moments of inertia about the local center of gravity. All defines the uncoupled blade bending coordinates including the radial shortening caused by bending. A12 is a velocity vector that includes the effects of bending and pitching velocities, steady bending displacements and pitch angles, and center of gravity offset. A13 defines the local radial velocity. Relations A14 through A27 are self-explanatory definitions of various coordinates and vectors.

The coordinates were transformed as follows:

(1) Translate through CG.

(2) Rotate through uncoupled blade flatwise and edgewise slopes and integrate to define the vector A11.

(3) Rotate through blade pitch and define the coupled coordinates given by A14 and A15.

(4) Rotate through blade rigid-body lag.

(5) Rotate through blade rigid-body flap.

(6) Translate through offset.

(7) Rotate through azimuth angle.

(8) Rotate through hub pitch.

(9) Rotate through hub roll.

(10) Translate through hub vertical, lateral, and longitudinal displacements.

Derivation of Subsystem Dynamic Characteristics

Rotor Blades

Consider first the kinetic energy. This can be broken down into two parts: that associated with translational motion and that associated with pure rotational motion.

Translantional Kinetic Energy

Using the coordinate system shown in Figure A1 and performing the required coordinate rotations and translations, it can be shown that the absolute translational motion of a blade element i at blade station $r_{n,i}$ on any blade n is given by

$$\bar{X}_{n,i} = A_{\bar{q}\theta Y} A_{\bar{q}\theta X} \Lambda_{\psi,n} (A_{\beta,n} A_{\gamma,n} \bar{q}_{n,i} + \bar{E}_n) + \bar{Q} \tag{A28}$$

where

$$\bar{q}_{n,i} = A_{\theta,n,i} q^c_{n,i}$$

$$= \{ -\bar{q}^c_{E,n,i}, \bar{r}_{n,i}, \bar{q}^c_{F,n,i} \} \tag{A28a}$$

Taking the first time derivative of $\bar{X}_{n,i}$ the total kinetic energy arising from translational motion of all elements of all blades can be written

$$T_{BT} = \tfrac{1}{2} \sum_{n=1}^{N} \left(\sum_{i=1}^{NB} (\dot{\bar{X}}_{n,i})^T (\dot{\bar{X}}_{n,i}) m_{n,i} \delta r_{n,i} \right) \tag{A29}$$

Rotational Kinetic Energy

Since angular velocity follows the rule $\dot{\theta}_A = \dot{\theta}_{A,B} + \dot{\theta}_B$, where $\dot{\theta}_{A,B}$ denotes the angular velocity of the coordinate system A relative to that of the coordinate system B, the angular velocity components of the blade can be expressed as the sum of the relative angular velocities between each of the coordinate systems given in Figure A1. Thus, the absolute angular velocity of any blade element i at blade station $r_{n,i}$ on any blade n is given by

$$\begin{aligned}\dot{\bar{\theta}}_{n,i} = {} & i_3\left(\sum_{t=1}^{NE} \phi'_{F,i,t}\dot{q}_{T,n,t}\right) + k_4\left(\sum_{t=1}^{NE} \phi'_{E,i,t}\dot{q}_{T,n,t}\right) \\ & - j_5\phi_{\theta,i}\dot{\theta}_{T,n} + k_6\dot{\gamma}_n + i_7\dot{\beta}_n + k_9\dot{\psi}_n \\ & + i_{10}\left(\sum_{s=1}^{NA} \phi_{\theta X,s}\dot{\bar{q}}_s\right) + j_{11}\left(\sum_{s=1}^{NA} \phi_{\theta Y,s}\dot{\bar{q}}_s\right)\end{aligned} \tag{A30}$$

The various components of this velocity vector are readily developed if we recognize that the i_k, j_k, k_k are the unit vectors associated with their corresponding rotational transformation matrices. Therefore, to obtain $\dot{\bar{\theta}}_{n,i}$ we must express the i_k, j_k, k_k in terms of i_2, j_2, k_2. Using the transformation matrices defined earlier, we can write

$$\begin{aligned} j_{11} = j_{10} &= j_9\cos\bar{q}\theta_x - k_9\sin\bar{q}\theta_x \\ i_{10} = i_9 &= i_7\cos\psi_n - j_7\sin\psi_n \\ j_9 &= i_7\sin\psi_n + j_7\cos\psi_n \\ k_9 = k_7 &= j_6\sin\beta_n + k_6\cos\beta_n \\ j_7 &= j_6\cos\beta_n - k_6\sin\beta_n \\ i_7 = i_6 &= i_5\cos\gamma_n - j_5\sin\gamma_n \\ j_6 &= i_5\sin\gamma_n + j_5\cos\gamma_n \end{aligned} \tag{A31}$$

$$
\begin{aligned}
k_6 = k_5 &= i_4 \sin\theta_{n,i} + k_4 \cos\theta_{n,i} \\
i_5 &= i_4 \cos\theta_{n,i} - k_4 \sin\theta_{n,i} \\
j_5 = j_4 &= i_3 \sin q^{c'}_{E,n,i} + j_3 \cos q^{c'}_{E,n,i} \\
i_4 &= i_3 \cos q^{c'}_{E,n,i} - j_3 \sin q^{c'}_{E,n,i} \\
k_4 = k_3 &= j_2 \sin q^{c'}_{F,n,i} + k_2 \cos q^{c'}_{F,n,i} \\
j_3 &= j_2 \cos q^{c'}_{F,n,i} - k_2 \sin q^{c'}_{F,n,i} \\
i_3 &= i_2
\end{aligned}
\qquad \text{(A31)}
$$

Substitution of the above in Equation A30 expresses the absolute rotational velocity in terms of the generalized coordinates and their derivatives.

These relationships allow us to write the absolute velocity vector $\dot{\bar{\theta}}_{n,i}$ in terms of the appropriate unit vectors at a blade element i.

Thus, the total kinetic energy arising from pure rotational motion of all elements of all blades can be written

$$
T_{BR} = \tfrac{1}{2} \sum_{n=1}^{N} \left(\sum_{i=1}^{NB} (\dot{\bar{\theta}}_{n,i})^T [I_{n,i}] (\dot{\bar{\theta}}_{n,i}) \delta r_{n,i} \right) \qquad \text{(A32)}
$$

Total Kinetic Energy

The total kinetic energy arising from translational and pure rotational motion of all elements of all blades is given by the sum of Equations A29 and A32, namely,

$$
T_{BTOT} = T_{BT} + T_{BR} \qquad \text{(A33)}
$$

Potential Energy

The blades have two direct sources of potential energy: that associated with blade bending and that associated with twisting deformations.

The bending potential energy of a blade can be written in the classical form which expresses this energy in terms of the fourth spanwise derivative of the flatwise and edgewise deformations. However, since in this analysis a modal approach is employed and it is assumed that all modal information relating to the blades is available for inclusion in the eigenanalysis, the total potential energy associated with bending of all blades is simply written as

$$V_{BB} = \tfrac{1}{2} \sum_{n=1}^{N} \left(\sum_{t=1}^{NE} \omega_{q,n,t}^2 M_{q,n,t} q_{T,n,t}^2 \right) \tag{A34}$$

The potential energy derived from torsional deformations of all blades is given by

$$V_{BT} = \tfrac{1}{2} \sum_{n=1}^{N} \left(\sum_{i=1}^{NB} (K_{n,i} \phi_{\theta,i}^2 \theta_{T,n}^2) \right) \tag{A35}$$

In this expression $K_{n,i}$ is the torsional stiffness of the blade n at the blade station $r_{n,i}$. It is obtained from the blade polar second moment of area distribution and the blade torsional modulus of elasticity using the relationship

$$1/K_{n,i} = \sum_{s=1}^{i} (\delta r_{n,s} / G_{n,s} J_{n,s}) \tag{A36}$$

Further sources of potential energy are contained in the root springs that may be used when the blades are considered inflexible. These root springs restrain both flapping and inplane motion and appear explicitly only in the rigid-body flap and lag equations. The total potential energy associated with the springs is given by

$$V_{BS} = \tfrac{1}{2} \sum_{n=1}^{N} (K_{\gamma,n} \gamma_n^2 + K_{\beta,n} \beta_n^2) \tag{A37}$$

It should be noted that, when the blade elastic modes are used, the potential energy from these springs is implied in Equation A34 since the springs determine the blade root boundary conditions.

Total Potential Energy

The total potential energy arising from bending, twisting, and rigid-body motions of all blades is given by the sum of Equations A34, A35, and A37, namely,

$$V_{BTOT} = V_{BB} + V_{BT} + V_{BS} \tag{A38}$$

Dissipation Potentials

We can immediately recognize two sources of energy dissipation associated with the blades: that resulting from bending deformations and that resulting from torsional deformations. Unfortunately, no realistic analytical definition of structional damping of any kind has ever been established. Nevertheless, it is known that structural damping does exist, no matter how small. Therefore, this may be included as a percentage of critical damping. We must, however, remember that in specifying a percentage of critical damping, we must also specify the frequency upon which it is based. In the case of blade bending, this presents no problem since the modal frequencies are obvious choices. However, in the case of blade torsion, the choice is not so obvious since coupling with the control system can cause radical changes in the torsional natural frequency. To circumvent this problem, the torsional damping is based on the rotor rotational speed, which is always known. It is then the privilege of the user of the analysis to choose the damping level that he feels most closely satisfies the condition being analyzed.

Based on the above, we can then write the total dissipation potential arising from blade bending as

$$D_{BB} = \tfrac{1}{2} \sum_{n=1}^{N} \left(\sum_{t=1}^{NE} 2\zeta_{q_{n,t}} M_{q_{n,t}} \omega_{q_{n,t}} \dot{q}_{T_{n,t}}^2 \right) \tag{A39}$$

and that arising from blade torsion as

$$D_{BT} = \tfrac{1}{2} \sum_{n=1}^{N} \left(2\zeta_{\theta,n} I_{T,n} \Omega \dot{\theta}_{T,n}^2 \right) \tag{A40}$$

Energy is also dissipated by the lag dampers that act on the rigid-body inplane degree of freedom. This dissipation potential is given by

$$D_{BD} = \tfrac{1}{2} \sum_{n=1}^{N} \left(2\zeta_{\gamma,n} I_{\gamma,n} \omega_{\gamma,n} \dot{\gamma}_n^2 \right) \tag{A41}$$

Total Dissipation Potential

The total energy dissipation arising from bending, twisting, and rigid-body inplane motion of all blades is given by the sum of Equations A39, A40, and A41, namely,

$$D_{BTOT} = D_{BB} + D_{BT} + D_{BD} \tag{A42}$$

Fixed, or Airframe, System

Neglecting aerodynamic interference effects between the rotor system and any part of the airframe and also, for the present, neglecting mechanical control coupling, the only coupling that can exist between rotor motions and airframe motions is that transmitted through the rotor hub. Therefore, knowing the dynamic characteristics of the airframe as seen at the rotor hub allows us to define a dynamically coupled rotor/airframe system. Such an approach is used in this analysis.

It is assumed that the airframe, or fixed system, dynamic characteristics are available either from shake test data or from a separate analysis. The data required for each of the NA airframe modes $\overline{q}$ are:

1. The generalized mass, M_A.
2. The modal frequency, ω_A.
3. The percentage of critical damping, ζ_A.
4. The modal components of motion at the rotor hub, ϕ_X, ϕ_Y, ϕ_Z, $\phi_{\theta X}$, $\phi_{\theta Y}$.

With this information, we are able to define the total kinetic and potential energies and the dissipation potential associated with the airframe system as follows:

Total Kinetic Energy

$$T_{ATOT} = \tfrac{1}{2} \sum_{s=1}^{NA} (M_{A,s} \dot{q}_s^2) \tag{A43}$$

Total Potential Energy

$$V_{ATOT} = \tfrac{1}{2} \sum_{s=1}^{NA} (\omega_{A,s}^2 M_{A,s} \overline{q}_s^2) \qquad (A44)$$

Total Dissipation Potential

$$D_{ATOT} = \tfrac{1}{2} \sum_{s=1}^{NA} (2\zeta_{A,s} M_{A,s} \omega_{A,s} \dot{\overline{q}}_s^2) \qquad (A45)$$

The modal components at the rotor hub provide the motion interface between the rotor and airframe systems.

Control Systems

This analysis considers both main and tail rotor systems. Normally, the control systems associated with these have little in common. For example, the conventional tail rotor has only collective pitch inputs. An assortment of cables, quadrants, control rods, and bell cranks may also feature in the design. The control servos can be close to, or some considerable distance away from, the rotor. On the other hand, the conventional main rotor has both collective and cyclic pitch inputs, necessitating the use of a swash plate arrangement. The primary control servos normally act directly on the stationary swash plate.

To accommodate the peculiar characteristics of both types of control system, each is modelled and analyzed separately.

The equations for the main and tail rotor servos are identical. Therefore, they are excluded from this section and developed later.

Tail Rotor Control System

Figure A2 shows the model used to describe this type of control system. The model simulates the collective pitch spider beam and actuator shaft backed up by three spring, mass, damper systems that can be used to describe the dynamics of control rod/quadrant/cable arrangements. The subsidiary spring, mass, damper systems can be used to describe the dynamics of appendages such as control surfaces and rudders.

In Figure A2, $X_{1,n}$ is the motion at the pushrod of blade n. It is defined by

$$X_{1,n} = L_{2,n} \tan\delta_{3,n} \beta_n + L_{2,n} \tan\alpha_{1,n} \gamma_n - L_{2,n} \phi_\theta PR\theta_{T,n}$$

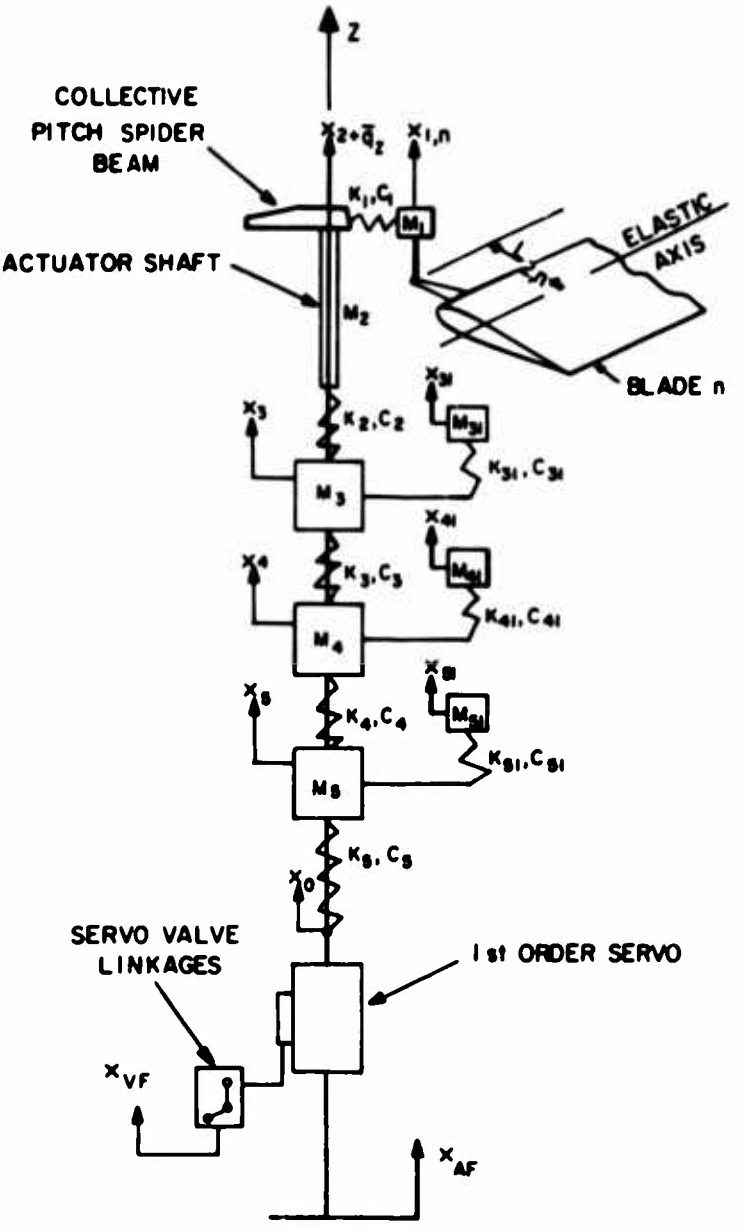

Figure A2. Tail Rotor Control System Model.

$$+ \sum_{i=1}^{NE} [\phi_{FPR,i} + (L_{2,n}\tan\alpha_{1,n}/(R_n - e_n))\phi_{ET,i}]q_{T,n,i}$$
$$+ \sum_{s=1}^{NA} (\phi_{Z,s}\bar{q}_s) \qquad \text{(A46)}$$

for pure collective type motion.

It is assumed that the actuator and collective pitch spider beam move with an amplitude $X_2 + \bar{q}_Z$ in the Z direction; the effects of all other components of hub motion are ignored. It is also assumed that airframe motions can be neglected in the remainder of the control system.

The energies associated with the collective motion of the tail rotor control system are then readily written as follows:

Total Kinetic Energy

$$T_{TTOT} = \tfrac{1}{2}\{ \sum_{n=1}^{N} (M_{1,n}\dot{X}_{1,n}^2) + \sum_{s=1}^{NA} (M_2\phi_{Z,s}\dot{\bar{q}}_s^2)$$
$$+ M_2\dot{X}_2^2 + M_3\dot{X}_3^2 + M_4\dot{X}_4^2 + M_5\dot{X}_5^2$$
$$+ M_{31}\dot{X}_{31}^2 + M_{41}\dot{X}_{41}^2 + M_{51}\dot{X}_{51}^2\} \qquad \text{(A47)}$$

Total Potential Energy

$$V_{TTOT} = \tfrac{1}{2}\{ \sum_{n=1}^{N} [K_{1,n}(X_{1,n} - X_2 - \sum_{s=1}^{NA} (\phi_{Z,s}\bar{q}_s))^2]$$
$$+ K_2(X_2 + \sum_{s=1}^{NA} (\phi_{Z,s}\bar{q}_s) - X_3)^2 + K_3(X_3 - X_4)^2$$
$$+ K_4(X_4 - X_5)^2 + K_5(X_5 - X_0)^2$$
$$+ K_{31}(X_{31} - X_3)^2 + K_{41}(X_{41} - X_4)^2$$
$$+ K_{51}(X_{51} - X_5)^2\} \qquad \text{(A48)}$$

Total Dissipation Potential

$$D_{TTOT} = \tfrac{1}{2}\{\sum_{n=1}^{N}[C_{1,n}(\dot{X}_{1,n} - \dot{X}_2 - \sum_{s=1}^{NA}(\phi_{Z,s}\dot{\bar{q}}_s))^2]$$
$$+ C_2(\dot{X}_2 + \sum_{s=1}^{NA}(\phi_{Z,s}\dot{\bar{q}}_s) - \dot{X}_3)^2 + C_3(\dot{X}_3 - \dot{X}_4)^2$$
$$+ C_4(\dot{X}_4 - \dot{X}_5)^2 + C_5(\dot{X}_5 - \dot{X}_0)^2$$
$$+ C_{31}(\dot{X}_{31} - \dot{X}_3)^2 + C_{41}(\dot{X}_{41} - \dot{X}_4)^2$$
$$+ C_{51}(\dot{X}_{51} - \dot{X}_5)^2\} \qquad (A49)$$

For pure cyclic motion of the rotating system generalized coordinates, it is assumed that the actuator shaft is subjected to a pure moment at its point of connection to the collective pitch spider beam. Under these circumstances, the control system stiffness to be associated with the motion $X_{1,n}$ is

$$K_{c,n} = 2K_{1,n}K_{MA}/(NK_{1,n}L_s^2 + 2K_{MA}) \qquad (A50)$$

Therefore, the total potential energy associated with cyclic motion of the control system is given by

$$V_{TCTOT} = \tfrac{1}{2}\sum_{n=1}^{N}(K_{c,n}X_{1,n}^2) \qquad (A51)$$

Main Rotor Control System

The model used to describe the main rotor control system is shown in Figure A3. This is depicted as a rigid swash plate supported on three spring/servo systems. The servos are situated at a radius R_S from the center of the swash plate with the forward servo being set at an angle δ_{FS} relative to the Y axis as shown. The blade pushrods are situated at a radius R_B from the center of the swash plate. The point P locates the position of the pushrod of blade n, and the angle $\delta_{B,n}$ that positions this point relative to the Y axis is given by

$$\delta_{B,n} = \delta_{FS} + \Omega t + 2\pi(n - 1)/N + \delta_{Pk,n} \qquad (A52)$$

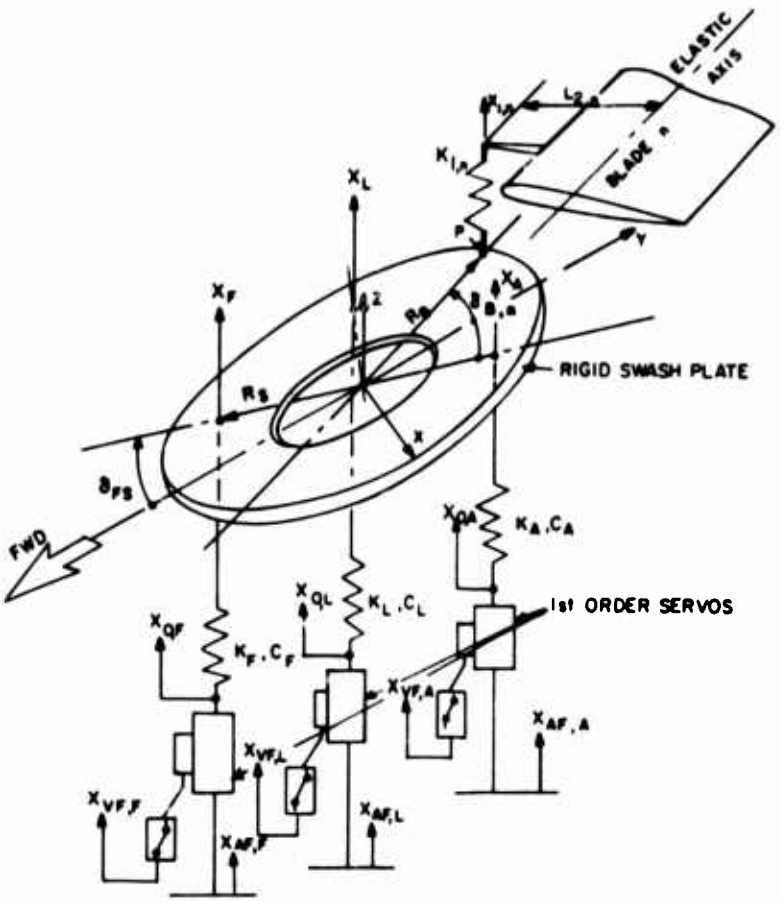

Figure A3. Main Rotor Control System Model.

where

$$\delta_{PR,n} = \tan^{-1}[L_{2,n}/(e_n + L_{2,n}\tan\delta_{3,n})] \tag{A53}$$

This definition neglects steady and dynamic deformations. The servos at X_L and X_A are positioned 90 degrees and 180 degrees respectively in the yaw right direction from the servo at X_F.

The displacement of the pushrod of blade n, $X_{1,n}$, is defined in exactly the same manner as in the tail rotor control system, Equation A46. The displacement of the point P on the swash plate is derived assuming that, in addition to its own dynamic displacements X_F, X_L, and X_A, the swash plate also follows the motions of the hub.

With these displacements defined, the energies associated with the main rotor control system can be shown to be as follows:

Total Kinetic Energy

$$\begin{aligned} T_{MTOT} = \tfrac{1}{2}\{ & \sum_{n=1}^{N} (M_{1,n}\dot{X}_{1,n}^2) \\ & + I_{FA}[{}^{1}/_{2R_S}(\dot{X}_A - \dot{X}_F) + \sum_{s=1}^{NA} (\phi_{\theta X,s}\dot{\bar{q}}_s)]^2 \\ & + I_L[{}^{1}/_{2R_S}(2\dot{X}_L - \dot{X}_A - \dot{X}_F) + \sum_{s=1}^{NA} (\phi_{\theta Y,s}\dot{\bar{q}}_s)]^2 \\ & + M_S[{}^{1}/_{2}(\dot{X}_A + \dot{X}_F) + \sum_{s=1}^{NA} (\phi_{Z,s}\dot{\bar{q}}_s)]^2\} \end{aligned} \tag{A54}$$

Total Potential Energy

$$\begin{aligned} V_{MTOT} = \tfrac{1}{2}\{ & \sum_{n=1}^{N} K_{1,n}[X_{1,n} - \sum_{s=1}^{NA} (\phi_{Z,s}\bar{q}_s) - \tfrac{1}{2}(X_A + X_F) \\ & - {}^{R_B}/_{R_S}({}^{1}/_{2}(X_A - X_F)(\cos\psi_n\cos\delta_n - \sin\psi_n\sin\delta_n)) \\ & - {}^{R_B}/_{R_S}({}^{1}/_{2}(2X_L - X_A - X_F)(\sin\psi_n\cos\delta_n + \cos\psi_n\sin\delta_n))]^2 \\ & + K_F(X_F - X_{OF})^2 + K_A(X_A - X_{OA})^2 \\ & + K_L(X_L - X_{OL})^2\} \end{aligned} \tag{A55}$$

where

$$\psi_n = \Omega t + 2\pi(n-1)/N \tag{A56}$$

and

$$\delta_n = \delta_{FS} + \delta_{PR,n} \tag{A57}$$

Total Dissipation Potential

$$\begin{aligned} D_{MTOT} = \tfrac{1}{2}\{ & \sum_{n=1}^{N} C_{1,n}[\dot{X}_{1,n} - \sum_{s=1}^{NA} (\phi_{Z,s}\dot{\bar{q}}_s) - \tfrac{1}{2}(\dot{X}_A + \dot{X}_F) \\ & - {}^{R_B}/_{R_S}({}^{1}/_{2}(\dot{X}_A - \dot{X}_F)(\cos\psi_n\cos\delta_n - \sin\psi_n\sin\delta_n)) \\ & - {}^{R_B}/_{R_S}({}^{1}/_{2}(2\dot{X}_L - \dot{X}_A - \dot{X}_F)(\sin\psi_n\cos\delta_n + \cos\psi_n\sin\delta_n))]^2 \\ & + C_F(\dot{X}_F - \dot{X}_{OF})^2 + C_A(\dot{X}_A - \dot{X}_{OA})^2 \\ & + C_{LL}(\dot{X}_L - \dot{X}_{OL})^2\} \end{aligned} \tag{A58}$$

Servo Systems

Only servos with first-order transfer functions were considered. Main and tail rotor servos were assumed to be governed by the same equation of motion; however, they may all have different dynamic properties. The model used to describe the servo system is shown in Figure A4. In this model the displacement X, in the case of the tail rotor control system, corresponds to X_5, and K corresponds to K_5; see Figure A2. Similar analogies can be made for the forward, lateral, and aft main rotor servos; see Figure A3.

From Figure A4, we can see that the displacement of the valve spool relative to the servo housing is $\epsilon_v = X_v - X_c$. This can be written in the general form

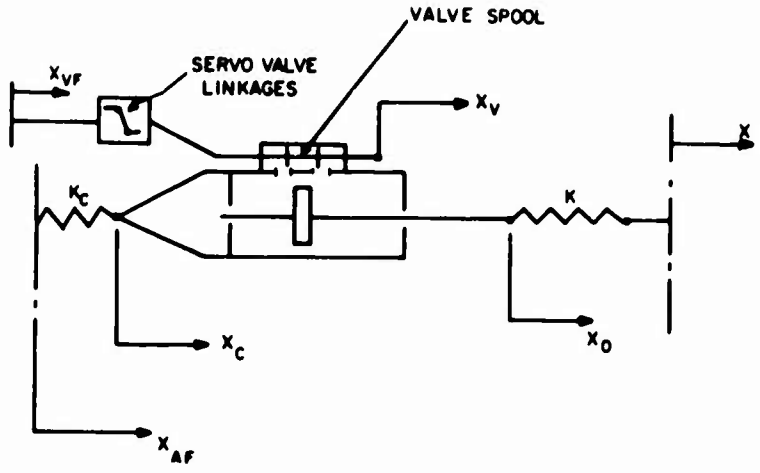

Figure A4. Control System Servo Model.

$$\varepsilon_V = R_1 X_{VF} + R_2 X_0 + R_3 X_C \tag{A59}$$

where the servo linkage ratios, R_1, R_2 and R_3, depend on the kinematics of the servo linkage arrangements.

Flow through the valve is given by

$$\begin{aligned} Q_V &= C_q \varepsilon_V - C_P \delta P \\ &= A_P(\dot{X}_C - \dot{X}_0) + C_{LS}\delta P + (V_T/4N_S)\dot{\delta P} \end{aligned} \tag{A60}$$

and since

$$K_C(X_C - X_{AF}) = A_P \delta P \tag{A61}$$

giving

$$X_C = A_P \delta P / K_C \cdots X_{AF} \tag{A62}$$

and

$$\dot{X}_C = A_P \dot{\delta P} / K_C + \dot{X}_{AF} \tag{A63}$$

it can be verified that

$$C_q R_1 X_{VF} + C_q R_2 X_0 + C_q R_3 X_{AF} - A_P \dot{X}_{AF} + A_P \dot{X}_0$$

$$- [(C_{LS} + C_P)/A_P - C_q R_3/K_C]A_P\delta P$$

$$- A_P[1/K_C + V_T/4N_S A_P^2]A_P\dot{\delta}P = 0 \qquad (A64)$$

If we express ε_V in the form

$$\varepsilon_V = R_2(R_1/R_2 X_{VF} + X_0 + R_3/R_2 X_C) \qquad (A65)$$

and let $R_2 = \alpha_S$ such that

$$\varepsilon_V = \alpha_S(R_1/\alpha_S X_{VF} + X_0 + R_3/\alpha_S X_C) \qquad (A66)$$

then using this form for ε_V and the identities

$$\mu_1 = [(C_{LS} + C_P)/C_q A_P - R_3/K_C] \qquad (A67)$$

$$\mu_2 = [1/K_C + V_T/4N_S A_P^2] \qquad (A68)$$

together with the equalities

$$A_P\delta P = - K(X_0 - X) \qquad (A69)$$

$$A_P\dot{\delta}P = - K(\dot{X}_0 - \dot{X}) \qquad (A70)$$

in Equations A60 and A64, it can be shown, after some algebraic manipulation, that the servos are governed by the equation

$$(\alpha_S/\mu_1)(A_P/\alpha_S C_q)(1 + \tau\mu_2)\ddot{X}_0 + (\alpha_S/\mu_1 + K)X_0$$

$$- (\alpha_S/\mu_1)(A_P/\alpha_S C_q)K\mu_2\dot{X} - KX + (\alpha_S/\mu_1)(R_1/\alpha_S)X_{VF}$$

$$+ (\alpha_S/\mu_1)(R_3/\alpha_S)X_{AF} - (\alpha_S/\mu_1)(A_P/\alpha_S C_q)\dot{X}_{AF} = 0 \qquad (A71)$$

Here, (a_g/μ_1) is the "Servo Power-On Stiffness With Locked Input," $(A_p/a_g C_q)$ is the "Servo Time Constant or Inverse of Velocity Gain," and (μ_2) is the "Reciprocal of Combined Actuator Hydraulic and Structural Series Stiffness."

In this analysis X_{VF} and X_{AF} were not considered to be independent degrees of freedom. Rather, they are assumed to be the result of airframe vibration. X_{VF} could, for example, be construed to be the result of vibration at the pilot station being transmitted through the control system, whereas X_{AF} gives a measure of the effect of the servo support vibrations. Since accurate measures of these quantities are not always available, it was considered that they could best be represented by expressing them as functions of the airframe motions at the hub using feedback factors for the support and valve to define relative participations as follows:

$$X_{VF} = \sum_{s=1}^{NA} (SF_{V,X}\phi_{X,s}\bar{q}_s + SF_{V,Y}\phi_{Y,s}\bar{q}_s + SF_{V,Z}\phi_{Z,s}\bar{q}_s + SF_{V,\theta X}\phi_{\theta X,s}\bar{q}_s + SF_{V,\theta Y}\phi_{\theta Y,s}\bar{q}_s) \quad (A72)$$

$$X_{AF} = \sum_{s=1}^{NA} (SF_{A,X}\phi_{X,s}\bar{q}_s + SF_{A,Y}\phi_{Y,s}\bar{q}_s + SF_{A,Z}\phi_{Z,s}\bar{q}_s + SF_{A,\theta X}\phi_{\theta X,s}\bar{q}_s + SF_{A,\theta Y}\phi_{\theta Y,s}\bar{q}_s) \quad (A73)$$

$$\dot{X}_{AF} = \sum_{s=1}^{NA} (SF_{A,X}\phi_{X,s}\dot{\bar{q}}_s + SF_{A,Y}\phi_{Y,s}\dot{\bar{q}}_s + SF_{A,Z}\phi_{Z,s}\dot{\bar{q}}_s + SF_{A,\theta X}\phi_{\theta X,s}\dot{\bar{q}}_s + SF_{A,\theta Y}\phi_{\theta Y,s}\dot{\bar{q}}_s) \quad (A74)$$

These expressions are substituted directly in Equation A71 to give the final form of the servo equation.

Final Form of Dynamic System Equations

Final forms of the dynamic system equations of motions are obtained by formally expanding all of the total kinetic and potential energy and dissipation potential expressions derived in the preceding sections, and then performing first-order perturbations of all of the generalized coordinates about specified steady initial values. This procedure, as mentioned earlier, requires an extensive amount of matrix manipulation. However, the methods employed are well known and, provided accuracy is maintained, there is no problem in principle in arriving at the final equations. For this reason, none of the expansions are repeated here.

The equations that follow are very lengthy. Therefore, to improve readability, they are all written in exactly the same format. Also, since two types of control system are treated, their contributions to the equations are written separately. Finally, the servo equations, as applied to each type of control system, are written.

The first block of equations contains all of the terms that arise from the coupled rotor/airframe system. It also includes all of the terms contributed by the motion at the pushrod as defined in Equation A46. Each equation first defines acceleration coefficients, then velocity coefficients, and then displacement coefficients.

In every equation, all generalized coordinates and physical properties associated with the rotor system have a subscript n, the blade number. This subscript is omitted from the equations without ambiguity. Also, to give added clarity, the equations are presented in integral form.

Airframe Mode Equations

$$\left\{\sum_{n=1}^{N}\sum_{i=1}^{NA}\left[\int_{0}^{R-e} m dr\{\phi_{X,j}(\phi_{X,i} + \phi_{\theta Y,i}[b_2 + r\beta_o]) + \phi_{Y,j}(\phi_{Y,i} - \phi_{\theta X,i}[b_2 + r\beta_o])\right.\right.$$

$$+ \phi_{Z,j}(\phi_{Z,i} + \phi_{\theta X,i}[(a_2 - r\gamma_o)\sin\psi + (e + r + a_2\gamma_o - b_2\beta_o)\cos\psi]$$

$$+ \phi_{\theta Y,i}[(e + r + a_2\gamma_o - b_2\beta_o)\sin\psi - (a_2 - r\gamma_o)\cos\psi]) + \phi_{\theta Y,j}((b_2 + r\beta_o)\phi_{X,i}$$

$$+ \phi_{Z,i}[(e + r + a_2\gamma_o - b_2\beta_o)\sin\psi - (a_2 - r\gamma_o)\cos\psi]) + \phi_{\theta X,j}(-(b_2 + r\beta_o)\phi_{Y,i}$$

$$+ \phi_{Z,i}[(e + r + a_2\gamma_o - b_2\beta_o)\cos\psi + (a_2 - r\gamma_o)\sin\psi])$$

$$+ \phi_{\theta Y,j}(\phi_{\theta Y,i}[(-a_2(a_2\gamma_o - b_2\beta_o) - (r + e)(a_2 - r\gamma_o))\sin 2\psi + ((r + e)^2$$

$$+ 2(r + e)(a_2\gamma_o - b_2\beta_o))\sin^2\psi + a_2(a_2 - 2r\gamma_o)\cos^2\psi + b_2(b_2 + 2r\beta_o)]$$

$$+ \phi_{\theta X,i}[\tfrac{1}{2}(-a_2(a_2 - 2r\gamma_o) + (r + e)^2 + 2(r + e)(a_2\gamma_o - b_2\beta_o))\sin 2\psi$$

$$+ (-(r + e)(a_2 - r\gamma_o) - a_2(a_2\gamma_o - b_2\beta_o))\cos 2\psi]) + \phi_{\theta X,j}(\phi_{\theta Y,i}[\tfrac{1}{2}(-a_2(a_2 - 2r\gamma_o)$$

$$+ (r + e)^2 + 2(r + e)(a_2\gamma_o - b_2\beta_o))\sin 2\psi + (-(r + e)(a_2 - r\gamma_o)$$

$$- a_2(a_2\gamma_o - b_2\beta_o))\cos 2\psi] + \phi_{\theta X,i}[(a_2(a_2\gamma_o - b_2\beta_o) + (r + e)(a_2 - r\gamma_o))\sin 2\psi$$

$$+ ((r + e)^2 + 2(r + e)(a_2\gamma_o - b_2\beta_o))\cos^2\psi + a_2(a_2 - 2r\gamma_o)\sin^2\psi$$

$$\left.\left. + b_2(b_2 + 2r\beta_o)]\right)\right\} + I_X dr\ \{\phi_{\theta Y,j} q'_{EO}(-\phi_{\theta Y,i}\cos\theta_o\sin 2\psi - \phi_{\theta X,i}\cos\theta_o\cos 2\psi)$$

$$+ \phi_{\theta X,j} q'_{EO}(-\phi_{\theta Y,i}\cos\theta_o\cos 2\psi + \phi_{\theta X,i}\cos\theta_o\sin 2\psi) + \phi_{\theta Y,j}(\phi_{\theta Y,i}(\cos^2\theta_o\sin^2\psi$$

$$+ (\gamma_o\cos^2\theta_o - \tfrac{1}{2}\beta_o\sin 2\theta_o)\sin 2\psi) + \phi_{\theta X,i}(\tfrac{1}{2}\cos^2\theta_o\sin 2\psi$$

$$+ (\gamma_o\cos^2\theta_o - \tfrac{1}{2}\beta_o\sin 2\theta_o)\cos 2\psi)) + \phi_{\theta X,j}(\phi_{\theta Y,i}(\tfrac{1}{2}\cos^2\theta_o\sin 2\psi + (\gamma_o\cos^2\theta_o$$

$$- \tfrac{1}{2}\beta_o\sin 2\theta_o)\cos 2\psi) + \phi_{\theta X,i}(\cos^2\theta_o\cos^2\psi - (\gamma_o\cos^2\theta_o - \tfrac{1}{2}\beta_o\sin 2\theta_o)\sin 2\psi))\}$$

$$+ I_Y dr\ \{\phi_{\theta Y,j}(\phi_{\theta Y,i}(q'_{EO}\cos\theta_o - q'_{FO}\sin\theta_o)\sin 2\psi + \phi_{\theta X,i}(q'_{EO}\cos\theta_o$$

$$- q'_{FO}\sin\theta_o)\cos 2\psi) + \phi_{\theta X,j}(\phi_{\theta Y,i}(q'_{EO}\cos\theta_o - q'_{FO}\sin\theta_o)\cos 2\psi$$

$$+ \phi_{\theta X,i}(-q'_{EO}\cos\theta_o + q'_{FO}\sin\theta_o)\sin 2\psi) + \phi_{\theta Y,j}(\phi_{\theta Y,i}(\cos^2\psi - \gamma_o\sin 2\psi)$$

$$+ \phi_{\theta X,i}(-\gamma_o\cos 2\psi - \tfrac{1}{2}\sin 2\psi)) + \phi_{\theta X,j}(\phi_{\theta Y,i}(-\gamma_o\cos 2\psi - \tfrac{1}{2}\sin 2\psi)$$

$$+ \phi_{\theta X,i}(\sin^2\psi + \gamma_o\sin 2\psi))\} + I_Z dr\{\phi_{\theta Y,j}q'_{FO}(\phi_{\theta Y,i}\sin\theta_o\sin 2\psi$$

$$+ \phi_{\theta X,i}\sin\theta_o\cos 2\psi) + \phi_{\theta X,j}q'_{FO}(\phi_{\theta Y,i}\sin\theta_o\cos 2\psi - \phi_{\theta X,i}\sin\theta_o\sin 2\psi)$$

$$+ \phi_{\theta Y,j}(\phi_{\theta Y,i}(\sin^2\theta_o\sin^2\psi + (\gamma_o\sin^2\theta_o + \tfrac{1}{2}\beta_o\sin 2\theta_o)\sin 2\psi)$$

$$+ \phi_{\theta X,i}(\tfrac{1}{2}\sin^2\theta_o\sin 2\psi + (\gamma_o\sin^2\theta_o + \tfrac{1}{2}\beta_o\sin 2\theta_o)\cos 2\psi))$$

$$+ \phi_{\theta X,j}(\phi_{\theta Y,i}(\tfrac{1}{2}\sin^2\theta_o\sin 2\psi + (\gamma_o\sin^2\theta_o + \tfrac{1}{2}\beta_o\sin 2\theta_o)\cos 2\psi)$$

$$+ \phi_{\theta X,i}(\sin^2\theta_o\cos^2\psi - (\gamma_o\sin^2\theta_o + \tfrac{1}{2}\beta_o\sin 2\theta_o)\sin 2\psi))\}\Big]\ddot{q}_i\Big\}$$

$$+ \left\{\sum_{i=1}^{NA}[\phi_{\theta X,i}\phi_{\theta X,j}I_{FA} + \phi_{\theta Y,i}\phi_{\theta Y,j}I_L + \phi_{Z,i}\phi_{Z,j}M_S]\ddot{q}_i\right\} + \left\{M_{A,j}\ddot{q}_j\right\}$$

$$+ \left\{\sum_{n=1}^{N}\Big[\int_o^{R-e} mdr\{\phi_{X,j}((b_2\gamma_o + a_2\beta_o)\sin\psi - b_2\cos\psi) + \phi_{Y,j}(-(b_2\gamma_o\right.\right.$$

$$+ a_2\beta_o)\cos\psi - b_2\sin\psi) + \phi_{Z,j}a_2 + \phi_{\theta Y,j}[((a_2^2 + b_2^2)\gamma_o + a_2(r + e))\sin\psi$$

$$- (a_2(a_2 - r\gamma_o) + b_2(b_2 + r\beta_o))\cos\psi] + \phi_{\theta X,j}[(a_2(a_2 - r\gamma_o)$$

$$+ b_2(b_2 + r\beta_o))\sin\psi + ((a_2^2 + b_2^2)\gamma_o + a_2(r + e))\cos\psi]\}$$

$$+ I_X dr\{\phi_{\theta Y,j}q'_{EO}\cos\theta_o\sin\psi + \phi_{\theta X,j}q'_{EO}\cos\theta_o\cos\psi\} + I_Y dr\{\phi_{\theta Y,j}(-q'_{EO}\cos\theta_o$$

$$+ q'_{FO}\sin\theta_o)\sin\psi + \phi_{\theta X,j}(-q'_{EO}\cos\theta_o + q'_{FO}\sin\theta_o)\cos\psi + \phi_{\theta Y,j}(\gamma_o\sin\psi$$

$$- \cos\psi) + \phi_{\theta X,j}(\gamma_o\cos\psi + \sin\psi)\} + I_Z dr\{-\phi_{\theta Y,j}q'_{FO}\sin\theta_o\sin\psi$$

$$\left.\left. - \phi_{\theta X,j}q'_{FO}\sin\theta_o\cos\psi\}\Big]\ddot{\theta}_T\right\} + \left\{\sum_{n=1}^{N}\Big[\int_o^{R-e} mdr\{\phi_{X,j}(b_2 + r\beta_o)\sin\psi - \phi_{Y,j}(b_2\right.\right.$$

$$+ r\beta_o)\cos\psi + \phi_{Z,j}(r + a_2\gamma_o - b_2\beta_o) + \phi_{\theta Y,j}[(e(a_2\gamma_o - b_2\beta_o) + r(r + e + 2a_2\gamma_o)$$

$$+ b_2^2)\sin\psi - (a_2(a_2\gamma_o - b_2\beta_o) + r(a_2 - r\gamma_o))\cos\psi] + \phi_{\theta X,j}[(a_2(a_2\gamma_o - b_2\beta_o)$$

$$+ r(a_2 - r\gamma_o))\sin\psi + (e(a_2\gamma_o - b_2\beta_o) + r(r + e + 2a_2\gamma_o) + b_2^2)\cos\psi]\}$$

$$+ I_X dr\{-\phi_{\theta Y,j}q'_{EO}\cos\theta_o\cos\psi + \phi_{\theta X,j}q'_{EO}\cos\theta_o\sin\psi + \phi_{\theta Y,j}(\cos^2\theta_o\sin\psi$$

$$+ (\gamma_o\cos^2\theta_o - \tfrac{1}{2}\beta_o\sin2\theta_o)\cos\psi) + \phi_{\theta X,j}(\cos^2\theta_o\cos\psi - (\gamma_o\cos^2\theta_o$$

$$- \tfrac{1}{2}\beta_o\sin2\theta_o)\sin\psi)\} + \tau_Y dr\{\phi_{\theta Y,j}(q'_{EO}\cos\theta_o - q'_{FO}\sin\theta_o)\cos\psi$$

$$+ \phi_{\theta X,j}(-q'_{EO}\cos\theta_o + q'_{FO}\sin\theta_o)\sin\psi + \phi_{\theta X,j}\gamma_o\sin\psi - \phi_{\theta Y,j}\gamma_o\cos\psi\}$$

$$+ I_Z dr\{\phi_{\theta Y,j}q'_{FO}\sin\theta_o\cos\psi - \phi_{\theta X,j}q'_{FO}\sin\theta_o\sin\psi + \phi_{\theta Y,j}(\sin^2\theta_o\sin\psi$$

$$+ (\gamma_o\sin^2\theta_o + \tfrac{1}{2}\beta_o\sin2\theta_o)\cos\psi) + \phi_{\theta X,j}(\sin^2\theta_o\cos\psi - (\gamma_o\sin^2\theta_o$$

$$+ \tfrac{1}{2}\beta_o\sin2\theta_o)\sin\psi)\}\Big]\ddot{\beta}\Big\} + \Big\{\sum_{n=1}^{N}\Big[\int_0^{R-e} mdr\{\phi_{X,j}(-(a_2 - r\gamma_o)\sin\psi - (a_2\gamma_o$$

$$+ r)\cos\psi) + \phi_{Y,j}(-(a_2\gamma_o + r)\sin\psi + (a_2 - r\gamma_o)\cos\psi) + \phi_{Z,j}a_2\beta_o$$

$$+ \phi_{\theta Y,j}[(-b_2(a_2 - r\gamma_o) + a_2e\beta_o)\sin\psi + (-(a_2^2 + r^2)\beta_o - b_2(a_2\gamma_o + r))\cos\psi]$$

$$+ \phi_{\theta X,j}[((a_2^2 + r^2)\beta_o + b_2(a_2\gamma_o + r))\sin\psi + (-b_2(a_2 - r\gamma_o) + a_2e\beta_o)\cos\psi]\}$$

$$+ I_X dr\{-\phi_{\theta Y,j}q'_{EO}\sin\theta_o\cos\psi + \phi_{\theta X,j}q'_{EO}\sin\theta_o\sin\psi + \phi_{\theta Y,j}[\tfrac{1}{2}\sin2\theta_o\sin\psi$$

$$+ (\tfrac{1}{2}\gamma_o\sin2\theta_o - \beta_o\sin^2\theta_o)\cos\psi] + \phi_{\theta X,j}[\tfrac{1}{2}\sin2\theta_o\cos\psi - (\tfrac{1}{2}\gamma_o\sin2\theta_o - \beta_o\sin^2\theta_o)\sin\psi]\}$$

$$+ I_Y dr\{\phi_{\theta Y,j}(q'_{EO}\sin\theta_o + q'_{FO}\cos\theta_o)\cos\psi + \phi_{\theta X,j}(-q'_{EO}\sin\theta_o$$

$$- q'_{FO}\cos\theta_o)\sin\psi\} + I_Z dr\{-\phi_{\theta Y,j}q'_{FO}\cos\theta_o\cos\psi + \phi_{\theta X,j}q'_{FO}\cos\theta_o\sin\psi$$

$$+ \phi_{\theta Y,j}[-\tfrac{1}{2}\sin2\theta_o\sin\psi - (\tfrac{1}{2}\gamma_o\sin2\theta_o + \beta_o\cos^2\theta_o)\cos\psi] + \phi_{\theta X,j}[-\tfrac{1}{2}\sin2\theta_o\cos\psi$$

$$+ (\tfrac{1}{2}\gamma_o\sin2\theta_o + \beta_o\cos^2\theta_o)\sin\psi]\}\Big]\ddot{\gamma}\Big\} + \Big\{\sum_{n=1}^{N}\sum_{i=1}^{NE}\Big[\int_0^{R-e} mdr\{\phi_{X,j}(\phi_{E,i}(\gamma_o\sin\psi - \cos\psi)$$

$$+ \nu_{1,i}\sin\psi + \phi_{F,i}\beta_o\sin\psi) + \phi_{Y,j}(\phi_{E,i}(-\sin\psi - \gamma_o\cos\psi) - \nu_{1,i}\cos\psi$$

$$- \phi_{F,i}\beta_o\cos\psi) + \phi_{Z,j}\phi_{F,i} + \phi_{\theta Y,j}[(\phi_{F,i}(a_2\gamma_o + r + e) + \phi_{E,i}b_2\gamma_o)\sin\psi$$

$$+ (-\phi_{F,i}(a_2 - r\gamma_o) - \phi_{E,i}(b_2 + r\beta_o))\cos\psi] + \phi_{\theta X,j}[(\phi_{F,i}(a_2 - r\gamma_o) + \phi_{E,i}(b_2$$

$$+ r\beta_o))\sin\psi + (\phi_{E,i}b_2\gamma_o + \phi_{F,i}(a_2\gamma_o + r + e))\cos\psi] + \phi_{\theta Y,j}\nu_{1,i}b_2\sin\psi$$

$$+ \phi_{\theta X,j}\nu_{1,i}b_2\cos\psi\} + I_X dr\{\phi_{\theta Y,j}[\cos\theta_o\sin\psi + (\gamma_o\cos\theta_o - \beta_o\sin\theta_o$$

$$- q'_{EO})\cos\psi]\phi'_{F,i} + \phi_{\theta X,j}[\cos\theta_o\cos\psi - (\gamma_o\cos\theta_o - \beta_o\sin\theta_o - q'_{EO})\sin\psi]\phi'_{F,i}\}$$

$$+ I_Y dr\{(\phi_{\theta Y,j} q'_{FO}\cos\psi - \phi_{\theta X,j} q'_{FO}\sin\psi)\phi'_{E,i}\}$$

$$+ I_Z dr\{\phi_{\theta Y,j}[-\sin\theta_o\sin\psi - (\gamma_o\sin\theta_o + \beta_o\cos\theta_o + q'_{FO})\cos\psi]\phi'_{E,i}$$

$$+ \phi_{\theta X,j}[-\sin\theta_o\cos\psi + (\gamma_o\sin\theta_o + \beta_o\cos\theta_o + q'_{FO})\sin\psi]\phi'_{E,i}\}\Big]\ddot{q}_{T,i}\Big\}$$

$$+ \left\{\tfrac{1}{2}\left[\frac{1}{R_S}(\phi_{\theta X,j} I_{FA} - \phi_{\theta Y,j} I_L) + \phi_{Z,j} M_S\right]\ddot{X}_A\right\} + \left\{\tfrac{1}{2}\left[\frac{1}{R_S}(-\phi_{\theta X,j} I_{FA} - \phi_{\theta Y,j} I_L)\right.\right.$$

$$\left.\left. + \phi_{Z,j} M_S\right]\ddot{X}_F\right\} + \left\{\frac{1}{R_S}\phi_{\theta Y,j} I_L \ddot{X}_L\right\} + \left\{\sum_{n=1}^{N}\sum_{i=1}^{NA}\int_0^{R-e} m dr\{2\Omega\phi_{Z,j}[\phi_{\theta X,i}((a_2 - r\gamma_o)\cos\psi\right.$$

$$- (e + r + a_2\gamma_o - b_2\beta_o)\sin\psi) + \phi_{\theta Y,i}((e + r + a_2\gamma_o - b_2\beta_o)\cos\psi$$

$$+ (a_2 - r\gamma_o)\sin\psi)] + \Omega\phi_{\theta Y,j}[\phi_{\theta Y,i}([(r + e)^2 + 2(r + e)(a_2\gamma_o - b_2\beta_o)$$

$$- a_2(a_2 - r\gamma_o)]\sin 2\psi + [-(r + e)(a_2 - r\gamma_o) - a_2(a_2\gamma_o - b_2\beta_o)]2\cos 2\psi)$$

$$+ \phi_{\theta X,i}([a_2(a_2\gamma_o - b_2\beta_o) + (r + e)(a_2 - r\gamma_o)]2\sin 2\psi + [(r + e)^2$$

$$- a_2(a_2 - 2r\gamma_o) + 2(r + e)(a_2\gamma_o - b_2\beta_o)]\cos 2\psi - a_2(a_2 - 2r\gamma_o) - (r + e)^2$$

$$- 2(r + e)(a_2\gamma_o - b_2\beta_o))] + \Omega\phi_{\theta X,j}[\phi_{\theta Y,i}([a_2(a_2\gamma_o - b_2\beta_o) + (r + e)(a_2$$

$$- r\gamma_o)]2\sin 2\psi + [-a_2(a_2 - 2r\gamma_o) + (r + e)^2 + 2(r + e)(a_2\gamma_o - b_2\beta_o)]\cos 2\psi$$

$$+ a_2(a_2 - 2r\gamma_o) + (r + e)^2 + 2(r + e)(a_2\gamma_o - b_2\beta_o)) + \phi_{\theta X,i}([-(r + e)^2$$

$$- 2(r + e)(a_2\gamma_o - b_2\beta_o) + a_2(a_2 - r\gamma_o)]\sin 2\psi + [(r + e)(a_2 - r\gamma_o)$$

$$\left.\left. + a_2(a_2\gamma_o - b_2\beta_o)]2\cos 2\psi)]\right\} + I_X dr\{2\Omega q'_{EO}(\phi_{\theta Y,j}[-\phi_{\theta Y,i}\cos\theta_o\cos 2\psi\right.$$

$$+ \phi_{\theta X,i}\cos\theta_o\sin 2\psi] + \phi_{\theta X,j}[\phi_{\theta Y,i}\cos\theta_o\sin 2\psi + \phi_{\theta X,i}\cos\theta_o\cos 2\psi])$$

$$+ \Omega(\phi_{\theta Y,j}[\phi_{\theta Y,i}(\cos^2\theta_o\sin 2\psi + (2\gamma_o\cos^2\theta_o - \beta_o\sin 2\theta_o)\cos 2\psi)$$

$$+ \phi_{\theta X,i}(\cos^2\theta_o\cos 2\psi - (2\gamma_o\cos^2\theta_o - \beta_o\sin 2\theta_o)\sin 2\psi) - \phi_{\theta X,i}\sin^2\theta_o]$$

$$+ \phi_{\theta X,j}[\phi_{\theta Y,i}(\cos^2\theta_o\cos 2\psi - (2\gamma_o\cos^2\theta_o - \beta_o\sin 2\theta_o)\sin 2\psi)$$

$$\left.\left. + \phi_{\theta X,i}(-\cos^2\theta_o\sin 2\phi - (2\gamma_o\cos^2\theta_o - \beta_o\sin 2\theta_o)\cos 2\psi) + \phi_{\theta Y,i}\sin^2\theta_o])\right\}$$

$$+ I_Y dr\{2\Omega(\phi_{\theta Y,j}[\phi_{\theta Y,i}(q'_{EO}\cos\theta_o - q'_{FO}\sin\theta_o)\cos 2\psi + \phi_{\theta X,i}(-q'_{EO}\cos\theta_o$$

$$+ q'_{FO}\sin\theta_o)\sin 2\psi] + \phi_{\theta X,j}[\phi_{\theta Y,i}(-q'_{EO}\cos\theta_o$$

$$+ q'_{FO}\sin\theta_o)\sin2\psi + \phi_{\theta X,i}(- q'_{EO}\cos\theta_o + q'_{FO}\sin\theta_o)\cos2\psi])$$

$$+ \Omega(\phi_{\theta Y,j}[\phi_{\theta Y,i}(- 2\gamma_o\cos2\psi - \sin2\psi) + \phi_{\theta X,i}(- \cos2\psi + 2\gamma_o\sin2\psi)]$$

$$+ \phi_{\theta X,j}[\phi_{\theta Y,i}(- \cos2\psi + 2\gamma_o\sin2\psi) + \phi_{\theta X,i}(2\gamma_o\cos2\psi + \sin2\psi)])\}$$

$$+ I_Z dr\{2\Omega q'_{FO}(\phi_{\theta Y,j}[\phi_{\theta Y,i}\sin\theta_o\cos2\psi - \phi_{\theta X,i}\sin\theta_o\cos2\psi] + \phi_{\theta X,j}[$$

$$- \phi_{\theta Y,i}\sin\theta_o\sin2\psi - \phi_{\theta X,i}\sin\theta_o\cos2\psi]) + \Omega(\phi_{\theta Y,j}[\phi_{\theta Y,i}(\sin^2\theta_o\sin2\psi + (2\gamma_o\sin^2\theta_o$$

$$+ \beta_o\sin2\theta_o)\cos2\psi) + \phi_{\theta X,i}(\sin^2\theta_o\cos2\psi - (2\gamma_o\sin^2\theta_o + \beta_o\sin2\theta_o)\sin2\psi)$$

$$- \phi_{\theta X,i}\cos^2\theta_o\ ] + \phi_{\theta X,j}\ [\phi_{\theta Y,i}(\sin^2\theta_o\cos2\psi - (2\gamma_o\sin^2\theta_o + \beta_o\sin2\theta_o)\sin2\psi)$$

$$+ \phi_{\theta X,i}(-\sin^2\theta_o\sin2\psi\ - (2\gamma_o\sin^2\theta_o\ + \beta_o\sin2\theta_o)\cos2\psi)$$

$$+ \phi_{\theta Y,i}\cos^2\theta_o\ ])\}\Big]\dot{\overline{q}}_j\Big\}\ + \Big\{2\zeta_{A,j}M_{A,j}\omega_{A,j}\ \dot{\overline{q}}_j\Big\}$$

$$+ \Big\{\sum_{n=1}^{N}\Big[\int_0^{R-e} mdr\{2\Omega\ (\phi_{X,j}\ ((b_2\gamma_o + a_2\beta_o)\cos\psi + b_2\sin\psi)$$

$$+ \phi_{Y,j}((b_2\gamma_o + a_2\beta_o)\sin\psi - b_2\cos\psi) + \phi_{\theta Y,j}(b_2(b_2$$

$$+ r\beta_o)\sin\psi + b_2(a_2\beta_o + b_2\gamma_o)\cos\psi)\ + \phi_{\theta X,j}(-b_2(b_2\gamma_o + a_2\beta_o)\sin\psi$$

$$+ b_2(b_2 + r\beta_o)\cos\psi))\} + I_X dr\{\Omega(\phi_{\theta Y,j}[\cos2\theta_o\sin\psi + (\gamma_o\cos2\theta_o$$

$$- \beta_o\sin2\theta_o)\cos\psi] + \phi_{\theta X,j}[\cos2\theta_o\cos\psi - (\gamma_o\cos2\theta_o - \beta_o\sin2\theta_o)\sin\psi\ ])\}$$

$$+ I_Y dr\{\Omega(\phi_{\theta Y,j}(\gamma_o\cos\psi + \sin\psi) + \phi_{\theta X,j}(\cos\psi - \gamma_o\sin\psi))\}$$

$$+ I_Z dr\{\Omega\ (\phi_{\theta Y,j}[-\cos2\theta_o\sin\psi - (\gamma_o\cos2\theta_o - \beta_o\sin2\theta_o)\cos\psi]$$

$$+ \phi_{\theta X,j}[\ - \cos2\theta_o\cos\psi + (\gamma_o\cos2\theta_o - \beta_o\sin2\theta_o)\sin\psi])\}\Big]\phi_\theta\dot{\theta}_T\Big\}$$

$$+ \Big\{\sum_{n=1}^{N}\Big[\int_0^{R-e} mdr\{2\Omega(\phi_{X,j}(b_2 + r\beta_o)\cos\psi + \phi_{Y,j}(b_2 + r\beta_o)\sin\psi$$

$$+ \phi_{\theta Y,j}b_2(b_2 + 2r\beta_o)\cos\psi - \phi_{\theta X,j}b_2(b_2 + 2r\beta_o)\sin\psi)\}$$

$$+ I_X dr\{\Omega(\phi_{\theta Y,j}\cos2\theta_o\cos\psi - \phi_{\theta X,j}\cos2\theta_o\sin\psi)\} + I_Y dr\{\Omega(\phi_{\theta Y,j}\cos\psi$$

$$- \phi_{\theta X,j}\sin\psi)\} + I_Z dr\{\Omega(- \phi_{\theta Y,j}\cos 2\theta_o\cos\psi + \phi_{\theta X,j}\cos 2\theta_o\sin\psi)\}\Big]\dot{\beta}\Big\}$$

$$+ \Big\{\sum_{n=1}^{N}\Big[\int_0^{R-e} mdr\{2\Omega(\phi_{X,j}[- (a_2 - r\gamma_o)\cos\psi + (a_2\gamma_o + r)\sin\psi]$$

$$+ \phi_{Y,j}[- (a_2\gamma_o + r)\cos\psi - (a_2 - r\gamma_o)\sin\psi] + \phi_{\theta Y,j}[(r^2\beta_o + b_2(a_2\gamma_o$$

$$+ r))\sin\psi - (b_2(a_2 - r\gamma_o) + a_2 r\beta_o)\cos\psi] + \phi_{\theta X,j}[(r^2\beta_o + b_2(a_2\gamma_o + r))\cos\psi$$

$$+ (b_2(a_2 - r\gamma_o) + a_2 r\beta_o)\sin\psi])\} + I_X dr\{2\Omega q'_{EO}(\phi_{\theta Y,j}\sin\theta_o\sin\psi$$

$$+ \phi_{\theta X,j}\sin\theta_o\cos\psi) + \Omega(\phi_{\theta Y,j}[\sin 2\theta_o\cos\psi - (\gamma_o\sin 2\theta_o - \beta_o)\sin\psi]$$

$$+ \phi_{\theta X,j}[- \sin 2\theta_o\sin\psi - (\gamma_o\sin 2\theta_o - \beta_o)\cos\psi])\}$$

$$+ I_Y dr\{2\Omega(\phi_{\theta Y,j}(- q'_{EO}\sin\theta_o - q'_{FO}\cos\theta_o)\sin\psi + \phi_{\theta X,j}(- q'_{EO}\sin\theta_o$$

$$- q'_{FO}\cos\theta_o)\cos\psi) + \Omega(-\phi_{\theta Y,j}\beta_o\sin\psi - \phi_{\theta X,j}\beta_o\cos\psi)\}$$

$$+ I_Z dr\{2\Omega q'_{FO}(\phi_{\theta Y,j}\cos\theta_o\sin\psi + \phi_{\theta X,j}\cos\theta_o\cos\psi) + \Omega(\phi_{\theta Y,j}(- \sin 2\theta_o\cos\psi$$

$$+ (\gamma_o\sin 2\theta_o + \beta_o)\sin\psi) + \phi_{\theta X,j}(\sin 2\theta_o\sin\psi + (\gamma_o\sin 2\theta_o + \beta_o)\cos\psi)\}\Big]\dot{\gamma}\Big\}$$

$$+ \Big\{\sum_{m=1}^{N}\sum_{i=1}^{NE}\Big[\int_0^{R-e} mdr\{2\Omega(\phi_{X,j}[\phi_{E,i}(\gamma_o\cos\psi + \sin\psi) + \nu_{1,i}\cos\psi$$

$$+ \phi_{F,i}\beta_o\cos\psi] + \phi_{Y,j}[- \phi_{E,i}(\cos\psi - \gamma_o\sin\psi) + \nu_{1,i}\sin\psi$$

$$+ \phi_{F,i}\beta_o\sin\psi] + \phi_{\theta Y,j}[\phi_{E,i}(b_2 + r\beta_o)\sin\psi + b_2(\phi_{F,i}\beta_o$$

$$+ \phi_{E,i}\gamma_o)\cos\psi] + \phi_{\theta X,j}[- b_2(\phi_{F,i}\beta_o + \phi_{E,i}\gamma_o)\sin\psi + \phi_{E,i}(b_2 + r\beta_o)\cos\psi]$$

$$+ \phi_{\theta Y,j}\nu_{1,i}b_2\cos\psi - \phi_{\theta X,j}\nu_{1,i}b_2\sin\psi)\} + I_X dr\{\Omega(\phi_{\theta Y,j}[(\sin\theta_o\cos\psi$$

$$+ (q'_{EO}\sin 2\theta_o - \gamma_o\sin\theta_o + \beta_o\cos\theta_o)\sin\psi)\phi'_{E,i}$$

$$+ (\cos\theta_o\cos\psi + (q'_{EO} - \gamma_o\cos\theta_o + \beta_o\sin\theta_o)\sin\psi)\phi'_{F,i}]$$

$$+ \phi_{\theta X,j}[(- \sin\theta_o\sin\psi + (q'_{EO}\sin 2\theta_o - \gamma_o\sin\theta_o + \beta_o\cos\theta_o)\cos\psi)\phi'_{E,i}$$

$$+ (- \cos\theta_o\sin\psi + (q'_{EO} - \gamma_o\cos\theta_o + \beta_o\sin\theta_o)\cos\psi)\phi'_{F,i}])\}$$

$$+ I_Y dr\{\Omega(\phi_{\theta Y,j}[\phi'_{E,i}(- \sin\theta_o\cos\psi + (- 2q'_{FO}\cos^2\theta_o - q'_{EO}\sin 2\theta_o$$
$$- \beta_o\cos\theta_o + \gamma_o\sin\theta_o)\sin\psi) + \phi'_{F,i}(\cos\theta_o\cos\psi + (- q'_{FO}\sin 2\theta_o + q'_{EO}\cos 2\theta_o$$
$$- \beta_o\sin\theta_o - \gamma_o\cos\theta_o)\sin\psi)] + \phi_{\theta X,j}[\phi'_{E,i}(\sin\theta_o\sin\psi + (- 2q'_{FO}\cos^2\theta_o$$
$$- q'_{EO}\sin 2\theta_o - \beta_o\cos\theta_o + \gamma_o\sin\theta_o)\cos\psi) + \phi'_{F,i}(- \cos\theta_o\sin\psi + (q'_{EO}\cos 2\theta_o$$
$$- q'_{FO}\sin 2\theta_o - \beta_o\sin\theta_o - \gamma_o\cos\theta_o)\cos\psi)])\} + I_Z dr\{\Omega(\phi_{\theta Y,j}[(- \sin\theta_o\cos\psi$$
$$+ (2q'_{FO}\cos^2\theta_o + \gamma_o\sin\theta_o + \beta_o\cos\theta_o)\sin\psi)\phi'_{E,i} + (- \cos\theta_o\cos\psi$$
$$+ (q'_{FO}\sin 2\theta_o + \gamma_o\cos\theta_o + \beta_o\sin\theta_o)\sin\psi)\phi'_{F,i}] + \phi_{\theta X,j}[(\sin\theta_o\sin\psi$$
$$+ (2q'_{FO}\cos^2\theta_o + \gamma_o\sin\theta_o + \beta_o\cos\theta_o)\cos\psi)\phi'_{E,i} + (\cos\theta_o\sin\psi + (q'_{FO}\sin 2\theta_o$$
$$- q'_{EO}\cos 2\theta_o + \gamma_o\cos\theta_o + \beta_o\sin\theta_o)\cos\psi)\phi'_{F,i}])\}\Big\}\ddot{q}_{T,i}\Big\}$$
$$+ \Big\{\sum_{n=1}^{N}\sum_{i=1}^{NA}\Big[\int_0^{R-e} mdr\{\Omega^2\phi_{Z,j}[\phi_{\theta X,i}(- (a_2 - r\gamma_o)\sin\psi - (e + r + a_2\gamma_o$$
$$- b_2\beta_o)\cos\psi) + \phi_{\theta Y,i}(- (e + r + a_2\gamma_o - b_2\beta_o)\sin\psi$$
$$+ (a_2 - r\gamma_o)\cos\psi)]\}\Big]\bar{q}_i\Big\} + \Big\{M_{A,j}\omega^2 A_{,j}\bar{q}_j\Big\}$$
$$+ \Big\{\sum_{n=1}^{N}\Big[\int_0^{R-e} mdr\{\Omega^2(\phi_{X,j}[- (b_2\gamma_o + a_2\beta_o)\sin\psi + b_2\cos\psi]$$
$$+ \phi_{Y,j}[(b_2\gamma_o + a_2\beta_o)\cos\psi + b_2\sin\psi] + \phi_{\theta Y,j}[(a_2(a_2\gamma_o + r + e - 2b_2\beta_o)$$
$$- b_2^2\gamma_o)\sin\psi + (- a_2(a_2 - r\gamma_o) + b_2(b_2 + r\beta_o))\cos\psi]$$
$$+ \phi_{\theta X,j}[(a_2(a_2 - r\gamma_o) - b_2(b_2 + r\beta_o))\sin\psi + (a_2(a_2\gamma_o + r + e - 2b_2\beta_o)$$
$$- b_2^2\gamma_o)\cos\psi])\} + I_X dr\{\Omega^2 q'_{EO}(\phi_{\theta Y,j}\cos\theta_o\sin\psi + \phi_{\theta X,j}\cos\theta_o\cos\psi)$$
$$+ \Omega^2[\phi_{\theta Y,j}(\cos 2\theta_o\cos\psi - (\gamma_o\cos 2\theta_o - \beta_o\sin 2\theta_o)\sin\psi) + \phi_{\theta X,j}(- \cos 2\theta_o\sin\psi$$
$$- (\gamma_o\cos 2\theta_o - \beta_o\sin 2\theta_o)\cos\psi)]\} + I_Y dr\{\Omega^2[\phi_{\theta Y,j}(- q'_{EO}\cos\theta_o + q'_{FO}\sin\theta_o)\sin\psi$$
$$+ \phi_{\theta Y,j}(- q'_{EO}\cos\theta_o + q'_{FO}\sin\theta_o)\cos\psi]\} + I_Z dr\{\Omega^2 q'_{FO}(- \phi_{\theta Y,j}\sin\theta_o\sin\psi$$

$$
- \phi_{\theta X,j}\sin\theta_o\cos\psi) + \Omega^2[\ \phi_{\theta Y,j}(\ -\cos2\theta_o\cos\psi + (\gamma_o\cos2\theta_o\ - \beta_o\sin2\theta_o)\sin\psi)
$$

$$
+ \phi_{\theta X,j}(\cos2\theta_o\sin\psi\ + (\gamma_o\cos2\theta_o - \beta_o\sin2\theta_o)\cos\psi)]\}\Big]\ \phi_\theta\theta_T\Big\}
$$

$$
+\ \Big\{\sum_{n=1}^{N}\Big[\int_6^{R-e} mdr\{\Omega^2[\ -\phi_{X,j}(b_2 + r\beta_o)\sin\psi + \phi_{Y,j}(b_2 + r\beta_o)\cos\psi
$$

$$
+ \phi_{\theta Y,j}([(r + e)\ (a_2\gamma_o + r - b_2\beta_o) + r(a_2\gamma_o - b_2\beta_o) - b_2(2r\beta_o + b_2)]\sin\psi
$$

$$
+ [\ -a_2(a_2\gamma_o + r - b_2\beta_o) - b_2(b_2 + 2r\beta_o) + r^2\gamma_o]\cos\psi)
$$

$$
+ \phi_{\theta X,j}([a_2(a_2\gamma_o + r - b_2\beta_o) + b_2(2r\beta_o + b_2) - r^2\gamma_o]\sin\psi
$$

$$
+ [(r + e)(a_2\gamma_o + r - b_2\beta_o) + r(a_2\gamma_o - b_2\beta_o) - b_2(b_2 + 2r\beta_o)]\cos\psi)]\}
$$

$$
+ I_X dr\{\Omega^2 q'_{EO}(-\phi_{\theta Y,j}\cos\theta_o\cos\psi + \phi_{\theta X,j}\cos\theta_o\sin\psi) + \Omega^2[\phi_{\theta Y,j}(\sin^2\theta_o\sin\psi
$$

$$
+ \gamma_o\cos^2\theta_o\cos\psi) + \phi_{\theta X,j}(\sin^2\theta_o\ \cos\psi\ + \gamma_o\cos^2\theta_o\sin\psi)]\}
$$

$$
+ I_Y dr\{\Omega^2[\phi_{\theta Y,j}(q'_{EO}\cos\theta_o - q'_{FO}\sin\theta_o)\cos\psi + \phi_{\theta X,j}(-q'_{EO}\cos\theta_o
$$

$$
+ q'_{FO}\sin\theta_o)\sin\psi + \phi_{\theta Y,j}(\ -\gamma_o\cos\psi - \sin\psi) + \phi_{\theta X,j}(\gamma_o\sin\psi - \cos\psi)]\}
$$

$$
+ I_Z dr\{\Omega^2 q'_{FO}(\phi_{\theta Y,j}\sin\theta_o\cos\psi\ - \phi_{\theta X,j}\sin\theta_o\sin\psi) + \Omega^2[\ \phi_{\theta Y,j}(\cos^2\theta_o\sin\psi
$$

$$
+ \gamma_o\ \sin^2\theta_o\cos\psi) + \phi_{\theta X,j}(\cos^2\theta_o\cos\psi - \gamma_o\sin^2\theta_o\sin\psi)]\}\Big]\ \beta\ \Big\}
$$

$$
+\ \Big\{\sum_{n=1}^{N}\Big[\int_6^{R-e} mdr\{\ \Omega^2[\ \phi_{X,j}((a_2 - r\gamma_o)\sin\psi + (a_2\gamma_o + r)\cos\psi)
$$

$$
+ \phi_{Y,j}\ ((a_2\gamma_o + r)\sin\psi - (a_2 - r\gamma_o)\cos\psi) + \phi_{\theta Y,j}[(r(a_2\beta_o - b_2\gamma_o)
$$

$$
- b_2(a_2\gamma_o + r) + a_2([\ r + e]\beta_o + b_2) - r^2\beta_o)\sin\psi + (b_2(a_2 - r\gamma_o)
$$

$$
+ b_2(a_2\gamma_o + r) - a_2(a_2\beta_o - r\beta_o) + r^2\beta_c)\cos\psi] + \phi_{\theta X,j}[(-b_2(a_2 - r\gamma_o)
$$

$$
- b_2(a_2\gamma_o + r) + a_2(a_2\beta_o - r\beta_o) - r^2\beta_o)\sin\psi + (r(a_2\beta_o - b_2\gamma_o) - b_2(a_2\gamma_o + r)
$$

$$
+ a_2([r + e]\beta_o\ + b_2) - r^2\beta_o)\cos\psi]]\}
$$

$$+ I_X dr\{\Omega^2 q'_{EO}(\phi_{\theta Y,j}\sin\theta_o\cos\psi - \phi_{\theta X,j}\sin\theta_o\sin\psi) + \Omega^2[\phi_{\theta Y,j}(\beta_o\cos^2\theta_o\cos\psi$$

$$- \tfrac{1}{2}\sin2\theta_o\sin\psi) + \phi_{\theta X,j}(-\beta_o\cos^2\theta_o\sin\psi - \tfrac{1}{2}\sin2\theta_o\cos\psi)]\}$$

$$+ I_Y dr\{\Omega^2[\phi_{\theta Y,j}(-q'_{EO}\sin\theta_o - q'_{FO}\cos\theta_o)\cos\psi + \phi_{\theta X,j}(q'_{EO}\sin\theta_o$$

$$+ q'_{FO}\cos\theta_o)\sin\psi - \phi_{\theta Y,j}\beta_o\cos\psi + \phi_{\theta X,j}\beta_o\sin\psi]\}$$

$$+ I_Z dr\{\Omega^2 q'_{FO}(\phi_{\theta Y,j}\cos\theta_o\cos\psi - \phi_{\theta X,j}\cos\theta_o\sin\psi) + \Omega^2[\phi_{\theta Y,j}(\tfrac{1}{2}\sin2\theta_o\sin\psi$$

$$+ \beta_o\sin^2\theta_o\cos\psi) + \phi_{\theta X,j}(\tfrac{1}{2}\sin2\theta_o\cos\psi - \beta_o\sin^2\theta_o\sin\psi)]\}\Big]\gamma\Big\}$$

$$+ \Big\{\sum_{n=1}^{N}\sum_{i=1}^{NE}\Big[\int_0^{R-e} mdr\{\Omega^2[\phi_{X,j}(-\phi_{E,i}(\gamma_o\sin\psi - \cos\psi) - \nu_{1,i}\sin\psi$$

$$- \phi_{F,i}\beta_o\sin\psi) + \phi_{Y,j}(\phi_{E,i}(\sin\psi + \gamma_o\cos\psi) + \nu_{1,i}\cos\psi + \phi_{F,i}\beta_o\cos\psi)$$

$$+ \phi_{\theta Y,j}((\phi_{F,i}(a_2\gamma_o + r + e - 2b_2\beta_o) - \phi_{E,i}b_2\gamma_o)\sin\psi + (-\phi_{F,i}(a_2 - r\gamma_o)$$

$$+ \phi_{E,i}(b_2 + r\beta_o))\cos\psi) + \phi_{\theta X,j}((\phi_{F,i}(a_2 - r\gamma_o) - \phi_{E,i}(b_2 + r\beta_o))\sin\psi$$

$$+ (\phi_{F,i}(a_2\gamma_o + r + e - 2b_2\beta_o) - \phi_{E,i}b_2\gamma_o)\cos\psi) - \phi_{\theta Y,j}\nu_{1,i}b_2\sin\psi$$

$$- \phi_{\theta X,j}\nu_{1,i}b_2\cos\psi]\} + I_X dr\{\Omega^2[\phi_{\theta Y,j}(-\sin\theta_o\sin\psi - (\gamma_o\sin\theta_o$$

$$- \beta_o\cos\theta_o)\cos\psi)\phi'_{E,i} + \phi_{\theta X,j}(-\sin\theta_o\cos\psi + (\gamma_o\sin\theta_c - \beta_o\cos\theta_o)\sin\psi)\phi'_{E,i}]\}$$

$$+ I_Y dr\{\Omega^2[\phi_{\theta Y,j}(\phi'_{E,i}(\sin\theta_o\sin\psi + (-q'_{EO}\sin2\theta_o - \beta_o\cos\theta_o - q'_{FO}\cos2\theta_o$$

$$+ \gamma_o\sin\theta_o)\cos\psi) + \phi'_{F,i}(-\cos\theta_o\sin\psi + (-q'_{FO}\sin2\theta_o - \beta_o\sin\theta_o$$

$$+ q'_{EO}\cos2\theta_o - \gamma_o\cos\theta_o)\cos\psi)) + \phi_{\theta X,j}(\phi'_{E,i}(\sin\theta_o\cos\psi + (q'_{EO}\sin2\theta_o$$

$$+ \beta_o\cos\theta_o + q'_{FO}\cos2\theta_o - \gamma_o\sin\theta_o)\sin\psi) + \phi'_{F,i}(-\cos\theta_o\cos\psi + (-q'_{EO}\cos2\theta_o$$

$$+ \beta_o\sin\theta_o + q'_{FO}\sin2\theta_o + \gamma_o\cos\theta_o)\sin\psi))]\} + I_Z dr\{\Omega^2[\phi_{\theta Y,j}((\cos\theta_o\sin\psi$$

$$+ (-q'_{EO}\cos2\theta_o + \gamma_o\cos\theta_o + \beta_o\sin\theta_o)\cos\psi)\phi'_{F,i} + \phi'_{E,i}q'_{FO}\cos2\theta_o\cos\psi)$$

$$+ \phi_{\theta X,j}((\cos\theta_o\cos\psi + (q'_{EO}\cos2\theta_o - \gamma_o\cos\theta_o - \beta_o\sin\theta_o)\sin\psi)\phi'_{F,i}$$

$$- \phi'_{E,i}q'_{FO}\cos2\theta_o\sin\psi)]\Big]q_{T,i}\Big\} = 0 \qquad \text{(A75)}$$

Blade Pitch Equations

$$\left\{\sum_{i=1}^{NA}\left[\int_0^{R-e} m dr\{\phi_{X,i}((b_2\gamma_o + a_2\beta_o)\sin\psi - b_2\cos\psi) + \phi_{Y,i}(-(b_2\gamma_o + a_2\beta_o)\cos\psi - b_2\sin\psi) + a_2\phi_{Z,i} + \phi_{\theta Y,i}[((a_2^2 + b_2^2)\gamma_o + a_2(r+e))\sin\psi + (-a_2(a_2 - r\gamma_o) - b_2(b_2 + r\beta_o))\cos\psi] + \phi_{\theta X,i}[(a_2(a_2 - r\gamma_o) + b_2(b_2 + r\beta_o))\sin\psi + ((a_2^2 + b_2^2)\gamma_o + a_2(r+e))\cos\psi]\}\right.\right.$$

$$+ I_X dr\{q'_{EO}(\phi_{\theta Y,i}\cos\theta_o\sin\psi + \phi_{\theta X,i}\cos\theta_o\cos\psi)\} + I_Y dr\{\phi_{\theta Y,i}(-q'_{EO}\cos\theta_o + q'_{FO}\sin\theta_o)\sin\psi + \phi_{\theta X,i}(-q'_{EO}\cos\theta_o + q'_{FO}\sin\theta_o)\cos\psi + \phi_{\theta Y,i}(\gamma_o\sin\psi - \cos\psi) + \phi_{\theta X,i}(\gamma_o\cos\psi + \sin\psi)\} + I_Z dr\{q'_{FO}(-\phi_{\theta Y,i}\sin\theta_o\sin\psi - \phi_{\theta X,i}\sin\theta_o\cos\psi)\}\left.\right] \phi_\theta \ddot{\bar{q}}_i \Bigg\}$$

$$+ \left\{\left[\int_0^{R-e} m dr\{(a_2^2 + b_2^2)\} + I_Y dr\{1\}\right]\phi_\theta^2 \ddot{\theta}_T\right\} + \left\{M_1 L_2^2 \phi_{\theta PR}^2 \ddot{\theta}_T\right\}$$

$$+ \left\{\left[\int_0^{R-e} m dr\{(a_2^2 + b_2^2)\gamma_o + a_2 r\} + I_X dr\{q'_{EO}\cos\theta_o\} + I_Y dr\{-q'_{EO}\cos\theta_o + q'_{FO}\sin\theta_o + \gamma_o\} + I_Z dr\{-q'_{FO}\sin\theta_o\}\right]\phi_\theta \ddot{\beta}\right\} + \left\{-M_1 L_2^2 \tan\delta_3 \phi_{\theta PR}\ddot{\beta}\right\}$$

$$+ \left\{\left[\int_0^{R-e} m dr\{b_2 r\} + I_X dr\{q'_{EO}\sin\theta_o\} + I_Y dr\{-q'_{EO}\sin\theta_o - q'_{FO}\cos\theta_o\} + I_Z dr\{q'_{FO}\cos\theta_o\}\right]\phi_\theta \ddot{\gamma}\right\} + \left\{-M_1 L_2^2 \tan\alpha_1 \phi_{\theta PR}\ddot{\gamma}\right\}$$

$$+ \left\{\sum_{i=1}^{NE}\left[\int_0^{R-e} m dr\{a_2\phi_{F,i} + b_2\phi_{E,i}\} + I_X dr\{q'_{EO}\phi'_{F,i}\} + I_Y dr\{-q'_{FO}\phi'_{E,i}\} + I_Z dr\{q'_{FO}\phi'_{E,i}\}\right]\phi_\theta \ddot{q}_{T,i}\right\} + \left\{\sum_{i=1}^{NE}(-M_1 L_2(\phi_{FPR,i} + [L_2\tan\alpha_1/(R-e)]\phi_{ET,i}))\phi_{\theta PR}\ddot{q}_{f,i}\right\}$$

$$+ \left\{\sum_{i=1}^{NA}\left[\int_0^{R-e} m dr\{2\Omega[\phi_{\theta Y,i}(a_2(a_2 - r\gamma_o)\sin\psi + a_2(a_2\gamma_o + r + e - b_2\beta_o)\cos\psi) + \phi_{\theta X,i}(-a_2(a_2\gamma_o + r + e - b_2\beta_o)\sin\psi + a_2(a_2 - r\gamma_o)\cos\psi)]\}\right.\right.$$

$$
\begin{aligned}
&+ I_X dr\{2\Omega q'_{EO}[\phi_{\theta Y,i}\cos\theta_o\cos\psi - \phi_{\theta X,i}\cos\theta_o\sin\psi] + \Omega[\phi_{\theta Y,i}(-\cos 2\theta_o\sin\psi \\
&- (\gamma_o\cos 2\theta_o - \beta_o\sin 2\theta_o)\cos\psi) + \phi_{\theta X,i}(-\cos 2\theta_o\cos\psi + (\gamma_o\cos 2\theta_o \\
&- \beta_o\sin 2\theta_o)\sin\psi)]\} + I_Y dr\{\Omega[\phi_{\theta Y,i}(-q'_{EO}\cos\theta_o + q'_{FO}\sin\theta_o)2\cos\psi \\
&+ \phi_{\theta X,i}(q'_{EO}\cos\theta_o - q'_{FO}\sin\theta_o)2\sin\psi + \phi_{\theta Y,i}(\gamma_o\cos\psi + \sin\psi) + \phi_{\theta X,i}(-\gamma_o\sin\psi \\
&+ \cos\psi)]\} + I_Z dr\{2\Omega q'_{FO}[-\phi_{\theta Y,i}\sin\theta_o\cos\psi + \phi_{\theta X,i}\sin\theta_o\sin\psi] \\
&+ \Omega[\phi_{\theta Y,i}(\cos 2\theta_o\sin\psi + (\gamma_o\cos 2\theta_o - \beta_o\sin 2\theta_o)\cos\psi) + \phi_{\theta X,i}(\cos 2\theta_o\cos\psi \\
&- (\gamma_o\cos 2\theta_o - \beta_o\sin 2\theta_o)\sin\psi)]\}\Big]\phi_\theta\dot{\bar{q}}_i \Big\} + \Big\{(2\zeta_\theta I_T\Omega + C_1L_2^2\phi_{\theta PR}^2)\dot{\theta}_T\Big\} \\
&+ \Big\{\Big[\int_0^{R-e} mdr\{2\Omega[-b_2(b_2 + r\beta_o)]\} + I_X dr\{-\Omega\cos 2\theta_o\} + I_Y dr\{-\Omega\} \\
&+ I_Z dr\{\Omega\cos 2\theta_o\}\Big]\phi_\theta\dot{\beta}\Big\} + \Big\{-C_1L_2^2\tan\delta_3\phi_{\theta PR}\dot{\beta}\Big\} + \Big\{\Big[\int_0^{R-e} mdr\{2\Omega[a_2(b_2 + r\beta_o)]\} \\
&+ I_X dr\{-\Omega\sin 2\theta_o\} + I_Z dr\{\Omega\sin 2\theta_o\}\Big]\phi_\theta\dot{\gamma}\Big\} + \Big\{-C_1L_2^2\tan\alpha_1\phi_{\theta PR}\dot{\gamma}\Big\} \\
&+ \Big\{\sum_{i=1}^{NE}\Big[\int_0^{R-e} mdr\{2\Omega(-\phi_{F,i}b_2\beta_o + \phi_{E,i}a_2\beta_o) - 2\Omega\nu_{1,i}b_2\} + I_X dr\{\Omega[-\phi'_{E,i}\sin\theta_o \\
&- \phi'_{F,i}\cos\theta_o]\} + I_Y dr\{\Omega[\phi'_{E,i}\sin\theta_o - \phi'_{F,i}\cos\theta_o]\} + I_Z dr\{\Omega[\phi'_{E,i}\sin\theta_o \\
&+ \phi'_{F,i}\cos\theta_o]\}\Big]\phi_\theta\dot{q}_{T,i}\Big\} + \Big\{\sum_{i=1}^{NE}(-C_1L_2(\phi_{FPR,i} \\
&+ [L_2\tan\alpha_1/(R-e)]\phi_{ET,i}))\phi_{\theta PR}\dot{q}_{T,i}\Big\} + \Big\{\Big[\int_0^{R-e} mdr\{\Omega^2[e(a_2\gamma_o - b_2\beta_o) \\
&- b_2(b_2 + r\beta_o) + a_2^2]\} + I_X dr\{-\Omega^2\cos 2\theta_o\} + I_Z dr\{\Omega^2\cos 2\theta_o\}\Big]\phi_\theta^2\theta_T\Big\} \\
&+ \Big\{\Big(\int_0^{R-e} K\phi_\theta^2\Big)\theta_T\Big\} + \Big\{K_1L_2^2\phi^2_{\theta PR}\theta_T\Big\} \\
&+ \Big\{\Big[\int_0^{R-e} mdr\{\Omega^2[a_2(a_2\gamma_o + r + e) - b_2(b_2\gamma_o - 2a_2\beta_o)]\} + I_X dr\{\Omega^2[q'_{EO}\cos\theta_o \\
&- \gamma_o\cos 2\theta_o]\} + I_Y dr\{\Omega^2(-q'_{EO}\cos\theta_o + q'_{FO}\sin\theta_o)\} + I_Z dr\{\Omega^2[-q'_{FO}\sin\theta_o \\
&+ \gamma_o\cos 2\theta_o]\}\Big]\phi_\theta\beta\Big\} + \Big\{-K_1L_2^2\tan\delta_3\phi_{\theta PR}\beta\Big\} + \Big\{\Big[\int_0^{R-e} mdr\{\Omega^2[-(a_2^2 + b_2^2)\beta_o \\
&+ eb_2]\} + I_X dr\{-\Omega^2\beta_o\cos 2\theta_o\} + I_Z dr\{\Omega^2\beta_o\cos 2\theta_o\}\Big]\phi_\theta\gamma\Big\}
\end{aligned}
$$

$$+ \left\{ - K_1 L_2^2 \tan\alpha_1 \phi_{\theta PR} \gamma \right\} + \left\{ \sum_{i=1}^{NE} \left[\int_0^{R-e} m dr \{ \Omega^2 [\phi_{F,i}(a_2 + e\gamma_o) - \phi_{E,i}(b_2 \right.\right.$$

$$+ (r + e)\beta_o)] \} + I_X dr \{ - \Omega^2 \beta_o \phi'_{E,i} \cos\theta_o \} + I_Y dr \{ \Omega^2 \beta_o (\phi'_{E,i} \cos\theta_o + \phi'_{F,i} \sin\theta_o) \}$$

$$\left.\left. + I_Z dr \{ \Omega^2 [- \phi'_{E,i} q'_{EO} \cos 2\theta_o + (q'_{EO} \cos 2\theta_o - \beta_o \sin\theta_o) \phi'_{F,i}] \} \right] \phi_\theta \, q_{T,i} \right\}$$

$$+ \left\{ \sum_1^{NE} (- K_1 L_2 (\phi_{FPR,i} + [L_2 \tan\alpha_1 / (R-e)] \phi_{ET,i})) \phi_{\theta PR} q_{T,i} \right\}$$

Tail rotor control system contribution:

$$+ C_1 L_2 \phi_{\theta PR} \dot{X}_2 + K_1 L_2 \phi_{\theta PR} X_2$$

Main rotor control system contribution:

$$+ [\tfrac{1}{2} C_1 L_2 {}^{R_B}/_{R_S} (-(\sin\delta + \cos\delta)\sin\psi + (\cos\delta - \sin\delta)\cos\psi)$$

$$+ \tfrac{1}{2} C_1 L_2] \phi_{\theta PR} \dot{X}_A + [\tfrac{1}{2} C_1 L_2 {}^{R_B}/_{R_S} ((\sin\delta - \cos\delta)\sin\psi$$

$$- (\cos\delta + \sin\delta)\cos\psi) + \tfrac{1}{2} C_1 L_2] \phi_{\theta PR} \dot{X}_F + [C_1 L_2 {}^{R_B}/_{R_S} (\cos\delta \sin\psi + \sin\delta \cos\psi)] \phi_{\theta PR} \dot{X}_L$$

+ The coefficients of X_A, X_F, and X_L, which are identical to those of $\dot{X}_A$, $\dot{X}_F$, and $\dot{X}_L$ respectively, with C_1 replaced by K_1.

$$= 0 \qquad \text{(A76)}$$

Blade Rigid-Body Flapping Equations

$$\left\{\sum_{i=1}^{NA}\left[\int_0^{R-e} m\,dr\{\phi_{X,i}(b_2 + r\beta_o)\sin\psi - \phi_{Y,i}(b_2 + r\beta_o)\cos\psi + \phi_{Z,i}(r + a_2\gamma_o - b_2\beta_o) + \phi_{\theta Y,i}[(e(a_2\gamma_o - b_2\beta_o) + r(r + e + 2a_2\gamma_o) + b_2^2)\sin\psi + (-a_2(a_2\gamma_o - b_2\beta_o) - r(a_2 - r\gamma_o))\cos\psi] + \phi_{\theta X,i}[(a_2(a_2\gamma_o - b_2\beta_o) + r(a_2 - r\gamma_o))\sin\psi + (e(a_2\gamma_o - b_2\beta_o) + r(r + e + 2a_2\gamma_o) + b_2^2)\cos\psi]\} + I_X dr\{q'_{EO}(-\phi_{\theta Y,i}\cos\theta_o\cos\psi + \phi_{\theta X,i}\cos\theta_o\sin\psi) + \phi_{\theta Y,i}(\cos^2\theta_o\sin\psi + (\gamma_o\cos^2\theta_o - \tfrac{1}{2}\beta_o\sin 2\theta_o)\cos\psi) + \phi_{\theta X,i}(\cos^2\theta_o\cos\psi - (\gamma_o\cos^2\theta_o - \tfrac{1}{2}\beta_o\sin 2\theta_o)\sin\psi)\} + I_Y dr\{\phi_{\theta Y,i}(q'_{EO}\cos\theta_o - q'_{FO}\sin\theta_o - \gamma_o)\cos\psi + \phi_{\theta X,i}(-q'_{EO}\cos\theta_o + q'_{FO}\sin\theta_o + \gamma_o)\sin\psi\} + I_Z dr\{q'_{FO}(\phi_{\theta Y,i}\sin\theta_o\cos\psi - \phi_{\theta X,i}\sin\theta_o\sin\psi) + \phi_{\theta Y,i}(\sin^2\theta_o\sin\psi + (\gamma_o\sin^2\theta_o + \tfrac{1}{2}\beta_o\sin 2\theta_o)\cos\psi) + \phi_{\theta X,i}(\sin^2\theta_o\cos\psi - (\gamma_o\sin^2\theta_o + \tfrac{1}{2}\beta_o\sin 2\theta_o)\sin\psi)\}\right]\ddot{\bar{q}}_i\right\}$$

$$+\left\{\left[\int_0^{R-e} m\,dr\{((a_2^2 + b_2^2)\gamma_o + a_2 r)\} + I_X dr\{q'_{EO}\cos\theta_o\} + I_Y dr\{(-q'_{EO}\cos\theta_o + q'_{FO}\sin\theta_o + \gamma_o)\} + I_Z dr\{-q'_{FO}\sin\theta_o\}\right]\ddot{\phi}_{\theta T}\right\} + \left\{-M_1 L_2^2\tan\delta_3\,\phi_{\theta PR}\ddot{\theta}_T\right\}$$

$$+\left\{\left[\int_0^{R-e} m\,dr\{r^2 + b_2^2 + 2a_2 r\gamma_o\} + I_X dr\{\cos^2\theta_o\} + I_Z dr\{\sin^2\theta_o\}\right]\ddot{\beta}\right\}$$

$$+\left\{M_1 L_2^2\tan^2\delta_3\,\ddot{\beta}\right\} + \left\{\left[\int_0^{R-e} m\,dr\{-b_2(a_2 - r\gamma_o)\} + I_X dr\{\tfrac{1}{2}\sin 2\theta_o\} + I_Z dr\{-\tfrac{1}{2}\sin 2\theta_o\}\right]\ddot{\gamma}\right\} + \left\{M_1 L_2^2\tan\delta_3\tan\alpha_1\,\ddot{\gamma}\right\} + \left\{\sum_{i=1}^{NE}\left[\int_0^{R-e} m\,dr\{\phi_{F,i}(a_2\gamma_o + r) + \phi_{E,i}b_2\gamma_o + \nu_{1,i}b_2\} + I_X dr\{\phi'_{F,i}\cos\theta_o\} + I_Z dr\{-\phi'_{E,i}\sin\theta_o\}\right]\ddot{q}_{T,i}\right\}$$

$$+\left\{\sum_{i=1}^{NE}(M_1 L_2\tan\delta_3(\phi_{FPR,i} + [L_2\tan\alpha_1/(R-e)]\phi_{ET,i}))\ddot{q}_{T,i}\right\}$$

$$+\left\{\sum_{i=1}^{NA}\left[\int_0^{R-e} m\,dr\{2\Omega[\phi_{\theta Y,i}((r(r + e + 2a_2\gamma_o) + e(a_2\gamma_o - b_2\beta_o) + b_2^2)\cos\psi + (a_2(a_2\gamma_o - b_2\beta_o) - r^2\gamma_o)\sin\psi) + \phi_{\theta X,i}((-r(r + e + 2a_2\gamma_o) - e(a_2\gamma_o$$

$$- b_2\beta_o) - b_2^2)\sin\psi + (a_2(a_2\gamma_o - b_2\beta_o) - r^2\gamma_o)\cos\psi)]\}$$

$$+ I_X dr\{2\Omega q'_{EO}(\phi_{\theta Y,i}\cos\theta_o\sin\psi + \phi_{\theta X,i}\cos\theta_o\cos\psi)$$

$$+ \Omega[\phi_{\theta Y,i}(\cos\psi - 2(\gamma_o\cos^2\theta_o - \tfrac{1}{2}\beta_o\sin 2\theta_o)\sin\psi) + \phi_{\theta X,i}(-\sin\psi - 2(\gamma_o\cos^2\theta_o$$

$$- \tfrac{1}{2}\beta_o\sin 2\theta_o)\cos\psi)]\} + I_Y dr\{\Omega[\phi_{\theta Y,i}(-q'_{EO}\cos\theta_o + q'_{FO}\sin\theta_o)2\sin\psi$$

$$+ \phi_{\theta X,i}(-q'_{EO}\cos\theta_o + q'_{FO}\sin\theta_o)2\cos\psi$$

$$+ \phi_{\theta Y,i}(2\gamma_o\sin\psi - \cos\psi) + \phi_{\theta X,i}(2\gamma_o\cos\psi + \sin\psi)]\} + I_Z dr\{2\Omega q'_{FO}[$$

$$- \phi_{\theta Y,i}\sin\theta_o\sin\psi - \phi_{\theta X,i}\sin\theta_o\cos\psi] + \Omega[\phi_{\theta Y,i}(\cos\psi - (2\gamma_o\sin^2\theta_o$$

$$+ \beta_o\sin 2\theta_o)\sin\psi) + \phi_{\theta X,i}(-\sin\psi - (2\gamma_o\sin^2\theta_o + \beta_o\sin 2\theta_o)\cos\psi)]\}\Big]\dot{\bar{q}}_i\Big\}$$

$$+ \Big\{\Big[\int_0^{R-e} mdr\{2\Omega b_2(b_2 + r\beta_o)\} + I_X dr\{\Omega\cos 2\theta_o\} + I_Y dr\{\Omega\} + I_Z dr\{-\Omega\cos 2\theta_o\}\Big]\phi_\theta\dot{\theta}_T\Big\}$$

$$+ \Big\{-C_1L_2^2\tan\delta_3\phi_{\theta PR}\dot{\theta}_T\Big\} + \Big\{C_1L_2^2\tan^2\delta_3\dot{\beta}\Big\} + \Big\{\Big[\int_0^{R-e} mdr\{2\Omega(b_2(a_2\gamma_o + r)$$

$$+ r^2\beta_o)\} + I_X dr\{\Omega(2q'_{EO}\sin\theta_o + \beta_o - \gamma_o\sin 2\theta_o)\} + I_Y dr\{\Omega(-2q'_{EO}\sin\theta_o$$

$$- 2q'_{FO}\cos\theta_o - \beta_o)\} + I_Z dr\{\Omega(2q'_{FO}\cos\theta_o + \gamma_o\sin 2\theta_o + \beta_o)\}\Big]\dot{\gamma}\Big\}$$

$$+ \Big\{C_1L_2^2\tan\delta_3\tan\alpha_1\dot{\gamma}\Big\} + \Big\{\sum_{i=1}^{NE}\Big[\int_0^{R-e} mdr\{2\Omega[\phi_{E,i}(b_2 + r\beta_o)]\}$$

$$+ I_X dr\{\Omega[\phi'_{E,i}(q'_{EO}\sin 2\theta_o + \beta_o\cos\theta_o - \gamma_o\sin\theta_o) + \phi'_{F,i}(q'_{EO} + \beta_o\sin\theta_o$$

$$- \gamma_o\cos\theta_o)]\} + I_Y dr\{\Omega[\phi'_{E,i}(-q'_{EO}\sin 2\theta_o - 2q'_{FO}\cos^2\theta_o + \gamma_o\sin\theta_o - \beta_o\cos\theta_o)$$

$$+ \phi'_{F,i}(q'_{EO}\cos 2\theta_o - q'_{FO}\sin 2\theta_o - \gamma_o\cos\theta_o - \beta_o\sin\theta_o)]\}$$

$$+ I_Z dr\{\Omega[\phi'_{E,i}(2q'_{FO}\cos^2\theta_o + \gamma_o\sin\theta_o + \beta_o\cos\theta_o) + \phi'_{F,i}(q'_{FO}\sin 2\theta_o + \gamma_o\cos\theta_o$$

$$+ \beta_o\sin\theta_o)]\}\Big]\dot{q}_{T,i}\Big\} + \Big\{\sum_{i=1}^{NE}(C_1L_2\tan\delta_3(\phi_{FPR,i} + [L_2\tan\alpha_1/(R-e)]\phi_{ET,i}))\dot{q}_{T,i}\Big\}$$

$$+ \Big\{\sum_{i=1}^{NA}\Big[\int_0^{R-e} mdr\{\Omega^2[\phi_{\theta Y,i}(-b_2(b_2 + 2r\beta_o))\cos\psi + \phi_{\theta X,i}(b_2(b_2 + 2r\beta_o))\sin\psi]\}\Big]\bar{q}_i\Big\}$$

$$+ \Big\{\Big[\int_0^{R-e} mdr\{\Omega^2[a_2(a_2\gamma_o + r + e) - b_2(b_2\gamma_o - 2a_2\beta_o)]\} + I_X dr\{\Omega^2[q'_{EO}\cos\theta_o$$

$$- \gamma_o\cos 2\theta_o + \beta_o\sin 2\theta_o]\} + I_Y dr\{\Omega^2[-q'_{EO}\cos\theta_o - q'_{FO}\sin\theta_o]\} + I_Z dr\{\Omega^2[q'_{FO}\sin\theta_o$$

$$+ \gamma_o \cos 2\theta_o - \beta_o \sin 2\theta_o]\Big]\phi_\theta \theta_T \Big\} + \Big\{ - K_1 L_2^2 \tan\delta_3 \phi_{\theta PR} \theta_T \Big\}$$

$$+ \Big\{ \Big[\int_0^{R-e} m dr \{ \Omega^2 [e(a_2 \gamma_o - b_2 \beta_o) + r(r+e) - 4r\beta_o b_2 + 2a_2 r\gamma_o - b_2^2] \}$$

$$+ I_X dr\{\Omega^2 \sin^2\theta_o\} + I_Y dr\{-\Omega^2\} + I_Z dr\{\Omega^2 \cos^2\theta_o\}\Big]\beta \Big\} + \Big\{ K_1 L_2^2 \tan^2\delta_3 \beta \Big\}$$

$$+ \Big\{ K_\beta \beta \Big\} + \Big\{ \Big[\int_0^{R-e} m dr \{ \Omega^2 [b_2 (a_2 - r\gamma_o) + a_2 \beta_o (2r + e)] \} + I_X dr \{$$

$$- \tfrac{1}{2}\Omega^2 \sin 2\theta_o \} + I_Z dr \{ \tfrac{1}{2}\Omega^2 \sin 2\theta_o \} \Big] \gamma \Big\} + \Big\{ K_1 L_2^2 \tan\delta_3 \tan\alpha_1 \gamma \Big\}$$

$$+ \Big\{ \sum_{i=1}^{NE} \Big[\int_0^{R-e} m dr \{ \Omega^2 [- \phi_{E,i} b_2 \gamma_o + \phi_{F,i} (a_2 \gamma_o + r + e + 2b_2 \beta_o) - \nu_{1,i} b_2] \}$$

$$+ I_X dr \{ - \Omega^2 \phi'_{E,i} \sin\theta_o \} + I_Y dr \{ \Omega^2 [\phi'_{E,i} \sin\theta_o + \phi'_{F,i} \cos\theta_o] \}$$

$$+ I_Z dr \{ - \Omega^2 [\phi'_{F,i} \cos\theta_o] \} \Big] q_{T,i} \Big\} + \Big\{ \sum_{i=1}^{NE} (K_1 L_2 \tan\delta_3 (\phi_{FPR,i}$$

$$+ [L_2 \tan\alpha_1 / (R-e)] \phi_{ET,i})) q_{T,i} \Big\}$$

Tail rotor control system contribution:

$$- C_1 L_2 \tan\delta_3 \dot{X}_2 - K_1 L_2 \tan\delta_3 X_2$$

Main Rotor Control system contribution:

$$+ [- \tfrac{1}{2} C_1 L_2 \tan\delta_3 {}^{R_B}/_{R_S} (-(\sin\delta + \cos\delta)\sin\psi + (\cos\delta - \sin\delta)\cos\psi)$$

$$- \tfrac{1}{2} C_1 L_2 \tan\delta_3] \dot{X}_A + [- \tfrac{1}{2} C_1 L_2 \tan\delta_3 {}^{R_B}/_{R_S} ((\sin\delta - \cos\delta)\sin\psi - (\cos\delta$$

$$+ \sin\delta)\cos\psi) - \tfrac{1}{2} C_1 L_2 \tan\delta_3] \dot{X}_F + [- C_1 L_2 \tan\delta_3 {}^{R_B}/_{R_S} (\cos\delta\sin\psi + \sin\delta\cos\psi)] \dot{X}_L$$

+ The coefficients of X_A, X_F, and X_L, which are identical to those of $\dot{X}_A$, $\dot{X}_F$, and $\dot{X}_L$ respectively, with C_1 replaced by K_1.

$$= 0 \qquad \text{(A77)}$$

Blade Rigid-Body Lagging Equations

$$\left\{\sum_{i=1}^{NA}\left[\int_0^{R-e} mdr\{\phi_{X,i}(-(a_2 - r\gamma_o)\sin\psi - (a_2\gamma_o + r)\cos\psi) + \phi_{Y,i}(-(a_2\gamma_o + r)\sin\psi\right.\right.$$

$$+ (a_2 - r\gamma_o)\cos\psi) + \phi_{Z,i}a_2\beta_o + \phi_{\theta Y,i}(([e\beta_o - b_2](a_2 - r\gamma_o))\sin\psi$$

$$+ (-b_2(a_2\gamma_o + r) - (a_2^2 + r^2)\beta_o)\cos\psi) + \phi_{\theta X,i}((b_2(a_2\gamma_o + r) + (a_2^2$$

$$+ r^2)\beta_o)\sin\psi + ([e\beta_o - b_2](a_2 - r\gamma_o))\cos\psi)\} + I_X dr\{q'_{EO}(-\phi_{\theta Y,i}\sin\theta_o\cos\psi$$

$$+ \phi_{\theta X,i}\sin\theta_o\sin\psi) + \phi_{\theta Y,i}(\tfrac{1}{2}\sin 2\theta_o\sin\psi + (\tfrac{1}{2}\gamma_o\sin 2\theta_o - \beta_o\sin^2\theta_o)\cos\psi)$$

$$+ \phi_{\theta X,i}(\tfrac{1}{2}\sin 2\theta_o\cos\psi - (\tfrac{1}{2}\gamma_o\sin 2\theta_o - \beta_o\sin^2\theta_o)\sin\psi)\} + I_Y dr\{\phi_{\theta Y,i}(q'_{EO}\sin\theta_o$$

$$+ q'_{FO}\cos\theta_o)\cos\psi + \phi_{\theta X,i}(-q'_{EO}\sin\theta_o - q'_{FO}\cos\theta_o)\sin\psi\} + I_Z dr\{q'_{FO}($$

$$- \phi_{\theta Y,i}\cos\theta_o\cos\psi + \phi_{\theta X,i}\cos\theta_o\sin\psi) + \phi_{\theta Y,i}(-\tfrac{1}{2}\sin 2\theta_o\sin\psi - (\tfrac{1}{2}\gamma_o\sin 2\theta_o$$

$$\left.\left.+ \beta_o\cos^2\theta_o)\cos\psi) + \phi_{\theta X,i}(-\tfrac{1}{2}\sin 2\theta_o\cos\psi + (\tfrac{1}{2}\gamma_o\sin 2\theta_o + \beta_o\cos^2\theta_o)\sin\psi)\right]\ddot{q}_i\right\}$$

$$+ \left\{\left[\int_0^{R-e} mdr\{b_2 r\} + I_X dr\{q'_{EO}\sin\theta_o\} + I_Y dr\{-q'_{EO}\sin\theta_o - q'_{FO}\cos\theta_o\}\right.\right.$$

$$\left.\left.+ I_Z dr\{q'_{FO}\cos\theta_o\}\right]\phi_\theta\ddot{\theta}_T\right\} + \left\{-M_1L_2^2\tan\alpha_1\phi_{\theta PR}\ddot{\theta}_T\right\} + \left\{\left[\int_0^{R-e} mdr\{-b_2(a_2\right.\right.$$

$$\left.\left.- r\gamma_o)\} + I_X dr\{\tfrac{1}{2}\sin 2\theta_o\} + I_Z dr\{-\tfrac{1}{2}\sin 2\theta_o\}\right]\ddot{\beta}\right\} + \left\{M_1L_2^2\tan\delta_3\tan\alpha_1\ddot{\beta}\right\}$$

$$+ \left\{\left[\int_0^{R-e} mdr\{a_2^2 + r^2\} + I_X dr\{\sin^2\theta_o\} + I_Z dr\{\cos^2\theta_o\}\right]\ddot{\gamma}\right\}$$

$$+ \left\{M_1L_2^2\tan^2\alpha_1\ddot{\gamma}\right\} + \left\{\sum_{i=1}^{NE}\left[\int_0^{R-e} mdr\{\phi_{E,i}r - a_2\nu_{1,i}\} + I_X dr\{\phi'_{F,i}\sin\theta_o\}\right.\right.$$

$$\left.\left.+ I_Z dr\{\phi'_{E,i}\cos\theta_o\}\right]\ddot{q}_{T,i}\right\} + \left\{\sum_{i=1}^{NE}(M_1L_2\tan\alpha_1(\phi_{FPR,i}\right.$$

$$\left.+ [L_2\tan\alpha_1/(R-e)]\phi_{ET,i}))\ddot{q}_{T,i}\right\} + \left\{\sum_{i=1}^{NA}\left[\int_0^{R-e} mdr\{2\Omega[\phi_{\theta Y,i}(a_2^2\beta_o\sin\psi\right.\right.$$

$$+ (r + e)a_2\beta_o\cos\psi) + \phi_{\theta X,i}(-(r + e)a_2\beta_o\sin\psi + a_2^2\beta_o\cos\psi)]\}$$

$$+ I_X dr\{\Omega[-\phi_{\theta Y,i}\beta_o\cos 2\theta_o\sin\psi - \phi_{\theta X,i}\beta_o\cos 2\theta_o\cos\psi]\} + I_Y dr\{\Omega\beta_o(\phi_{\theta Y,i}\sin\psi$$

$$\left.\left.+ \phi_{\theta X,i}\cos\psi)\} + I_Z dr\{\Omega\beta_o(\phi_{\theta Y,i}\cos 2\theta_o\sin\psi + \phi_{\theta X,i}\cos 2\theta_o\cos\psi)\}\right]\dot{\tilde{q}}_i\right\}$$

$$+ \left\{\left[\int_0^{R-e} mdr\{-2\Omega a_2(b_2 + r\beta_o)\} + I_X dr\{\Omega\sin 2\theta_o\} + I_Z dr\{-\Omega\sin 2\theta_o\}\right]\phi_\theta\dot{\delta}_T\right\}$$

$$+ \left\{ - C_1 L_2^2 \tan\alpha_1 \phi_\theta \dot{\theta}_T \right\}$$

$$+ \left\{ \left[\int_0^{R-e} m dr\{ - 2\Omega(r^2\beta_o + b_2(a_2\gamma_o + r))\} + I_X dr\{\Omega(- 2q'_{EO}\sin\theta_o + \gamma_o \sin 2\theta_o - \beta_o)\} + I_Y dr\{\Omega\beta_o\} + I_Z dr\{\Omega(- 2q'_{FO}\cos\theta_o - \gamma_o \sin 2\theta_o - \beta_o)\} \right] \dot{\beta} \right\}$$

$$+ \left\{ C_1 L_2^2 \tan\delta_3 \tan\alpha_1 \dot{\beta} \right\} + \left\{ (2\zeta_\gamma I_\gamma \omega_\gamma + C_1 L_2^2 \tan^2\alpha_1)\dot{\gamma} \right\}$$

$$\left\{ \sum_{i=1}^{NE} \left[\int_0^{R-e} m dr\{ - 2\Omega(a_2\phi_{E,i} + r\beta_o\phi_{F,i}) - 2\Omega r\nu_{1,i}\} + I_X dr\{\Omega[\phi'_{E,i}(2q'_{EO}\sin^2\theta_o + \beta_o \sin\theta_o) - \phi'_{F,i}\beta_o\cos\theta_o]\} + I_Y dr\{\Omega[\phi'_{E,i}(- 2q'_{EO}\sin^2\theta_o - q'_{FO}\sin 2\theta_o - \beta_o \sin\theta_o) + \phi'_{F,i}(q'_{EO}\sin 2\theta_o + 2q'_{FO}\cos^2\theta_o + \beta_o\cos\theta_o)]\} + I_Z dr\{\Omega[\phi'_{E,i}(q'_{FO}\sin 2\theta_o + \beta_o \sin\theta_o) + \phi'_{F,i}(- 2q'_{FO}\cos^2\theta_o - \beta_o\cos\theta_o)]\} \right] \dot{q}_{T,i} \right\} + \left\{ \sum_{i=1}^{NE} (C_1 L_2 \tan\alpha_1 (\phi_{FPR,i} + [L_2\tan\alpha_1/(R-e)]\phi_{ET,i}))\dot{q}_{T,i} \right\}$$

$$+ \left\{ \sum_{i=1}^{NA} \left[\int_0^{R-e} m dr\{\Omega^2[\phi_{\theta Y,i}((- b_2(a_2\gamma_o + r) - r^2\beta_o)\sin\psi + (b_2(a_2 - r\gamma_o) + a_2 r\beta_o)\cos\psi) + \phi_{\theta X,i}((- b_2(a_2 - r\gamma_o) - a_2 r\beta_o)\sin\psi + (- b_2(a_2\gamma_o + r) - r^2\beta_o)\cos\psi)]\} \right] \bar{q}_i \right\} + \left\{ \left[\int_0^{R-e} m dr\{\Omega^2[- (b_2^2 + a_2^2)\beta_o + eb_2]\} + I_X dr\{ - \Omega^2\beta_o \cos 2\theta_o\} + I_Z dr\{\Omega^2\beta_o\cos 2\theta_o\} \right] \phi_\theta \theta_T \right\} + \left\{ - K_1 L_2^2 \tan\alpha_1 \phi_{\theta PR}\theta_T \right\}$$

$$+ \left\{ \left[\int_0^{R-e} m dr\{\Omega^2[b_2(a_2 - r\gamma_o) + a_2\beta_o(2r + e)]\} + I_X dr\{- \tfrac{1}{2}\Omega^2 \sin 2\theta_o\} + I_Z dr\{\tfrac{1}{2}\Omega^2 \sin 2\theta_o\} \right] \beta \right\} + \left\{ K_1 L_2^2 \tan\delta_3 \tan\alpha_1 \beta \right\} + \left\{ \left[\int_0^{R-e} m dr\{\Omega^2[e(r - a_2\gamma_o) - b_2 r\beta_o]\} + I_Z dr\{- \Omega^2\beta_o \sin^2\theta_o\} \right] \gamma \right\} + \left\{ K_1 L_2^2 \tan^2\alpha_1 \gamma \right\} + \left\{ K_\gamma \gamma \right\}$$

$$+ \left\{ \sum_{i=1}^{NE} \int_0^{R-e} m dr\{\Omega^2[- \phi_{E,i}(b_2\beta_o - e) - a_2\beta_o\phi_{F,i}]\} q_{T,i} \right\}$$

$$+ \left\{ \sum_{i=1}^{NE} (K_1 L_2 \tan\alpha_1 (\phi_{FPR,i} + [L_2\tan\alpha_1/(R-e)]\phi_{ET,i}))q_{T,i} \right\}$$

Tail rotor control system contribution:

$$- C_1 L_2 \tan\alpha_1 \dot{X}_2 - K_1 L_2 \tan\alpha_1 X_2$$

Main rotor control system contribution:

$$+ \left[-\tfrac{1}{2}C_1L_2\tan\alpha_1 {}^{R_B}/_{R_S} \left(-(\sin\delta + \cos\delta)\sin\psi + (\cos\delta - \sin\delta)\cos\psi\right) \right.$$

$$\left. - \tfrac{1}{2}C_1L_2\tan\alpha_1 \right]\dot{X}_A + \left[-\tfrac{1}{2}C_1L_2\tan\alpha_1 {}^{R_B}/_{R_S} \left((\sin\delta - \cos\delta)\sin\psi - (\cos\delta \right.\right.$$

$$\left.\left. + \sin\delta)\cos\psi\right) - \tfrac{1}{2}C_1L_2\tan\alpha_1 \right]\dot{X}_F + \left[-C_1L_2\tan\alpha_1 {}^{R_B}/_{R_S} (\cos\delta\sin\psi + \sin\delta\cos\psi) \right]\dot{X}_L$$

+ The coefficients of X_A, X_F, and X_L, which are identical to those of $\dot{X}_A$, $\dot{X}_F$, and $\dot{X}_L$, respectively, with C_1 replaced by K_1.

$$= 0 \qquad \text{(A78)}$$

Blade Bending Equations

$$\Bigg\{\sum_{i=1}^{NA}\Big[\int_0^{R-e} mdr\{\phi_{X,i}[\phi_{E,j}(\gamma_o\sin\psi - \cos\psi) + \nu_{1,j}\sin\psi + \phi_{F,j}\beta_o\sin\psi]$$

$$+ \phi_{Y,i}[\phi_{E,j}(-\gamma_o\cos\psi - \sin\psi) - \nu_{1,j}\cos\psi - \phi_{F,j}\beta_o\cos\psi] + \phi_{Z,i}\phi_{F,j}$$

$$+ \phi_{\theta Y,i}[(\phi_{E,j}b_2\gamma_o + \phi_{F,j}(a_2\gamma_o + r + e))\sin\psi + (-\phi_{F,j}(a_2 - r\gamma_o)$$

$$- \phi_{E,j}(b_2 + r\beta_o))\cos\psi] + \phi_{\theta X,i}[(\phi_{F,j}(a_2 - r\gamma_o) + \phi_{E,j}(b_2 + r\beta_o))\sin\psi$$

$$+ (\phi_{E,j}b_2\gamma_o + \phi_{F,j}(a_2\gamma_o + r + e))\cos\psi] + \phi_{\zeta,i}b_2\nu_{1,j}\sin\psi + \phi_{\theta X,i}b_2\nu_{1,j}\cos\psi\}$$

$$+ I_X dr\{\phi'_{F,j}[\phi_{\theta Y,i}(\cos\theta_o\sin\psi + (\gamma_o\cos\theta_o - \beta_o\sin\theta_o - q'_{EO})\cos\psi)$$

$$+ \phi_{\theta X,i}(\cos\theta_o\cos\psi - (\gamma_o\cos\theta_o - \beta_o\sin\theta_o - q'_{EO})\sin\psi)]\}$$

$$+ I_Y dr\{\phi'_{E,j}[\phi_{\theta Y,i}q'_{FO}\cos\psi - \phi_{\theta X,i}q'_{FO}\sin\psi]\} + I_Z dr\{\phi'_{E,j}[\phi_{\theta Y,i}(-\sin\theta_o\sin\psi$$

$$- (\gamma_o\sin\theta_o + \beta_o\cos\theta_o + q'_{FO})\cos\psi) + \phi_{\theta X,i}(-\sin\theta_o\cos\psi + (\gamma_o\sin\theta_o + \beta_o\cos\theta_o$$

$$+ q'_{FO})\sin\psi)]\}\Big]\ddot{q}_i\Bigg\} + \Bigg\{\Big[\int_0^{R-e} mdr\{b_2\phi_{E,j} + a_2\phi_{F,j}\} + I_X dr\{q'_{EO}\phi'_{F,j}\}$$

$$+ I_Y dr\{-q'_{FO}\phi'_{E,j}\} + I_Z dr\{q'_{FO}\phi'_{E,j}\}\Big]\phi_\theta\ddot{\theta}_T\Bigg\} + \Bigg\{-M_1L_2\phi_{\theta PR}(\phi_{FPR,j}$$

$$+ [L_2\tan\alpha_1/(R-e)]\phi_{ET,j})\ddot{\theta}_T\Bigg\} + \Bigg\{\Big[\int_0^{R-e} mdr\{\phi_{F,j}(a_2\gamma_o + r) + \phi_{E,j}b_2\gamma_o$$

$$+ b_2\nu_{1,j}\} + I_X dr\{\phi'_{F,j}\cos\theta_o\} + I_Z dr\{-\phi_{E,j}\sin\theta_o\}\Big]\ddot{\beta}\Bigg\} + \Bigg\{M_1L_2\tan\delta_3(\phi_{FPR,j}$$

$$+ [L_2\tan\alpha_1/(R-e)]\phi_{ET,j})\ddot{\beta}\Bigg\} + \Bigg\{\Big[\int_0^{R-e} mdr\{\phi_{E,j}r - a_2\nu_{1,j}\} + I_X dr\{\phi'_{F,j}\sin\theta_o\}$$

$$+ I_Z dr\{\phi'_{E,j}\cos\theta_o\}\Big]\ddot{\gamma}\Bigg\} + \Bigg\{M_1L_2\tan\alpha_1(\phi_{FPR,j} + [L_2\tan\alpha_1/(R-e)]\phi_{ET,j})\ddot{\gamma}\Bigg\}$$

$$+ \Bigg\{\sum_{i=1}^{NE}\Big[\int_0^{R-e} mdr\{\phi^2_{E,j} + \phi^2_{F,j}\} + I_X dr\{\phi'_{F,j}\phi'_{F,i}\} + I_Z dr\{\phi'_{E,j}\phi'_{E,i}\}\Big]\ddot{q}_{T,i}\Bigg\}$$

$$+ \Bigg\{(\phi_{FPR,j} + [L_2\tan\alpha_1/(R-e)]\phi_{ET,j})\sum_{i=1}^{NE}(M_1(\phi_{FPR,i}$$

$$+ [L_2\tan\alpha_1/(R-e)]\phi_{ET,i}))\ddot{q}_{T,i}\Bigg\} + \Bigg\{\sum_{i=1}^{NA}\Big[\int_0^{R-e} mdr\{2\Omega[\phi_{\theta Y,i}(\phi_{F,j}(a_2 - r\gamma_o)\sin\psi$$

$$+ \phi_{F,j}(a_2\gamma_o + r + e - b_2\beta_o)\cos\psi) + \phi_{\theta X,i}(-\phi_{F,j}(a_2\gamma_o + r + e - b_2\beta_o)\sin\psi$$

$$+ \phi_{F,j}(a_2 - r\gamma_o)\cos\psi)] + I_X dr\{\Omega[\phi'_{F,j}(\phi_{\theta Y,i}(\cos\theta_o\cos\psi - (\gamma_o\cos\theta_o - q'_{EO}$$

$$- \beta_o \sin\theta_o)\sin\psi) + \phi_{\theta X,i}(- \cos\theta_o \sin\psi - (\gamma_o \cos\theta_o - q'_{EO} - \beta_o \sin\theta_o)\cos\psi))$$

$$+ \phi'_{E,j}(\phi_{\theta Y,i}(- \sin\theta_o \cos\psi + (\gamma_o \sin\theta_o - \beta_o \cos\theta_o - q'_{EO} \sin 2\theta_o)\sin\psi)$$

$$+ \phi_{\theta X,i}(\sin\theta_o \sin\psi + (\gamma_o \sin\theta_o - \beta_o \cos\theta_o - q'_{EO} \sin 2\theta_o)\cos\psi))]\}$$

$$+ I_Y dr\{\Omega[\phi'_{E,j}(\phi_{\theta Y,i}(\sin\theta_o \cos\psi + (q'_{EO} \sin 2\theta_o - 2q'_{FO} \sin^2\theta_o$$

$$+ \beta_o \cos\theta_o - \gamma_o \sin\theta_o)\sin\psi) + \phi_{\theta X,i}(- \sin\theta_o \sin\psi + (q'_{EO} \sin 2\theta_o - 2q'_{FO} \sin^2\theta_o$$

$$+ \beta_o \cos\theta_o - \gamma_o \sin\theta_o)\cos\psi)) + \phi'_{F,j}(\phi_{\theta Y,i}(- \cos\theta_o \cos\psi + (- q'_{EO} \cos 2\theta_o$$

$$+ q'_{FO} \sin 2\theta_o + \beta_o \sin\theta_o + \gamma_o \cos\theta_o)\sin\psi) + \phi_{\theta X,i}(\cos\theta_o \sin\psi + (- q'_{EO} \cos 2\theta_o$$

$$+ q'_{FO} \sin 2\theta_o + \beta_o \sin\theta_o + \gamma_o \cos\theta_o)\cos\psi))]\} + I_Z dr\{\Omega[\phi'_{F,j}(\phi_{\theta Y,i}(\cos\theta_o \cos\psi$$

$$-(q'_{FO} \sin 2\theta_o - q'_{EO} \cos 2\theta_o + \gamma_o \cos\theta_o + \beta_o \sin\theta_o)\sin\psi) + \phi_{\theta X,i}(- \cos\theta_o \sin\psi$$

$$- (q'_{FO} \sin 2\theta_o - q'_{EO} \cos 2\theta_o + \gamma \cos\theta_o + \beta_o \sin\theta_o)\cos\psi)) + \phi'_{E,j}((- \sin\theta_o \cos\psi$$

$$+ (2q'_{FO} \sin^2\theta_o + \gamma_o \sin\theta_o + \beta_o \cos\theta_o)\sin\psi)\phi_{\theta Y,i} + \phi_{\theta X,i}(\sin\theta_o \sin\psi$$

$$+ (2q'_{FO} \sin^2\theta_o + \gamma_o \sin\theta_o + \beta_o \cos\theta_o)\cos\psi))]\}\Big] \ddot{q}_i \Big\} + \Big\{ \Big[\int_0^{R-e} mdr\{2\Omega(\phi_{F,j} b_2 \beta_o$$

$$- \phi_{E,j} a_2 \beta_o) + 2\Omega \nu_{1,j} b_2\} + I_X dr\{\Omega(\phi'_{F,j} \cos\theta_o + \phi'_{E,j} \sin\theta_o)\}$$

$$+ I_Y dr\{\Omega(- \phi'_{E,j} \sin\theta_o + \phi'_{F,j} \cos\theta_o)\} + I_Z dr\{\Omega($$

$$- \phi'_{E,j} \sin\theta_o - \phi'_{F,j} \cos\theta_o)\}\Big] \phi_\theta \dot{\theta}_T \Big\} + \Big\{ - C_1 L_2 \phi_{\theta PR}(\phi_{FPR,j}$$

$$+ [L_2 \tan\alpha_1/(R-e)]\phi_{ET,j}) \dot{\theta}_T \Big\} + \Big\{ \Big[\int_0^{R-e} mdr\{- 2\Omega\phi_{E,j}(b_2 + r\beta_o)\}$$

$$+ I_X dr\{\Omega[\phi'_{F,j}(\gamma_o \cos\theta_o - \beta_o \sin\theta_o - q'_{EO}) + \phi'_{E,j}(\gamma_o \sin\theta_o - \beta_o \cos\theta_o$$

$$- q'_{EO} \sin 2\theta_o)]\} + I_Y dr\{\Omega[\phi'_{E,j}(q'_{EO} \sin 2\theta_o + 2q'_{FO} \cos^2\theta_o - \gamma_o \sin\theta_o$$

$$+ \beta_o \cos\theta_o) + \phi'_{F,j}(- q'_{EO} \cos 2\theta_o + q'_{FO} \sin 2\theta_o + \gamma_o \cos\theta_o + \beta_o \sin\theta_o)]\}$$

$$+ I_Z dr\{\Omega[\phi'_{E,j}(- 2q'_{FO} \cos^2\theta_o - \gamma_o \sin\theta_o - \beta_o \cos\theta_o) + \phi'_{F,j}(- q'_{FO} \sin 2\theta_o$$

$$+ q'_{EO}\cos 2\theta_o - \gamma_o \cos\theta_o - \beta_o \sin\theta_o)]\}\Big] \dot{\beta} \Big\} + \Big\{ C_3 L_2 \tan\delta_3 (\phi_{FPR,j}$$

$$+ [L_2 \tan\alpha_1/(R-e)]\phi_{ET,j})\, \dot{\beta} \Big\} + \Big\{ \Big[\int_0^{R-e} mdr\{2\Omega(a_2 \phi_{E,j} + r\beta_o \phi_{F,j} + \nu_{1,j} r)\}$$

$$+ I_X dr\{\Omega[\phi'_{F,j}\beta_o \cos\theta_o - \phi'_{E,j}(\beta_o \sin\theta_o + 2q'_{EO}\sin^2\theta_o)]\}$$

$$+ I_Y dr\{\Omega[\phi'_{E,j}(2q'_{EO}\sin^2\theta_o + q'_{FO}\sin 2\theta_o + \beta_o \sin\theta_o) + \phi'_{F,j}(- q'_{EO}\sin 2\theta_o$$

$$- 2q'_{FO}\cos^2\theta_o - \beta_o \cos\theta_o)]\} + I_Z dr\{\Omega[\phi'_{E,j}(- q'_{FO}\sin 2\theta_o - \beta_o \sin\theta_o)$$

$$+ \phi'_{F,j}(2q'_{FO}\cos^2\theta_o + q'_{EO}\sin 2\theta_o + \beta_o \cos\theta_o)]\}\Big] \dot{\gamma} \Big\} + \Big\{ C_1 L_2 \tan\alpha_1 (\phi_{FPR,j}$$

$$+ [L_2 \tan\alpha_1/(R-e)]\phi_{ET,j})\dot{\gamma} \Big\} \Big\{ \sum_{i=1}^{NE} \Big[\int_0^{R-e} mdr\{2\Omega[\nu_{1,j}\phi_{E,i} - \nu_{1,i}\phi_{E,j}$$

$$+ \beta_o(\phi_{F,j}\phi_{E,i} - \phi_{F,i}\phi_{E,j})]\} + I_X dr\{\Omega(\beta_o$$

$$+ q'_{EO}\sin\theta_o)(\phi'_{F,j}\phi'_{E,i} - \phi'_{E,j}\phi'_{F,i})\}$$

$$+ I_Y dr\{\Omega(q'_{EO}\sin\theta_o + 2q'_{FO}\cos\theta_o + \beta_o)(\phi'_{E,j}\phi'_{F,i} - \phi'_{F,j}\phi'_{E,i})\}$$

$$+ I_Z dr\{\Omega(q'_{EO}\sin\theta_o - 2q'_{FO}\cos\theta_o - \beta_o)(- \phi'_{F,j}\phi'_{E,i} + \phi'_{E,j}\phi'_{F,i})\}\Big] \dot{q}_{T,i} \Big\}$$

$$+ \Big\{ C_1(\phi_{FPR,j} + [L_2 \tan\alpha_1/(R-e)]\phi_{ET,j}) \sum_{i=1}^{NE} (\phi_{FPR,i}$$

$$+ [L_2 \tan\alpha_1/(R-e)]\phi_{ET,i})\dot{q}_{T,i} \Big\} + \Big\{ 2\zeta_{q,j} M_{q,j} \omega_{q,j}\, \dot{q}_{T,j} \Big\}$$

$$+ \Big\{ \Big[\int_0^{R-e} mdr\{\Omega^2[\phi_{F,j}(a_2 + e\gamma_o) - \phi_{E,j}(\beta_o(r+e) + b_2)]\}$$

$$+ I_X dr\{- \Omega^2 \phi'_{E,j}(q'_{EO}\sin 2\theta_o + \beta_o \cos\theta_o)\} + I_Y dr\{\Omega^2[\phi'_{E,j}(q'_{EO}\sin 2\theta_o$$

$$+ q'_{FO}\cos 2\theta_o + \beta_o \cos\theta_o) + \phi'_{F,j}(- q'_{EO}\cos 2\theta_o + q'_{FO}\sin 2\theta_o + \beta_o \sin\theta_o)]\}$$

$$+ I_Z dr\{\Omega^2[- \phi'_{E,j} q'_{FO}\cos 2\theta_o + \phi'_{F,j}(- q'_{FO}\sin 2\theta_o + q'_{EO}\cos 2\theta_o$$

$$- \beta_o \sin\theta_o)]\}\Big] \phi_\theta \theta_T \Big\} + \Big\{ - K_1 L_2 \phi_{\theta PR}(\phi_{FPR,j} + [L_2 \tan\alpha_1/(R-e)]\phi_{ET,j})\theta_T \Big\}$$

$$+ \Big\{ \Big[\int_0^{R-e} mdr\{\Omega^2[- \phi_{E,j} b_2 \gamma_o + \phi_{F,j}(a_2 \gamma_o + r + e + 2b_2 \beta_o) - \nu_{1,j} b_2]\}$$

$$+ I_X dr\{- \Omega^2 \phi'_{E,j}\sin\theta_o\} + I_Y dr\{\Omega^2(\phi'_{E,j}\sin\theta_o - \phi'_{F,j}\cos\theta_o)\}$$

$$+ I_Z dr\{\Omega^2 \phi'_{F,j} \cos\theta_o\}\Big]\beta\Big\{ + \Big\{ K_1 L_2 \tan\delta_3 (\phi_{FPR,j} + [L_2 \tan\alpha_1/(R-E)]\phi_{ET,j})\ \beta\Big\}$$

$$+ \Big\{\Big[\int_0^{R-e} mdr\{\Omega^2[-\phi_{E,j}(b_2\beta_o - e) - \phi_{F,j}a_2\beta_o]\}\Big]\gamma\Big\} + \Big\{ K_1 L_2 \tan\alpha_1 (\phi_{FPR,j}$$

$$+ [L_2 \tan\alpha_1/(R-e)]\phi_{ET,j})\gamma\Big\} + \Big\{\sum_{i=1}^{NE}\Big[\int_0^{R-e} mdr\{-\Omega^2 b_2 \beta_o \nu_{2,i,j}\}$$

$$+ I_X dr\{\Omega^2 \sin^2\theta_o \phi'_{E,j}\phi'_{E,i}\} + I_Y dr\{\Omega^2[\phi'_{E,j}(-\phi'_{E,i}\sin^2\theta_o + \tfrac{1}{2}\phi'_{F,i}\sin 2\theta_o)$$

$$+ \phi'_{F,j}(\tfrac{1}{2}\phi'_{E,i}\sin 2\theta_o - \phi'_{F,i}\cos^2\theta_o)]\} + I_Z dr\{\Omega^2[-\tfrac{1}{2}\phi'_{E,j}\phi'_{F,i}\sin 2\theta_o$$

$$+ \phi'_{F,j}(-\tfrac{1}{2}\phi'_{E,i}\sin 2\theta_o + \phi'_{F,i}\cos^2\theta_o)]\}\Big]q_{T,i}\Big\} + \Big\{ K_1 (\phi_{FPR,j}$$

$$+ [L_2 \tan\alpha_1/(R-e)]\phi_{ET,j}) \sum_{i=1}^{NE} (\phi_{FPR,i} + [L_2 \tan\alpha_1/(R-e)]\phi_{ET,i})q_{T,i}\Big\}$$

$$+ \Big\{ \omega^2_{q,j} M_{q,j} q_{T,j} \Big\}$$

Tail rotor control system contribution:

$$- C_1(\phi_{FPR,j} + [L_2 \tan\alpha_1/(R-e)]\phi_{ET,j})\dot{X}_2$$

$$- K_1(\phi_{FPR,j} + [L_2 \tan\alpha_1/(R-e)]\phi_{ET,j})X_2$$

Main rotor control system contribution:

$$+ [-\tfrac{1}{2}C_1(\phi_{FPR,j} + [L_2 \tan\alpha_1/(R-e)]\phi_{ET,j})(1 + {}^{R_B}/_{R_S}(-(\sin\delta + \cos\delta)\sin\psi$$

$$+ (\cos\delta - \sin\delta)\cos\psi))]\dot{X}_A + [-\tfrac{1}{2}C_1(\phi_{FPR,j} + [L_2 \tan\alpha_1/(R-e)]\phi_{ET,j})(1$$

$$+ {}^{R_B}/_{R_S}((\sin\delta - \cos\delta)\sin\psi - (\cos\delta + \sin\delta)\cos\psi))]\dot{X}_F + [-C_1(\phi_{FPR,j}$$

$$+ [L_2 \tan\alpha_1/(R-e)]\phi_{ET,j})(\cos\delta\sin\psi + \sin\delta\cos\psi)]\dot{X}_L$$

+ The coefficients of X_A, X_F, and X_L which are identical to those of $\dot{X}_A$, $\dot{X}_F$, and $\dot{X}_L$ respectively, with C_1 replaced by K_1.

$$= 0 \qquad \text{(A79)}$$

Tail Rotor Control System Equations

$$M_2\ddot{X}_2$$

$$+\sum_{n=1}^{N}\{C_1L_2\phi_{\theta PR}\dot{\theta}_T - C_1L_2\tan\delta_3\dot{\beta} - C_1L_2\tan\alpha_1\dot{\gamma} - \sum_{i=1}^{NE}(C_1(\phi_{FPR,i}$$

$$+ [L_2\tan\alpha_1/(R-e)]\phi_{ET,i})\dot{q}_{T,i}) + C_1\dot{X}_2\} + C_2\dot{X}_2 - C_2\dot{X}_3$$

$$+\sum_{n=1}^{N}\{K_1L_2\phi_{\theta PR}\theta_T - K_1L_2\tan\delta_3\beta - K_1L_2\tan\alpha_1\gamma$$

$$- \sum_{i=1}^{NE}(K_1(\phi_{FPR,i} + [L_2\tan\alpha_1/(R-e)]\phi_{ET,i})q_{T,i}) + K_1X_2\} + K_2X_2 - K_2X_3 = 0$$

(A80)

$$M_3\ddot{X}_3 + (C_2 + C_3 + C_{31})\dot{X}_3 - C_2\dot{X}_2 - C_{31}\dot{X}_{31} - C_3\dot{X}_4 + (K_2 + K_3 + K_{31})X_3$$

$$- K_2X_2 - K_{31}X_{31} - K_3X_4 = 0$$

(A81)

$$M_4\ddot{X}_4 + (C_3 + C_4 + C_{41})\dot{X}_4 - C_3\dot{X}_3 - C_{41}\dot{X}_{41} - C_4\dot{X}_5 + (K_3 + K_4 + K_{41})X_4$$

$$- K_3X_3 - K_{31}X_{31} - K_4X_5 = 0$$

(A82)

$$M_5\ddot{X}_5 + (C_4 + C_5 + C_{51})\dot{X}_5 - C_4\dot{X}_4 - C_{51}\dot{X}_{51}$$

$$+ (K_4 + K_5 + K_{51})X_5 - K_4X_4 - K_{51}X_{51} - K_6X_0 = 0$$

(A83)

When the servo is included, the damper C_5 is not used.

$$M_{31}\ddot{X}_{31} + C_{31}\dot{X}_{31} - C_{31}\dot{X}_3 + K_{31}X_{31} - K_{31}X_3 = 0 \quad \text{(A84)}$$

$$M_{41}\ddot{X}_{41} + C_{41}\dot{X}_{41} - C_{41}\dot{X}_4 + K_{41}X_{41} - K_{41}X_4 = 0 \quad \text{(A85)}$$

$$M_{51}\ddot{X}_{51} + C_{51}\dot{X}_{51} - C_{51}\dot{X}_5 + K_{51}X_{51} - K_{51}X_5 = 0 \quad \text{(A86)}$$

The computer program of the analysis allows the user to include or omit any of the above tail rotor control system degrees of freedom as desired.

Main Rotor Control System Equations

$$[\tfrac{1}{4}(1/R_S^2(I_{FA} + I_L) + M_S)]\ddot{X}_A + [\tfrac{1}{4}(1/R_S^2(I_L - I_{FA}) + M_S)]\ddot{X}_F + [1/2R_S^2(-I_L)]\ddot{X}_L$$

$$+ [\sum_{i=1}^{NA}(1/2R_S(\phi_{\theta X,i}I_{FA} - \phi_{\theta Y,i}I_L) + \tfrac{1}{2}\phi_{Z,i}M_S)\ddot{q}_i] + \sum_{n=1}^{N}\{\tfrac{1}{2}C_1L_2(1 - R_B/R_S([\sin\delta$$

$$+ \cos\delta]\sin\psi + [\sin\delta - \cos\delta]\cos\psi))\phi_{\theta PR}\dot{\theta}_T - \tfrac{1}{2}C_1L_2\tan\delta_3(1 - R_B/R_S([\sin\delta$$

$$+ \cos\delta]\sin\psi + [\sin\delta - \cos\delta]\cos\psi))\dot{\beta} - \tfrac{1}{2}C_1L_2\tan\alpha_1(1 - R_B/R_S([\sin\delta + \cos\delta]\sin\psi$$

$$+ [\sin\delta - \cos\delta]\cos\psi))\dot{\gamma} - \sum_{i=1}^{NE}(\tfrac{1}{2}C_1(\phi_{FPR,i} + [L_2\tan\alpha_1/(R-e)]\phi_{ET,i})(1$$

$$- R_B/R_S([\sin\delta + \cos\delta]\sin\psi + [\sin\delta - \cos\delta]\cos\psi))\dot{q}_{T,i}) + (\tfrac{1}{2}C_1(R_B/R_S)^2[-(\sin\delta$$

$$+ \cos\delta)\sin\psi - (\sin\delta - \cos\delta)\cos\psi - \tfrac{1}{2}\cos2\delta\sin2\psi - \tfrac{1}{2}\sin2\delta\cos2\psi + \tfrac{1}{2}] + \tfrac{1}{4}C_1)\dot{X}_A\}$$

$$+ C_A\dot{X}_A + \sum_{n=1}^{N}\{(\tfrac{1}{4}C_1(R_B/R_S)^2[-2\cos\delta\sin\psi - 2\sin\delta\cos\psi + \sin2\delta\sin2\psi - \cos2\delta\cos2\psi]$$

$$+ \tfrac{1}{4}C_1)\dot{X}_F\} + \sum_{n=1}^{N}\{\tfrac{1}{2}C_1(R_B/R_S)^2[\cos\delta\sin\psi + \sin\delta\cos\psi + \tfrac{1}{2}(\cos2\delta - \sin2\delta)\sin2\psi$$

$$- (\sin\delta + \cos\delta)\cos\delta\sin^2\psi - (\sin\delta - \cos\delta)\sin\delta\cos^2\psi]\dot{X}_L\}$$

+ Displacement coefficients which are identical to the velocity coefficients, with C_1 and C_A replaced by K_1 and K_A respectively.

$$- K_AX_{OA} = 0 \qquad \text{(A87)}$$

$$[\tfrac{1}{4}(1/R_S^2(I_L - I_{FA}) + M_S)]\ddot{X}_A + [\tfrac{1}{4}(1/R_S^2(I_{FA} + I_L) + M_S)]\ddot{X}_F + [1/2R_S^2(-I_L)]\ddot{X}_L$$

$$+ [\sum_{i=1}^{NA}(1/2R_S(-\phi_{\theta X,i}I_{FA} - \phi_{\theta Y,i}I_L) + \tfrac{1}{2}\phi_{Z,i}M_S)\ddot{q}_i] + \sum_{n=1}^{N}\{\tfrac{1}{2}C_1L_2(1$$

$$- R_B/R_S([\cos\delta - \sin\delta]\sin\psi + [\sin\delta + \cos\delta]\cos\psi))\phi_{\theta PR}\dot{\theta}_I - \tfrac{1}{2}C_1L_2\tan\delta_3(1$$

$$- R_B/R_S([\cos\delta - \sin\delta]\sin\psi + [\sin\delta + \cos\delta]\cos\psi))\dot{\beta} - \tfrac{1}{2}C_1L_2\tan\alpha_1(1$$

$$- R_B/R_S([\cos\delta - \sin\delta]\sin\psi + [\sin\delta + \cos\delta]\cos\psi))\dot{\gamma} - \sum_{i=1}^{NE}(\tfrac{1}{2}C_1(\phi_{FPR,i}$$

$$+ [L_2 \tan\alpha_1/(R-e)]\phi_{ET,i})(1 - {}^{R_S}/_{R_S}([\cos\delta - \sin\delta]\sin\psi + [\sin\delta +$$

$$+ \cos\delta]\cos\psi))\dot{q}_{T,i} + (\tfrac{1}{4}C_1({}^{R_B}/_{R_S})^2[- 2\cos\delta\sin\psi - 2\sin\delta\cos\psi + \sin2\delta\sin2\psi$$

$$- \cos2\delta\cos2\psi] + \tfrac{1}{4}C_1)\dot{X}_A\} + \sum_{n=1}^{N}\{(\tfrac{1}{2}C_1({}^{R_B}/_{R_S})^2[(\sin\delta - \cos\delta)\sin\psi - (\cos\delta$$

$$+ \sin\delta)\cos\psi + \tfrac{1}{2}\cos2\delta\sin2\psi + \tfrac{1}{2}\sin2\delta\cos2\psi + \tfrac{1}{2}] + \tfrac{1}{4}C_1)\dot{X}_F\} + C_F\dot{X}_F$$

$$+ \sum_{n=1}^{N}\{\tfrac{1}{2}C_1({}^{R_B}/_{R_S})^2[\cos\delta\sin\psi + \sin\delta\cos\psi - \tfrac{1}{2}(\cos2\delta + \sin2\delta)\sin2\psi - (\cos\delta$$

$$- \sin\delta)\cos\delta\sin^2\psi - (\cos\delta + \sin\delta)\sin\delta\cos^2\psi]\dot{X}_L\}$$

+ Displacement coefficients which are identical to the velocity coefficients, with C_1 and C_F replaced by K_1 and K_F respectively.

$$- K_F X_{OF} = 0 \qquad \text{(A88)}$$

$$[{}^{1}/_{2R_S^2}(- I_L)]\ddot{X}_A$$

$$+ [{}^{1}/_{2R_S^2}(- I_L)]\ddot{X}_F$$

$$+ [{}^{1}/_{R_S^2}(I_L)]\ddot{X}_L$$

$$+ [\sum_{i=1}^{NA}({}^{1}/_{R_S}(\phi_{\theta Y,i}I_L))\ddot{q}_i]$$

$$+ \sum_{i=1}^{N}\{C_1L_2{}^{R_B}/_{R_S}(\cos\delta\sin\psi + \sin\delta\cos\psi)\phi_{\theta PR}\dot{\theta}_T - C_1L_2\tan\delta_3{}^{R_B}/_{R_S}(\cos\delta\sin\psi$$

$$+ \sin\delta\cos\psi)\dot{\beta} - C_1L_2\tan\alpha_1{}^{R_B}/_{R_S}(\cos\delta\sin\psi + \sin\delta\cos\psi)\dot{\gamma} + \sum_{i=1}^{NE}(- C_1(\phi_{FPR,i}$$

$$+ [L_2\tan\alpha_1/(R-e)]\phi_{ET,i})(\cos\delta\sin\psi + \sin\delta\cos\psi))\dot{q}_{T,i} + (\tfrac{1}{2}C_1({}^{R_B}/_{R_S})^2(\cos\delta\sin\psi$$

$$+ \sin\delta\cos\psi + \tfrac{1}{2}(\cos2\delta - \sin2\delta)\sin2\psi - (\sin\delta + \cos\delta)\cos\delta\sin^2\psi + (\cos\delta$$

$$- \sin\delta)\sin\delta\cos^2\psi))\dot{X}_A + (\tfrac{1}{2}C_1({}^{R_B}/_{R_S})^2(\cos\delta\sin\psi + \sin\delta\cos\psi - \tfrac{1}{2}(\cos2\delta$$

$$+ \sin2\delta)\sin2\psi + (\sin\delta - \cos\delta)\cos\delta\sin^2\psi - (\cos\delta + \sin\delta)\sin\delta\cos^2\psi))\dot{X}_F$$

$$+ (\tfrac{1}{2}C_l(R_B/R_S)^2(\sin2\delta\sin2\psi + 2\cos^2\delta\sin^2\psi + 2\sin^2\delta\cos^2\psi))\dot{X}_L\} + C_L\dot{X}_L$$

+ Displacement coefficients which are identical to the velocity coefficients, with C_l and C_L replaced by K_l and K_L respectively.

$$- K_L X_{OL} = 0 \qquad \text{(A89)}$$

When the servos are included, the dampers C_A, C_F, and C_L are not used.

Tail Rotor Servo Equation

$$
\begin{aligned}
&(\alpha_S/\mu_1)(A_P/\alpha_S C_q)(1 + K\mu_2)\dot{X}_o \\
&- (\alpha_S/\mu_1)(A_P/\alpha_S C_q)K\mu_2\dot{X} \\
&- (\alpha_S/\mu_1)(A_P/\alpha_S C_q)\Big(\sum_{i=1}^{NA}(SF_{A,X}\phi_{X,i} + SF_{A,Y}\phi_{Y,i} + SF_{A,Z}\phi_{Z,i} \\
&+ SF_{A,\theta X}\phi_{\theta X,i} + SF_{A,\theta Y}\phi_{\theta Y,i})\dot{\bar{q}}_i\Big) + (\alpha_S/\mu_1 + K)X_o - KX \\
&- (\alpha_S/\mu_1)(R_3/\alpha_S)\Big(\sum_{i=1}^{NA}(SF_{A,X}\phi_{X,i} + SF_{A,Y}\phi_{Y,i} + SF_{A,Z}\phi_{Z,i} \\
&+ SF_{A,\theta X}\phi_{\theta X,i} + SF_{A,\theta Y}\phi_{\theta Y,i})\bar{q}_i\Big) \\
&+ (\alpha_S/\mu_1)(R_1/\alpha_S)\Big(\sum_{i=1}^{NA}(SF_{V,X}\phi_{X,i} + SF_{V,Y}\phi_{Y,i} + SF_{V,Z}\phi_{Z,i} \\
&+ SF_{V,\theta X}\phi_{\theta X,i} + SF_{V,\theta Y}\phi_{\theta Y,i})\bar{q}_i\Big) = 0
\end{aligned}
\qquad \text{(A90)}
$$

In this equation K represents K_5 or K_4, etc., in the tail rotor control system shown in Figure A2, depending on which elements are included in the model employed by the user. The computer program of the analysis automatically incorporates the appropriate value and also allows inclusion or omission of the servo, as desired.

Main Rotor Servo Equations
Aft Servo

$$(\alpha_{S,A}/\mu_{1,A})(A_{P,A}/\alpha_{S,A}\,C_{q,A})(1 + K_A\mu_{2,A})\dot{X}_{O,A}$$

$$- (\alpha_{S,A}/\mu_{1,A})(A_{P,A}/\alpha_{S,A}C_{q,A})K_A\mu_{2,A}\dot{X}_A$$

$$- (\alpha_{S,A}/\mu_{1,A})(A_{P,A}/\alpha_{S,A}C_{qA})\Big(\sum_{i=1}^{NA}(SF_{A,X,A}\phi_{X,i} + SF_{A,Y,A}\phi_{Y,i}$$

$$+ SF_{A,Z,A}\phi_{Z,i} + SF_{A,\theta X,A}\phi_{\theta X,i} + SF_{A,\theta Y,A}\phi_{\theta Y,i})\dot{\bar{q}}_i\Big)$$

$$+ (\alpha_{S,A}/\mu_{1,A} + K_A)X_{O,A}$$

$$- K_A X_A$$

$$- (\alpha_{S,A}/\mu_{1,A})(R_{3,A}/\alpha_{S,A})\Big(\sum_{i=1}^{NA}(SF_{A,X,A}\phi_{X,i} + SF_{A,Y,A}\phi_{Y,i} + SF_{A,Z,A,}\phi_{Z,i}$$

$$+ SF_{A,\theta X,A}\phi_{\theta X,i} + SF_{A,\theta Y,A}\phi_{\theta Y,i})\bar{q}_i\Big)$$

$$+ (\alpha_{S,A}/\mu_{1,A})(R_{1,A}/\alpha_{S,A})\Big(\sum_{i=1}^{NA}(SF_{V,X,A}\phi_{X,i} + SF_{V,Y,A}\phi_{Y,i} + SF_{V,Z,A}\phi_{Z,i}$$

$$+ SF_{V,\theta X,A}\phi_{\theta X,i} + SF_{V,\theta Y,A}\phi_{\theta Y,i})\bar{q}_i\Big) = 0 \qquad (A91)$$

The equations for the forward and lateral servos are identical to the above, with the subscript A replaced by F and L respectively.

The computer program of the analysis allows the user to omit or include any or all of the servos, as desired.

Aerodynamic Forces

At this juncture, we have developed the differential equations that govern the free vibration of the dynamic system. These were developed using Lagrangian procedures and Lagrange's equations in the form of Equation A1. We now wish to add the influence of aerodynamic forces on the system such that Langrange's equations become

$$\frac{d}{dt}\left(\frac{\partial T}{\partial \dot{q}_j}\right) - \frac{\partial T}{\partial q_j} + \frac{\partial V}{\partial q_j} + \frac{\partial D}{\partial \dot{q}_j} = Q_j \qquad \text{(A92)}$$

where the Q_j are the generalized aerodynamic forces.

Since we are interested in the stability of the system and not particularly in forced response phenomena, the Q_j will be those forces that arise from motions of the dynamic system. That is, Equation A92 will define a set of homogeneous differential equations in the generalized coordinates, q_j. This being a linear analysis, the Q_j can be obtained by the method of small perturbations.

Although the analysis is linear, it is worth pointing out that the coordinate perturbations are performed about certain steady initial values of the generalized coordinates that do not necessarily correspond to regions of linear lift coefficient, drag coefficient, etc. Rather, it is assumed that the perturbations are small enough for the behavior of the system to be considered linear at that instant. This allows us to include stall and compressibility effects even though the generalized aerodynamic forces developed represent quasi-steady effects. In a later section, we shall further refine the aerodynamics by adding circulatory and noncirculatory unsteady effects of the types postulated by Theodorsen[1] and Loewy.[2]

---

(1) Theodorsen, T., General Theory of Aerodynamic Instability and the Mechanism of Flutter, NACA Report 496, National Advisory Committee for Aeronautics, Langley Aeronautical Laboratory, Langley Field, Virginia.

(2) Loewy, R. G., "A Two-Dimensional Approximation to the Unsteady Aerodynamics of Rotary Wings," Journal of the Aeronautical Sciences, Vol. 24, February, 1957.

Blade Elemental Aerodynamic Forces

The elemental aerodynamic lift, drag, and pitching moment on any element i of any blade n are given by

$$dL_{n,i} = \tfrac{1}{2}\rho C_{n,i} U^2_{n,i} C_{L,n,i} \delta r_{n,i} \tag{A93}$$

$$dD_{n,i} = \tfrac{1}{2}\rho C_{n,i} U^2_{n,i} C_{D,n,i} \delta r_{n,i} \tag{A94}$$

$$dM_{n,i} = \tfrac{1}{2}\rho C_{n,i}{}^2 U^2_{n,i} C_{M,n,i} \delta r_{n,i} \tag{A95}$$

Here, $dM_{n,i}$ is the aerodynamic pitching moment at the airfoil aerodynamic center, and $dL_{n,i}$ and $dD_{n,i}$ act in the directions shown in Figure A5. The lift and drag forces can be resolved into the X_5, Y_5, Z_5 axis system to give elemental T and H forces defined by

$$dT_{n,i} = dL_{n,i}\cos\phi_{n,i} - dD_{n,i}\sin\phi_{n,i} \tag{A96}$$

$$dH_{n,i} = dL_{n,i}\sin\phi_{n,i} + dD_{n,i}\cos\phi_{n,i} \tag{A97}$$

where the local inflow angle is defined

$$\phi_{n,i} = \tan^{-1}(U_{P,n,i}/U_{T,n,i}) \tag{A98}$$

Thus, to evaluate $dT_{n,i}$, $dH_{n,i}$, and $dM_{n,i}$, we must know the values of $U_{n,i}$, $U_{P,n,i}$, $U_{T,n,i}$, $C_{L,n,i}$, $C_{D,n,i}$, and $C_{M,n,i}$.

$C_{L,n,i}$, $C_{D,n,i}$, and $C_{M,n,i}$ depend on the local angle of attack, and this is seen from Figure A5 to be given by

$$\alpha_{n,i} = \vartheta_{P,n,i} - \theta_{n,i} - \phi_{n,i} \tag{A99}$$

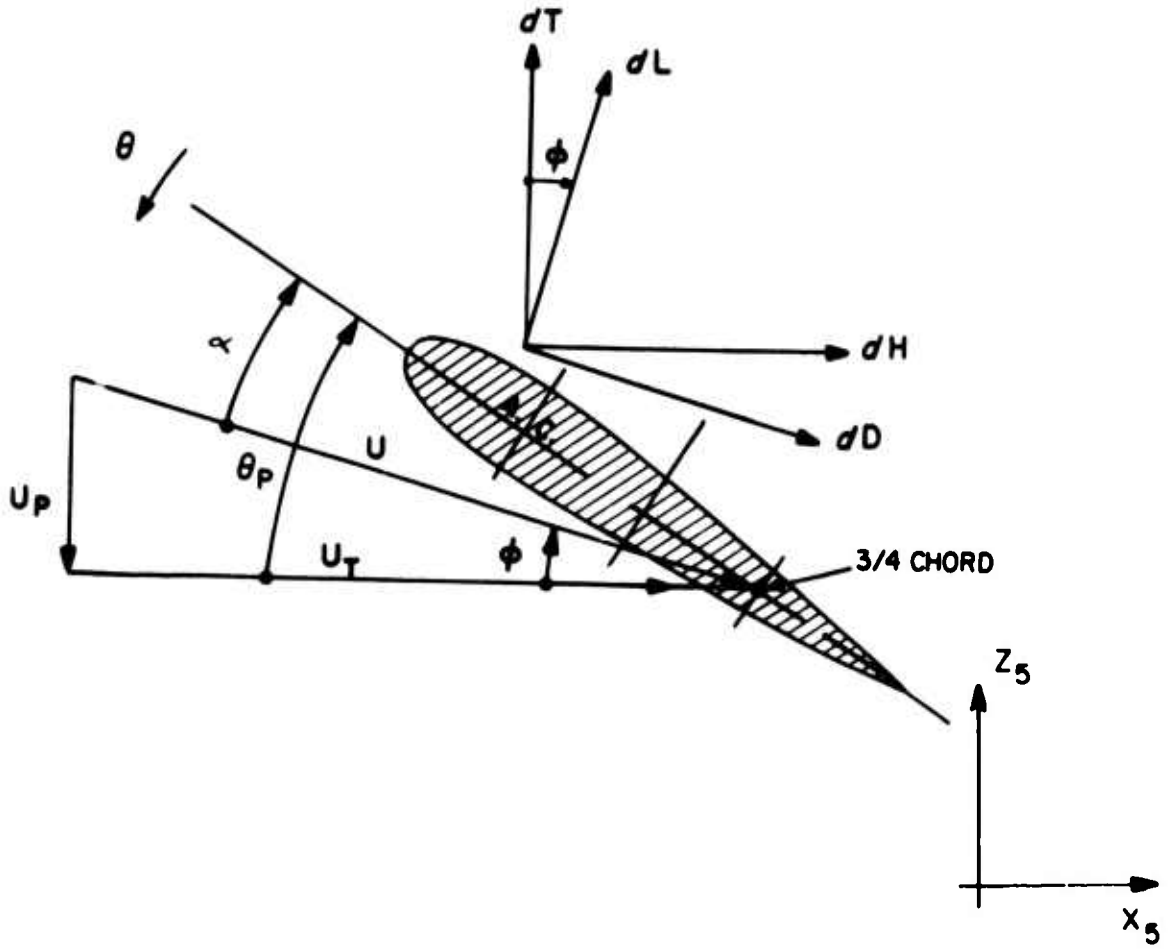

Figure A5. Forces and Velocities at a Local Blade Element.

Also from Figure A5, it is apparent that

$$U_{n,i} = (U^2_{P,n,i} + U^2_{T,n,i})^{\frac{1}{2}} \tag{A100}$$

$U_{P,n,i}$ and $U_{T,n,i}$, being the local relative velocities in the X_5, Y_5, Z_5 axis system, are obtained as follows:

Neglecting, for the moment, the forward velocity component, it is readily established by inspection of Figure A1 and using Equation A28 to define $\bar{X}_{n,i}$ that the absolute velocity of any blade element i on any blade n is given by

$$\bar{V}_{n,i} = \bar{V} - \dot{\bar{X}}_{n,i} \tag{A101}$$

where $\bar{V} = \{0, 0, -V_A\}$

The local relative velocities at any blade element are obtained by appropriate transformation of $\bar{V}_{n,i}$. Thus

$$\{\bar{U}_{T,n,i}, \bar{U}_{R,n,i}, -\bar{U}_{P,n,i}\} = [A_{\bar{q}_{\theta Y}} A_{\bar{q}_{\theta X}} A_{\psi,n} A_{\beta,n} A_{\gamma,n} A_{q_{E,n,i}c'} A_{q_{F,n,i}c'}]^T \{\bar{V}_{n,i}\} \tag{A102}$$

Therefore, in the X_5, Y_5, Z_5 axis system, the local relative velocities are

$$\{U_{T,n,i}, U_{R,n,i}, -U_{P,n,i}\} = [A_{q_{E,n,i}c'} A_{q_{F,n,i}c'}]\{\bar{U}_{T,n,i}, \bar{U}_{R,n,i} - \bar{U}_{P,n,i}\} \tag{A103}$$

Inserting the steady initial displacements of the generalized coordinates and assuming zero initial velocities of the generalized coordinates in this expression, it can be shown that, initially,

$$U_{T,n,i} = \Omega[e_n + r_{n,i} + a_{n,i}\gamma_{o,n} - b_{n,i}\beta_{o,n} - (a_{n,i} - r_{n,i}\gamma_{o,n})(\gamma_{o,n} - q'_{EO,n,i})] - V_A\beta_{o,n}[\gamma_{o,n} - q'_{EO,n,i}] \quad \text{(A104)}$$

$$U_{P,n,i} = -\Omega[(e_n + r_{n,i})q'_{FO,n,i}(\gamma_{o,n} - q'_{EO,n,i}) + (a_{n,i} - r_{n,i}\gamma_{o,n})(\beta_{o,n} + q'_{FO,n,i})] + V_A \quad \text{(A105)}$$

Since the angle of attack is measured at the 3/4 chord, the appropriate definitions of $a_{n,i}$ and $b_{n,i}$ in Equations A104 and A105 are

$$a_{n,i} = q_{EO,n,i} + (C_{n,i}/4 - EA_{n,i})\cos\theta_{on,i} \quad \text{(A106)}$$

$$b_{n,i} = q_{EO,n,i} + (C_{n,i}/4 - EA_{n,i})\sin\theta_{on,i} \quad \text{(A107)}$$

These quantities define the position of the 3/4 chord on the deformed blade relative to the blade feathering, or elastic, axis.

$U_{R,n,i}$ is the local relative radial velocity and is ignored since the effects of radial flow are not taken into account in this analysis.

We are now in a position to calculate the blade elemental aerodynamic forces and, therefore, the generalized aerodynamic forces.

Generalized Aerodynamic Forces

If we apply the principle of virtual work, it can readily be established that the system generalized aerodynamic forces are given by

$$Q_{n,i} = \sum_{i=1}^{NB} (\{dF_{n,i}\}^T \frac{\partial}{\partial q_{n,j}} \{\bar{X}_{n,i}\} + \{d\bar{M}_{n,i}\}^T \frac{\partial}{\partial q_{n,j}} \{\bar{\Theta}_{n,i}\}) \quad \text{(A108)}$$

for $q_{n,j}$ in the rotating system, and

$$Q_j = \sum_{n=1}^{N} \sum_{i=1}^{NB} \left(\{dF_{n,i}\}^T \frac{\partial}{\partial q_{n,j}} \{\bar{X}_{n,i}\} + \{d\bar{M}_{n,i}\}^T \frac{\partial}{\partial q_{n,j}} \{\bar{\theta}_{n,i}\} \right) \tag{A109}$$

for $q_{n,j}$ in the fixed system.

$\{dF_{n,i}\}$ is obtained by rotating the blade elemental T and H forces such that they act in the directions of the absolute displacements. Thus,

$$\{dF_{n,i}\} = [A_{q\theta Y} A_{q\theta X} A_{\psi,n} A_{\beta,n} A_{\gamma,n}]\{dH_{n,i}, 0, dT_{n,i}\} \tag{A110}$$

$\{dM_{n,i}\}$ is obtained by transforming the local blade elemental pitching moment vector to the absolute axis system. Thus,

$$\{dM_{n,i}\} = [A_{q\theta Y} A_{q\theta X} A_{\psi,n} A_{\beta,n} A_{\gamma,n}]\{0, dM_{n,i} 0\} \tag{A111}$$

$\{\bar{\theta}_{n,i}\}$ is the rotational displacement vector in the absolute axis system on which $\{dM_{n,i}\}$ acts. It is given by

$$\{\bar{\theta}_{n,i}\} = [A_{q\theta Y} A_{q\theta X} A_{\psi,n} A_{\beta,n} A_{\gamma,n}]\{0, -\theta_{n,i}, 0\} \tag{A112}$$

If we now perturb the generalized forces given by Equations A106 and A107 such that, in general,

$$Q_j = (Q_j)_o + \delta Q_j \tag{A113}$$

where the $(Q_j)_o$ are the values of the generalized forces at the steady initial values of the generalized coordinates, and the δQ_j are increments of the generalized forces resulting from small perturbations of the generalized coordinates, it can be shown that if we make a first-order Taylor expansion of the δQ_j about the steady values $(Q_j)_o$, then the perturbation forces are given by the following general expression:

$$\delta Q_j = \Big(\sum \Big(\frac{\partial Q_j}{\partial q_t}\Big)_o \delta q_t$$

$$+ \Big(\frac{\partial Q_j}{\partial T}\frac{\partial T}{\partial U_T} + \frac{\partial Q_j}{\partial H}\frac{\partial H}{\partial U_T} + \frac{\partial Q_j}{\partial M}\frac{\partial M}{\partial U_T}\Big)_o \Big(\Big(\frac{\partial U_T}{\partial q_t}\Big)_o \delta q_t + \Big(\frac{\partial U_T}{\partial \dot{q}_t}\Big)_o \delta \dot{q}_t\Big)$$

$$+ \Big(\frac{\partial Q_j}{\partial T}\frac{\partial T}{\partial U_P} + \frac{\partial Q_j}{\partial H}\frac{\partial H}{\partial U_P} + \frac{\partial Q_j}{\partial M}\frac{\partial M}{\partial U_P}\Big)_o \Big(\Big(\frac{\partial U_P}{\partial q_t}\Big)_o \delta q_t + \Big(\frac{\partial U_P}{\partial \dot{q}_t}\Big)_o \delta \dot{q}_t\Big)$$

$$+ \Big(\frac{\partial Q_j}{\partial T}\frac{\partial T}{\partial \alpha} + \frac{\partial Q_j}{\partial H}\frac{\partial H}{\partial \alpha} + \frac{\partial Q_j}{\partial M}\frac{\partial M}{\partial \alpha}\Big)_o \Big(\Big(\frac{\partial \alpha}{\partial q_t}\Big)_o \delta q_t + \Big(\frac{\partial \alpha}{\partial \dot{q}_t}\Big)_o \delta \dot{q}_t\Big)\Big) \qquad \text{(A114)}$$

where the summation is performed over the number of generalized coordinates.

The subscript o in this expression implies that the quantities are to be evaluated at the steady initial values of the generalized coordinates. It will be remembered that a summation over all blades is implicit when the generalized coordinates are in the fixed system.

Equations A108 and A109 give the values of the generalized aerodynamic forces, and they both contain the absolute displacement vector $\bar{X}_{n,i}$. When $\bar{X}_{n,i}$ as defined by Equation A28 was developed, we were at that time concerned with the displacement of the center of gravity of the blade element i. However, we are now concerned with aerodynamic forces; and if we consider these forces to act at the element aerodynamic center, then it is the displacement of this point that must be defined. This is easily accomplished by substituting $AC_{n,i}$ for $CG_{n,i}$ in the expression for $\bar{X}_{n,i}$.

It now only remains to define the derivatives given in Equation A114 to establish the values of the generalized aerodynamic forces Q_j required in A72.

The following list of aerodynamic forces and derivatives is presented without subscripts to preserve clarity. This also applies to the generalized force expressions, which are presented in integral form. Nevertheless, it should be remembered that in these force expressions, all generalized coordinates and physical properties associated with the rotor system have a subscript n, the blade number.

$$dT = \tfrac{1}{2}\rho cU[C_L U_T - C_D U_P] \tag{A115}$$

$$dH = \tfrac{1}{2}\rho cU[C_L U_P + C_D U_T] \tag{A116}$$

$$dM = \tfrac{1}{2}\rho c^2 U^2 C_M \tag{A117}$$

$$t_1 = \frac{\partial(dT)}{\partial U_T} = \tfrac{1}{2}\rho c\,{}^1/_U[C_L(U^2 + U_T^2) - C_D U_T U_P + C_{L,\alpha} U_T U_P - C_{D,\alpha} U_P^2] + \tfrac{1}{2}\rho c\,{}^1/_v[C_{L,M} U_T^2 - C_{D,M} U_T U_P] \tag{A118}$$

$$t_2 = \frac{\partial(dT)}{\partial U_P} = \tfrac{1}{2}\rho c\,{}^1/_U[C_L U_T U_P - C_D(U^2 + U_P^2) - C_{L,\alpha} U_T^2 + C_{D,\alpha} U_T U_P] + \tfrac{1}{2}\rho c\,{}^1/_v[C_{L,M} U_T U_P - C_{D,M} U_P^2] \tag{A119}$$

$$t_3 = \frac{\partial(dT)}{\partial \alpha} = \tfrac{1}{2}\rho cU[C_{L,\alpha} U_T - C_{D,\alpha} U_P] \tag{A120}$$

$$h_1 = \frac{\partial(dH)}{\partial U_T} = \tfrac{1}{2}\rho c\,{}^1/_U[C_L U_T U_P + C_D(U^2 + U_T^2) + C_{L,\alpha} U_P^2 + C_{D,\alpha} U_T U_P] + \tfrac{1}{2}\rho c\,{}^1/_v[C_{L,M} U_T U_P + C_{D,M} U_T^2] \tag{A121}$$

$$h_2 = \frac{\partial(dH)}{\partial U_P} = \tfrac{1}{2}\rho c\,{}^1/_U[C_L(U^2 + U_P^2) + C_D U_T U_P - C_{L,\alpha} U_T U_P - C_{D,\alpha} U_T^2] + \tfrac{1}{2}\rho c\,{}^1/_v[C_{L,M} U_P^2 + C_{D,M} U_T U_P] \tag{A122}$$

$$h_3 = \frac{\partial(dH)}{\partial \alpha} = \tfrac{1}{2}\rho cU[C_{L,\alpha} U_P + C_{D,\alpha} U_T] \tag{A123}$$

$$m_1 = \frac{\partial(dM)}{\partial U_T} = \tfrac{1}{2}\rho c^2[C_M 2U_T + C_{M,\alpha} U_P] + \tfrac{1}{2}\rho c^2\,{}^1/_v C_{M,M} U_T U \tag{A124}$$

$$m_2 = \frac{\partial(dM)}{\partial U_P} = \tfrac{1}{2}\rho c^2[C_M 2U_P - C_{M,\alpha} U_T] + \tfrac{1}{2}\rho c^2\,{}^1/_v C_{M,M} U_P U \tag{A125}$$

$$L_3 = \frac{\partial(dM)}{\partial \alpha} = \tfrac{1}{2}\rho c^2 C_{M,\alpha} U^2 \tag{A126}$$

$$\delta U_T = \frac{\partial U_T}{\partial q} + \frac{\partial U_T}{\partial \dot{q}}$$

$$= \sum_{i=1}^{NA} \{\phi_{\theta Y,i}(U_P\cos\psi - U_P[\gamma_o - q'_{EO}]\sin\psi)$$

$$- \phi_{\theta X,i}(U_P[\gamma_o - q'_{EO}]\cos\psi + U_P\sin\psi)\}\bar{q}_i$$

$$- \{\Omega(a\beta_o + bq'_{EO})\}\phi_\theta\theta_T$$

$$- \{\Omega(b + r\beta_o) + U_P(\gamma_o - q'_{EO})\}\beta$$

$$- \{\Omega e(\gamma_o - q'_{EO}) + U_P\beta_o\}\gamma$$

$$+ \sum_{i=1}^{NE} \{\Omega[\phi'_{E,i}(-a - e\gamma_o + (r + e)q'_{EO}) - \phi_{E,i}q'_{EO} - \phi_{F,i}\beta_o$$

$$+ r_i] - U_P[\phi'_{E,i}(\beta_o + q'_{FO}) + \phi'_{F,i}(\gamma_o - q'_{EO})]\}q_{T,i}$$

$$+ \sum_{i=1}^{NA} \{\phi_{\theta Y,i}[b(\gamma_o - q'_{EO})\sin\psi - (b + r\beta_o)\cos\psi] + \phi_{\theta X,i}[b(\gamma_o - q'_{EO})\cos\psi$$

$$+ (b + r\beta_o)\sin\psi] + \phi_{X,i}[(\gamma_o - q'_{EO})\sin\psi - \cos\psi] + \phi_{Y,i}[-(\gamma_o$$

$$- q'_{EO})\cos\psi - \sin\psi]\}\dot{\bar{q}}_i$$

$$+ \{b\}\phi_\theta\dot{\theta}_T$$

$$+ \{b(\gamma_o - q'_{EO})\}\dot{\beta}$$

$$+ \{r + aq'_{EO}\}\dot{\gamma}$$

$$+ \sum_{i=1}^{NE} \{\dot{r}_i q'_{EO} + \phi_{E,i}\}\dot{q}_{T,i} \qquad \text{(A127)}$$

$$\delta U_P = \frac{\partial U_P}{\partial q} + \frac{\partial U_P}{\partial \dot{q}}$$

$$= \sum_{i=1}^{NA} \{\phi_{\theta Y,i}(- U_P(\beta_o + q'_{FO})\sin\psi) - \phi_{\theta X,i}(U_P(\beta_o + q'_{FO})\cos\psi)\}\bar{q}_i$$

$$+ \{\Omega b(\beta_o + q'_{FO})\phi_\theta\}\theta_T$$

$$- \{\Omega(a - r\gamma_o) + U_P(\beta_o + q'_{FO})\}\beta$$

$$+ \{\Omega(r\beta_o - eq'_{FO})\}\gamma$$

$$+ \sum_{i=1}^{NE} \{\Omega[\phi'_{F,i}(-a + r\gamma_o) + \phi_{E,i}(\beta_o + q'_{FO})] - U_P\phi'_{F,i}(\beta_o + q'_{FO})\}q_{T,i}$$

$$+ \sum_{i=1}^{NA} \{(-(a - r\gamma_o)\cos\psi + (r + e + bq'_{FO} + a\gamma_o)\sin\psi)\phi_{\theta Y,i}$$

$$+ ((a - r\gamma_o)\sin\psi + (r + e + bq'_{FO} + a\gamma_o)\cos\psi)\phi_{\theta X,i}$$

$$+ \phi_{X,i}(\beta_o + q'_{FO})\sin\psi - \phi_{Y,i}(\beta_o + q'_{FO})\cos\psi$$

$$+ \phi_{Z,i}\}\dot{\bar{q}}_i$$

$$+ \{a\}\phi_\theta\dot{\theta}_T$$

$$+ \{a\gamma_o + r + bq'_{FO}\}\dot{\beta}$$

$$- \{aq'_{FO}\}\dot{\gamma}$$

$$+ \sum_{i=1}^{NE} \{-\dot{r}_i q'_{FO} + \phi_{F,i}\}\dot{q}_{T,i} \qquad \text{(A128)}$$

$$\delta\alpha = \frac{\partial\alpha}{\partial q} + \frac{\partial\alpha}{\partial\dot{q}} = \{-1\}\phi_\theta\theta_T \qquad \text{(A129)}$$

Equations A115 through A129 and used in the computation of the generalized aerodynamic forces. These forces comprise the right-hand side of Equation A92 and have the following forms:

$$Q_{\bar{q}_j} = \left\{\int_b^{R-e}\left[\sum_{n=1}^{N}\{\sum_{i=1}^{NA}\{\phi_{\theta X,i}[\phi_{\theta Y,j}((-b_1\beta_o + a_1q'_{EO} + r + e)dH\right.\right.$$

$$+ a_1(\beta_o + q'_{FO})dT)] + \phi_{X,j}[\phi_{\theta Y,i}dT] - \phi_{Y,j}[\phi_{\theta X,i}dT]\}\bar{q}_i$$

$$+ \{\phi_{\theta X,j}[(-a_1\sin\psi - a_1(\gamma_o - q'_{EO})\cos\psi)dH - (b_1\sin\psi - (a_1q'_{FO}$$

$$- b_1\gamma_o)\cos\psi)dT] + \phi_{\theta Y,j}[(a_1\cos\psi - a_1(\gamma_o - q'_{EO})\sin\psi)dH + (b_1\cos\psi$$

$$+ (a_1q'_{FO} - b_1\gamma_o)\sin\psi)dT]\}\phi_\theta\theta_T$$

$$+ \{\phi_{\theta X,j}[((b_1\beta_o - r - a_1q'_{EO})\sin\psi + e(\gamma_o - q'_{EO})\cos\psi)dH$$

$$- (a_1(\beta_o + q'_{FO})\sin\psi + e(\beta_o + q'_{FO})\cos\psi)dT] + \phi_{\theta Y,j}[((- b_1\beta_o + r$$

$$+ a_1 q'_{EO})\cos\psi + e(\gamma_o - q'_{EO})\sin\psi)dH + (a_1(\beta_o + q'_{FO})\cos\psi - e(\beta_o$$

$$+ q'_{FO})\sin\psi)dT] + \phi_{X,j}\sin\psi dT - \phi_{Y,j}\cos\psi dT + \phi_{Z,j}((\gamma_o - q'_{EO})dH$$

$$- (\beta_o + q'_{FO})dT)\}\beta$$

$$+ \{\phi_{\theta X,j}[(b_1(\gamma_o - q'_{EO})\sin\psi + (e\beta_o - b_1)\cos\psi)dH - ((b_1 q'_{FO} + a_1\gamma_o$$

$$+ r)\sin\psi - (a_1 - r\gamma_o)\cos\psi)dT] - \phi_{\theta Y,j}[(b_1(\gamma_o - q'_{EO})\cos\psi - (e\beta_o$$

$$- b_1)\sin\psi)dH + ((- b_1 q'_{FO} - a_1\gamma_o - r)\cos\psi - (a_1 - r\gamma_o)\sin\psi)dT]$$

$$- \phi_{X,j}[((\gamma_o - q'_{EO})\cos\psi + \sin\psi)dH - q'_{FO}\cos\psi dT] - \phi_{Y,j}[((\gamma_o - q'_{EO})\sin\psi$$

$$- \cos\psi)dH - q'_{FO}\sin\psi dT] + \phi_{Z,j}\beta_o dH\}\gamma$$

$$+ \sum_{i=1}^{NE} \{\phi_{\theta X,j}[((- \phi_{F,i} + b_1(\gamma_o - q'_{EO}\ \phi'_{E,i} + a_1\beta_o\phi'_{E,i})\sin\psi$$

$$- (\phi_{F,i}(\gamma_o - q'_{EO}) + b_1\phi'_{E,i} - e\beta_o\phi'_{E,i})\cos\psi)dH - ((\phi_{E,i} + b_1(\gamma_o$$

$$- q'_{EO})\phi'_{F,i} + a_1(\beta_o + q'_{FO})\phi'_{F,i} + b_1 q'_{FO}\phi'_{E,i})\sin\psi + (\phi_{E,i}\gamma_o$$

$$- r_i - q'_{FO}\phi_{F,i} + (r + e)q'_{FO}\phi'_{F,i})\cos\psi)dT] - \phi_{\theta Y,j}[((- \phi_{F,i}$$

$$+ b_1(\gamma_o - q'_{EO})\phi'_{E,i} + a_1\beta_o\phi'_{E,i})\cos\psi + (\phi_{F,i}(\gamma_o - q'_{EO}) + b_1\phi'_{E,i}$$

$$- e\beta_o\phi'_{E,i})\sin\psi)dH + ((- \phi_{E,i} - b_1(\gamma_o - q'_{EO})\phi'_{F,i} - a_1(\beta_o + q'_{FO})\phi'_{F,i}$$

$$- b_1 q'_{FO}\phi'_{E,i})\cos\psi + (\phi_{E,i}\gamma_o - r_i - q'_{FO}\phi_{F,i} + (r + e)q'_{FO}\phi'_{F,i})\sin\psi)dT]$$

$$- \phi_{X,j}[(\phi'_{E,i}\sin\psi + \phi'_{E,i}(\gamma_o - q'_{EO})\cos\psi)dH + (- \phi'_{F,i}\sin\psi - (\phi'_{F,i}(\gamma_o$$

$$- q'_{EO}) + q'_{FO}\phi'_{E,i})\cos\psi)dT] - \phi_{Y,j}[(- \phi'_{E,i}\cos\psi + \phi'_{E,i}(\gamma_o$$

$$- q'_{EO})\sin\psi)dH + (\phi'_{F,i}\cos\psi - (\phi'_{F,i}(\gamma_o - q'_{EO}) + q'_{FO}\phi'_{E,i})\sin\psi)dT]$$

$$- \phi_{Z,j}[- \beta_o\phi'_{E,i}dH + \phi'_{F,i}(\beta_o + q'_{FO})dT]\}q_{T,i} + [(\phi_{\theta X,j}(a_1\gamma_o + r + e$$

$$+ b_1 q'_{FO}) - \phi_{\theta Y,j}(a_1 - r\gamma_o)$$

$$- \phi_{Y,j}(\beta_o + q'_{FO}))\cos\psi + (\phi_{\theta X,j}(a_1 - r\gamma_o) + \phi_{\theta Y,j}(a_1\gamma_o + r + e$$

$$+ b_1 q'_{FO}) + \phi_{X,j}(\beta_o + q'_{FO}))\sin\psi + \phi_{Z,j}][t_1\delta U_T + t_2\delta U_P + t_3\delta\alpha]$$

$$+ [(- \phi_{\theta X,j} b_1(\gamma_o - q'_{EO}) + \phi_{\theta Y,j}(b_1 + r\beta_o) + \phi_{Y,j}(\gamma_o - q'_{EO})$$

$$+ \phi_{X,j})\cos\psi - (\phi_{\theta X,j}(b_1 + r\beta_o) + \phi_{\theta Y,j} b_1(\gamma_o - q'_{EO}) + \phi_{X,j}(\gamma_o - q'_{EO})$$

$$- \phi_{Y,j})\sin\psi][h_1\delta U_T + h_2\delta U_P + h_3\delta\alpha]\}\Big]dr\Big\} \tag{A130}$$

$$Q_{\theta T} = \Big\{\int_0^{R-e}\Big[(- a_1 dH - b_1 dT)\phi_\theta^2\theta_T$$

$$+ \sum_{i=1}^{NE}((- \phi_{F,i} - \phi'_{E,i} q'_{EO} b_1)dH - (\phi_{E,i} + \phi'_{E,i} q'_{FO} b_1$$

$$- \phi'_{F,i}(q'_{EO} b_1 - q'_{FO} a_1))dT)\phi_\theta q_{T,i}$$

$$+ a_1(t_1\delta U_T + t_2\delta U_P + t_3\delta\alpha)\phi_\theta$$

$$- b_1(h_1\delta U_T + h_2\delta U_P + h_3\delta\alpha)\phi_\theta$$

$$- (m_1\delta U_T + m_2\delta U_P + m_3\delta\alpha)\phi_\theta\Big]dr\Big\} \tag{A131}$$

$$Q_\beta = \Big\{\int_0^{R-e}\Big[(- a_1(\gamma_o - q'_{EO})dH - (b_1\gamma_o - a_1 q'_{FO})dT)\phi_\theta\theta_T$$

$$- (b_1 dH - (a_1 - r\gamma_o)dT)\gamma$$

$$+ \sum_{i=1}^{NE}((- \phi_{F,i}(\gamma_o - q'_{EO}) - \phi'_{E,i} b_1)dH - (\phi_{E,i}\gamma_o - \phi_{F,i} q'_{FO}$$

$$- r_i - \phi'_{F,i}(b_1 - r q'_{FO}))dT)q_{T,i}$$

$$+ (a_1\gamma_o + r + b_1 q'_{FO})(t_1\delta U_T + t_2\delta U_P + t_3\delta\alpha)$$

$$- (b_1(\gamma_o - q'_{EO}))(h_1\delta U_T + h_2\delta U_P + h_3\delta\alpha)\Big]dr\Big\} \tag{A132}$$

$$
\begin{aligned}
Q_\gamma = \Bigg\{ \int_0^{R-e} \Big[& (b_1 q'_{EO} dH + b_1 q'_{FO} dT) \phi_\theta \theta_T \\
& + \sum_{i=1}^{NE} \big((\phi_{E,i} q'_{EO} - r_i + \phi'_{E,i}(a_1 - r q'_{EO})) dH \\
& + (\phi_{E,i} q'_{FO} - r \phi'_{E,i} q'_{FO} - \phi'_{F,i}(a_1 - r q'_{EO})) dT \big) q_{T,i} \\
& - (a_1 q'_{FO})(t_1 \delta U_T + t_2 \delta U_P + t_3 \delta \alpha) \\
& - (a_1 q'_{EO} + r)(h_1 \delta U_T + h_2 \delta U_P + h_3 \delta \alpha) \Big] dr \Bigg\}
\end{aligned}
\tag{A133}
$$

$$
\begin{aligned}
Q_{q_{T,j}} = \Bigg\{ \int_0^{R-e} \Big[& (- \phi_{F,j} dH - \phi_{E,j} dT) \phi_\theta \theta_T \\
& + \sum_{i=1}^{NE} \big((- q'_{EO} r_{j,i} - \phi'_{E,i}(q'_{EO} \phi_{E,j} - r_j)) dH \\
& - (q'_{FO} \phi_{E,j} \phi'_{E,i} + \phi'_{F,i}(- q'_{EO} \phi_{E,j} + r_j + q'_{FO} \phi_{F,j}) \\
& + q'_{FO} r_{j,i}) dT \big) q_{T,i} \\
& + \phi_{F,j}(t_1 \delta U_T + t_2 \delta U_P + t_3 \delta \alpha) \\
& - \phi_{E,j}(h_1 \delta U_T + h_2 \delta U_P + h_3 \delta \alpha) \Big] dr \Bigg\}
\end{aligned}
\tag{A134}
$$

Unsteady Aerodynamics

Circulatory Components

The importance of the effect of unsteady aerodynamics on rotor stability has been demonstrated by a number of investigators. Anderson and Watts[3] give a good account of some of the work that has been done. Their discussions generally relate to flutter phenomena experienced by unstalled blades in hover conditions. Under such conditions, the unsteady aerodynamic theories postulated by Theodorsen and Loewy can be used. These theories differ only in that, if Theodorsen functions are employed, the effects of wakes from previous blades either are ignored or are negligible, whereas the use of Loewy functions permits the effects of preceding blades to be taken into account. Theodorsen analysis, therefore, necessarily constitutes a single blade analysis, while Loewy analysis yields a multiblade solution.

Both approaches define circulatory unsteady effects and are readily accommodated by employing the unsteady aerodynamic lift deficiency function $C' = F' + iG'$ defined by

$$C' = \frac{H_1^{(2)}(k) + 2J_1(k)W}{H_1^{(2)}(k) + iH_0^{(2)}(k) + 2[J_1(k) + iJ_0(k)]W} \qquad \text{(A135)}$$

This expression defines the Loewy lift deficiency function. When $W = 0$, Theodorsen lift deficiency functions are defined.

In Equation A135, the modifier W, which is used only when multiblade or preceding blade wake effects are considered, is given by

$$W = \frac{1 + \sum_{n=1}^{N-1} \left[e^{khN} e^{i2\pi m}\right]^{\frac{N-n}{N}} e^{i\phi_n}}{e^{khN} e^{i2\pi m} - 1} \qquad \text{(A136)}$$

where $k = \frac{\omega c}{2U}$ is a reduced frequency parameter, ω is the flutter frequency, c is the chord, and U is the total inflow velocity. $m = \omega/\Omega$ is the ratio of the flutter frequency and the rotor speed. $h = 4\pi U\rho/c\Omega$ is the nondimensional vertical wake spacing. ϕ_n is the interblade phase which depends on the type of mode being analyzed.

---

(3) Anderson, W. D., and Watts, G. A., Rotor Blade Wake Flutter, Lockheed Report LR 26213, December, 1973.

For collective modes, $\phi_n = 0$

For reactionless modes, $\phi_n = \pi n$

For advancing modes, $\phi_n = (-\pi/2)n$

For regressing modes, $\phi_n = (\pi/2)n$

Here, $n = 1, 2, \ldots (N - 1)$

Using all of the foregoing, C' can be defined at every blade radial station.

In this analysis, it is assumed that the rotor is in some steady-state condition when the perturbations of the generalized coordinates are made. Therefore, circulatory unsteady aerodynamic effects are incorporated as follows:

We have previously derived expressions for all of the generalized aerodynamic forces resulting from the perturbations of the generalized coordinates, Equations A130 through A134. Clearly, these will exist whether or not unsteady effects are present. Therefore, any unsteady effects must be added to these.

Hence, the unsteady aerodynamics are assumed to affect only the derivatives of the lift curve slope with respect to angle of attack and Mach number, and those aerodynamic derivatives associated with the T and H forces, Equations A118 through A123. They are assumed to have no effect on steady lift, drag, or pitching moment, or pitching moment derivatives, Equations A115 through A117 and A124 through A126. Therefore, the circulatory unsteady components of the generalized aerodynamic forces are obtained by first setting Equations A115 through A117 and A124 through A126 to zero, setting C_L, C_D, $C_{D,\alpha}$, and $C_{D,M}$ to zero, and multiplying Equations A118 through A123 by C'. The quantities given by Equations A115 through A126 are then substituted for their equivalents in the generalized aerodynamic force expressions, Equations A130 through A134.

Noncirculatory Components

In addition to the circulatory effects just discussed, noncirculatory forces and moments exist that do not depend on wake effects. These are produced by air mass accelerations and can be shown to be given by expressions of the form

$$L_{NC} = \rho U^2 b_h \pi \left[i \frac{k}{U} \dot{h}_o + (a_h k^2 + ik)\alpha_o \right] \tag{A137}$$

$$M_{NC} = \rho U^2 b_h^2 \pi \left[i \frac{K}{U} a_h \dot{h}_o + \left(\left(a_h^2 + \frac{1}{8} \right) k^2 - \left(\tfrac{1}{2} - a_h \right) ik \right) \alpha_o \right] \tag{A138}$$

where h_o corresponds to a blade plunging coordinate, defined positive down, and α_o is a blade pitching coordinate, defined positive nose up. L_{NC} and M_{NC} are defined positive up and nose up and act at the quarter chord and elastic axis respectively. The quantity $a_h b_h = a_h c/2 = EA$. h_o is measured at the semi-chord.

These equations have the form

$$L_{NC} = \frac{\partial L_{NC}}{\partial \dot{h}_o} \dot{h}_o + \frac{\partial L_{NC}}{\partial \alpha} \frac{\partial \alpha}{\partial \theta_o} \alpha_o \tag{A139}$$

$$M_{NC} = \frac{\partial M_{NC}}{\partial \dot{h}_o} \dot{h}_o + \frac{\partial M_{NC}}{\partial \alpha} \frac{\partial \alpha}{\partial \theta_o} \alpha_o \tag{A140}$$

We can now make analogies between the coordinates $\dot{h}_o$ and α_o and the equivalent quantities in the present analysis. $\dot{h}_o$ is the equivalent of a change in inflow velocity and α_o is a blade pitch coordinate. Therefore, we can write

$$\frac{\partial L_{NC}}{\partial \dot{h}_o} \dot{h}_o = - \frac{\partial L_{NC}}{\partial U_P} \delta U_P \tag{A141}$$

$$\frac{\partial M_{NC}}{\partial \dot{h}_o} \dot{h}_o = - \frac{\partial M_{NC}}{\partial U_P} \delta U_P \tag{A142}$$

$$\frac{\partial \alpha}{\partial \alpha_o} \alpha_o = - \frac{\partial \alpha}{\partial \theta} \theta \tag{A143}$$

In addition, from equations A96 and A97 we can write

$$\delta T = \delta L \cos\phi \tag{A144}$$

$$\delta H = \delta L \sin\phi \tag{A145}$$

where ϕ is given by Equation A98.

Substituting Equations A139 in Equations A144 and A145, and using the equivalencies A141 through A143, the following noncirculatory unsteady T and H force derivatives can be defined.

$$t_2' = \frac{\partial T_{NC}}{\partial U_P} = -i\rho U_T \frac{C}{2} \pi k \tag{A146}$$

$$t_3' = \frac{\partial T_{NC}}{\partial \alpha} = \rho U U_T \frac{C}{2} \pi (a_h k^2 + ik) \tag{A147}$$

$$h_2' = \frac{\partial H_{NC}}{\partial U_P} = -i\rho U_P \frac{C}{2} \pi k \tag{A148}$$

$$h_3' = \frac{\partial H_{NC}}{\partial \alpha} = \rho U U_P \frac{C}{2} \pi (a_h k^2 + ik) \tag{A149}$$

Using Equations A142 and A143, the noncirculatory unsteady moment derivatives can be shown to be given by

$$m_2' = \frac{\partial M_{NC}}{\partial U_P} = -i\rho U \frac{C^2}{4} a_h \pi k \tag{A150}$$

$$m_3' = \frac{\partial M_{NC}}{\partial \alpha} = \rho U^2 \frac{C^2}{4} \left[\left(a_h^2 + \frac{1}{8} \right) k^2 - i \left(\frac{1}{2} - a_h \right) k \right] \pi \tag{A151}$$

The noncirculatory components of the generalized aerodynamic forces are obtained by setting Equations A115 through A126 to zero and substituting the quantities defined by Equations A146 through A151 for their equivalents in the generalized aerodynamic force expressions, Equations A130 through A134.

Total Aerodynamic Effect

The total generalized aerodynamic forces are obtained by adding the quasi-steady, the circulatory unsteady, and the noncirculatory unsteady components.

All of the above derivations have been discussed in general terms. However, it should be remembered that the aerodynamic derivatives and lift deficiency functions depend on the local environment and geometry of the particular blade element under consideration. Therefore, these quantities and the parameters on which they depend are functions of the blade radius.

Flutter Solutions

Clearly, the values of the unsteady quantities depend, among other things, on the value of ω, the flutter frequency. This is normally an assumed quantity. If, for example, we are employing Theodorsen functions, we would assume a flutter frequency ω and solve the set of equations. If one of the roots in our solution corresponds identically with ω, we have a valid solution. If not, we would try more values of ω and iterate on a solution. When Loewy functions are employed, only one additional complication is added; that is, in addition to specifying the flutter frequency, we must also specify the mode of flutter, namely, reactionless, collective, etc.

Having specified the mode of flutter, we proceed as described for cases employing Theodorsen functions. This should be repeated for all modes of flutter.

Coordinate Transformation

Hingeless or Articulated Rotors

The dynamic system equations and generalized aerodynamic force expressions that we have derived are expressed in terms of the system generalized coordinates. The coefficients are seen to contain time-dependent quantities. These could be solved directly and the transient response of the system determined. However, transient responses, although useful from the viewpoint of forced response phenomena, are less satisfactory for determining whether or not a system is stable. This ambiguity derives from the fact that transient responses contain contributions from all of the system modes, and spectral analysis may be required to separate individual modal contributions. This is a costly and time-consuming procedure. Experience has shown that there are, in the majority of cases, only a few modes that are cause for concern, that is, in regard to stability. Generally, these are the fundamental modes. The higher order modes are normally important more in relation to forced response. Consequently, in order to obtain eigensolutions of the system of equations we have developed, other than using Floquet type theory, it is necessary that we remove the time dependence of the coefficients. This is achieved by assuming a form of response of the rotating system coordinates and making the required coordinate transformations.

In this analysis, it was assumed that each rotating system generalized coordinate q could be expressed in the form

$$q = {}^{1}/_{N}q_o + {}^{1}/_{N}q_D(-1)^n + {}^{2}/_{N}q_s\sin\psi_n + {}^{2}/_{N}q_c\cos\psi_n \qquad \text{(A152)}$$

Thus, each individual blade mode is replaced by four rotor modes. q_o defines collective motion, q_D defines differential collective or reactionless motion, and q_s and q_c combine to define cyclic motion. The reactionless motion as defined here can only occur in rotors with an even number of blades. The rotor warping motions involving terms in 2ψ, 3ψ, etc., were neglected.

To express the differential equations of the rotating system degrees of freedom in terms of the rotor modes, the transformation, Equation A152, and its first and second time derivatives, Equations A150 and A151, are substituted directly in Equations A76 through A79 and in the generalized aerodynamic force expressions, Equations A131 through A134. The required time derivatives are

$$\dot{q} = {}^{1}/_{N}\dot{q}_o + {}^{1}/_{N}\dot{q}_D(-1)^n + {}^{2}/_{N}(\dot{q}_s - \Omega q_c)\sin\psi_n + {}^{2}/_{N}(\dot{q}_c + \Omega q_s)\cos\psi_n \qquad \text{(A153)}$$

$$\ddot{q} = {}^{1}/_{N}\ddot{q}_o + {}^{1}/_{N}\ddot{q}_D(-1)^n + {}^{2}/_{N}(\ddot{q}_s - 2\Omega\dot{q}_c - \Omega^2 q_s)\sin\psi_n + {}^{2}/_{N}(\ddot{q}_c + 2\Omega\dot{q}_s - \Omega^2 q_c)\cos\psi_n \qquad \text{(A154)}$$

In making these substitutions, it is found that the equations still contain time dependent coefficients. This time dependence involves terms in $\sin\psi$, $\cos\psi$, $\sin 2\psi$, $\cos 2\psi$, $\sin^2\psi$, and $\cos^2\psi$, which can be removed for rotors that have polar symmetry, i.e., rotors with any number of equally spaced blades greater than two, by employing the following identities:

$$\sum^{N} q = q_o, \quad \sum^{N} \dot{q} = \dot{q}_o, \quad \sum^{N} \ddot{q} = \ddot{q}_o$$

$$\sum^{N} q(-1)^n = q_D, \quad \sum^{N} \dot{q}(-1)^n = \dot{q}_D, \quad \sum^{N} \ddot{q}(-1)^n = \ddot{q}_D$$

$$\sum^{N} q\sin\psi_n = q_s, \quad \sum^{N} q\cos\psi_n = q_c$$

$$\sum^{N} \dot{q}\sin\psi_n = \dot{q}_s - \Omega q_c$$

$$\sum^{N} \dot{q}\cos\psi_n = \dot{q}_c + \Omega q_s$$

$$\sum^{N} \ddot{q}\sin\psi_n = \ddot{q}_s - 2\Omega\dot{q}_c - \Omega^2 q_s$$

$$\sum^{N} \ddot{q}\cos\psi_n = \ddot{q}_c + 2\Omega\dot{q}_s - \Omega^2 q_c$$

$$\sum^{N} \sin\psi_n = \sum^{N} \cos\psi_n = 0$$

$$\sum^{N} \sin 2\psi_n = \sum^{N} \cos 2\psi_n = 0$$

$$\sum^{N} \sin^2\psi_n = \sum^{N} \cos^2\psi_n = {}^{N}/_{2}\ , \quad N>2$$

The method of obtaining these will be illustrated by example. If equation A152 is summed from n=1 to N, and it is recognized that because of the polar symmetry $\sum (-1)^n = \sum \sin\psi_n = \sum \cos\psi_n = 0$, it can be seen that $\sum q = {}^{1}/_{N} \sum q_o = q_o$. Similarly, if Equation A152 is multiplied by $\sin\psi_n$ followed by summation from n=1 to N, then again recognizing that because of the polar symmetry $\sum \sin\psi_n = \sum (-1)^n \sin\psi_n = \sum \sin\psi_n \cos\psi_n = 0$, it can be seen that $\sum q\sin\psi_n = {}^{2}/_{N} q_s \sum \sin^2\psi_n$. It can be shown that $\sum \sin^2\psi_n = {}^{N}/_{2}$ for N>2, which leads to the result $\sum q\sin\psi_n = q_s$. Continuing in this manner using Equations A149, A150, and A151, the remaining terms are readily established.

It is clear from the above that, provided the polar symmetry requirement is satisfied, the time dependence of the coefficients can be removed. This is accomplished in the following manner. Suppose we are dealing with the blade rigid-body flapping equations given by Equations A77 and A132. By making appropriate substitutions from Equations A152, A153, and A154 in Equations A77 and A132, the flapping equations will be expressed in terms of the rotor modes described earlier. However, the coefficients will contain time-dependent terms. This is removed in exactly the same manner as described above. By summing the equations that are expressed in terms of rotor modes from n=1 to N, the equation of motion of the collective flapping (β_{col}) is defined. By multiplying the equations by $(-1)^n$, then summing from n=1 to N, the reactionless flapping (β_D) equation is defined. Multiplying the equations by $\sin\psi_n$, then summing from n=1 to N defines the cyclic flapping (β_S) equation; while multiplying by $\cos\psi_n$, then summing from n=1 to N defines the cyclic flapping (β_C) equation. This procedure is repeated for all rotating system equations of motion.

The fixed system and control system equations are expressed in terms of the rotor modes by substituting from Equations A152, A153, and A154 in Equations A75, A80, A87, A88, and A89, and in the generalized aerodynamic force expression A130. In this case, the coefficient time dependence is removed by simply summing each equation from n=1 to N and applying the above identities as appropriate.

Because of the length of the equations involved, no attempt was made to rewrite them in their transformed form. Instead, the transformations were performed in the computer program of the analysis.

Gimbaled Rotors

All of the foregoing can be applied only to rotors that are not gimbaled. However, the gimbaled rotor is readily accommodated since the equations are expressed in terms of rotor modes. The method employed is best illustrated by example.

Consider a four-bladed gimbaled rotor system whose blades can move only in an out-of-plane direction. For zero spring restraint on the gimbal the first mode of the blades will be rigid-body flapping, and since blade motions are transmitted across the hub, the mode will be purely cyclic. Therefore, for this mode, the coordinate transformation will be as given by Equation A152 with q_o and q_D set to zero. The next blade mode will be a bending mode that is the equivalent of the first bending mode of a rotating, cantilevered beam. This mode will be purely collective, or reactionless, and its coordinate transformation will, therefore, be as given by Equation A152 with q_s and q_c set to zero. The next mode will be the equivalent of the first bending mode of a hinged, rotating beam. The mode will be purely cyclic, and its coordinate transformation will, therefore, be as given by Equation A152 with q_o and q_D set to zero. Continuing in this manner, all of the rotor modes and their respective coordinate transformations can be defined.

An approach similar to the above is employed in this analysis to describe the gimbaled rotor dynamics. Since the blade modes used are fully coupled flatwise/edgewise, mode selection is slightly different but the logic is the same. Mode selection and coordinate transformations are carried out automatically in the computer program of the analysis whenever gimbaled rotors are being studied. This is done in the following manner.

The blade root boundary condition in the plane of the rotor is always assumed to be cantilevered. The gimbal is restrained with the spring k_β, which may of course be zero. Excluding torsion, five blade modes are automatically used which are, by virtue of the coordinate transformations, described in terms of rotor modes. These, together with the coordinate transformations used, are shown below.

Mode	Out-of-Plane Root Bdry. Cond.	Type	Coord. Trans.
1	k_β	Rigid Body Flap	q_s, q_c
2	Cantilevered	1st Flatwise	q_o, q_D
3	k_β	1st Flatwise	q_o, q_D, q_s, q_c
4	k_β	2nd Flatwise	q_s, q_c
5	Cantilevered	2nd Flatwise	q_o, q_D

Thus, we have two modes that are purely cyclic, two modes that are purely collective, or reactionless, and one mode that has collective, reactionless, and cyclic components. It should be remembered that the reactionless components occur only in rotors with an even number of blades.

Solution of Equations

To compute the eigenvalues of the second-degree matrix system, it is first necessary to reduce the problem to the standard eigenvalue form. This is accomplished by multiplying through by the inverse of the stiffness matrix, and forming the companion matrix. This companion matrix is then balanced to improve the accuracy in the case where corresponding rows and columns have very different norms. The balanced matrix is then reduced to upper Hessenberg form by stabilized elementary similarity transformations, and finally the eigenvalues are extracted using the modified LR method.

For a given eigenvalue, the corresponding eigenvector is found by using the eigenvalue to combine the matrices into one NxN matrix, thus yielding a redundant system of N simultaneous equations in N unknowns. This system is solved by setting the ith component of the eigenvector to 1.0 and solving the reduced system obtained by placing the ith column in the solution vector position and deleting the ith row by the Gauss-Jordon method with interchanging.

APPENDIX B

FORWARD-FLIGHT ANALYSIS

This appendix gives details of a forward-flight analysis that approximates forward-flight effects by neglecting certain periodic terms in the equations of motion. It will be seen in what follows that the analysis is essentially the hover analysis developed in Appendix A, appropriately modified to account for both dynamic and aerodynamic forward-flight effects.

Important assumptions are noted below.

ASSUMPTIONS

1. Aerodynamic trim loads and derivatives with respect to perturbations in blade section total velocities and angle of attack are obtained from any desired aerodynamic analysis (linear or nonlinear). Steady, first and second harmonics of these quantities are retained.

2. The trim inflow velocity distribution is determined from any appropriate analysis. Steady and first harmonics are retained.

3. The trim values of the blade rigid-body and elastic deflections and slopes are determined from any appropriate analysis. Steady and first harmonics are retained.

4. Trim values of steady and first harmonic pitch at each station are retained.

5. Trim values of blade velocity as they affect the trim dynamic forces acting on the blades are neglected as higher order.

6. Products of trim quantities are generally neglected in the aerodynamic force terms, but they are retained in the dynamic system equations where deemed appropriate. Products of trim quantities involving aerodynamic offset (which is assumed to be of the same order as the trim deflections) are generally neglected.

7. All products of perturbation quantities have been dropped.

8. Terms involving products of a perturbational quantity and a first-order trim quantity are retained.

9. The approach used implies implicit retention of some "higher order" terms because terms involving products of aerodynamic derivatives, first-order trim, and first-order perturbation are retained. To the extent that the aerodynamic derivative is a function of trim quantities, higher order terms will be present.

DEVELOPMENT OF FORWARD-FLIGHT ANALYSIS

In Appendix A, we developed a stability analysis for rotors in hover or conditions of pure axial flow. The equations were written with all periodicity retained, and it was shown that by making appropriate rotating system generalized coordinate transformations, the periodicity could be removed, leading to a set of constant coefficient equations in a fixed-axis system. Making this coordinate transformation necessitated that each rotating system degree of freedom be assumed to respond in a prescribed number and type of modes. This was done to allow computation of system eigenvalues and eigenvectors for stability analysis.

Such an approach is not essential; we could have solved the equations directly, obtained the system transient response characteristics, and assessed stability from these. However, this approach is not entirely satisfactory since the transients contain components of response from all modes and it is not always apparent, without making runs that involve excessive computer time, whether a system is stable or unstable. We could also have employed analytical techniques that determine eigenvalues of systems with time-dependent coefficients. Floquet theory is one such technique. Here, again, the time to obtain solutions has to be considered. In multi-degree-of-freedom systems Floquet solutions can be costly, and their physical implications require a degree of expertise not required in solutions for constant coefficient systems.

When forward-flight effects are added to the equations of motion of the system, it is not possible, by a simple coordinate transformation, to remove the resultant periodicity in the coefficients. For exact solutions, we have to revert to either of the alternatives mentioned above. However, approximate solutions can be obtained without recourse to these alternatives if certain higher harmonic periodic terms are neglected.

If the same coordinate transformation that was used in the hover analysis is also used in the forward-flight equations, it is found that in the fixed system equations, a substantial amount of the periodicity disappears by virtue of the summation over the number of blades, rotor system polar symmetry being implied. However, in the rotating system equations, terms in all rotor harmonics higher than the first can appear. We do not, therefore, have a system of constant coefficient equations. If it is assumed that these higher harmonic terms can be neglected, constant coefficiert equations result that are identical in form to the hover equations except that they now contain terms that are functions of advance ratio. These can then be solved using standard eigenvalue approaches.

Hohenemser[4] suggests that the approach gives valid results up to advance ratios as high as 0.5. Biggers[5] reached this same conclusion but suggests that the approximation be used with caution when higher frequency modes are important.

Considering the conclusions reached by these researchers, and remembering Biggers' caution, it was decided to apply this approximate technique to the stability equations derived in Appendix A. The approach used is described in what follows.

By way of example, let us examine a single aerodynamic force component on a fixed system coordinate $\overline{q}_i$ arising from an inplane bending perturbation q_E of the blades of a rotor in forward flight. The condition is illustrated in Figure B1. Considering only that part of the force caused by changes in the blade tangential velocity, it can be seen that for small perturbations, the moment in the direction θ_Y is given by

$$\delta M = \sum_{n=1}^{N} \left(\int_0^{R-e} \left(\left(\frac{\partial (dT)}{\partial U_T} \right) \delta U_T (r + e) \sin\psi \right) dr \right) \tag{B1}$$

From Figure B1,

$$\delta U_T = [\Omega(r + e) - V_F \sin\psi \cos(q'_E + \gamma_o)] - [\Omega(r + e) - V_F \sin\psi] = V_F q'_E \gamma_o \sin\psi \tag{B2}$$

With $q'_E = \sum_{i=1}^{NE} \phi'_{E,i} q_{T,i}$, the moment becomes

$$\delta M = \sum_{n=1}^{N} \left(\int_0^{R-e} \left(V_F (r + e) \gamma_o \left(\frac{\partial (dT)}{\partial U_T} \right) \sin^2\psi \sum_{i=1}^{NE} (\phi'_{E,i} q_{T,i}) \right) dr \right) \tag{B3}$$

---

(4) Hohenemser, K. H., "Some Applications of the Method of Multiblade Coordinates," Journal of the American Helicopter Society, Vol. 17, No. 3, July, 1972.

(5) Biggers, J. B., "Some Approximations to the Flapping Stability of Helicopter Rotors," AHS/NASA-Ames Specialists Meeting on Rotorcraft Dynamics, Feb. 13-15, 1974.

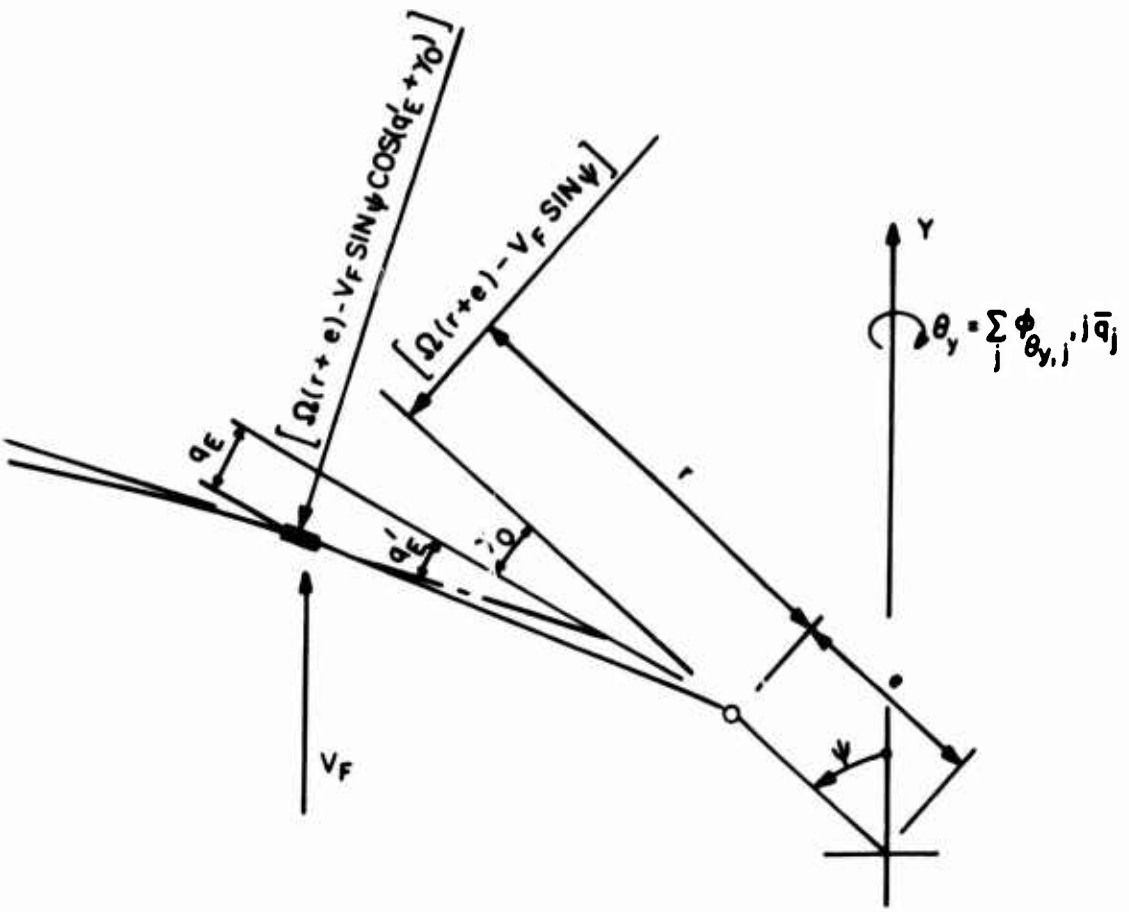

Figure B1. Source of Force Component Resulting From an Inplane Blade Bending Perturbation.

The force on the coordinate $\bar{q}_j$ is then given by

$$\delta F_j = \phi_{\theta Y,j}\delta M$$
$$= \left(\int_0^{R-e}\left(\sum_{i=1}^{NE}(V_F(r+e)\phi'_{E,i}\phi_{\theta Y,j}\sum_{n=1}^{N}(\gamma_o(\frac{\partial(dT)}{\partial U_T})\sin^2\psi q_{T,i}))\right)dr\right) \tag{B4}$$

An examination of Equation B4 reveals that only the terms under the $\sum^{N}$ are time dependent. If we know the time histories of these terms for each blade, we could compute the force component δF_j. However, this is not our immediate objective. We are, rather, more concerned with expressing Equation B4 in an analytical form suitable for inclusion in an eigenanalysis. If the transients of γ_o and $(\frac{\partial(dT)}{\partial U_T})$ were available, we could represent these as Fourier series in harmonics of ψ. In addition, if the response of the generalized coordinate $q_{T,i}$ has known analytical form, it is apparent that δF_j can be expressed analytically.

In Appendix A, we made a coordinate transformation that expressed $q_{T,i}$ in the form

$$q_{T,i} = {}^1/_N q_{To,i} + {}^1/_N(-1)^n q_{TD,i} + {}^2/_N q_{Ts,i}\sin\psi + {}^2/_N q_{Tc,i}\cos\psi \tag{B5}$$

Suppose we now assume that the Fourier series expressions for γ and $(\frac{\partial(dT)}{\partial U_T})$ can be truncated such that

$$\gamma_o = \gamma_{o1} + \gamma_{s1}\sin\psi + \gamma_{c1}\cos\psi \tag{B6}$$

and

$$(\frac{\partial(dT)}{\partial U_T}) = t_1 = t_{o1} + t_{1s}\sin\psi + t_{1c}\cos\psi + t_{1s2}\sin2\psi + t_{1c2}\cos2\psi \tag{B7}$$

At this juncture, let us also assume that β_o, q_{FO}, q_{EO}, q'_{FO}, q'_{EO}, θ_o, and U_P are all expressible in the form of Equation B6 and that t_2, t_3, h_1, h_2, h_3, m_1, m_2, m_3, dT, dH, and dM are all expressible in the form of Equation B7.

Substituting Equations B5, B6, and B7 in Equation B4 gives

$$\delta F_j = \left(\int_0^{R-e}\left(\sum_{i=1}^{NE}\left(V_F(r+e)\phi'_{E,i}\phi_{\theta Y,j}\right.\right.\right.$$
$$\times \sum_{n=1}^{N}\left[(\gamma_{o1} + \gamma_{s1}\sin\psi + \gamma_{c1}\cos\psi)\right.$$
$$\times (t_{o1} + t_{1s}\sin\psi + t_{1c}\cos\psi + t_{1s2}\sin 2\psi + t_{1c2}\cos 2\psi)$$
$$\times \left({}^{1}/_{N}q_{To,i} + {}^{1}/_{N}(-1)^n q_{TD,i} + {}^{2}/_{N}q_{Ts,i}\sin\psi + {}^{2}/_{N}q_{Tc,i}\cos\psi\right)$$
$$\left.\left.\left.\times \sin^2\psi\right]\right)\right)dr\right) \qquad (B8)$$

After expansion of the harmonic terms in this equation and appropriate summation over the number of blades N, it can be shown that

$$\delta F_j = \left(\int_0^{R-e}\left(\sum_{i=1}^{NE}\left(V_F(r+e)\phi'_{E,i}\phi_{\theta Y,j}\left[C_o q_{To,i} + C_s q_{Ts,i} + C_c q_{Tc,i}\right.\right.\right.\right.$$
$$\left.\left.\left.\left. + \text{terms involving products of } q_{To,i},\ q_{TD,i},\ q_{Ts,i}, \text{ and } q_{Tc,i} \text{ and harmonics of } \psi \text{ equal to or greater than 2}\right]\right)\right)dr\right) \qquad (B9)$$

where C_o, C_s, and C_c are constants that are functions of γ_{o1}, γ_{s1}, γ_{c1}, t_{o1}, t_{1s}, t_{1c}, t_{1s2}, and t_{1c2}.

If we assume that the harmonic terms in Equation B9 can be neglected, then performing the required integration we can write

$$\delta F_j = \sum_{i=1}^{NE}\left(A_o q_{To,i} + A_s q_{Ts,i} + A_c q_{Tc,i}\right) \qquad (B10)$$

where A_o, A_s, and A_c are quantities that are independent of time. This equation expresses the element of force δF_j in an identical form to the force elements in the hover analysis.

It will be noticed that the removal of the harmonic terms in Equation B9 results in the elimination of the reactionless coordinate $q_{TD,i}$ from the q_j, or fixed system, equations. This was mathematically correct in the hover analysis since, as the name implies, the mode is indeed reactionless. It is therefore apparent that coupling of the reactionless mode with the fixed system modes can occur only if harmonics of ψ greater than the first are retained in the analysis.

The total force on the coordinate $\bar{q}_j$ resulting from the blade inplane bending perturbation q_E is the sum of all of the δF_j resulting from this perturbation. We derived above a single component caused by changes in tangential velocity. Clearly, other components arise from changes in inflow velocity, changes in thrust, changes in drag, etc. Also, additional components of force result from blade out-of-plane bending perturbations, and yet others arise from blade inplane and out-of-plane bending velocity perturbations. In any event, by following the procedure outlined above, all of the elements of force resulting from the blade bending displacement perturbations can be expressed in the form of Equation B10, while those resulting from blade bending velocity perturbations will have exactly the same form except that they will be in terms of $\dot{q}_{To,i}$, $\dot{q}_{Ts,i}$, and $\dot{q}_{Tc,i}$. Summing all of the force elements resulting from the displacement perturbations gives the complete aerodynamic coefficients of $q_{To,i}$, $q_{Ts,i}$, and $q_{Tc,i}$ in the $\bar{q}_j$ equation. Likewise, summing all of the force elements resulting from the velocity perturbation gives the complete aerodynamic coefficients of $\dot{q}_{To,i}$, $\dot{q}_{Ts,i}$, and $\dot{q}_{Tc,i}$ in the $\bar{q}_j$ equation.

Any coefficient of any displacement, velocity, or acceleration of any of the system generalized coordinates in the $\bar{q}_j$ equation can be obtained in the same way. This is so whether the coefficients arise from purely dynamic considerations or aerodynamic considerations, or both.

All of the dynamic and aerodynamic force elements in each coefficient in the $\bar{q}_j$ equation for a purely axial flow condition were derived in Appendix A. To include the forward-flight aerodynamic effects, it is only necessary to modify the expressions for δU_T and δU_P given in Appendix A by adding the quantities given below.

$$\begin{aligned}\delta U_T(\text{fwd. flt.}) = &\Big[\sum_{i=1}^{NE}\left(V_F(-\phi'_{E,i}[\gamma_o - q'_{EO}]\sin\psi + \phi'_{E,i}\cos\psi)q_{T,i}\right)\Big] \\ &+ [V_F(-\beta_o[\gamma_o - q'_{EO}]\cos\psi)\beta] \\ &+ [V_F(-[\gamma_o - q'_{EO}]\sin\psi + \cos\psi)\gamma] \\ &+ \Big[\sum_{i=1}^{NA}\left(-\phi_{\theta X,i}V_F\beta_o[\gamma_o - q'_{EO}]\right)\bar{q}_i\Big]\end{aligned} \tag{B11}$$

$$\delta U_P(\text{fwd. flt.}) =$$

$$[\sum_{i=1}^{NE}(V_F((-\phi'_{E,i}q'_{FO} - \phi'_{F,i}[\gamma_o - q'_{EO}])\sin\psi + \phi'_{F,i}\cos\psi)q_{T,i})]$$

$$+ [V_F\cos\psi\beta]$$

$$+ [V_F(-q'_{FO}\sin\psi - q'_{FO}[\gamma_o - q'_{EO}]\cos\psi)\gamma]$$

$$+ [\sum_{i=1}^{NA}(\phi_{\theta X,i}V_F)\bar{q}_i] \qquad \text{(B12)}$$

Although we have discussed only the construction of the fixed system equations, the procedure outlined is equally applicable to the construction of the rotating system equations. The only difference is that, whereas a summation over the number of blades appears in the fixed system equations, as seen in Equation B8, no such summation appears in the rotating system equations. Therefore, the force components in the rotating system equations will have a form similar to that of Equation B8 with the $\sum^{N}$ omitted.

Again by way of example, a typical aerodynamic force element in the rigid-body flapping, β , equation resulting from a blade out-of-plane bending perturbation is

$$\delta F_\beta = (\sum_{i=1}^{NE}(-r\phi'_{F,i}U_P(\beta_o + q'_{FO})(\frac{\partial(dT)}{\partial U_P}))q_{T,i}) \qquad \text{(B13)}$$

Using the assumed forms for the time-dependent quantities as defined earlier, this can be rewritten

$$\delta F_\beta = (\int_0^{R-e}(\sum_{i=1}^{NE}(-r\phi'_{F,i}[(U_{PO} + U_{PS}\sin\psi +$$

$$+ U_{PC}\cos\psi)(\beta_{o_1} + q'_{FO_1} + [\beta_{os} + q'_{FOs}]\sin\psi$$

$$+ [\beta_{oc} + q'_{FOc}]\cos\psi)(t_{o2} + t_{2s}\sin\psi + t_{2c}\cos\psi$$

$$+ t_{2s2}\sin 2\psi + t_{2c2}\cos 2\psi)(^1/_N q_{To,i} + {}^1/_N(-1)^n q_{TD,i}$$

$$+ {}^2/_N q_{Ts,i}\sin\psi + {}^2/_N q_{Tc,i}\cos\psi)]))dr) \qquad \text{(B14)}$$

It is clear that if the harmonic terms in this are expanded, the result can be expressed in the general form

$$a + b\sin\psi + c\cos\psi + d\sin 2\psi + e\cos 2\psi + \ldots \tag{B15}$$

where the a, b, c, etc., are functions of the U_p, β, q'_F, t, and q_T.

If in B15 we ignore harmonics higher than the first, then after substituting back into Equation B14 and performing the required integration, the result can be written

$$\begin{aligned}\delta F_\beta = \sum_{i=1}^{NE} \Big[& (A_{o1} q_{To,i} + A_{o1}(-1)^n q_{TD,i} + A_{s1} q_{Ts,i} + A_{c1} q_{Tc,i}) \\ & + (A_{s1} q_{To,i} + A_{s1}(-1)^n q_{TD,i} + A_{s2} q_{Ts,i} + A_{c2} q_{Tc,i})\sin\psi \\ & + (A_{c1} q_{To,i} + A_{c1}(-1)^n q_{TD,i} + A_{c2} q_{Ts,i} + A_{c3} q_{Tc,i})\cos\psi\Big]\end{aligned} \tag{B16}$$

where the A's are quantities that are independent of time. This equation expresses the element of force δF_β in an identical form to the force elements in the hover analysis. The total force on the rigid-body flapping resulting from the blade out-of-plane bending perturbation is the sum of all of the δF_β resulting from this perturbation. Similarly, the forces from all other perturbations of any generalized coordinates, whether they be displacement, velocity, or acceleration or arise from purely dynamic or aerodynamic considerations, or both, are obtained in the same manner and can be expressed in the same form as Equation B16.

If each of the rotating system equations, expressed in the form of Equation B16, is multiplied by $(-1)^n$ and summed over the number of blades N, the reactionless mode equations are obtained. Summing each equation over the number of blades gives the collective mode equations. Multiplying each equation by $\sin\psi$ and $\cos\psi$, respectively, and summing over the number of blades gives the cyclic mode equations. On completing these manipulations, it is again found that the reactionless mode is completely decoupled due to the harmonics of ψ above the first being discarded.

In some of the system equations, products involving $\sin\theta_o$ and $\cos\theta_o$ are encountered. In this analysis, the blade angle θ_o is not considered to be small. Therefore, when substitutions of the form given in Equation B6 are made for θ_o, we get

$$\sin\theta_o = \sin(\theta_{o_1} + \theta_{s_1}\sin\psi + \theta_{c_1}\cos\psi)$$

$$\cos\theta_o = \cos(\theta_{o_1} + \theta_{s_1}\sin\psi + \theta_{c_1}\cos\psi) \qquad \text{(B17)}$$

These were expressed in terms of Bessel functions such that

$$\begin{aligned}
\sin\theta_o &= B_1\sin\theta_{o_1} + B_2\cos\theta_{o_1} \\
&= [J_o(\theta_{s_1})J_o(\theta_{c_1}) + (2(J_2(\theta_{s_1})J_o(\theta_{c_1}) \\
&\quad - J_2(\theta_{c_1})J_o(\theta_{s_1})))\cos 2\psi \\
&\quad - 2J_1(\theta_{s_1})J_1(\theta_{c_1})\sin 2\psi \\
&\quad - 4J_2(\theta_{s_1})J_2(\theta_{c_1})\cos^2 2\psi]\sin\theta_{o_1} \\
&\quad + [2J_1(\theta_{s_1})J_o(\theta_{c_1})\sin\psi \\
&\quad - 4J_1(\theta_{s_1})J_2(\theta_{c_1})\sin\psi\cos 2\psi \\
&\quad + 2J_1(\theta_{c_1})J_o(\theta_{s_1})\cos\psi \\
&\quad + 4J_1(\theta_{c_1})J_2(\theta_{s_1})\cos\psi\cos 2\psi]\cos\theta_{o_1}
\end{aligned}$$

$$\cos\theta_o = B_1\cos\theta_{o_1} - B_2\sin\theta_{o_1} \qquad \text{(B18)}$$

The Bessel series was trucated at J_2 due to the rapid decrease in the magnitudes of the functions beyond this point at typical values of the arguments.

It should be clear from what has preceded that literal expression of the forward-flight equations would indeed be a monumental task. Therefore, this task was left to the computer. Special routines were developed that perform all of the manipulations described here, the end product always being the stability matrices from which the system eigenvalues and eigenvectors are extracted.

LIST OF SYMBOLS

a	$= q_{EO} + (c/4 - EA)\cos\theta_o$
a_1	$= q_{EO} - AC\cos\theta_o$
a_2	$= q_{EO} - CG\cos\theta_o$
a_h	$= EA/b_h$
A_p	Servo piston area
AC	Distance from blade elastic axis to aerodynamic center--positive toward leading edge
A_o, A_{o1}, A_s, A_{s1}, A_{s2}, A_c, A_{c1}, A_{c2}, A_{c3}	Non-time dependent coefficients arising from expansions of products of harmonic series in forward flight analysis
$A_{q_{\theta Y}}$	Hub roll transformation matrix
$A_{q_{\theta X}}$	Hub pitch transformation matrix
A_ψ	Blade azimuth transformation matrix
A_β	Blade flapping transformation matrix
A_γ	Blade lagging transformation matrix
A_θ	Blade pitch transformation matrix
$A_{q_E}^{c'}$	Blade inplane bending slope transformation matrix
$A_{q_F}^{c'}$	Blade out-of-plane bending slope transformation matrix
b	$= q_{FO} + (c/4 - EA)\sin\theta_o$

b_1 = $q_{FO} - AC\sin\theta_o$

b_2 = $q_{FO} - CG\sin\theta_o$

b_h Chord /2

C Chord

C' Lift deficiency function

C_1 Damping constant at pushrod

$C_{2,3,4,5}$ Tail rotor control system damping constants

$C_{31,41,51}$ Tail rotor control system damping constants

C_L Lift coefficient

C_D Drag coefficient

C_M Pitching moment coefficient

C_F Damping constant at forward main rotor servo

C_A Damping constant at aft main rotor servo

C_{LL} Damping constant at lateral main rotor servo

C_q Servo valve flow gain

C_P Servo valve pressure gain

C_o, C_s, C_c Non-time dependent coefficients arising from expansions of products of harmonic series in forward flight analysis

C_{LS} Servo leakage coefficient

$C_{L,\alpha}$ Slope of lift curve

$C_{D,\alpha}$ Slope of drag curve

$C_{M,\alpha}$ Slope of pitching moment curve

$C_{L,M}$ Partial derivative of lift coefficient with respect to Mach number

$C_{D,M}$ Partial derivative of drag coefficient with respect to Mach number

$C_{M,M}$	Partial derivative of pitching moment coefficient with respect to Mach number
CG	Distance from blade elastic axis to center of gravity--positive toward leading edge
dL	Elemental lift
dD	Elemental drag
dM	Elemental pitching moment
dT	Elemental thrust
dH	Elemental inplane force
$\{d\bar{F}\}$	Blade elemental lift and drag force vector in absolute coordinate system
$\{d\bar{M}\}$	Blade elemental pitching moment vector in absolute coordinate system
D	Dissipation potential
e	Blade offset
$\{\bar{E}\}$	Blade offset vector
EA	Distance from blade semi-chord to elastic axis--positive toward trailing edge
F'	Real part of lift deficiency function
G	Blade torsional modulus of elasticity
G'	Imaginary part of lift deficiency function
$H_r^{(2)}$	Hankel function of second type of order
h	Wake spacing parameter
h_o	Blade plunging coordinate used in definition of unsteady aerodynamics
h_1	Partial derivative of drag with respect to local blade tangential velocity
h_2	Partial derivative of drag with respect to local blade vertical velocity

h_3	Partial derivative of drag with respect to local blade angle of attack
$[I]$	Blade flatwise, edgewise, torsional mass moment of inertia matrix
I_θ	Blade torsional mass moment of inertia
I_{YY}	Blade edgewise second moment of area
I_X	Elemental blade flatwise mass moment of inertia
I_Y	Elemental blade torsional mass moment of inertia
I_Z	Elemental blade chordwise mass moment of inertia
I_T	Total blade torsional mass moment of inertia
I_γ	Blade mass moment of inertia about lag hinge
I_{FA}	Main rotor swash plate fore/aft mass moment of inertia
I_L	Main rotor swash plate lateral mass moment of inertia
J	Local blade polar second moment of area
J_r	Bessel function of first kind of order
K	Blade torsional stiffness
K_G	Airframe mode generalized stiffness
K_γ	Blade lag hinge spring rate
K_β	Blade flapping hinge spring rate
K_1	Pitch beam stiffness or stiffness at main or tail rotor blade pushrod
$K_{2,3,4,5}$	Tail rotor control system spring rates
$K_{31,41,51}$	Tail rotor control system spring rates
K_{MA}	Stiffness of tail rotor pitch actuator for pure moment applied at pitch beam end
K_F	Spring rate at forward main rotor servo
K_A	Spring rate at aft main rotor servo
K_L	Spring rate at lateral main rotor servo

K_C	Spring rate at servo support
k	Reduced frequency parameter
L_2	Distance from blade elastic axis to pushrod--positive toward leading edge
L_3	Radial location of blade pitch horn
L_1	Length of one arm of tail rotor blade pitch spider beam
L_{NC}	Noncirculatory lift
L_s	Length of tail rotor pitch beam arm
m	Blade elemental mass and flutter frequency ratio
M_G	Airframe mode generalized mass
M_{NC}	Noncirculatory pitching moment
M_q	Generalized mass of blade bending modes
M_A	Generalized mass of fixed system modes
M_1	Mass at pushrod
$M_{2,3,4,5}$	Tail rotor control system masses
$M_{31,41,51}$	Tail rotor control system masses
M_S	Main rotor swash plate mass
M	Mach number
m_1	Partial derivative of pitching moment with respect to local blade tangential velocity
m_2	Partial derivative of pitching moment with respect to local blade vertical velocity
m_3	Partial derivative of pitching moment with respect to local blade angle of attack
n	Blade number
N	Number of blades
NE	Number of blade bending modes
NA	Number of fixed system modes

N_S	Bulk modulus of servo fluid
$\bar{q}_j$	Fixed system mode generalized coordinate
$q_{T,j}$	Blade bending mode generalized coordinate--bending up and leading positive
q_{FO}	Steady blade flatwise deflection--up positive
q_{EO}	Steady blade inplane deflection--lag positive
$\bar{q}_{\theta X}$	Hub pitch coordinate
$\bar{q}_{\theta Y}$	Hub roll coordinate
$\bar{q}_X$	Hub lateral coordinate
$\bar{q}_Y$	Hub longitudinal coordinate
$\bar{q}_Z$	Hub vertical coordinate
q_o	Collective mode coordinate
q_D	Reactionless mode coordinate
q_s	Sine cyclic coordinate
q_c	Cosine cyclic coordinate
q_{To}, q_{TD}, q_{Ts}, q_{Tc}	Blade bending collective, reactionless, sine cyclic, and cosine cyclic coordinates
q'_{FO}, q'_{FOs}, q'_{FOc}	Blade flatwise bending slope steady, and sine and cosine coefficient components
$\bar{Q}$	Generalized forces
$Q_{q,j}$	Generalized force on J'th fixed system mode
$Q_{\theta T}$	Generalized force on blade pitch
Q_β	Generalized force on blade flapping
Q_γ	Generalized force on blade lagging

$Q_{q_{T,j}}$	Generalized force on j'th blade bending mode
Q_V	Flow through servo valve
Q_j	Generalized aerodynamic force
r	Radius of local blade element from offset
r_1	Radial location of inner snubber of crossbeam rotor
r_2	Radial location of outer snubber of crossbeam rotor
R	Rotor radius
R_S	Radius to servo connections on main rotor swash plate
R_B	Radius to pushrod connections on main rotor swash plate
$R_{1,2,3}$	Servo linkage ratios
$SF_{V,X,Y,Z,\theta_X,\theta_Y}$	Servo valve feedback factors
$SF_{,X,Y,Z,\theta_X,\theta_Y}$	Servo support feedback factors
T	Kinetic energy
t_1	Partial derivative of thrust with respect to local blade tangential velocity
t_2	Partial derivative of thrust with respect to local blade vertical velocity
t_3	Partial derivative of thrust with respect to local blade angle of attack
t_{o1}, t_{1s}, t_{1c}, t_{1s2}, t_{1c2}	Steady, first, and second harmonic coefficients of the partial of thrust with respect to tangential velocity
t_{o2}, t_{2s}, t_{2c}, t_{2s2}, t_{2c2}	Steady, first, and second harmonic coefficients of the partial of thrust with respect to inflow velocity
U	Total local blade inflow velocity

U_P	Local blade vertical velocity
U_{PO}, U_{PS}, U_{PC}	Steady and first harmonic coefficients of inflow velocity
U_T	Local blade tangential velocity
v	Speed of sound
V	Potential energy
V_T	Total volume of servo fluid under compression
V_A	Rotor axial velocity
V_F	Forward-flight speed
$\{\overline{V}\}$	Airspeed vector
W	Loewy unsteady aerodynamics factor--Equation A136
$\{\overline{X}\}$	Absolute displacement vector
X_1	Displacement at blade pushrod
$X_{2,3,4,5}$	Tail rotor control system motions
$X_{31,41,51}$	Tail rotor control system motions
X_F	Motion of main rotor swash plate at forward servo
X_A	Motion of main rotor swash plate at aft servo
X_L	Motion of main rotor swash plate at lateral servo
X_{OF}	Motion of output of forward main rotor servo
X_{OA}	Motion of output of aft main rotor servo
X_{OL}	Motion of output of lateral main rotor servo
X_{VF}	Feedback motion at servo valve
X_{AF}	Feedback motion at servo support
X_O	Motion at output of tail rotor servo
X_C	Motion at servo support

α	Local blade angle of attack
α_o	Blade pitch coordinate used in definition of unsteady aerodynamics
α_1	Pitch-lag coupling--lead, pitch-up positive
α_s	Servo linkage ratio
β	Blade rigid-body flapping generalized coordinate--up positive
β_o	Steady blade coning--up positive
β_{col}, β_D, β_s, β_c	Blade flapping collective, reactionless, sine cyclic, and cosine cyclic coordinates
β_{o1}, β_{os}, β_{oc}	Steady and first harmonic coefficients of blade flapping
γ	Blade rigid-body lag generalized coordinate--lead positive
γ_o	Steady blade lag--lead positive
γ_{o1}, γ_{s1}, γ_{c1}	Steady and first harmonic coefficients of blade lagging
δ_3	Pitch-flap coupling--flap up, pitch-down positive
δP	Servo differential pressure
δ_{FB}	Angle between airframe longitudinal axis and main rotor fore/aft servo axis--yaw right positive
δ_{PR}	Angle measured at center of rotation from blade feathering axis to pushrod--positive in direction of rotation
δr	Element of blade radius
δF	Perturbation force
δM	Perturbation moment
δF_β	Perturbation force on flapping coordinate

δU_P	Change in inflow velocity resulting from displacement and velocity perturbations
δU_T	Change in tangential velocity resulting from displacement and velocity perturbations
ϵ_v	Motion of servo valve relative to housing
ζ_q	Fraction of critical structural damping of blade bending modes--based on modal frequency
ζ_θ	Fraction of critical structural damping of blade pitch mode--based on rotor speed
ζ_γ	Fraction of critical rigid-body lag damping--based on uncoupled lag frequency
ζ_A	Fraction of critical structural damping of fixed system modes--based on modal frequency
θ	Blade pitch generalized coordinate--leading edge down positive
θ_o	Steady blade pitch angle--leading edge down positive
θ_T	Blade pitch normal coordinate
θ_P	Geometric blade pitch angle--leading edge up positive
θ_{o1}, θ_{s1}, θ_{c1}	Steady and first harmonic coefficients of blade pitching
$\dot{\theta}_X$, $\dot{\theta}_Y$, $\dot{\theta}_Z$	Blade flatwise, torsional, and edgewise angular velocities
$\{\dot{\bar{\theta}}\}$	Absolute blade angular velocity vector
μ_1	Servo parameter--Equation A67
μ_2	Servo parameter--Equation A68
ν_1	$= (\int_0^r (-\phi'_{E,i} q'_{EO} + \phi'_{F,i} q'_{FO}) dr) = -r_i$
ν_2	$= (\int_0^r (\phi'_{E,i} \phi'_{E,j} + \phi'_{F,i} \phi'_{F,j}) dr) = -\dot{r}_i = -r_{i,j}$
ρ	Air mass density

ϕ	Local blade inflow angle
$\phi_{X,Y,Z}$	Fixed system translational mode shapes at hub
$\phi_{\theta X,\theta Y}$	Fixed system rotational mode shapes at hub
ϕ_F	Blade flatwise bending mode shape
ϕ_E	Blade inplane bending mode shape
ϕ_θ	Blade torsional mode shape
$\phi_{\theta PR}$	Blade torsional mode shape at pushrod radial station
ϕ_{FPR}	Blade flatwise bending mode shape at pushrod radial station
ϕ_{ET}	Blade inplane bending mode shape at tip radius
ϕ_n	Wake phase angle parameter
ψ	Blade azimuthal angle
ω_{T1}	Blade asymmetric torsional frequency
ω_{T2}	Blade symmetric torsional frequency
ω_P	Hub pitch frequency
ω_Y	Hub yaw frequency
ω_{EN}	Blade edgewise natural frequency
ω_q	Frequency of blade bending modes
ω_γ	Uncoupled rigid-body lag frequency
ω_A	Frequency of fixed system modes
ω	Flutter frequency
Ω	Rotor speed

Subscripts

A	Refers to aft servo
F	Refers to forward servo
L	Refers to lateral servo
i	Refers to blade element or mode number

j	Refers to mode or force number
s, t	Refers to mode number
r	Refers to blade number
PR	Refers to pushrod
X, Y, Z	Refers to hub lateral, longitudinal, and vertical directions
θ_X, θ_Y	Refers to hub pitch and roll directions

Superscripts

c	Means coupled
u	Means uncoupled

Differential Notation

$'$	Differentiation with respect to radius
$\dot{}$	Differentiation with respect to time
$\ddot{}$	Second differential with respect to time